European Droughts under Climate Change: Projections and Uncertainties

by

Rita Man Sze Yu

Thesis
Submitted to the University of East Anglia
for the degree of
Doctor of Philosophy

Supervisors: Dr Timothy Osborn, Dr Rachel Warren and Prof. Declan Conway

Climatic Research Unit
School of Environmental Sciences
September 2013

Abstract

Droughts are one of the most damaging natural hazards, and anthropogenic climate change has and will continue to alter their characteristics. Better understanding of changes in drought characteristics under potential future climates is vital for managing drought risks and impacts, yet projections are very uncertain. This thesis examines the effects of climate change on European drought characteristics through a multi-scenario and multi-model approach. It explores the uncertainty associated with emission scenarios, global and spatial climate projections, and with the identification and characterisation of droughts.

Climate projections simulated by the simple climate model MAGICC6.0 and pattern-scaling climate scenario generator ClimGen are assessed, emulating eighteen CMIP3 general circulation models (GCMs) under ten emission scenarios. Drought severity (magnitude times duration) and spatial extent are analysed for both 3-month and 12-month events.

Drought projections vary substantially depending on the GCM, emission scenario, region, season and definition of drought. Overall, climate change enhances drought conditions across the study region, with marked increases simulated for the southern latitudes; reductions are projected for the northern latitudes, especially in winter and spring. Perturbations in the interannual variability of precipitation tend to enhance drought conditions caused by mean precipitation changes, or to moderate or reverse their reductions. Hydrological drought parameters are highly sensitive to potential evapotranspiration (PET), which shows the importance of the PET calculation method. Greater agreement in the direction of change tends to occur in the high- and low-latitudes, and in summer and autumn. Both meteorological and hydrological drought results generally indicate the same direction of change, with the latter having larger magnitudes. Projection ranges tend to increase with time and magnitude of warming; intra-GCM spread dominates other sources of uncertainty. The implications of the large uncertainties include that decision-making should be based on multi-scenario and multi-model results, and with consideration of drought definition.

Acknowledgements

Firstly, I would like to thank my supervisors, Tim Osborn, Rachel Warren and Declan Conway for their guidance and support throughout the period of my PhD. Thanks to Rachel for helping me to obtain the AXA Research Doctoral Fellowship. A special thanks to Tim for his willingness to help with anything, and everything he has done for me.

I am very grateful to the AXA Research Fund who provided three years of funding for my PhD. I also thank the School of Environmental Sciences who provided financial support for a 6-month extension to my AXA fellowship.

I thank Robin Hankin who assisted with statistical interpretation and methodological design. I also thank my fellow PhD students and researchers, as well as the people I have met throughout this period, for their support and advice.

I thank my parents, my family and friends in Hong Kong and elsewhere for their continuous support.

Finally, I thank my two examiners, Christel Prudhomme and Phil Jones, for their interest in my work, as well as their thoughtful and constructive comments that make the viva examination such a positive experience for me.

Contents

List of tables

List of figures

Chapter 1

Introduction

1.1 Rationale

Extreme weather/climate events have significant environmental and societal impacts, and anthropogenic climate change has and will continue to alter their characteristics. Droughts (e.g. the 2003 European heatwave and drought; Fink *et al.*, 2004; Stott *et al.*, 2004) are one of the most damaging natural hazards in human, environmental and economic terms (Sheffield and Wood, 2008b; Kirono *et al.*, 2011). Regional changes in drought patterns in the 20th century have been observed (see Section 2.3) and their future changes have been simulated (see Section 2.4). Climate change is stimulating demand from public and private sector decision-makers, as well as other stakeholders, for better understanding of potential future drought characteristics. Such knowledge is the initial step to assessing the impacts of drought (Bordi *et al.*, 2009). It also has both strategic and policy implications by informing effective adaptation and planning strategies (Graham *et al.*, 2007) for managing drought risks and impacts.

Until recently, studies on the projections of extreme weather events, such as drought, have often been based upon a few general circulation models (GCMs), regional climate models (RCMs), and/or emission scenarios, partly due to availability. Only a few studies (e.g. Burke, 2011) have considered the changes in drought under a perturbed climate using a large ensemble of simulations. In addition to the uncertainties due to climate modelling, droughts can be represented by a wide range of indices depending on the purpose of application, and events can be quantified in various ways (see Section 2.2). The different concepts and methods of representing drought events applied in different studies make

inter-comparing results from different analysis challenging (IPCC, 2012). Few studies have investigated the uncertainties associated with the definitional issues of drought, such as the use of a fixed or a seasonally-varying drought threshold, or how the results could differ between meteorological and hydrological droughts (e.g. Wong *et al.*, 2011). Therefore, a systematic approach to analyse the uncertainties in drought projections under a changing climate is desirable.

Changes in the variability of variables are also an important consideration in a changing climate as they may mask/moderate or exacerbate the direction and/or magnitude of an anthropogenic signal. For example, perturbations in interannual climate variability could have implications on the Iberian hydroelectric production (Trigo *et al.*, 2004), agriculture (Skuras and Psaltopoulos, 2012), food production and forestry (Salinger, 2005); exacerbated precipitation variability could raise drought risks (Bates *et al.*, 2008). Future interannual precipitation variability could enhance or alleviate changes in drought characteristics caused by mean precipitation changes, but their spatial and temporal effects have not been well studied.

Climate and hydrological models may be physically sound, but their use in climate change and hydrological impacts studies are subject to various sources of uncertainties that range from the choice of emission scenarios, models and model calibration methodologies (Schaake, 1990; Sankarasubramanian *et al.*, 2001), to the difficulties in the interpretation of multi-model results (see Section 2.6 for further discussion). Decision makers often have time and/or resource constraints, making climate change vulnerability and adaptation assessments based on a physical model a less appropriate support tool in practical applications. Assessing the sensitivity of a system to a particular trigger thus offers an alternative approach, which may provide some indication of the urgency of the issue (Weiss and Alcamo, 2011) without the level of complexity associated with physical modelling. Runoff sensitivity to climatic (e.g. precipitation) changes has been estimated (e.g. by Wigley and Jones, 1985) using various approaches on both global (Chiew *et al.*, 2006) and regional scales (Sankarasubramanian *et al.*, 2001; Chiew and McMahon, 2002; Fu *et al.*, 2007a; Zheng *et al.*, 2009; Liu and Cui, 2011; Renner and Bernhofer, 2012), but few studies have focused on Europe (except for Arnell, 1992; Weiss and Alcamo, 2011). Hence, there is a need to study the spatial and temporal variations of runoff sensitivity

for the European study region. Also, the applicability of such an approach for estimating runoff under a perturbed climate has barely been explored.

This thesis advances from the author's Master of Research dissertation, which examined the implications of future changes in drought frequency in Europe under both unmitigated and mitigated climate change scenarios. The former set of scenarios were represented by four Intergovernmental Panel on Climate Change (IPCC) Special Report on Emissions Scenarios (SRES) emission scenarios (Nakicenovich and Swart, 2000) and the latter, by three stabilisation scenarios at CO_2-equivalent levels of approximately 450, 500 and 550 ppm. This previous work, now published in Warren *et al.* (2012), was based on the standardized precipitation index (SPI) and precipitation scenarios simulated using four previous generation GCMs. Results indicated marked increases in drought frequency over the 21st century, particularly in Southern Europe, under all climate change scenarios examined. It also demonstrated that stringent mitigation measures would be required to reduce these increases in drought conditions.

1.2 Research Aim

GCMs are widely applied in climate change studies. In spite of advanced GCMs and improved knowledge, considerable levels of uncertainty remain in climate change projections, particularly in relation to extreme events. Uncertainties arise not only from the various emission scenarios and GCMs, but also from the different classifications of drought (namely meteorological, agricultural, hydrological, socio-economic and groundwater droughts), and a number of indices have been developed to quantify them. This PhD aims to examine the impacts of climate change projections on drought characteristics for the European study region, and to explore the various sources of uncertainties in drought projections. Specifically, the robustness of these projections is illustrated by quantifying the effects of using different emission scenarios, GCMs and definitions of drought.

1.3 Study Approach

Building on current scientific knowledge, this thesis addresses some of the gaps in existing research by not only examining the potential changes in European drought characteristics due to climate change, but also the associated uncertainties in the projections through the application of a range of emission scenarios and GCMs. The study approach adopted in this thesis is outlined below. The general methods applied are described in Chapter 3; more details related to specific analysis are elaborated in the relevant chapters.

GCM simulations are available for limited emission scenarios due to the computational cost of running large ensembles. Therefore, climate projections simulated by the simple climate model MAGICC6.0 and pattern-scaling climate scenario generator ClimGen are assessed as they can emulate simulations beyond the available GCM ensemble. These include emulations of eighteen Coupled Model Intercomparison Project (CMIP3) GCMs under six IPCC SRES emission scenarios (Nakicenovich and Swart, 2000) and four Representative Concentration Pathway scenarios (RCPs; Moss *et al.*, 2010).

Drought severity (i.e. magnitude times duration) and spatial extent are analysed for both short (3-month) and long (12-month) events, for the European study region (see Section 3.9). Results for two future periods, 2001–2050 and 2051–21100, are compared to the baseline period of 1951–2000. Changes in meteorological droughts are quantified by the Standardised Precipitation Index (SPI) (see Chapter 4). A subset of these climate projections are also used as input to a global hydrological model, Mac-PDM.09, to generate runoff data for characterising changes in hydrological droughts (see Chapter 5). As there are various ways of defining drought, Chapter 5 also investigates the uncertainties arising from definitional issues, including the classification of drought (i.e. meteorological and hydrological droughts), the choice of threshold and the definition of when a drought terminates. Drought analyses based on the monthly time step of precipitation and runoff are considered appropriate given the relatively large spatial coverage and temporal extent (see Sections 3.9 and 3.6, respectively).

To assess the spatial and temporal effects of climate-change-induced changes in inter-annual precipitation variability in the projected meteorological and hydrological droughts, results from two experiments are compared (see Chapter 6). In the first experiment, the

future precipitation scenarios account for changes in both precipitation mean and variability (as represented by the coefficient of variation, CV, or equivalently by the shape parameter of a gamma distribution; see Section 3.2). In the second experiment, the future precipitation scenarios consider only the changes in mean precipitation while keeping the CV constant (hence precipitation standard deviation changes in proportion to the mean; see Section 3.2).

The spatial and temporal variations of runoff sensitivity for the European study region are studied by the elasticity approach using a non-parametric (empirical) estimator. The applicability of this elasticity approach for estimating runoff under a perturbed climate is assessed by comparing the level of agreement between mean runoff values estimated by the elasticity method and those simulated by hydrological modelling using Mac-PDM.09.

1.4 Thesis Structure

This thesis is presented in eight chapters, including this Introduction, and is organised as follows. Chapter 2 provides an overview of the drought concept, the various classifications of drought and methods for their quantification. It presents the observed and projected changes in drought, along with the drivers of their occurrence. This chapter also discusses the various sources of uncertainties in climate modelling and the challenges in projecting future drought characteristics. Chapter 3 describes the general methods applied in this study, including the modelling framework, the approach for identifying and measuring drought, the study area and regions.

Chapter 4 examines the effects of climate change on European meteorological drought characteristics for both 3-month (SPI3) and 12-month (SPI12) events. It assesses the uncertainties that arise from ten emission scenarios and eighteen GCMs, as well as their relative contribution. Using runoff data simulated by Mac-PDM.09, Chapter 5 assesses the effects of climate change on European hydrological droughts, for both 3-month and 12-month events. In order to do so, the uncertainties associated with drought definitional issues are considered, which includes the choice of threshold that identifies drought condition from “normal” climate, the definition of when a drought terminates, and a comparison between the results derived using the meteorological and hydrological drought classifications.

Chapter 6 explores the spatial and temporal effects of climate-change-induced changes in interannual precipitation variability on the projected meteorological and hydrological droughts, based on the 12-month results obtained in Chapters 4 and 5. Chapter 7 studies the spatial and temporal variations of sensitivity of runoff for the study region using the elasticity approach, and explores the applicability of elasticity values for estimating runoff under a perturbed climate. Chapter 8 summarises the key findings revealed from this thesis, and presents some concluding remarks about the policy implications and areas for future research.

Chapter 2

Literature Review

2.1 Introduction

Climate variability and extreme weather/climate events are of great concern (Katz and Brown, 1992) as they produce disproportionately large climate-related damages (Easterling *et al.*, 2000; Meehl *et al.*, 2000). There is growing confidence (Smith *et al.*, 2009a) that human-induced climate change can alter/raise the risk of extreme events (Meehl *et al.*, 2000; Trenberth, 2006; Smith *et al.*, 2009a), which have implications for regional and local adaptation and risk reduction strategies (van Aalst, 2006; Berrang-Ford *et al.*, 2011). This chapter describes the importance of drought events, and provides an overview of the drought concept, the various classifications of drought and methods for their quantification. The observed and projected drought trends are then presented, along with the drivers of drought and their variations. This chapter also discusses the various sources of uncertainties in climate modelling and the challenges in projecting future drought characteristics.

Drought is one of the most damaging natural hazards, in human, environmental and economic terms (Sheffield and Wood, 2008b; Kirono *et al.*, 2011). It affects agriculture (Dai *et al.*, 2004; Fink *et al.*, 2004; Motha and Baier, 2005), irrigation (Döll, 2002) and food production (Li *et al.*, 2009; Piao *et al.*, 2010). Droughts also have implications for hydrological (e.g. groundwater and reservoir storage; Marsh *et al.*, 2007; Vidal and Wade, 2009) and ecological (Ciais *et al.*, 2005; Gobron *et al.*, 2005; Archer and Predick, 2008) systems, e.g. aquatic ecosystems (Kirono *et al.*, 2011). Their impacts on socio-economic systems (Alston and Kent, 2004; Fink *et al.*, 2004; Ding *et al.*, 2011) include

municipal and industrial water supply (Blenkinsop and Fowler, 2007a; Zhang *et al.*, 2011), hydro-power generation, recreation, industry (Panu and Sharma, 2002), and navigation (Graham *et al.*, 2007). Increasing drought conditions can lead to human health concerns (Quevauviller, 2011), e.g. famine in northern Nigeria (Tarhule and Woo, 1997), as they could counteract the effects of the anticipated longer growing seasons. Droughts can also impact on ecosystem goods and services (e.g. in the Alps; Jasper *et al.*, 2004; Bigler *et al.*, 2006; Moser *et al.*, 2011) include the loss of sequestered forest carbon and associated atmospheric feedbacks (Ciais *et al.*, 2005; Allen *et al.*, 2010). Global wildfire potential may also increase (Liu *et al.*, 2010), e.g. more fires in eastern Iberian Peninsula with dry summers (Pausas, 2004).

Notable episodes of droughts include the 1930s and 1950s soil moisture and runoff droughts over continental U.S. and the early 2000s in western U.S. (Andreadis *et al.*, 2005), the Sahel drying since the late 1960s (Dore, 2005), the Australian "Big Dry" since 1995 (Cai *et al.*, 2009), the 1975–1976 UK drought (Gallagher *et al.*, 1976; Perry, 1976; Ratcliffe *et al.*, 1978; Marsh *et al.*, 2007) and the 2003 European heatwave and drought (Fink *et al.*, 2004; Stott *et al.*, 2004). Globally, there were 296 large-scale ($>$500,000 km^2 and $>$3 months) soil moisture droughts during 1950–2000, based on simulations driven by a hybrid observation-reanalysis meteorological dataset that combines gridded observations with data from the National Centers for Environmental Prediction National Center for Atmospheric Research (NCEP–NCAR) reanalysis of global terrestrial hydrologic using the VIC model (Sheffield *et al.*, 2009).

Current management practices may be insufficient to cope with future changes in sustainability, quantity and quality of water resources (Bates *et al.*, 2008), and many developments are planned in drought-prone areas (e.g. the Thames Gateway; Walden, 2009). Drought by itself does not necessarily imply a disaster. While drought risk generally increases with warming and drying (Dai *et al.*, 2004), local and global social and environmental changes influence vulnerability (Iglesias *et al.*, 2006; García-Ruiz *et al.*, 2011). Human activities (e.g. overfarming, excessive irrigation, deforestation, over-exploiting available water and erosion) can alter the land's ability to capture and hold water (Mishra and Singh, 2010). The slow-onset nature of drought can allow human actions to shape the impacts, especially if reliable seasonal forecasts can be made (Li *et al.*, 2009). Climate

change can be incorporated into existing disaster risk reduction and development planning strategies (van Aalst, 2006). For instance, (improved) water management, water pricing and water recycling policies may reduce the population exposed to water stress (Arnell, 2004a; García-Ruiz *et al.*, 2011).

Despite advances in science and improved technology, drought remains one of the major challenges of climate variability worldwide (Piao *et al.*, 2010). Impact assessment and adaptation decisions require specific information about the spatial and temporal characteristics of drought risk (Loukas and Vasiliades, 2004; Mechler *et al.*, 2010). A better understanding of potential future drought evolution could facilitate the implementation of effective adaptation, preparedness and disaster risk reduction measures (Wilhite, 1997).

2.2 Drought

2.2.1 Drought as a Concept

Palmer (1965), Yevjevich (1967), Dracup *et al.* (1980), Wilhite and Glantz (1985), Le Houérou (1996), Panu and Sharma (2002), Wilhite (2005), Paulo and Pereira (2006), WMO (2006), Mishra and Singh (2010) and Dai (2011) have comprehensively reviewed the concept of drought, whcih can be defined and understood in many ways. Sections 2.2.1–2.2.7 are based on these and other studies.

Drought is a natural, temporary and recurrent feature of variability, characterised by a cumulative precipitation deficit from the long-term mean (Bordi *et al.*, 2009; Vidal and Wade, 2009). The predominant driver is low precipitation, but high evaporation rates (available energy; Burke, 2011) also play a role (van Lanen *et al.*, 2007; Li *et al.*, 2009). Although drought (depending on the variability and how it is defined) is common in arid and semi-arid regions, it can affect virtually all climate regimes (Vidal and Wade, 2009), e.g. in cold regions, sub-zero temperatures can produce winter droughts (van Lanen *et al.*, 2007). This also universal phenomenon therefore needs to be considered a relative, rather than an absolute, condition; its characteristics also vary significantly from one region to another (Mpelasoka *et al.*, 2008). The effects of rainfall deficiency may take weeks or months to become apparent. A prolonged and more spatially extensive meteorological drought may induce other types of drought (Mpelasoka *et al.*, 2008) (see Section 2.2.2).

Desertification generally refers to progressive land degradation in arid, semi-arid and dry sub-humid areas caused by climate variability and/or human activities, whereas drought impacts are typically temporary, affecting production rather than long-term productivity (Le Houérou, 1996). However, drought may trigger desertification; since the 1970s, drying over west Africa, southern Europe, East and South Asia, and eastern Australia have substantially increased global aridity (Dai, 2011).

2.2.2 Drought Classifications, Characterisation and Indices

A single drought event can span different climate zones and affect various human activities (Fleig *et al.*, 2006). A standard methodology for characterising droughts under different hydroclimatological and hydrogeological conditions would help monitoring and forecasting of regional episodes (Fleig *et al.*, 2006). However, each event has unique climatic characteristics, spatial extent and impacts (Wilhite, 2005). The wide range of geographical and temporal distribution of droughts (thus the varying concepts), their complexity and interdisciplinary nature, and differing perspectives held by various stakeholders, make the onset and end of a drought difficult to determine. Hence, a precise, systematic and universal drought definition is lacking (Heim Jr., 2002; Andreadis *et al.*, 2005; Quiring, 2009b). Definitions also vary according to the variable (e.g. precipitation, streamflow or soil moisture) used to describe the drought (Mishra and Singh, 2010).

Conceptually, a drought refers to a water shortage (the demand) relative to the supply (Dracup *et al.*, 1980) that originates from the absence or reduction in precipitation due to atmospheric conditions. Droughts are commonly classified into meteorological, agricultural, hydrological and socio-economic droughts (AMS, 2004; see Sections 2.2.3–2.2.7). Meteorological drought is a more common and natural event, whereas agricultural, hydrological and socio-economic droughts emphasise more the human or social aspects (WMO, 2006). The sequence begins with meteorological drought; persistent dry conditions may induce agricultural, hydrological and water resources droughts (Andreadis *et al.*, 2005; Vidal and Wade, 2009).

Mishra and Singh (2011) discussed the various components and methodologies in drought modelling, including forecasting, probabilistic characterisation, spatio-temporal

analysis, the use of general circulation models (GCMs) and land data assimilation systems. Drought indices are commonly used by public and private sector stakeholders (Quiring, 2009b) for event detection, monitoring and evaluation as they enable spatial and temporal comparisons (Roudier and Mahe, 2010). Besides its scientific merits and ability to quantify events at different timescales, which requires a long timeseries (Mishra and Singh, 2010), a "good" indicator should also be valuable and informative to decision-makers (Steinemann *et al.*, 2005; Steinemann and Cavalcanti, 2006).

Many statistical techniques exist for drought analysis (Panu and Sharma, 2002). The choice of a suitable drought characteristic for a specific study is subjective and complicated by hydroclimatology and the nature of the region, type of event considered, societal vulnerability, study aim and data availability (Dracup *et al.*, 1980; Fleig *et al.*, 2006). As different types of drought may not occur simultaneously nor exhibit the same severity, they should be characterised separately (Fleig *et al.*, 2006). Many studies (e.g. Hayes, 1998; Byun and Wilhite, 1999; Heim Jr., 2002; Keyantash and Dracup, 2002; Steinemann, 2003; Quiring, 2009b) have reviewed and/or evaluated the various indicators; some of these are mentioned in Sections 2.2.3–2.2.7. Besides the classical drought definitions, drought analysis methods may be based on frequency/probability, regression and moisture adequacy index (MAI) (Panu and Sharma, 2002).

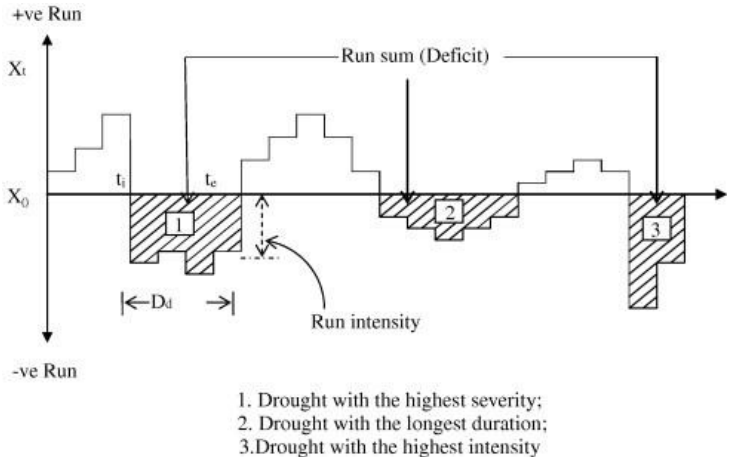

Figure 2.1: Drought characteristics using the run theory for a given threshold level. Source: Figure 1 in Mishra and Singh (2010).

Drought is generally analysed using timeseries of different variables on timescales that vary from months to years (Mishra and Singh, 2010; Panu and Sharma, 2002) based on a threshold approach that originated from the theory of runs (Yevjevich, 1967; Dracup

et al., 1980; Hisdal *et al.*, 2004). This allows various statistical drought parameters, including frequency, duration, intensity and severity, to be determined. Figure 2.1 (from Mishra and Singh, 2010) presents a schematic diagram of a drought variable (X_t), which is intersected at several places by the truncation level (X_0) that produces three drought events. A negative (positive) run occurs when all values of the timeseries of drought variable (X_t) are below (above) the pre-determined threshold (X_0). Drought initiation time (t_i) specifies the start of the deficit period, i.e. when the drought begins; drought termination time (t_e) denotes the time when the drought ends. Drought duration (D_d) is defined as the number of consecutive time-steps with below-threshold values (Byun and Wilhite, 1999), i.e. the time period between the initiation and termination of a drought. While drought severity (S_d) indicates the cumulative departure from a threshold, drought intensity (I_d) represents the averaged cumulative anomaly for that duration, i.e. the average magnitude of an event (Andreadis *et al.*, 2005). With a gridded dataset, the components in Figure 2.1 enable the determination of the areal extent of droughts, which is important as it (together with duration) can influence the range and scale of impacts (Marsh *et al.*, 2007). It can be measured by the Drought Area Index (DAI). DAI estimates the proportion of the area affected by drought by simply counting the number of cells with values of the timeseries, in any given timescale (e.g. month or year), falling below a given threshold divided by the total number of cells over a given domain (Cook *et al.*, 1997; 2004).

Frequency provides no information on the event intensity or duration; it also varies with the chosen timescale, e.g. shorter (longer) events tend to generate higher (lower) frequency (Vicente-Serrano and López-Moreno, 2005). Nevertheless, frequency analysis of critical events helps to determine design criteria in water resource projects (i.e. hydrological drought) and selecting a cropping system or pattern (i.e. agricultural drought) (Panu and Sharma, 2002). Duration strongly correlates to severity (Bonacci, 1993; Woo and Tarhule, 1994; Tarhule and Woo, 1997), which is important for studying hydrological drought (Andreadis *et al.*, 2005). Panu and Sharma (2002) defined severity as a function of duration and probability distribution of the drought variable and its autocorrelation structure. Critical duration, even with lower severity, is important for agricultural drought (Panu and Sharma, 2002). Areal drought characteristics, rather than point values, is useful for water resources management of large regions (Hisdal and Tallaksen, 2003). Droughts

can be spatially identified on a local, regional or national scale (Mishra and Singh, 2010); their maximum size is limited by the size and shape of continental landmasses (Sheffield *et al.*, 2009).

The size, duration and location of a drought depends on a pre-defined threshold of a sequence (e.g. SPI or runoff timeseries) below which an event occurs (Yevjevich, 1967; Dracup *et al.*, 1980). The threshold, either a constant or a function of time of the year, is of significant importance as it distinguishes the variable timeseries into "deficit" and "surplus" (Panu and Sharma, 2002). It may be in absolute (e.g. deficit volumes in mm) or relative (e.g. the 80th percentile) terms. The former may be more meaningful for practitioners engaged in drought monitoring, forecasting and management operations, whereas the latter enables comparisons with other regions that have different hydro-climatic characteristics. Different thresholds (e.g. mean, median and percentiles) characterise events of different intensities (Mishra and Singh, 2010), depending on the needs or applications and location (WMO, 2006).

2.2.3 Meteorological Drought

Meteorological drought typically refers to below-normal precipitation over a period of time over a region (Bordi *et al.*, 2009); it may also be described by temperature and evapotranspiration. It can develop quickly and end abruptly. The high temporal and spatial variability of precipitation and insufficient observation stations can pose analytical challenges.

Meteorological indices include percentile ranking methods (e.g. quartiles and deciles; Gibbs and Maher., 1967), percent of normal precipitation, consecutive dry days (CDD), Rainfall Anomaly Index (RAI; van Rooy, 1965), Effective Drought Index (EDI; Byun and Wilhite, 1999), and Standardized Precipitation Index (SPI; see Section 4.2.2) (Mckee *et al.*, 1993).

2.2.4 Agricultural Drought

Agricultural drought is often characterised by insufficient moisture in the surface soil layers to support crop and forage growth (Das, 2003), even with saturated deeper soil layers, through its control on transpiration and thus vegetative vigor (Sheffield and Wood,

2008a), without referring to surface water resources. Factors that cause meteorological (Section 2.2.3) and hydrological (Section 2.2.5) drought events, differences between actual and potential evapotranspiration (PET), plant biology and physics, and soil properties (e.g. water-holding capacity), all influence soil moisture, which is determined by the fluxes of precipitation, evapotranspiration and runoff (Sheffield and Wood, 2008a). However, precipitation amounts do not directly relate to soil infiltration.

Agricultural drought indices often combine precipitation, temperature and soil moisture to measure soil moisture and crop yield. Numerous indices exist (Hayes *et al.*, 2011), including a soil moisture index, normalised difference vegetation index (NDVI), water balance, heat stress, Palmer Moisture Anomaly Index (Z-index, which also measures meteorological drought; Palmer, 1965), Crop Moisture Index (CMI; Palmer, 1968), Soil Moisture Anomaly Index (Bergman *et al.*, 1988), and Palmer Drought Severity Index (PDSI; Palmer, 1965).

The PDSI has been widely applied especially in the U.S. (Soulé, 1992; Kangas and Brown, 2007; Gutzler and Robbins, 2011), but also in Europe (Briffa *et al.*, 1994; Lloyd-Hughes and Saunders, 2002; Dubrovsky *et al.*, 2008; van der Schrier *et al.*, 2010; Sousa *et al.*, 2011) and China (Zou *et al.*, 2005; Li *et al.*, 2007a; Fang *et al.*, 2009; Lei and Duan, 2011), and more recently, globally (Dai *et al.*, 2004; Burke *et al.*, 2006; Sheffield *et al.*, 2012). Alley (1984), Karl (1986) and Heddinghaus and Sabol (1991) discussed its limitations and assumptions. PDSI, although originally developed to monitor long-term meteorological events, is a soil moisture algorithm calibrated for relatively homogeneous regions, and has been extensively used to describe agricultural droughts (Panu and Sharma, 2002). Although the traditional PDSI excludes snow accumulation and subsequent runoff, van der Schrier *et al.* (2013) produced a new global dataset of monthly self-calibrating Palmer Drought Severity Index (scPDSI) that accounts for seasonal snowpack dynamics in the water balance model for 1901–2009.

2.2.5 Hydrological Drought

Surface waters (e.g. lakes and streams) are used for many purposes, including hydropower, irrigation and drinking water supply (Hisdal and Tallaksen, 2003). Hydrological drought is generally defined as a period of inadequate surface and subsurface water

supplies for use of a given water resource management system (Bordi *et al.*, 2009). Potential triggers include precipitation and/or soil moisture deficits (Andreadis *et al.*, 2005) (possibly due to more intense but less frequent precipitation), storage conditions, high evaporative losses (Hisdal and Tallaksen, 2003), poor water management and erosion. It usually lags behind meteorological and agricultural events (Hisdal and Tallaksen, 2003), develops slowly as it involves stored water that is depleted but not replenished (Dai, 2011), and persists longer (Steinemann *et al.*, 2005). Although surface and subsurface components recover slowly due to the long recharge periods, runoff may recover in response to precipitation more quickly than soil moisture (Andreadis *et al.*, 2005).

Hydrological droughts may be reflected by total water deficit or cumulative streamflow anomaly based on streamflow, reservoir and lake levels. Other indicators include the surface water supply index (SWSI), Palmer Hydrological Drought Severity Index (PHDI), Reclamation Drought Index (RDI; Weghorst, 1996), aggregate dryness index (ADI) that considers all meteorological, hydrological and agricultural aspects (Keyantash and Dracup, 2004), normalized ADI (NADI), low-flows (Smakhtin, 2001), and streamflow drought index (SDI; Nalbantis and Tsakiris, 2008). A new "composite index" based on streamflow, precipitation, reservoir levels, snowpack, and groundwater levels has been recommended (Hayes *et al.*, 2011). van Huijgevoort *et al.* (2012) presented a method that combines characteristics of the classical variable threshold-level method, and CDDs, which consistently identifies global-scale drought across climate regimes.

2.2.6 Groundwater Drought

Surface water drought may progress to groundwater drought, which is less extensively studied than other drought categories, particularly its spatial distribution (Peters *et al.*, 2005; 2006; Mishra and Singh, 2010). It occurs when groundwater levels, storage and discharge decline with some combination of low precipitation, high evapotranspiration, low soil moisture content and thus reduce groundwater recharge. The propagation of groundwater drought from recharge to discharge and the influence of aquifer characteristics on the propagation has been studied by (Eltahir and Yeh, 1999; Peters *et al.*, 2003; Peters and van Lanen, 2003). Abstraction and overexploitation may create/enhance a groundwater drought.

Mendicino *et al.* (2008) derived the Groundwater Resource Index (GRI) from a simple distributed water balance model for monitoring and forecasting. van Lanen and Peters (2002) identified natural groundwater droughts (recharge deficits) by applying transient recharge models and reservoir theory (Sequent Peak Algorithm). Peters *et al.* (2005) evaluated groundwater recharge and discharge for three reservoir coefficient values with respect to droughts. They used reliability, resilience and vulnerability, and a combination of these three indicators (Loucks' sustainability index), along with three newly-defined overall performance indicators that combine drought severity and frequency.

2.2.7 Socio-economic Drought

Socio-economic drought characterises the supply and demand of some precipitation-dependent commodity or economic good (e.g. water, livestock forage or hydroelectric power) that may affect society's productive and consumptive activities (Dracup *et al.*, 1980). Supply depends on precipitation or water availability that fluctuates annually. Demand is a function of human use and often correlates positively with increasing population and development. Temporal and spatial scales of supply and demand should be considered when defining a socio-economic drought. Water stress indicators include annual withdrawals-to-availability ratio, the consumption-to-Q90 ratio, and per capita water availability (Alcamo *et al.*, 2007b). It is worth noting that demand for freshwater resources could change over time even with an unchanged climate. For instance, demand could increase with an increase in development, or the construction of reservoirs could enhance resilience to future climate change.

2.2.8 Discussion

The choice of drought index determines the spatial patterns of drought characteristics (Soulé, 1992). The wide range of drought definitions discussed in this subsection implies that one or more indices may be consulted as each has its own advantages and weaknesses (Bonacci, 1993; Hayes *et al.*, 2007). Drought definitions thus need to be region- and application- or impact-specific (WMO, 2006), with the appropriate timescales chosen (Kangas and Brown, 2007). Nonetheless, few definitions adequately address drought impacts (Wilhite and Glantz, 1985).

PET is an input to the PDSI and is an important consideration in hydrologic modelling or water resource management studies; the uncertainty of which was also highlighted by Miller *et al.* (2011). PET is commonly estimated with Thornthwaite (Thornthwaite, 1948) and Penman-Monteith parameterisations (Allen *et al.*, 1994a;b). van der Schrier *et al.* (2011) found little difference in global scPDSI values computed using these two approaches due to the calculations in the simple water balance model of the PDSI algorithm. However, output from the global hydrological model, Mac-PDM.09, is sensitive to the PET calculation method (Penman-Monteith or Priestley-Taylor; Gosling and Arnell, 2011).

2.3 Past Changes in Drought

This subsection presents an overview of the historic changes in drought globally.

While long-term global drought trends are complex and there are no emergent coherent patterns of behaviour (IPCC, 2012), there have been regional-scale spatial and temporal variations (Easterling *et al.*, 2000). During the last 500–1000 years, North America, West Africa (Shanahan *et al.*, 2009), and East Asia have experienced multi-year to multi-decade dry periods (Dai, 2011).

Globally, the maximum number of CDD has generally reduced, except for parts of South Africa, Canada and eastern Asia (Frich *et al.*, 2002). Areas affected by severe drought increased slightly over 1900–1995 (Dore, 2005). PDSI trends revealed drying along the Guinea Coast, southern Africa, parts of Canada, and southern and central Europe during 1900–1949 (Dai *et al.*, 2004).

Global very dry (PDSI<-3.0) areas decreased by 7% over 1950–1972, but have increased by 12–30% since 1970s, particularly in early 1980s with an ENSO-induced precipitation decline and surface warming (Dai *et al.*, 2004; Dai, 2011). Since the mid-20th century, increased wetness occurred over the central U.S., Argentina and northern high-latitude areas whereas most of Africa, southern Europe, southeast Asia, and eastern Australia, (Dai *et al.*, 2004; Dai, 2011; 2013; as shown in Figure 2.2) with more frequent and intense drought (Dore, 2005). The U.S. and Europe had both increases in the percentage of areas with severe drought or moisture surplus (Huntington, 2006). Less frequent/intense, or shorter droughts have occurred in central North America and northwestern Australia

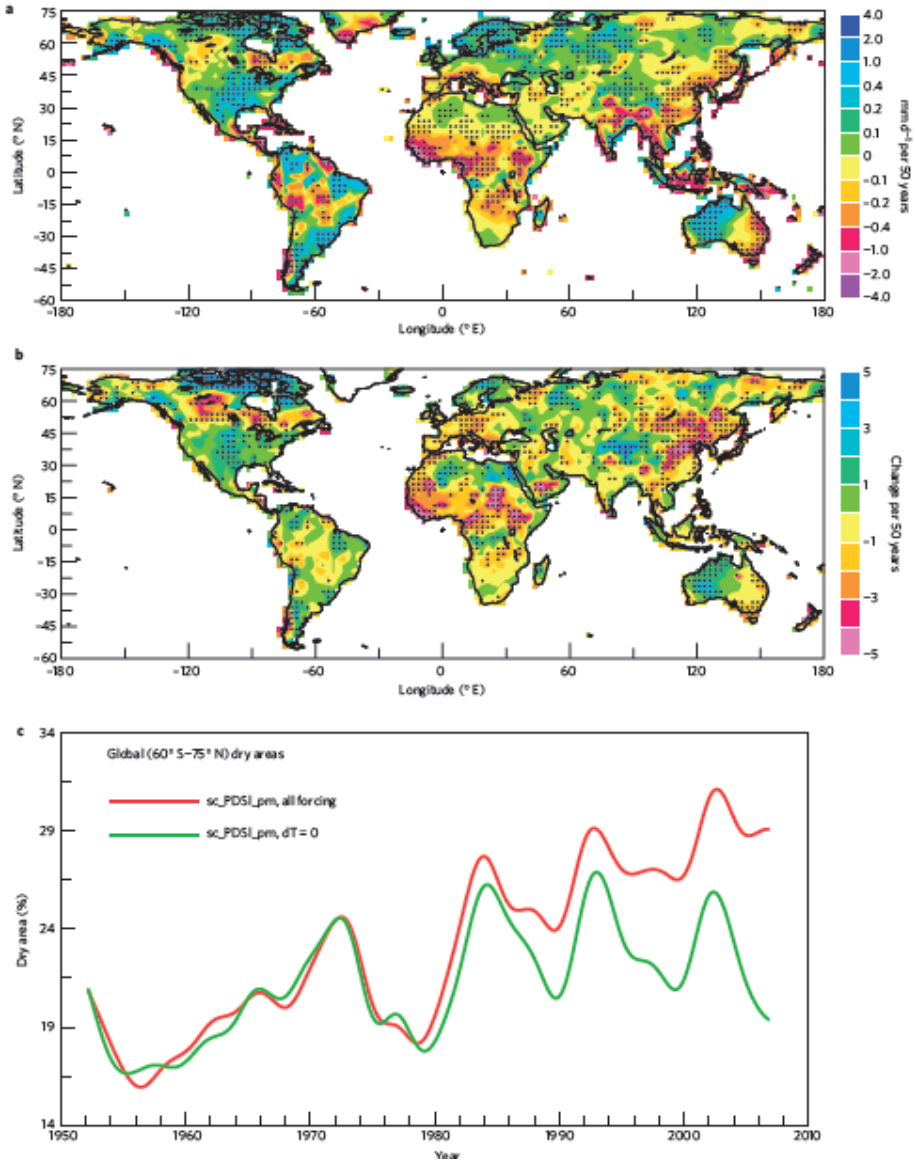

Figure 2.2: Trend maps for precipitation and scPDSI [scPDSI with PET estimated using the Penman–Monteith equation] and time series of percentage dry areas. Long-term trends from 1950 to 2010 in annual mean **a**, observed precipitation and **b**, calculated scPDSI using observation-based forcing. The stippling indicates the trend is statistically significant at the 5% level, with the effective degree of freedom computed. Note a change of 0.5 in the scPDSI is significant in the sense that a value of PDSI between –0.5 to –1.0, –1.0 to –2.0, –2.0 to –3.0 and –3.0 to –4.0 indicates, respectively, a dry spell, mild drought, moderate drought and severe drought. **c**, Smoothed time series of the drought area as a percentage of global land areas based on the scPDSI computed with (red line) and without (green line) the observed surface warming. The drought areas are defined locally as the cases when scPDSI is below the value of the twentieth percentile of the 1950–1979 period (results are similar for drought defined as PDSI<-2.0 and for using a longer base period from 1948 to 2010). Source: Figure 1 in Dai (2013).

(IPCC, 2012). For global soil moisture, although increasing precipitation over 1950–2000 has reduced drought extent by 0.021–0.035% yr^{-1}, high northern latitudes in particular, have dried with warming since the 1970s; West Africa has dried substantially with lower Sahel precipitation (Sheffield and Wood, 2008a).

However, after accounting for changes in available energy, humidity and wind speed, Sheffield *et al.* (2012) found little change in global drought since 1950, and that previously reported increases were overestimated due to the simple representation of PET in PDSI that responds only to perturbed temperature. Based on a new global scPDSI dataset calculated for 1901–2009, although van der Schrier *et al.* (2013) found more widespread drought in some regions such as the Mediterranean due to increasing temperature and PET, they did not find evidence for unusually strong or widespread drying. They also found that the selection of a calibration period of the scPDSI (rather than the formulation of PET) to be the cause for the differences in global drying trends in the literature. Moreover, robustness in the observed trends can be constrained by data inhomogeneities and relative sparseness of station density (Moberg *et al.*, 2006). There are also considerable regional variations in the reconstructed 20th-century runoff trends (Labat *et al.*, 2004).

These studies have reported spatial and temporal variations in the drying and drought trends. Such differences may be associated with the different datasets used for drought analysis, e.g. Dai *et al.* (2004) used observed/historical precipitation and temperature datasets, whereas Sheffield and Wood (2008a) used soil moisture simulation from the Variable Infiltration Capacity (VIC) land surface hydrological model driven by a hybrid dataset of precipitation, near-surface meteorological and radiation data derived from the National Centers for Environmental Prediction–National Center for Atmospheric Research (NCEP–NCAR) reanalysis and a suite of global observation-based products. Also, the different definitions and methodologies applied for drought quantification and computation (e.g. in the calculation of PDSI) can also contribute to some of the inconsistencies in the trends. Despite the variations in the trends found in different studies, drying and/or worsening drought conditions have consistently been found in southern Europe.

2.3.1 Europe

This subsection focuses mainly on the historic trends in precipitation/drought found for Europe, which has been used as the study region in this thesis (see Section 3.9).

Over the 20th century, while drought (SPI<-1) area coverage increased (Bordi *et al.*, 2009), the area affected by extreme and/or moderate droughts (according to both SPI and PDSI; Lloyd-Hughes and Saunders, 2002) and summer moisture availability (van der Schrier *et al.*, 2010) revealed insignificant changes; widespread and unusual drying over the last few decades is also not evident (van der Schrier *et al.*, 2010).

Between 1976–2000 and 1951–1975, much of the European region experienced reduced summer precipitation while the opposite trend occurred over Western Russia and Finland (Pal *et al.*, 2004). Trends of precipitation and scPDSI for the 20th century indicate a drying trend across much of the western and central Mediterranean (Sousa *et al.*, 2011). For England and Wales, while 12-month drought (based on rainfall deficiencies) frequency reveals no clear trend during 1800–2006, summer drought severity increased with 20th-century warming (Marsh *et al.*, 2007). Central eastern Europe and western Russia experienced significant drying (based on trends in SPI and PDSI values), with trends being strongest in winter/spring and weakest in summer/autumn (Lloyd-Hughes and Saunders, 2002). Extreme droughts (PDSI≤-4) became more frequent within the interior of continental Europe, and less frequent along the northwest European and Mediterranean coast, and the Alps (Lloyd-Hughes and Saunders, 2002). It is worth noting that the chosen calibration period of the PDSI can influence the interpretation of the index values based on Palmer's classification (van der Schrier *et al.*, 2013).

For Europe as a whole, long-term trends in streamflow drought are generally inconclusive (Hisdal *et al.*, 2001), and hydrological (represented by SPI24) drought area coverage varies with the time section considered due to the high spatial variability (Bordi *et al.*, 2009). However, distinct regional differences have been found. Since the 1960s, low flows reduced; annual streamflow generally decreased (increased) in southern and eastern regions (across Europe) and in summer (winter) (Stahl *et al.*, 2010). During 1962–1990, drought deficit volumes increased in Spain and eastern part of Eastern Europe, but decreased in much of Central Europe and western part of Eastern Europe; results for the UK are mixed, with more severe droughts in areas with limited storage capacity (e.g. Wales

and southwest England), and less severe droughts in areas that have large aquifers (e.g. southeast England). These trends are related to seasonal precipitation deviations or artificial influences in the catchments (Hisdal *et al.*, 2001). More severe summer streamflow droughts occurred in southern and eastern Norway due to altered snowmelt hydrology (Wilson *et al.*, 2010). Extended drought periods (that affected $\geq$40% of grid cells) occurred in autumn 1975 to late summer 1976, and spring/summer of 1990 (Tallaksen *et al.*, 2011).

Summer moisture availability increased from end of 17th century to beginning of 19th century; continuous drying has since occurred (Briffa *et al.*, 2009). The mid-1940s to early 1950s was a persistent and exceptionally dry period (van der Schrier *et al.*, 2010). Widespread summer drought in the last two decades with anomalous warming, particularly in central Europe (Briffa *et al.*, 2009).

2.4 Projected Changes in Drought

This subsection presents an overview of the projected changes in drought under future climates globally.

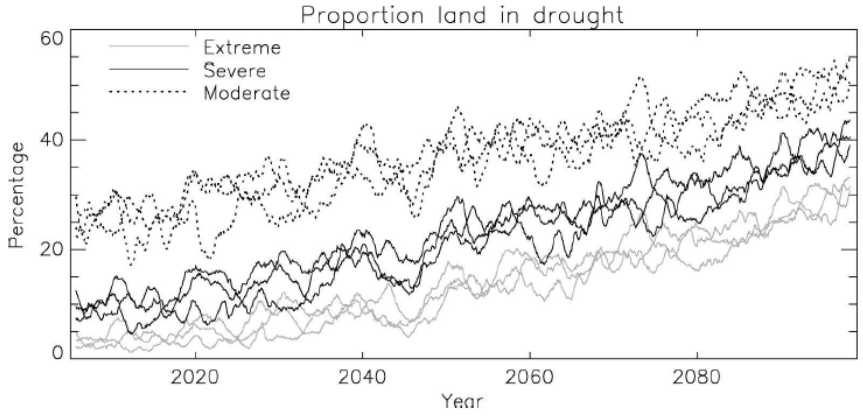

Figure 2.3: The proportion of the land surface in drought each month. Drought is defined as extreme, severe, or moderate, which represents 1%, 5%, and 20%, respectively, of the land surface in drought under present-day conditions. In each case results from the three simulations made using the A2 emissions scenario are shown. Source: Figure 9 in Burke *et al.* (2006).

Compared to high precipitation extremes, projected trends for global dry events appear weaker and less consistent (Planton *et al.*, 2008). Due to the range of definitions that correspond to different classifications of drought and inconsistencies in the model projections when based on different dryness indices (e.g. short- vs. long-term events), there is

medium confidence in future drought projections IPCC (2012). Despite the considerable regional variations, studies generally suggest a net overall global drying trend is projected over the 21st century. Over the 21st century, dry day frequency increases under A2 and A1B emission scenarios but varies little under B1 (Tebaldi *et al.*, 2006). The area of land surface in extreme drought increases from 1–30% (present-day) to 30–50% (by 2100) under A2 scenario, with slightly less frequent but much longer events (Burke *et al.*, 2006; Bates *et al.*, 2008; as shown in Figure 2.3). Using a drought risk index (based on a revised PDSI) that accounts for the effects of drought-disaster frequency, drought severity, production (yield) and extent of irrigation, results from 20 GCMs indicate that global drought disaster-affected area increases from 15% (present-day) to 44% (2100) (Li *et al.*, 2009).

The frequency of dry days are projected to increase (decrease) in sub-tropical latitudes of northern and southern hemispheres (high-latitude northern hemisphere), according to nine GCMs (Tebaldi *et al.*, 2006). Future droughts (on the annual timescale and based on both soil moisture anomalies and CDD) intensify in southern and central Europe, central North America, Central America and Mexico, northeast Brazil, and southern Africa (during December-January-February; Lyon, 2009) (IPCC, 2012). Decadal-mean scPDSI calculated using the ensemble-means from 22 GCMs suggest increasing aridity between the 1950s and 2090s over most of Africa, southern Europe and the Middle East, most of the Americas, Australia, and Southeast Asia; persistent droughts may also occur in the U.S. in the first half of the 21st century Dai (2011). Continental summer drying and droughts are likely with reduced precipitation, higher temperature and evaporation (Meehl *et al.*, 2000), especially in the sub-tropics (Shindell, 2007), low- and mid-latitudes (Bates *et al.*, 2008). In southern Europe and central North America, dry soil, frequency of low precipitation and long dry spells (due to fewer daily rainfall events, rather than lower mean precipitation) in summer could increase (Gregory *et al.*, 1997).

According to 21 GCMs under SRES A1B scenario, by 2100, soil moisture is projected to decline globally, causing droughts in tropics and subtropics, including southwest North America, Central America, the Mediterranean, Australia, much of the Amazon and South and West Africa in June-July-August and the Asian monsoon (in winter) region (Wang, 2005). The frequency of long-term soil moisture droughts is projected to triple, and the spatial extent of severe soil moisture deficits and frequency of short-term

(4–6-month) droughts double based on eight GCMs, with lower precipitation, higher temperatures and evaporation; greater evaporation may offset precipitation increases in some regions (Sheffield and Wood, 2008b).

Considerable streamflow variations are expected by 2100 (Todd *et al.*, 2011). Annual mean precipitation, evaporation, and runoff (by 10–30%; Milly *et al.*, 2005) decrease in mid-latitudes and sub-tropics (Arnell, 1999b), e.g. southern Europe, southern Africa and mid-latitude western North America (Nohara *et al.*, 2006). River discharge simulated by a land surface sub-module (MATSIRO) of the MIROC GCM indicate that North and South America, central and southern Africa, the Middle East, central to western Australia, and Indochina to southern China to experience significantly more frequent drought days by 2070–2100 (Hirabayashi *et al.*, 2008). Frequency of flow below the current 10-year return period minimum annual runoff, simulated by an enhanced version of the Macro-PDM hydrological model, is projected to be three (two) times more frequent in Europe and southern Africa (North America) by the 2050s (Arnell, 2003a).

Results from these studies have revealed the range of projected future changes in dryness/drought. Some of the inconsistencies may be attributed to the use of different variables (e.g. precipitation, soil moisture, streamflow), drought definitions and parameters (e.g. dry day frequency, proportion of land being drought-affected, the use of percentile), the different timescales and periods studied (e.g. seasonal, annual), as well as the various emission scenarios and climate/hydrological models applied. Despite the difficulties in inter-comparing drought projections from different analysis, positive trends in dryness and/or drought conditions are commonly projected for southern Europe. The projected future *European* drought characteristics from other studies are compared with the results obtained in this thesis, which are presented in Chapters 4 and 5.

2.5 Causes of Drought and its Characteristics

Meteorological droughts are mainly driven by precipitation and available energy; perturbations in the mean and/or the variability of either, or both, of these drivers can alter drought patterns (Burke, 2011). For instance, decreasing mean precipitation, increasing standard deviation of precipitation, increasing mean available energy and decreasing standard deviation of available energy tend to increase drought (Burke, 2011). On longer

timescales, runoff is roughly equal to the difference between land precipitation and evapotranspiration; hydrological droughts occur with a decline in precipitation and/or an increase in evapotranspiration, which depends on energy and water availability, near-surface atmospheric conditions and the control of transpiration by plants (Gedney *et al.*, 2006). The interactions between perturbations in precipitation, temperature and hydrologic processes through their frequency, intensity and seasonality (especially in snow-dominated regions) makes it difficult to assess the relative importance of temperature and precipitation in changes in drought events (Sheffield and Wood, 2008b), e.g. the recent drought in western North America, particularly the Southwest (Overpeck and Udall, 2010).

Global warming can alter future PET, an increase of which may induce soil moisture deficits and vegetation desiccation (Rind *et al.*, 1990). Drought intensification has been understated in most GCM simulations, due to their lack of realistic land surface components (Rind *et al.*, 1990). However, a detailed parameterisation of land evapotranspiration in mesoscale or global climate models is challenging (Dickinson, 2013). The various methods for PET estimation (e.g. Thornthwaite, Blaney-Criddle, Hargreaves, Samani-Hargreaves, Jensen-Haise, Priestley-Taylor, Penman, and Penman-Monteith) implies that the characterisation of the PET climate change signal is an important source of uncertainty, particularly in regions where precipitation is closely in balance with PET (Kingston *et al.*, 2009). The sensitivity of PET to climate changes depends on both data requirements and calculation method; it can also vary by location and by time of year (McKenney and Rosenberg, 1993). In addition to temperature, changes in humidity, solar radiation, wind speed and vegetation can offset or intensify the effects of warming on PET (McKenney and Rosenberg, 1993). Although Kingston *et al.* (2009) found a consistent global increase in PET with a 2°C global warming according to six different calculation methods, the magnitude of the PET climate change signal differ substantially; for certain regions and GCMs, choice of PET method determines the direction of projections of future water availability. Similarly, Lu *et al.* (2005) found significantly different PET values calculated from six different methods across 36 forested watersheds in the southeastern U.S. Moreover, runoff simulated by hydrological models (such as Mac-PDM.09; Gosling and Arnell, 2011) may be highly sensitive to the choice of PET calculation method.

While PET generally increases with temperature, actual evaporation may be amplified/alleviated with higher/lower precipitation (Sheffield and Wood, 2008b). For example, fluctuations in the Yellow River flow tend to be influenced by temperature (precipitation) changes in the long- (short-) term (Liang *et al.*, 2010). For some vegetation covers, the relationship between actual and potential evapotranspiration may be sensitive to the changing atmospheric CO_2 levels Lockwood (1999). Some of the processes/influences that can lead to the perturbations in these climatic/hydrological variables, which can subsequently modify the characteristics of droughts are discussed below.

2.5.1 Natural Causes of Drought

Global-scale atmospheric circulation changes can alter large-scale pattern of precipitation, temperature and cloudiness (Dai, 2011). Atmospheric circulation patterns that affect precipitation (which has a notable seasonality) are easier to distinguish than those responsible for spatial variations of drought, which tend to be more continuous (Vicente-Serrano, 2006). Changes in annual/heavy precipitation, or differences between precipitation and evapotranspiration cannot simply explain drought and flood changes, e.g. in some regions, both drought and flood frequencies increase with less frequent precipitation days but more frequent heavy precipitation days (Hirabayashi *et al.*, 2008).

Teleconnection-drought relationships have been observed (Bates *et al.*, 2008). These include inter-decadal and multi-decadal climate variability (Dore, 2005) and anomalous tropical sea surface temperatures (SSTs) (Hoerling and Kumar, 2003; Dai, 2011) that, for example, could weaken the East Asian summer monsoon (EASM) (Li *et al.*, 2010). Some of the effects of El Niño Southern Oscillation (ENSO), North Atlantic Oscillation (NAO) and other phenomenona are briefly described below.

ENSO is one of the major modes of climate variability. Since the late 1970s, a shift in ENSO towards more warm events, which corresponded with record high global-mean temperatures, has altered severely drought-affected areas (Dore, 2005). More (less) short-term droughts have coincided with El Niño (La Niña) episodes (Sheffield *et al.*, 2009). El-Niño-like conditions promote drought in Australia, Indonesia (Salinger, 2005), East China and South Africa (Herweijer *et al.*, 2007; Collier *et al.*, 2008; Lyon, 2009; Dai, 2011). La Niña-like conditions promote drought in North America (Schubert *et al.*, 2009), e.g.

Colorado River Basin during fall and winter (Ellis *et al.*, 2009); in the Yellow River Basin, average annual precipitation (and also streamflow) in La Niña years is 18.8% higher than in El Niño years (Fu *et al.*, 2007c).

NAO (Greatbatch, 2000) has made a significant contribution to high inter-decadal variability on precipitation and streamflow in Europe (Trigo *et al.*, 2004). Since the 1950s, the effects of positive (negative) NAO phases on droughts have strengthened (weakened) due to perturbed wintertime sea-level pressure fields, producing more (less) drought conditions in southern (northern) Europe (López-Moreno and Vicente-Serrano, 2008). The winter NAO pattern has significant implications for European climate (Hurrell, 1995) and water resources throughout the year (López-Moreno and Vicente-Serrano, 2008), e.g. the interannual flow variability in Spain and Portugal may affect hydroelectric production (Trigo *et al.*, 2004). As the western and central Mediterranean have precipitation maxima during winter (and to a lesser extent, Fennoscandia and the Baltic states during late summer), fluctuations in precipitation totals between positive and negative phases can significantly influence drought conditions during the succeeding months (López-Moreno and Vicente-Serrano, 2008). Along with the NAO, the Scandinavian Pattern (between winter and summer) influence Western and central Mediterranean (not Turkey) (Sousa *et al.*, 2011). The NAO also regulates Middle Eastern interannual to decadal rainfall-driven runoff (December–March) through local precipitation and temperature (Cullen *et al.*, 2002). Although the Alps exhibits the strongest European interannual variability of winter precipitation, this is only weakly correlated with the Northern Annular Mode (NAM) and the NAO (Bartolini *et al.*, 2009).

However, drought response to the positive and negative phases of NAO across Europe is asymmetrical, e.g. it varies spatially, and with the month, decade and timescale of the analysis (López-Moreno and Vicente-Serrano, 2008). The positive (negative) phase correlates with negative (positive) SPI values in central and southern Europe (northern Europe and the UK), producing winter/spring soil moisture droughts and summer/autumn hydrological droughts (López-Moreno and Vicente-Serrano, 2008). For instance, persistent meteorological and hydrological drought conditions in the 1980s and 1990s in southern Romania coincided with the positive phase (Stefan *et al.*, 2004).

Regional climate patterns may not only vary with ENSO and NAO, as discussed

above, but can also be affected by the interactions between different modes of climate variability. For instance, according to European dendroclimatic precipitation reconstruction, interaction between ENSO and NAO may have produced a multi-centennial medieval megadrought during the Medieval Climate Anomaly, and significant drying in northern Europe (Helama *et al.*, 2009). Risk for severe and synchronised mid-latitude drying increases if tropical mean SSTs or their interannual variability increase the equatorial ocean's west-east contrast, e.g. the 1998–2002 droughts spanning the U.S., southern Europe, and Southwest/Central Asia (Hoerling and Kumar, 2003). Drought conditions increase in the U.S. and southern South America with a cold equatorial Pacific anomaly, and in southern Central America, northern South America, and central Africa with a cold Atlantic anomaly; these are reversed by warm Pacific and Atlantic anomalies (Findell and Delworth, 2010). The Sahel droughts occurred as the warmest Atlantic SSTs migrated southward and the Indian Ocean warmed (Dai, 2011). ENSO, Pacific Decadal Oscillation (PDO), and NAM drove the North American (e.g. the Great Plain; Hu and Huang, 2009) droughts (Gutowski *et al.*, 2008). Variations in the Southern Annular Mode (SAM) and ENSO may perturb regional synoptic patterns and affect Victorian climate, Australia (Kiem and Verdon-Kidd, 2010). The NAO (and ENSO) determine southern European climate (Rodó *et al.*, 1997).

2.5.2 Anthropogenic Influences

Although natural causes have contributed to some of the recent regional trends in dryness or drought, anthropogenic influences may have exacerbated or dampened these trends (Sheffield and Wood, 2008a). Climate change will redistribute precipitation globally (Dore, 2005). Human-induced rapid warming since the 1970s has increased atmospheric moisture demand and likely altered atmospheric circulation patterns (Schär and Jendritzky, 2004; Dai, 2011). According to the Clausius-Clapeyron relation (Held and Soden, 2000), warming implies higher atmospheric moisture-holding capacity, and where available, more water vapour for the precipitating weather systems (Alexander

et al., 2006). The decreasing ratio between precipitation and precipitable water (Douville *et al.*, 2002) suggests an enhanced global hydrological cycle (Dore, 2005; Huntington, 2006). On a global scale, this could be a result of strengthened horizontal moisture transports, assuming that atmospheric circulation remains constant (Held and Soden, 2006). This occurs as more moisture (with increased atmospheric water vapour concentrations) is transported from areas where evaporation exceeds precipitation ($P-E<0$; e.g. in the sub-tropical oceans) to areas where precipitation exceeds evaporation ($P-E>0$; e.g. the higher latitudes) (Hegerl *et al.*, 2013). Therefore, drying intensifies in areas where $P-E<0$ and wetting amplifies in areas where $P-E>0$. Although an increase in precipitable water may increase precipitation initially, greater convection would warm the mid-upper troposphere due to the condensation of water vapour. If the net radiative cooling of the troposphere does not increase, the rate of convection would slow as it stabilises. Assuming that relative humidity changes little in the long term (Allen and Ingram, 2002), this process could limit global precipitation under increased warming (Hegerl *et al.*, 2013). Note that Simmons *et al.* (2010) found a reduction in relative humidity over low-latitude and mid-latitude land areas around the first decade of the 21st century, which would further limit an increase of global precipitation.

An enhanced global hydrological cycle, together with higher atmospheric demand for evapotranspiration — which may be dampened (enhanced) by higher (lower) precipitation or atmospheric humidity — especially during warmer seasons (Sheffield and Wood, 2008b; Weiss *et al.*, 2009), suggest enhanced drought conditions (Sheffield and Wood, 2008a; Vasiliades *et al.*, 2009) as the interannual variability of precipitation minus evaporation becomes stronger (Seager *et al.*, 2012). For example, global warming may have intensified the Australian Murray-Darling Basin drought severity and impacts through enhanced evaporation and evapotranspiration (Nicholls, 2004); however, the 2000–2007 nation-wide episodes may not be human-induced as they have a return period of 200–300 years (Hunt, 2009).

Human-induced changes in global land precipitation could be a result of GHG and black carbon/sulphate aerosols emissions (Frieler *et al.*, 2011), which have led to the global drying trend since 1952 (Burke *et al.*, 2006). For instance, the Asian monsoons are affected by black carbon/sulphate aerosols (Xu, 2001; Cheng *et al.*, 2005; Lau *et al.*, 2006;

Lau and Kim, 2006; Li *et al.*, 2007b; Ramanathan and Feng, 2009; Kuhlmann and Quaas, 2010). These, together with land use changes, have weakened the East Asian summer and winter monsoon, producing droughts in North China (Ding *et al.*, 2007; Liu *et al.*, 2009). Since 1960, the second aerosol indirect effect (i.e. more numerous and smaller cloud droplets reduce precipitation efficiency), higher SSTs in the South China Sea and Indian Ocean, and GHGs have altered low-level cloud cover (LCC) and reduced early summer precipitation in the drought region of Southern China (Cheng *et al.*, 2005; Shen *et al.*, 2008).

Anthropogenic influences can also alter both runoff volume and distribution. Relatively small temperature/precipitation changes can have large impacts on runoff (Frederick and Major, 1997). Although the geographical distribution of precipitation and runoff variations tend to correspond with that in the river discharge, upstream runoff changes influence downstream flows (Nohara *et al.*, 2006). Temperature strongly affects the seasonal distribution of snow-related runoff and hydrologic variables (Adam *et al.*, 2009), even with unchanged precipitation amount, particularly in lower lying valley areas and low-altitude mountain ranges where baseline climate is closer to freezing thresholds (Bureau of Reclamation, 2011). Decreased fraction of annual precipitation falling as snow have been found in recent decades in the Norwegian Arctic (Svalbard region), despite the increased measured annual precipitation (Forland and Hanssen-Bauer, 2003). This suggests that warming could lead to more rainfall due to the more efficient rainfall processes compared to snow falling. If more precipitation falls as rain than snow, temporary storage of precipitation as snow and ice will reduce (Feyen and Dankers, 2009; Todd *et al.*, 2011), minimum cool-season rainfall-runoff and probability of floods increase, e.g. in Norway (Roald *et al.*, 2004; Engen-Skaugen *et al.*, 2005; Roald *et al.*, 2006; Beldring *et al.*, 2008) and Denmark (Thodsen, 2007), together with an earlier and less intense spring peak in flow. Retreating glacierised areas (e.g. European glaciers of <3 km^2 could halve in area by 2050; Huss, 2011) implies lower warm-season snowmelt-runoff and annual minimum flows occur later in summer/autumn (Hisdal and Tallaksen, 2000; Chang *et al.*, 2002; Eckhardt and Ulbrich, 2003; Jasper *et al.*, 2004; Barnett *et al.*, 2005; van Lanen *et al.*, 2007; Laghari *et al.*, 2012). However, interannual runoff variability can increase even with unchanged interannual precipitation variability, for instance, in areas where flow volumes

are determined by groundwater recharge (Arnell, 2003a).

Although climate change can alter the volume and timing of streamflows and groundwater storage, its influence on exposure to water-related hazards, access to and future water resource availability also depends on demographic and socio-economic factors (Arnell, 2006). Population and economic growth, freshwater and groundwater withdrawals (Frederick and Major, 1997) may induce, enhance or prolong drought, e.g. the 1930s North American Dust Bowl drought (Dai, 2011). Without climate change, changes in population alone suggests 36–40% of the world's population (2.9–3.3 billion people) living in water-stressed watersheds by 2025, and 3.4–5.6 billion people by 2055 (Arnell, 2004a). While natural multi-decadal climate variability primarily drives average annual runoff in the 2020s, and population growth is primarily responsible for water stress under a 2°C warming; climate change becomes more dominant in a 4°C world and/or by the 2080s (Arnell, 2003a; Fung *et al.*, 2011).

Warming can enhance water stress in river basins (Fung *et al.*, 2011). This could affect a bigger population; perturbations in precipitation could also alter the number of people living in water-stressed watersheds, e.g. in the Mediterranean, parts of Europe, central and southern America, and southern Africa (Arnell, 2004a). Alcamo *et al.* (2007b) projected water stress increases (decreases) over 62.0–75.8% (19.7–29.0%) of total river basin area by 2050s primarily due to greater domestic water-use with higher income and growing water withdrawals. In southern and eastern Asia, insufficient storage implies that increased wet season runoff may not be available for the dry season (Arnell, 2004a). Land use/land cover change (and snowmelt) may alter regional/local moisture recycling (van der Ent *et al.*, 2010); it has altered Australian droughts (McAlpine *et al.*, 2009) and Middle Eastern streamflow variability during April–June (Cullen *et al.*, 2002).

2.5.3 Summary

This subsection has discussed some of the natural and anthropogenic drivers that can alter precipitation, temperature and runoff characteristics, thus modifying drought conditions. Natural causes of drought include changes in atmospheric circulation and modes of climate variability (e.g. ENSO and NAO) — the characteristics of which may also be modified by human activities. Humans can also influence drought patterns through GHG

and black carbon/sulphate aerosols emissions, as well as changes in land use and land cover, population and socio-economic activities. However, it may be difficult to distinguish between the effects of climate change and human activities, for example, on runoff variations (Piao *et al.*, 2010). In addition, basin-scale effects of climate, soil and vegetation (i.e. suppressed plant transpiration due to CO_2-induced stomatal closure; Gedney *et al.*, 2006) may alter streamflow (Liu and Cui, 2011). Furthermore, droughts have been produced by past large, widespread, abrupt climate changes, which may be triggered by human influences (Alley *et al.*, 2003). Therefore, drought occurrence and changes in their characteristics can be a result of any combination of climatic and hydrological elements, land surface conditions, and anthropogenic activities.

2.6 Uncertainties in Climate Modelling

Despite advanced climate models and improved knowledge, considerable levels of uncertainty remain in climate change projections, particularly in relation to extreme events such as future drought characteristics (Vasiliades *et al.*, 2009). Uncertainties on large spatial and longer temporal scales may be estimated (Knutti, 2008). Uncertainties arise from future human activities and the associated response of the climate system. The former are represented by future GHG and aerosol emissions (Section 2.6.1); the latter are explored with different climate model parameters and structures (Sections 2.6.2–2.6.11) and include natural climate variability (Section 2.6.12) (Seneviratne *et al.*, 2012).

2.6.1 Forcing Uncertainty

Human activities have influenced 20th-century temperature (Stott, 2003) and precipitation trends (Zhang *et al.*, 2007). Forcing uncertainty arises from non-climate factors that affect the climate system (Stainforth *et al.*, 2007a), e.g. population changes (Arnell, 2004a). It is often examined by applying various scenarios of prescribed atmospheric GHG concentrations (Stainforth *et al.*, 2007a) that may contain assumptions about future world economic and social development, and political decisions. A range of emissions scenarios — notably the IPCC SRES (Nakicenovich and Swart, 2000) and Representative

Concentration Pathways (RCPs; Moss *et al.*, 2010) (see Section 3.4) — have been developed. The relative likelihood of these is difficult to determine (Christensen and Christensen, 2007; Tebaldi and Knutti, 2007; Knutti *et al.*, 2010). Temperature-related impacts tend to scale with the amount of anthropogenic emissions and the associated global-mean temperature change (Arnell, 2003a; Tebaldi *et al.*, 2006; Sheffield and Wood, 2008b; Chen and Sun, 2009; Vidal and Wade, 2009; Xu *et al.*, 2009).

2.6.2 Initial Condition Uncertainty (ICU)

ICU arises from the initialisation of models (the initial state, or ensemble of states) from which they are integrated forward in time (Stainforth *et al.*, 2007a). The incomplete knowledge of the current state of the system introduces macroscopic ICU, which affects the predicted state variable distributions that have relatively "large" slowly mixing scales; microscopic ICU is due to the imprecise knowledge of "small" rapidly mixing scales (Stainforth *et al.*, 2007a). While ICU may affect modelled climate distributions (Stainforth *et al.*, 2007a), it is the primary error source in weather forecasting (Collins and Allen, 2002). The initial ocean state provides the "memory" of the system, which may be useful on interannual timescales (e.g. the forecasting of ENSO; Collins and Allen, 2002), but it is less relevant for longer-term (decadal) climate projections and multi-model simulations (Tebaldi and Knutti, 2007; Knutti *et al.*, 2010).

2.6.3 Boundary Condition Uncertainty (BCU)

Boundary conditions are prescribed externally to the model, experiments of which are otherwise self-contained (Tebaldi and Knutti, 2007). External influences can cause climate change beyond the "noise" of climate variability (Collins and Allen, 2002). These can be natural (the solar cycle or volcano eruptions; see Section 2.6.12), which may not be predictable in a deterministic sense (Collins and Allen, 2002), or anthropogenic (GHG emissions; see Section 2.6.1).

2.6.4 Model Imperfections

Model imperfection results from our limited understanding of, and ability to simulate, the Earth's climate (Stainforth *et al.*, 2007a). Model imperfection takes two forms:

inadequacy and uncertainty.

2.6.4.1 Model Inadequacy

Even the most sophisticated models are unrealistic representations of many relevant aspects of the climate system (Stainforth *et al.*, 2007a). Model inadequacy (structural uncertainties) relate to grid resolution (therefore particularly relevant for regional simulations) and missing/approximated processes (Stainforth *et al.*, 2007a) that cannot be accurately described in the model (Knutti *et al.*, 2010). Different choices made by modeling groups (Meinshausen *et al.*, 2008) may be due to *limited knowledge* that includes incomplete understanding of deterministic processes, and limited resources to measure and obtain empirical information (see van Asselt and Rotmans, 2002). For example, the simulation of convection and its effect on the water vapour and cloud distribution within the atmosphere, feedbacks from vegetation change to climate change and land cover changes, aerosol (e.g. black carbon) effects on clouds and precipitation (Bates *et al.*, 2008; Knutti *et al.*, 2010) are often omitted or implicitly represented in climate models. In addition, climate models exclude some natural processes (e.g. vegetation dynamics and wildfire) and anthropogenic forcings (e.g. irrigation, water diversion and land use that directly affect drought occurrence), which are difficult to quantify, even historically (Sheffield and Wood, 2008b).

2.6.4.2 Model Uncertainty

Model (parameter) uncertainty represents the impact of known uncertainties (Stainforth *et al.*, 2007a). It is introduced during model calibration/tuning when estimating parameters based on either limited observations or physical understanding (Knutti, 2008; Meinshausen *et al.*, 2008; Knutti *et al.*, 2010).

Processes to be included in a model and their parameterisation (e.g. factors that affect albedo and subgrid-scale mixing in oceanic GCMs; CCSP, 2008) may be subjectively chosen based on expert knowledge and experience (Tebaldi and Knutti, 2007). Similar sets of primitive dynamical equations may be solved by different numerical algorithms (CCSP, 2008). Different parameterisations contribute to diverging model response due to different realisations of a given forcing scenario (Goodess *et al.*, 2003a; Déqué *et al.*,

2007), e.g. the grand ensemble of climate*prediction*.net (Stainforth *et al.*, 2004) reveals climate sensitivities that range from below 2 K to over 11 K (Stainforth *et al.*, 2005).

Perturbed physics ensembles (PPE) have been employed to address parameter uncertainties (Tebaldi and Knutti, 2007); however, they cannot characterise inter-model variability to the extent that a multi-model ensemble can (Foley, 2010).

2.6.5 Multi-Model Ensembles (MMEs)

Simplifications, assumptions and parameterisation choices made during model construction lead to model and projection errors (Tebaldi and Knutti, 2007). Thus, it is impossible to designate a "best model" when simulation skill for mean precipitation, for instance, varies both temporally and spatially (Blenkinsop and Fowler, 2007a). Since each simulation provides a projected distribution, a multi-model approach can present the range of behaviour in the variables of interest across different models (Stainforth *et al.*, 2005; 2007b), and enables sensitivity analysis of the models' structural choices (Knutti *et al.*, 2010). This may capture much of the uncertainty (CCSP, 2008), and multi-model mean implicitly imply improved skill, reliability and consistency of model projections (Tebaldi and Knutti, 2007; Knutti *et al.*, 2010). An ensemble of different models or model versions, MMEs (e.g. Stainforth *et al.*, 2005), refers to a set of model simulations from structurally different models where each model has one or more initial condition ensembles (Tebaldi and Knutti, 2007). A multi-model approach has been recommended (Haylock *et al.*, 2006; Blenkinsop and Fowler, 2007a; Feyen and Dankers, 2009; Lopez *et al.*, 2009; Valle *et al.*, 2009; Todd *et al.*, 2011; Wilby, 2010; Gudmundsson *et al.*, 2011; Zhang *et al.*, 2011), possibly due to the cancelling the offsetting errors in the individual GCMs (Pierce *et al.*, 2009) although the exact reason remains unclear (Reichler and Kim, 2008). Examples include a regional study that includes measures of variability (Pierce *et al.*, 2009), in reproducing observed European annual low flows (Gudmundsson *et al.*, 2012a), and in planning public water supply in the UK (Lopez *et al.*, 2009). Stainforth *et al.* (2007b) provided an analysis pathway for how climate model ensembles may inform decisions. MMEs, and their frequency distributions, are valuable for model development (Stainforth *et al.*, 2007a) as they reveal the amplitude of the uncertainties, hence areas for improving predictability (Déqué *et al.*, 2007; Knutti *et al.*, 2010).

MME mean (e.g. Gudmundsson *et al.*, 2012a) is often used and uncertainty is often represented by the standard deviation or some other measure of spread of individual model results; ensemble median may outperform ensemble mean (Corso-Perez *et al.*, 2011). Models can also be weighted; weighted averages may perform better if there is sufficient available information to derive the weights (Knutti *et al.*, 2010).

2.6.5.1 Probabilistic Assessments

Probabilistic climate change information is the estimation of a frequency/probability distribution, and thus is potentially more informative than a scenario-based impact assessment (New *et al.*, 2007) by providing quantitative "risk" profiles to inform decision making (Todd *et al.*, 2011). An example of this is the UK Climate Projections (UKCP09) (Murphy *et al.*, 2009). However, an end-to-end probabilistic assessment, such as the UKCP09, may be resource-intensive (New *et al.*, 2007). Probabilistic projections based on MMEs are derived from a variety of statistical methods (Tebaldi and Knutti, 2007) for quantifying uncertainty and constructing probability density functions (PDFs) of future climate change. The Bayesian approach is one example (e.g. Tebaldi *et al.*, 2005; Buser *et al.*, 2009; Raje and Mujumdar, 2010; Smith *et al.*, 2009b; Tao *et al.*, 2009; Tebaldi and Sansó, 2009; Harris *et al.*, 2010; Potter *et al.*, 2010). It assigns probability to propositions that are uncertain and interprets probability as a measure of a "state of knowledge", which can be subjective (Foley, 2010). However, the creation of probabilistic projections from MME information is not an easy proposition, relying on assumptions about how to weight models and how to take account of structural uncertainties that lie beyond the available MME. In the case of the UKCP09, future climate projections are weighted based on their ability to reproduce the past climate. These issues are noted above and in the following subsections.

2.6.6 Challenges in Interpreting Multi-Model Projections

It is tempting to infer more from ensemble results as outcomes that are not simulated are similarly plausible (Parker, 2010a). Since uncertainty in multi-model or PPEs is expected to widen with model development, increased physical realism (Stainforth *et al.*,

2007a;b) and incorporation of additional processes or methods (Zhang *et al.*, 2011), current ensembles provides a lower bound on the maximum range of uncertainty (Stainforth *et al.*, 2007a), which may be constrained by the methods used to assess a model's ability to inform us about real-world variables (Stainforth *et al.*, 2007b).

Therefore, when constructing and interpreting MME climate results (in the form of climate change probability distributions or averages and measures of variability across models), a number of issues need to be considered (Stainforth *et al.*, 2007a), as discussed below.

2.6.7 Interpreting Multi-Model Ensemble (MME) Results

The shape, spread and central tendency of estimated climate projection density functions (e.g. global moisture budget and dry zone extension; Liepert and Previdi, 2012) from a MME is governed by the methodology applied (Brekke *et al.*, 2008). This includes the number and characteristics of the forcing scenarios, ICU, base model and the parameterisation explored, as well as the concerned timescale. The probability estimated may not relate to the probability of real-world behaviour, thus not providing the decision-relevant distributions desired (Stainforth *et al.*, 2007a; Tebaldi and Knutti, 2007; Vidal and Wade, 2009; Knutti *et al.*, 2010; Xu *et al.*, 2011). While an ensemble mean may outperform single model results, it does not appropriately generalise climate change impact, may demonstrate characteristics (some may be physically implausible) that are not reflected in any single model, and may cause a loss of signal that has barely been addressed (Knutti *et al.*, 2010). Uncertainty is often not adequately characterised (e.g. by standard deviation) due to the same biases in groups of GCMs (Chiew *et al.*, 2009; see Section 2.6.9), e.g. as in projected changes in summer runoff and indicators of low flows (Arnell, 2011). The assumed normal distribution of MME may not be true in projected hydrological changes, which are not even necessarily uni-modal (Arnell, 2011). The commonly reported mean annual river flows may mask the magnitude of uncertainty in flows of most importance to water managers (Xu *et al.*, 2011).

PDFs can be misleading as they imply much greater confidence than the underlying assumptions justify with the unknown reliability of these probabilistic projections (Parker, 2010a). Meaningful PDFs for future climate cannot be constructed by simply combining

MMEs/PPEs results due to the inability to weight models and to define the space of possible models (Stainforth *et al.*, 2007a). PDFs therefore should be interpreted cautiously — they indicate what outcomes may be more plausible than others, and are a way to communicate uncertainty, rather than as a strict mathematical representation of it (Knutti, 2008). The choice between subjective and objective (Berger *et al.*, 2001; Berger, 2006) Bayesian approaches for constructing PDFs introduces further statistical assumptions (Foley, 2010), resulting in a different risk-based decision (New *et al.*, 2007). PDFs are also conditional on the model, observational constraints (Knutti *et al.*, 2010) and the sources of uncertainties considered (Knutti, 2008). Therefore, blind use of a single generation of probabilistic impact information could lead to mal-adaptation (New *et al.*, 2007).

Nevertheless, ensembles are valuable for understanding present-day limitations (Stainforth *et al.*, 2007a). Uncertainty in climate response can be presented as histograms of change, as empirical distribution functions fitted to the distributions of change, or as intermediate ranges (Arnell, 2011). Histograms reveal all the information, but similarities in the climate model representations and the model sample used, rather than clustering in potential physical responses, may produce artificial clustering. Empirical distribution functions can be seen as simply smoothed histograms, and clustering in scenarios will manifest itself in "steps" in the empirical distribution function. An intermediate range (e.g. the 10–90% or inter-quantile ranges) better represent the spread of possible outcomes as using extremes (highest to lowest) may be misleading if "outliers" are present; the use of several quantiles provides information on the distribution of responses within the range.

2.6.8 The "Ensemble of Opportunity"

"Ensembles of opportunity" refers to multi-model datasets, such as the regional climate change simulations from the CORDEX (Coordinated Regional Climate Downscaling Experiment) initiative of the World Climate Research Program (http://www.meteo.unican.es/en/projects/CORDEX). MMEs are created by those willing to contribute, and neither systematically nor randomly (Tebaldi and Knutti, 2007). The models neither span the full range of likely behaviour nor uncertainty due to the small

number of models involved (Tebaldi and Knutti, 2007; Knutti, 2008). Subsequent versions of a model usually build on previous versions, suggesting a process of convergence (Tebaldi and Knutti, 2007). Moreover, the likelihoods of impacts may change over time with more data and resources or an alternative research design (New *et al.*, 2007).

2.6.9 Inter-Model Dependencies and Common Biases

The use of MMEs to obtain uncertainty estimates or PDFs (that rely on assumptions, except, for example, some weighting schemes) may assume that all GCM projections are equally credible and independent (Knutti, 2008; Arnell, 2011), and models can be averaged (i.e. one model, one vote). The idea of uncertainty decreases with more models relies on the fundamental assumption that random errors tend to cancel with independent models (Tebaldi and Knutti, 2007; Knutti *et al.*, 2010). While random errors may cancel, systematic errors associated with limited knowledge and misrepresented/unresolved processes will not improve with more models of similar quality (Tebaldi and Knutti, 2007). Models have similar resolution and the same theoretical arguments for their parameterisations; their inter-dependence (e.g. shared grids and numerical calculations) imply correlated errors; Stainforth *et al.*, 2007a; Tebaldi and Knutti, 2007). Provided that models are based on the same knowledge, make similar assumptions, or share parts of the code of existing models, our confidence should therefore not be infinitely improved by large number of models (Knutti *et al.*, 2010) and that we should not be over-optimistic about consensus estimates (Stainforth *et al.*, 2007a; Tebaldi and Knutti, 2007).

2.6.10 Lack of Verification, Model Tuning and Evaluation

The equations, parameterisations and assumptions built into a model are assumed to be extrapolated beyond the observed climate regime of where they are evaluated (Knutti, 2008). Hydrological models calibrated over the historical period are commonly assumed to be valid for use under a perturbed climate (Vaze *et al.*, 2010). Model accuracy (evaluation) is commonly measured by the ability to replicate observed climate variability and the terrestrial water cycle, for instance (Tebaldi and Knutti, 2007). Typical simulation biases relate to errors in the large-scale circulation in the GCMs — up to 3.4 °C for temperature and 100% for precipitation (Kjellström *et al.*, 2011). How models should be assessed

remains questionable (Blenkinsop and Fowler, 2007a).

Objective methodologies for climate model tuning and model evaluation (often based on expert judgement and/or not documented; Knutti *et al.*, 2010) are yet to be developed (Tebaldi and Knutti, 2007). Models may use the same set of observations for deriving parameterisations, tuning and evaluation (Tebaldi and Knutti, 2007), hence a risk of double-counting information, overconfidence, or circular logic (Knutti *et al.*, 2010). Ideally, independent datasets should be used for model evaluation (Tebaldi and Knutti, 2007). Also, observations and reanalysis datasets contain biases (Tebaldi and Knutti, 2007; Knutti *et al.*, 2010). Model calibration (Section 2.6.4.2) may change parameters unrelated to the problem as not all processes are included in models (Tebaldi and Knutti, 2007). Bias correction in climate projections may merely represent an ad hoc curve-fitting exercise of convenience, rather than a result of impeccable physically-based theory (Kundzewicz and Stakhiv, 2010); uncertainty in bias-corrected GCM outputs may be of the same order of magnitude as those related to GCM or GHM choice (Hagemann *et al.*, 2011).

Agreement across climate models and with observations suggest that models may be an empirically adequate rather than accurate representation of the processes governing the observed climate system behaviour (Knutti, 2008). While models lacking key mechanisms that are indispensable for meaningful climate projections can be omitted from an ensemble (Kundzewicz and Stakhiv, 2010), discounting a model based on inconsistent results may be unwise as models were designed based on an incomplete understanding of the climate system (Foley, 2010).

There appears to be an argument for constraining poorly performing models based on present-day skill (Foley, 2010), e.g. Nohara *et al.* (2006) used a weighted ensemble mean (WEM) to reduce model bias and uncertainty. Weighting models based on observations (Knutti *et al.*, 2010) is difficult and results depend on the choice of metric/criteria for defining model performance (Blenkinsop and Fowler, 2007a; Tebaldi and Knutti, 2007). Arnell (2011) described the practical and conceptual challenges in "optimum weighting" different model projections and to cull "poorly-performing" models from the analysis. While optimum weighting can in principle reduce projection errors, it requires accurate knowledge of the single model skill, the relative contributions of the joint model error and

unpredictable noise (Kundzewicz and Stakhiv, 2010). Multiple diagnostics and metrics of performance are needed as weights for future projections may differ from those optimal for present-day climate (Tebaldi and Knutti, 2007). Studies have shown, however, that weighting/culling has relatively little effect on the estimated range of climate change impacts (Brekke *et al.*, 2008; Chiew *et al.*, 2009; Weigel *et al.*, 2010), due to an absence of correlation between observed quantities and the models' future projections (Knutti *et al.*, 2010). Weighted combinations of results may not provide decision-relevant probabilities (Stainforth *et al.*, 2007a).

Furthermore, model convergence or present-day skill does not guarantee equal legitimacy in future climates (Charles *et al.*, 1999; Stainforth *et al.*, 2007a; Foley, 2010; Knutti *et al.*, 2010) since long-term climate projections cannot be validated directly through observations (Tebaldi and Knutti, 2007; Knutti, 2008).

2.6.11 Uncertainties in Downscaling

Downscaling refines, spatially and/or temporally, coarse GCM output to scales more useful to decision makers, and improves physical realism at sub-grid scale (Wilby and Wigley, 1997; Goodess *et al.*, 2003a; Wilby, 2010). Downscaling may be dynamical or statistical (Hewitson and Crane, 1996). Dynamical downscaling involves nesting a finer-scale regional climate model (RCM) within the coarser GCM (STARDEX, 2005) that defines the (time-varying) boundary conditions (Wilby and Wigley, 1997; Kundzewicz and Stakhiv, 2010). Statistical downscaling is used either to directly downscale GCM information or to downscale further from RCM simulations (Paeth *et al.*, 2011). It assumes stationarity (Charles *et al.*, 1999) as it involves applying statistical relationships between the large and smaller-scale, identified in the observations (i.e. empirical), to GCM output (STARDEX, 2005) in a targeted area, using the predictor fields from GCMs for scenarios construction (Schmidli *et al.*, 2007).

As demonstrated in the PRUDENCE project (Christensen *et al.*, 2007) and other studies, different methodologies have varying strengths and weaknesses (Hewitson and Crane, 1996; Wood *et al.*, 2004; Fowler and Wilby, 2007). Regional simulations also inherent the limitations from the parent GCM(s) (CCSP, 2008). Skill varies temporally and spatially (Mearns *et al.*, 1999; Schmidli *et al.*, 2007; Paeth *et al.*, 2011; Stoll *et al.*, 2011;

Teutschbein *et al.*, 2011), and with variables (Murphy, 1999; 2000; Haylock *et al.*, 2006; Iizumi *et al.*, 2011). Considering additional finer scale-processes increases uncertainty (Rowell, 2006), particularly regarding extreme events (Vicente-Serrano *et al.*, 2004), and may not improve confidence (Hewitson and Crane, 2006; Zhang *et al.*, 2011), e.g. RCMs cannot capture all the important physical processes responsible for precipitation despite their finer resolution (Blenkinsop and Fowler, 2007a; Maraun *et al.*, 2010). As no single downscaling model is more superior (STARDEX, 2005; Haylock *et al.*, 2006), a multi-model approach is recommended (Chen *et al.*, 2011; Zhang *et al.*, 2011). It is worth noting that, although skills vary amongst the various downscaling techniques, studies have shown that GCMs tend to be the largest source of uncertainty.

2.6.12 Uncertainties in Natural Climate Variability

Even without anthropogenic forcings, natural climate variations (both in terms of mean and extremes) are present and can alter climate on a range of timescales (Stuiver *et al.*, 1995; Overpeck *et al.*, 1997; Foley, 2010). This variability can be internally-generated or externally-forced, as described below. Annual to multi-decadal natural variability may contribute significant uncertainty (Kendon *et al.*, 2008) especially in the near-future (Kjellström *et al.*, 2011), e.g. for mean European runoff (Hulme *et al.*, 1999).

2.6.12.1 Internal variability

Internal interactions between components of the climate system produce internal variability, both in terms of mean and extremes (Hegerl *et al.*, 2007). It includes processes intrinsic to the atmosphere (annular modes of circulation variability in mid- and high-latitudes), the ocean (Bradley, 2000), and the coupled ocean-atmosphere system, e.g. ENSO in the tropics, (Deser *et al.*, 2012). It is more dominant in seasonal than annual results and earlier in the 21st century, and less important when climate changes are averaged over larger areas (Räisänen, 2001). Internal variability accounts for at least half of the inter-model spread in projected climate trends during 2005–2060 in the CMIP3 multi-model ensemble (Deser *et al.*, 2012).

2.6.12.2 External variability

External forcings refer to solar variability and stratospheric aerosol from volcanic eruptions, the primary forcings of decadal-to-centennial climate variations during the pre-industrial era (Shindell *et al.*, 2003; Foley, 2010). Solar variability may have affected the earth's climate on decadal-centennial timescales (Kelly and Wigley, 1992; Crowley and Kim, 1996; Haigh, 1999; Bond *et al.*, 2001), possibly via global cloud coverage (Svensmark and Friis-Christensen, 1997; although Lockwood (2012) provided an alterative view on this), such as during the Maunder Minimum (1645–1715; Lean *et al.*, 1995; Shindell *et al.*, 2001).

Volcanic forcing is important for climate change on both interannual, regional, and long-term global scales (Shindell *et al.*, 2003). For instance, the eruptions of Toba (Sumatra) 73,500 years ago (Rampino and Self, 1992) and more recently, Mount Pinatubo in 1991 (Hansen *et al.*, 1992; Kelly *et al.*, 1996; Hansen *et al.*, 1997), amongst others, generated aerosols that warm the stratosphere and cool the surface globally, causing a tendency for regional surface cooling during the subsequent years (Robock, 2000).

The relative contribution of external natural variability are greatest early in the century (Stott and Kettleborough, 2002), and may be intrinsic and irreducible (Knutti, 2008).

2.6.13 Discussion

Model simulations have a number of limitations. GCMs generally reproduce the overall and broad geographic (e.g. spatial mean annual) patterns of observed climate trends (Arnell, 2004a; Milly *et al.*, 2005). However, models may accurately simulate one metric but not another (Brekke *et al.*, 2008; Foley, 2010). Projected precipitation changes, which are important for hydrological modelling (Zhang *et al.*, 2011), are less spatially coherent (Alexander *et al.*, 2006; Sheffield and Wood, 2008b), weaker and more uncertain than temperature (Tebaldi *et al.*, 2006; Planton *et al.*, 2008; Bureau of Reclamation, 2011; Zhang *et al.*, 2011; Lavaysse *et al.*, 2012). Models have difficulties simulating precipitation response to large-scale climate variability (e.g. ECHAM5; Hagemann *et al.*, 2006), and river flows (Todd *et al.*, 2011; Xu *et al.*, 2011; Gudmundsson *et al.*, 2012a). Model skill may also vary regionally (Burke *et al.*, 2006; Alexander and Arblaster, 2009; Foley, 2010), seasonally (Jacob *et al.*, 2007; Chiew *et al.*, 2009; Grimm, 2010) and temporally

(Blenkinsop and Fowler, 2007b), and with horizontal (Blenkinsop and Fowler, 2007a) or vertical (Hagemann *et al.*, 2006) resolution. Simulated magnitude (and sometimes direction) of change often diverges.

Models that reproduce the mean climate may not necessarily perform well at replicating the observed climate extremes (McCrary and Randall, 2010; Williams *et al.*, 2010), e.g. dry days (Tebaldi *et al.*, 2006), and their associated impacts such as drought. The spatial distribution of model errors for drought indices differ from those for simulated mean precipitation (Blenkinsop and Fowler, 2007a), possibly due to natural variability, model errors in simulating large-scale flows and poorly represented regional processes and feedbacks (Burke *et al.*, 2006). Projections for future extreme events (e.g. Q95 flow) are more uncertain than for the mean (e.g. annual flow) (Xu *et al.*, 2011), e.g. Sheffield and Wood (2008b) found large model spread and overestimated drought duration and frequency.

A climate model that reasonably simulates present-day regional precipitation variability may produce less uncertain future drought projections (Burke, 2011), however, this also depends on the models' ability to simulate tropical SSTs (Dai, 2011) (see Section 2.5). Haddeland *et al.* (2011) assessed the results simulated by six land surface models and five global hydrological models (GHMs) that participated in the Water Model Intercomparison Project (WaterMIP). They found evaporation and runoff results diverged mainly due to model differences, with the largest absolute (relative) runoff differences in the tropics (arid regions).

2.7 Uncertainties in Hydrological Modelling

In addition to uncertainties related to climate modelling, those arising from hydrological modelling are also important. In recent years, model intercomparison studies that consider the global water balance have emerged. For instance, Haddeland *et al.* (2011) assessed the results simulated by six land surface models (LSMs) and five global hydrological models (GHMs) from the Water Model Intercomparison Project (WaterMIP). They found evaporation and runoff results diverged mainly due to model differences, with the largest absolute (relative) runoff differences in the tropics (arid regions). Gudmundsson *et al.* (2012b) assessed the ability of nine large-scale hydrological models in capturing the mean annual runoff cycle based on observed runoff from a large number of small,

near-natural catchments in Europe. Although they found large differences in model performance, the ensemble mean (mean of all model simulations) yielded rather robust predictions; also a relatively good regional average performance was found despite some large local uncertainties. However, model performance was poor in cold regions, due to shortcomings in simulating the timing of snow accumulation and melt. Prudhomme *et al.* (2011) assessed the ability of three GHMs from the WaterMIP (Joint U.K. Land Environment Simulator (JULES), Water Global Assessment and Prognosis (WaterGAP), and Max Planck Institute Hydrological Model (MPI-HM)) in reproducing large-scale hydrological extremes. They found that all models can broadly reproduce the spatio-temporal evolution of historical droughts (based on the regional deficiency index; RDI) and high flows (regional flood index; RFI) in Europe to varying degrees. Van Loon *et al.* (2012) found that most drought propagation processes in contrasting catchments in Europe are reasonably well reproduced by the ensemble mean of ten large-scale LSMs and GHMs that participated in the model intercomparison project of WATCH (WaterMIP). Nonetheless, hydrological drought simulation at large scales remains highly uncertain, especially in catchments with cold and semi-arid climates and catchments with large storage in aquifers or lakes.

Relatively few studies have applied multiple impact models in climate change impact studies. Hagemann *et al.* (2012), for instance, systematically assessed the hydrological response to climate change and project the future global water availability using three global climate and eight hydrological models. Their results demonstrated larger spread of the impacts than that of the climate models in some regions, primarily cased by the different representations of hydrological processes (e.g. evapotranspiration) in the GHMs.

These studies indicate that, similar to climate projections, climate change impact studies should not be based on the output of single impact models (Hagemann *et al.*, 2012). Specifically in relation to drought simulation using large-scale models, there is a need for better representation of evapotranspiration, snow accumulation and melt, storage and the parametrisation of storage processes (e.g. land and aquifer characteristics) (Van Loon *et al.*, 2012).

2.8 Challenges in Projecting Future Drought Conditions

Droughts are one of the most damaging natural hazards in human, environmental and economic terms. Anthropogenic climate change has and will continue to alter their characteristics. A better understanding of potential future drought characteristics and the uncertainties associated with the various methodologies to derive them are vital for identifying effective measures to manage drought risks and any direct/indirect impacts. However, confidence in drought projections is constrained by definitional issues (see Section 2.2), lack of observational data and the limitations of climate models (IPCC, 2012). Some of the uncertainties associated with drought identification and quantification are presented in Section 2.2, those related to climate modelling are discussed in Section 2.7. Hence, it is important to characterise the uncertainties associated with future drought simulations (Vasiliades *et al.*, 2009).

Projecting future climate remains very challenging. Present-day climate and its natural variability, climate change, and the sensitivity of drought metrics to these changes all define future drought changes (Burke, 2011). The strength of the change (signal) against the background of natural variability (noise) governs the detectability of any changes, and hence their statistical significance (Sheffield and Wood, 2008b). Future shifts in modes of climate variability (e.g. ENSO; Collins, 2004; Dore, 2005) remains uncertain. Moreover, climate change effects may not be felt in the near future at regional scales (Sheffield and Wood, 2008b).

Understanding and quantifying climate change impacts (natural and/or anthropogenic) on the hydrological cycle and water resources requires robust modelling which considers the underlying physical mechanisms that drive the regional hydroclimatology (Kiem and Verdon-Kidd, 2010). Despite the limitations discussed in Section 2.7, GCMs are valuable tools for studying climate change and the related impacts as each simulation presents a "what-if" scenario (Stainforth *et al.*, 2007a). However, GCMs were originally constructed for assessing the global climate system response to varying emissions (Wilby, 2010) and facilitating mitigation efforts, rather than informing adaptation-type analysis (Kundzewicz and Stakhiv, 2010). They also differ in their design and outcomes. GCMs (especially their representation of changes in the large-scale circulation) often dominate other sources of uncertainties in climate change impacts on hydrological change and water resources, e.g.

emission scenarios or hydrological model parameterisation (Arnell, 2004a; Graham *et al.*, 2007; Vidal and Wade, 2009; Xu *et al.*, 2011; Arnell, 2011; Gosling *et al.*, 2011b). Since each model has its own set of strengths and weaknesses (Knutti, 2008), no one model is particularly good or bad (Alexander and Arblaster, 2009), and a multi-model approach is desirable.

To evaluate the robustness of projections of European drought characteristics under climate change, the effects of applying different emission scenarios and GCMs are explored in this thesis (particularly Chapters 4 and 5). In most cases, however, resource and financial constraints have prevented the running of large ensembles of GCM experiments. The simple climate model MAGICC6 thus offers a practical solution as it enables emulation of a wide range of emission scenarios and GCMs. As GCM simulations do not span all the emission scenarios, ClimGen is used to emulate GCM simulations beyond the available GCM ensemble by using the pattern-scaling approach. Since the spatial resolution varies with the GCM, ClimGen is also used to interpolate the GCM pattern at the original resolution onto a $0.5^\circ \times 0.5^\circ$ grid. MAGICC6 and ClimGen are described in Chapter 3. Uncertainties associated with the different types and definitions of drought are examined in Chapter 5.

Chapter 3

General Methodology

This chapter presents the general methodology, including the modelling framework, study area and drought identification, applicable to Chapters 4–7. More specific details are elaborated in the individual sections.

3.1 MAGICC6

MAGICC (Model for the Assessment of Greenhouse-gas Induced Climate Change) is a simple/reduced complexity coupled gas-cycle/climate model (Wigley and Raper, 1987; 1992). It has been used in the previous IPCC Assessment Reports to produce projections of future global-mean temperature and sea level rise, e.g. the 4.2 version was used in the IPCC Fourth Assessment Report (AR4), Working Group 1.

The climate model in MAGICC is an upwelling-diffusion, energy-balance model that produces global- and hemispheric-mean temperature output and results for oceanic thermal expansion. MAGICC is based on a simple global-mean energy balance approximation:

$$\Delta Q = \lambda \Delta T + F \tag{3.1}$$

where ΔQ is the global-mean radiative forcing at the top of the troposphere. It is the balance between the climate system heat content change (F) and outgoing long-wave radiative heat loss to space ($\lambda \Delta T$). This outgoing energy flux is a linear function of surface temperature perturbation (ΔT) and the global-mean feedback factor (λ), which

itself is inversely proportional to the climate sensitivity.

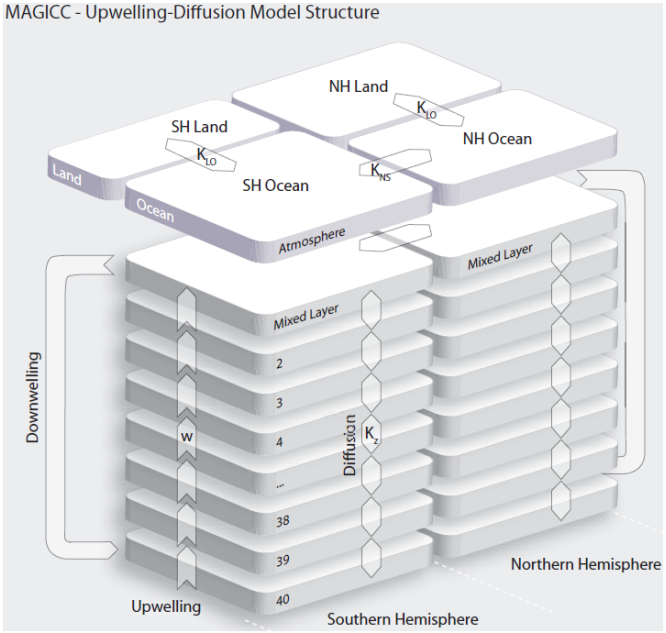

Figure 3.1: The schematic structure of MAGICC's upwelling-diffusion energy balance module with land and ocean boxes in each hemisphere. The processes for heat transport in the ocean are deepwater formation, upwelling, diffusion, and heat exchange between the hemispheres. Not shown is the entrainment and the vertically depth-dependent area of the ocean layers. Source: Figure A1 in Meinshausen *et al.* (2011a).

MAGICC's atmosphere consists of four boxes (one over land and one over ocean for each hemisphere) with zero heat capacity (Figure 3.1). The hemispherically averaged upwelling-diffusion ocean is coupled to an atmosphere layer. It determines the air temperature over land and ocean separately, by considering a radiative energy-balance combined with heat transfers between the land and ocean and between the two hemispheres (the latter occurring only between the ocean boxes of the hemispheres) and ocean heat uptake. Vertical diffusion and advection drive the heat exchange between the oceanic layers. MAGICC also has a globally averaged carbon cycle model. MAGICC6 is an updated version of MAGICC. MAGICC6 and its calibration to higher complexity models are detailed in Meinshausen *et al.* (2011a) and Meinshausen *et al.* (2011b). Therefore it is only briefly described here.

MAGICC encompasses a suite of coupled gas-cycle, climate and ice-melt models that account for feedbacks between the carbon cycle and the climate. The radiative forcing, climate sensitivity and ocean heat uptake efficiency determine the CO_2 concentrations

and global-mean temperature change that result from a given timeseries of GHG emissions. MAGICC6 has enhanced representation of time-varying climate sensitivities, carbon cycle feedbacks, aerosol forcings and ocean heat uptake characteristics. The internal consistency of MAGICC, while in its coupled mode, implies that the climate model response drives the climate feedbacks on the carbon cycle, thus CO_2 concentrations. Model component results can be uncoupled separately for consistent analysis of the joint response and feedback of different combinations of high complexity carbon cycle models and GCMs. MAGICC6 has therefore been calibrated to emulate the World Climate Research Programme's (WCRP's) phase 3 of the Coupled Model Intercomparison Project (CMIP3; Meehl *et al.*, 2007) GCMs and the Coupled Carbon Cycle Climate Model Intercomparison Project (C^4MIP; Huntingford *et al.*, 2009) carbon cycle model responses with considerable accuracy.

MAGICC6 has been used in this thesis for four reasons (Meinshausen *et al.*, 2011a). Firstly, MAGICC6 can emulate GCM results, which avoids the computational cost of running large ensembles with GCMs. Secondly, it can capture the structural uncertainties associated with parametrisation across the range of CMIP3 and C^4MIP models. Thirdly, it can help isolate the effects of various components, e.g. different forcings or climate responses. Lastly, MAGICC6 can be uncoupled to examine the effects of different combinations of forcings and more complex models.

MAGICC6 converts the CO_2 concentrations from an emission scenario to CO_2 emissions that drive a carbon cycle model. The global-mean surface temperature changes simulated by MAGICC6 for the 21st century were used as inputs in ClimGen (Section 3.2).

3.2 ClimGen

ClimGen version 1-02 (hereafter, ClimGen) has been applied, as a stand-alone application, as a climate scenario generator. It is detailed in Osborn (2009) as an extension to the approach described by Mitchell *et al.* (2004). It outputs monthly climate datasets and scenarios for the observed (1901–2005) climate, for both CRU TS2.1 (Mitchell and Jones, 2005) and CRU TS3.10 (Harris *et al.*, 2013; as used in this thesis), as well as future (2001–2100) climate scenarios (Mitchell *et al.*, 2004), for the entire terrestrial land

surface except Antarctica. ClimGen currently produces eight climate variables: mean, maximum and minimum temperature (thus information for diurnal temperature range), precipitation, vapour pressure, cloud cover and wet day frequency, at monthly, seasonal, or annual time-scale, or averaged over a specified time slice. Monthly precipitation, and temperature (for the hydrological drought analysis), are the primarily variables considered in this thesis.

ClimGen is based on the pattern scaling method (Santer *et al.*, 1990; Goodess *et al.*, 2003a; Mitchell, 2003), which separates the global-mean and spatial-pattern components of future climate change, and in some cases, the latter can be further distinguished into GHG and aerosol components. GCM simulations provide the geographical, seasonal and multi-variable structure of change for most scenarios of future climate change. ClimGen contains a database of standardised climate change patterns from 22 CMIP3 GCMs. For two time-periods, e.g. 2071–2100 and 1961–1990, it calculates the difference between the future 30-year average climate for 2071–2100, and the 1961–1990 mean climate, both simulated by the GCM and then divide by the global-mean warming for the particular climate change experiment between 2071–2100 and 1961–1990. The resultant standardised climate change pattern (that consists of GHG and aerosol components) P is expressed per °C global warming. The pattern P for regional temperature change, per degree C, for GCM g, scenario s, cell i, and month m, is given by:

$$P_{gsim} = \frac{T_{gsim}(2071-2100) - T_{gsim}(1961-1990)}{Tglobe_{gs}(2071-2100) - Tglobe_{gs}(1961-1990)} \tag{3.2}$$

Following the recommendations of Mitchell (2003), the CMIP3 GCM patterns in ClimGen are derived using all running 30-year mean periods and linear regression between these and the global-mean temperatures (instead of the simpler difference equation (3.2)). To strengthen the signal to noise ratio (where signal is the response to the externally-forced global warming and noise is the internal variability in an individual model simulation), all ensemble members from simulations under the SRES A2 and A1B were pooled together for each GCM. Global-mean temperature change from MAGICC6 (Section 3.1) for a given year, emissions scenario and set of climate model parameters is then used to re-scale these patterns P to generate a space-time pattern of changing mean climate that reflects a particular emission scenario.

ClimGen employs distance-weighted averaging to interpolate each of the patterns of standardised coefficients obtained from each GCM simulation at the original resolution onto a $0.5^\circ \times 0.5^\circ$ grid. Any changes relative to the baseline would be attributable to climate change and not to internal climate variability as ClimGen uses the same sequence of observed variability to generate each series of data, whether for 1951–2000, 2001–2050 or 2051–2100.

A climate change signal is combined with interannual variability and a climatological mean from the observational archive to generate future climates. Future scenarios can be generated by the *additive* (or "absolute changes") method, where GCM-derived changes in mean climate are added to the observations, i.e. interannual variability remains unchanged in the future. For precipitation, the *multiplicative* method (or "relative changes") is also an option ("Option 3" in ClimGen; as applied in Chapter 6). Perturbed mean precipitation is obtained by multiplying the observations by the GCM-derived mean precipitation changes. This requires the pattern-scaled GCM precipitation change to be expressed as a fractional change from present-day precipitation (e.g. a fractional change of 1.2 implies a 20% increase) rather than as an absolute change (e.g. an increase of 20 mm/month). The magnitude of mean precipitation change varies exponentially with the global-mean temperature change. The exponential function, calibrated using a start and end value provided by GCM data, avoids zero precipitation being generated as the rate of change decelerates with warming in regions of decrease. Interannual variability is modified in such a way that the coefficient of variation (CV; standard deviation:mean ratio) is roughly constant. Therefore, for the *multiplicative* method (where only the mean precipitation changes as CV is kept constant), the pattern P for regional temperature change, per degree C, for GCM g, scenario s, cell i, month m and year y, is given by:

$$P_{gsimy} = \bar{o}_{im} o'_{imy} e^{P_{gim} \Delta T_{gsy}} \tag{3.3}$$

where $\bar{o}_{im}$ is the 1961–1990 observed mean precipitation for cell i and month m, o'_{imy} is the observed precipitation anomaly (relative to the mean precipitation) for cell i, month m and year y, P_{gim} is the standardised climate change pattern for GCM g for cell i and month m, and ΔT_{gsy} is the global-mean temperature change under scenario s for GCM g in year y.

In regions where the temporal distribution of precipitation becomes more skewed (i.e. with increased low or high extremes, or both) or less skewed (i.e. with decreased low and/or high extremes), interannual variability may change independently of mean precipitation, and the "Osborn-Gamma" method ("Option 4" in ClimGen) is applied, as in this thesis. It uses the Gamma shape method (described by Goodess *et al.*, 2003b) where the observed interannual variability is perturbed so that it becomes consistent with the GCM-derived perturbed precipitation probability distributions. It is parameterised via the shape parameter, α, of the gamma distribution, which measures the distribution skewness. Similar to the multiplicative method, altered mean precipitation are derived the same way; the changes in mean precipitation and precipitation distribution shape are linear (exponential) functions of global-mean temperature in regions where they increase (decrease). α is derived from the GCM simulations and then scaled by the global-mean temperature change in the same way as the changes in mean climate are pattern-scaled. Hence, the projected gamma shape parameter α, per degree C, for GCM g, scenario s, cell i, year y and month m, is given by Equations 3.4 (for areas with increasing precipitation) and 3.5 (for areas with decreasing precipitation):

$$\alpha_{gsimy} = \bar{\alpha}_{im}(1 + S_{gim}\Delta T_{gsy}) \tag{3.4}$$

$$\alpha_{gsimy} = \bar{\alpha}_{im}e^{S_{gim}\Delta T_{gsy}} \tag{3.5}$$

where $\bar{\alpha}_{im}$ is the shape parameter of the 1951–2000 observed precipitation calculation period for cell i and month m, S_{gim} is the standardised pattern of change in gamma shape parameter pre-calculated from GCM g for cell i and month m (c.f. Equation 3.2). The gamma shape parameter is fitted to monthly precipitation values after they have been expressed as fractional deviations from the 30-year smoothed precipitation (i.e. they are divided by the latter). Thus, the gradual changes in mean precipitation are removed.

Similar to Equation 3.3, the pattern P for regional temperature change for the *Osborn-Gamma* method (where both precipitation mean and variability change), per degree C, for GCM g, scenario s, cell i, month m and year y, is given by Equations 3.6 (for areas with increasing precipitation) and 3.7 (for areas with decreasing precipitation):

$$P_{gsimy} = \bar{o}_{im}\tilde{o}_{imy}(1 + P_{gim}\Delta T_{gsy}) \tag{3.6}$$

$$P_{gsimy} = \bar{o}_{im}\tilde{o}_{imy}e^{P_{gim}\Delta T_{gsy}} \tag{3.7}$$

where $\tilde{o}_{imy}$ is the observed precipitation anomaly for cell i, month m and year y after transformation so that its gamma shape parameter is modified to match the projected shape parameter.

ClimGen is constrained by pattern scaling, which assumes a linear (or exponential) relationship between local climate change and global-mean temperature change, that the spatial pattern of change would remain over time, and that all GHGs have the same climate responses (Goodess *et al.*, 2003a). Also, future changes in aerosols are not represented as most emission scenarios have low aerosol emissions due to clean air assumptions.

3.3 Global Hydrological Model: Mac-PDM.09

The Macro-scale–Probability-Distributed Moisture model (Mac-PDM), a global hydrological model (GHM), is a grid-based conceptual water-balance accounting model. Evolution of the various water balance components is calculated at a daily time step. The first version was described in Arnell (1999a) and a revised version was used in Arnell (2003a). Here, the latest version, Mac-PDM.09, which is detailed in Gosling and Arnell (2011) and briefly outlined below, have been used.

Mac-PDM.09 can be forced with monthly or daily climate data. The inputs used for this study were 50-year monthly climate data from ClimGen (see Section 3.2). These include monthly timeseries of temperature and precipitation, along with long-term mean (present or future) monthly averages of temperature, precipitation, number of wet days, vapour pressure, cloud cover (converted internally to net radiation) and baseline (1961–1990) windspeed (the latter assumed to remain unchanged in the future). For the snow component, Mac-PDM.09 interpolates monthly temperature data to the daily time step and adds a random component to the rather smooth temperature series; a normal distribution with a standard deviation of 2°C is assumed for the departures from the smoothed data.

Mac-PDM.09 stochastically calculates daily precipitation for each cell using monthly precipitation data and wet-day frequency, and the hydrological output is calculated from the mean of 20 repetitions of a model run. Daily precipitation intensity is assumed to follow an exponential distribution based on the gridded observed coefficient of variation (CV) of daily rainfall.

The water balance of each cell (either regular or catchment shaped) is calculated independently, hence no routing of runoff between grid cells. This is considered appropriate as the aim is to examine the spatial pattern of climate change impacts, rather than to estimate runoff at specific locations (Arnell, 2003a). Precipitation, which is equally distributed across the cell, falls as snow if temperature falls below a defined threshold; if temperature rises above another threshold, snow melts at a constant rate per degree per day. Precipitation that exceeds interception capacity falls to the ground. Information on soil and vegetation characteristics is obtained from spatial datasets. The type of land cover (i.e. vegetation type) determines the amount of precipitation intercepted, potential evaporation (calculated using the Penman-Monteith method), and soil moisture storage capacity through soil texture and root depth. Actual evaporation is determined by potential evaporation and soil moisture content (Arnell, 1999a). When water reaches the ground, saturated soil generates "quickflow" (but not necessarily overland flow) whereas unsaturated soil allows infiltration. Evaporation and drainage to groundwater (which is not stored) and stream ("slowflow") deplete soil moisture. As soil moisture storage capacity varies statistically across the cell/catchment, quickflow can be generated from the saturated proportion of cell area. Quickflow and slowflow are then routed separately to the outlet of the cell to create daily river runoff, which is "indicative" and monthly runoff is a much more credible output. All runoff generated within the grid cell is assumed to reach the cell outlet.

Key caveats of Mac-PDM.09 include the exclusion of transmission losses along the river network or evaporation of infiltrated overland flow, which could overestimate runoff and underestimate the percentage effect of climate change on the amount of water in rivers in dry regions (Arnell, 2003a), and human interventions. In addition, Mac-PDM.09 does not incorporate the effects of seasonal freezing and thawing of permafrost, or glacial melt, therefore underestimates future runoff in catchments below melting glaciers (Arnell,

2003a).

3.4 Emission Scenarios

This thesis has examined the effects of a range of emission scenarios including the IPCC SRES scenarios and RCPs, as outlined below.

3.4.1 IPCC SRES Scenarios

The Intergovernmental Panel on Climate Change (IPCC)'s Special Report on Emission Scenarios (SRES; Nakicenovich and Swart, 2000) has detailed the SRES scenarios. Forty non-mitigation possible future world states were developed and structured into six subgroups based on plausible common storylines. The SRES scenarios are presented as four equally plausible storylines labelled A1, A2, B1 and B2. They represent different world futures in two dimensions: a focus on economic (the "A" scenarios) or environmental (the "B" scenarios) concerns, and global or regional development patterns. The characteristics of the four storylines and scenario families are summarised as follows:

- A1: A global and independent world with very rapid economic growth, global population peaks in mid-century and declines thereafter, rapid technological change, convergence of regions, capacity building, increased social interaction, reduced region differences in per capita income. The three A1 groups have distinguished technological change in the energy system: fossil intensive (A1FI), non-fossil fuels (A1T) or a balance across all sources (A1B).
- A2: A heterogeneous, market-led world with self-reliance and local identities preserved, high population growth, regionally oriented economic growth, fragmented economic and technological development.
- B1: A convergent world with low population growth as A1, transition to service and information economy, resource productivity improvements, clean and efficient technology towards global solutions.
- B2: A divergent world with emphasis on local solutions to economic, social, and environmental sustainability, moderate population growth, intermediate economic development, less rapid technological change.

3.4.2 Representative Concentration Pathways (RCPs)

The Representative Concentration Pathways (RCPs; Moss *et al.*, 2010) represent the full range of potential future radiative forcing pathways that are considered to be feasible, which are compatible with the full range of stabilisation, mitigation and baseline emission scenarios available in the scientific literature. Unlike the SRES scenarios that were developed sequentially (i.e. from detailed socio-economic storylines which determine GHG emissions to radiative forcing), the RCPs were developed through the parallel approach, where important characteristics for scenarios of radiative forcings, such as the level of radiative forcing in the year 2100, was first identified.

Four individual modeling groups developed four independent pathways for the RCPs (Table 3.1) using integrated assessment models that combine economics, technology, and physical processes. The scenarios include a full suite of GHG concentrations, spatially explicit emissions for pollutant gases and aerosols, and spatially explicit land-use and land-use change information. The differences between the RCPs may be partly attributable to differences between models and scenario assumptions (scientific, economic, and technological), but cannot directly be interpreted as a result of climate policy or particular socioeconomic developments.

Although the RCPs were not developed to mimic specific SRES scenarios, temperature projections for RCP8.5, RCP6 and RCP4.5 are similar to those for the SRES A1FI, B2 and B1 scenarios, respectively. Temperature estimates for the RCPs span a larger range than for the SRES scenarios, as the former span a large range of stabilisation, mitigation and non-mitigation pathways while the latter cover only non-mitigation scenarios (Rogelj *et al.*, 2012).

Scenario	Modelling team / models	Characteristics	References
RCP8.5	International Institute for Applies Systems Analysis (IIASA) / MESSAGE	High GHG concentration levels; increasing GHG emissions over time	Riahi *et al.* (2007)
RCP6.0	National Institute for Environmental Studies (NIES) / AIM	Stabilisation scenario; total radiative forcing stabilises after 2100	Fujino *et al.* (2006), Hijioka *et al.* (2008)
RCP4.5	Pacific Northwest National Laboratory (PNNL)'s Joint Global Change Research Institute (JGCRI) / MiniCAM	Stabilisation scenario; total radiative forcing stabilises before 2100	Clarke *et al.* (2007), Smith and Wigley (2006), Wise *et al.* (2009)
RCP3-PD (or RCP2.6)	Netherlands Environmental Assessment Agency (PBL) / IMAGE	Very low GHG concentration levels; radiative forcing level first reaches ∼3.1 W/m^2 mid-century before returning to 2.6 W/m^2 by 2100; GHG emissions (and indirectly emissions of air pollutants) are reduced substantially over time	van Vuuren *et al.* (2007)

Table 3.1: Representative Concentration Pathways (RCPs)

3.5 Characterising Uncertainty

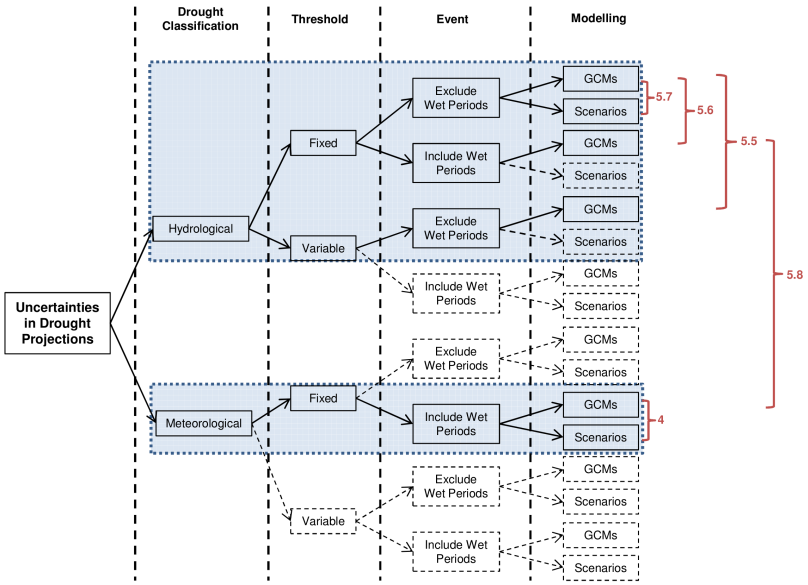

Figure 3.2: Some of the sources of uncertainty in drought projections. The blue shading highlights those examined in this thesis, along with their respective Sections (e.g. "5.8" denotes Section 5.8). The "threshold" category indicates whether the threshold used to identify drought conditions in seasonally-varying or fixed throughout the year. The "event" category indicates whether a temporary return to wetter conditions is included in a drought or not.

There is no single "best model" for reproducing mean precipitation and drought statistics across Europe; model skills also vary temporally, even on the catchment scale (Blenkinsop and Fowler, 2007b). Projections of future climate inevitably contain uncertainty that is typically addressed by using a variety of scenarios to generate a range of

Emission scenarios	Carbon cycle models	GCMs
SRES A1FI	BERN-CC	CCCMA-CGCM3.1(T47)
SRES A1B	CLIMBER2-LPJ	CNRM-CM3
SRES A1T	CSM-1*	CSIRO-Mk3.0
SRES A2	FRCGC	GFDL-CM2.0
SRES B1	HADCM3LC	GFDL-CM2. 1
SRES B2	IPSAL	INM-CM3.0
RCP 8.5	LLNL	IPSL-CM4
RCP 6	MPI	LASG-FGOALS-g1.0
RCP 4.5	UMD	MPI-OM-ECHAM5
RCP 3-PD	UVic-2.7	MRI-CGCM2.3.2
		NASA-GISS-ER
		NASA-GISS-EH
		NCAR-CCSM3
		NCAR-PCM
		NIES-MIROC3.2(hires)
		NIES-MIROC3.2(medres)
		UKMO-HadCM3
		UKMO-HadGEM1

Table 3.2: Emission scenarios, carbon cycle models and GCMs used. All ten carbon cycle models were used in an initial study but results presented in this thesis are only based on CSM-1.

possible outcomes. Using MAGICC6 and ClimGen, Chapters 4 and 5 examine some of the uncertainties associated with drought projections, specifically those introduced by climate modelling and the definition of drought, respectively (Figure 3.2).

Modelling uncertainties were assessed by using a range of emission scenarios and models. A subset of the options shown in Table 3.2 were applied in Chapters 4–7. It should be noted that although ClimGen can derive climate change patterns from 22 CMIP3 GCMs, MAGICC6 has only been tuned to emulate 18 of them, therefore this thesis was limited to those listed in Table 3.2. For the same CO_2 emissions, different carbon cycle models produce different atmospheric CO_2 concentrations and radiative forcings. This carbon cycle uncertainty is estimated to be $\sim$40% of that of the physical climate properties (e.g. equilibrium climate sensitivity and global heat capacity; Huntingford *et al.*, 2009). However, an initial study (not shown) involving ten carbon cycle models (Table 3.2) indicated that this source represented $<$5% of total variance that also encompassed GCM and emission scenario uncertainties, therefore is negligible for the concerned timescale. Consequently, this thesis has been based on the MAGICC emulation of only one carbon cycle model, CSM-1, which yields moderate global-mean temperature change.

Since there is no universal definition of drought (Section 2.2), two classifications were studied: meterorological and hydrological events. Meteorological droughts have been quantified by the precipitation-only Standardised Precipitation Index (SPI; see Section

4.2.2). A subset of the climate projections (Table 3.2) were used as input to the global hydrological model, Mac-PDM.09, to generate runoff data for characterising changes in hydrological droughts (Chapter 5).

3.6 Timescales and Study Periods

Different timescales may be useful for monitoring different drought classifications (Vicente-Serrano and López-Moreno, 2005). A 3–6 month drought describes a surface-water drought, whereas a 6+ month drought represents a water resource drought that could affect groundwater resources (Fowler and Kilsby, 2004; Blenkinsop and Fowler, 2007a). For meteorological events, SPI timescales of 1–3 (7–10) months better represent river discharges, e.g. in a mountain hydrological system with intense runoff, high precipitation and quick runoff generation (large reservoir storages) (Vicente-Serrano and López-Moreno, 2005). Intense spring/summer rainfall deficiencies of 4–9 months can threaten water supplies in areas dependent on surface water (e.g. parts of northern and southwest England); notably dry winters may prevent adequate recharge of groundwater resources (e.g. in eastern/southern England; Marsh *et al.*, 2007). SPI timescales of 12+ months seem not effective in monitoring droughts of any classification in mountainous areas (e.g. the Aragon River Basin, central Spanish Pyrenees; Vicente-Serrano and López-Moreno, 2005).

Both short (3-month) and long (12-month) droughts were studied here; meteorological events were denoted by SPI3 and SPI12, respectively. Prior to SPI computation (for meteorological drought; Section 4.2.2) or hydrological drought quantification (for hydrological drought; Section 5.3), a 3/12-month lagged moving average of the raw monthly precipitation/runoff timeseries was derived. This accounts for conditions in the preceding months, as a drought is a cumulative precipitation/runoff deficit.

Droughts were characterised for the baseline period (1951–2000), and two future periods (2001–2050 and 2050–2100). The 50-year period was chosen in order to sample a range of (e.g. multi-year) events and a range of natural variability; a shorter timescale may result in zero drought events being identified in some cells of the study region (see Section 3.9) during 1951–2000, thus the percentage change in future events would not be able to be determined.

3.7 Drought Identification

Both meteorological and hydrological droughts were characterised using a threshold approach (see Section 2.2.2): a meteorological/hydrological event occurs when the value of the lagged moving average SPI/runoff timeseries falls below the threshold. For meteorological events, the focus is on the *severely* or *extremely* dry conditions (see Table 4.1) — i.e. a drought was considered to begin when SPI≤ -1.5. For SPIm (where m represents the timescale concerned), when the SPI values of over m consecutive months remained SPI> -1.5, an event terminated in the first month when the SPI value rises above SPI-1.5. Hence, two separate events occurred only when there were over m months of SPI> -1.5; persisting dry conditions (e.g. several years) with occasional wet periods that could only temporarily alleviate the drying were regarded as a single event, i.e. lower frequency despite extensive drought conditions. The effects of including/excluding these excess periods for both meteorological and hydrological events are explored in Section 5.6. Hydrological droughts were identified using a runoff threshold based on SPI-1.5 (see Section 3.7.1).

3.7.1 Drought Threshold Expressed as Runoff

Hydrological drought thresholds in absolute runoff values may provide more information and/or a better indication for end-users on the level of runoff deficit. Therefore, a fixed runoff threshold was derived for each cell of the study region (Figure 3.3) — similar to the drought threshold in absolute precipitation values (Figure 4.1, Section 4.3), the runoff threshold for each cell is comparable to SPI-1.5 as both imply the same percentile exceedence.

To obtain the runoff thresholds, a percentile was determined based on the number of months of the SPI timeseries with values being ≤ -1.5 in the 1951–2000 period. This percentile was then applied to the 1951–2000 lagged moving average runoff timeseries to extract the threshold in absolute runoff. This means that for any particular cell, the probability of the runoff timeseries falling below the identified runoff threshold is the same as the SPI value being ≤ -1.5 in the 1951–2000 period.

Figure 3.3 shows that runoff threshold varies from just above zero to over 16 mm. Both 3- and 12-month events demonstrate similar spatial patterns, with 12-month having

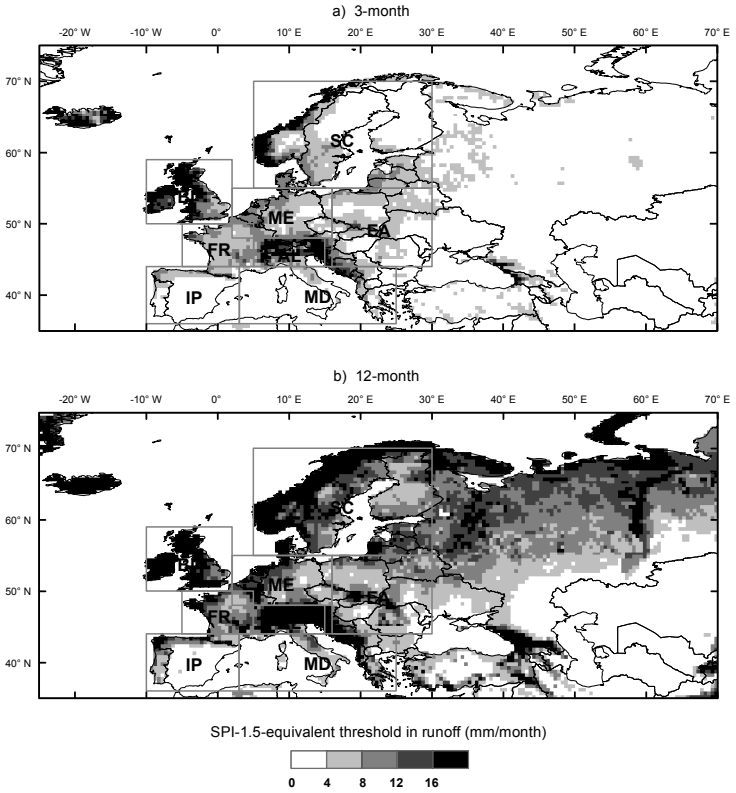

Figure 3.3: Threshold in runoff (mm/month), used for defining hydrological drought, that has the same percentile exceedence as SPI -1.5 during 1951–2000 for (a) 3-month and (b) 12-month events.

higher runoff threshold values due to the longer duration. For 3-month events, a majority of the study area has threshold values of under 8 mm. Higher values ($>$8 mm) tend to concentrate along the southwestern coast of Norway, the British Isles except southeastern England, and the Alps. For 12-month events, runoff threshold values of $>$12 mm are widespread in the higher latitudes of Scandinavia and Russia, much of the British Isles and western Europe, the Alps, as well as areas towards east of Mediterranean and the Black Sea.

The patterns of absolute runoff threshold correspond to those for absolute precipitation threshold (Figure 4.1). However, the patterns of absolute precipitation threshold are more spatially-coherent than their runoff counterparts.

3.8 Drought Parameters

As discussed in Section 2.2.2, precipitation/runoff deficit has been characterised by different parameters. This thesis has quantified meteorological and hydrological droughts

by considering their severity and spatial extent. Drought severity for cell i represents the cumulative deficit from the threshold over a 50-year period, and is given by:

$$Severity_i = \sum_{t=i}^{t=e} X_0 - X_t \tag{3.8}$$

where X_0 is the threshold, X_t is the drought variable at month t, and $t = i$ and $t = e$ represent the start and the end of the drought event, respectively (c.f. Figure 2.1). Severity provides no information on the timing of the events. For hydrological events, severity is equivalent to deficit volume in units of mm. Therefore, drought intensity represents the averaged magnitude and is denoted by:

$$Intensity = \frac{Severity}{t_e - t_i + 1} \tag{3.9}$$

The spatial extent of drought is expressed by the Drought Area Index (DAI), which measures the proportion of a region being affected by precipitation/runoff drought at month i:

$$DAI_i = \frac{Nd_i}{N_i} \cdot 100\% \tag{3.10}$$

where DAI_i represents the percentage of the region being drought-affected at month i, Nd_i is the number of cells of the region being drought affected at month i, and N_i is the total number of cells of the region. DAI does not consider the intensity of the events, and no area weighting has been applied. DAI25 (DAI50) denotes the percentage of the 50-year period during which $\geq$25% (50%) of the region being drought-affected.

DAI25 and DAI50 are regional drought parameters. Drought severity values obtained for each grid of the study region were averaged spatially for regional drought analysis. The use of these parameters provides no information on the timing of the events as they describe drought conditions over the 50-year period. For instance, in Section 5.8, it would not be possible to determine whether a meteorological drought event coincides with/lags a hydrological event. The study area and regions are detailed in Section 3.9.

3.9 Study Area and Regions

The European study area is defined as 35°–70°N, 25°W–70°E. For each simulation, meteorological (hydrological) severity results and the percentage of the region being drought-affected were generated for each of the 9140 (8385) cells within this area, before being averaged geographically and/or climatically (Figure 3.4).

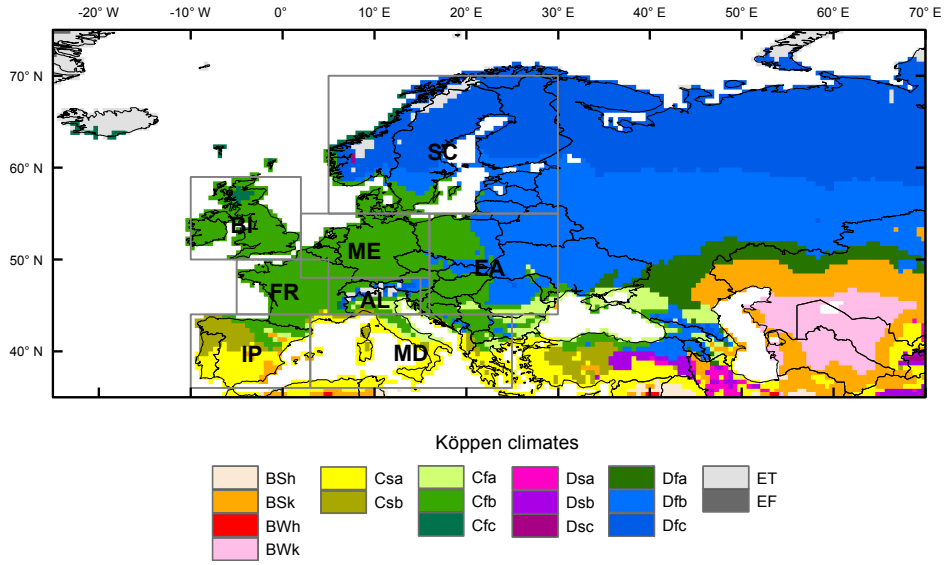

Figure 3.4: Study area and regions. Geographic (PRUDENCE) regions (Table 3.3) are found westwards of 30°E. Climate (Köppen) zones, as specified in the legend, span the entire study area.

Geographically-averaged results are based on the sub-regions of the PRUDENCE project (Christensen *et al.*, 2007; Table 3.3); they are referred to as "PRUDENCE results" in this thesis. Since significant climatic variations may occur within a PRUDENCE region (e.g. IP), climatically-averaged results may compliment the PRUDENCE results. The Köppen climate classification is one of the most frequently used. Classification information was obtained from the Supplementary Material of Peel *et al.* (2007); information at the 0.5° was extracted from the $0.1° \times 0.1°$ map. Based on vegetation, temperature and precipitation, 17 classes were differentiated for the study area (Figure 3.4); "EF" climate occurs in only five cells, hence was omitted from the analyses. Regional results in this thesis therefore enable comparisons with previous and subsequent studies.

Area	West	East	South	North
British Isles (BI)	–10	2	50	59
Iberian Peninsula (IP)	–10	3	36	44
France (FR)	–5	5	44	50
Mid-Europe (ME)	2	16	48	55
Scandinavia (SC)	5	30	55	70
Alps (AL)	5	15	44	48
Mediterranean (MD)	3	25	36	44
Eastern Europe (EA)	16	30	44	55

Table 3.3: European sub-regions defined in the "PRUDENCE" project (Christensen and Christensen, 2007)

3.9.1 Köppen Climates

The Köppen climate classification, detailed in Henderson-Sellers and Robinson (1986) and Peel *et al.* (2007) (particularly Table 1), is briefly described here. The study area contains four main climate types: arid B, temperate C, cold D and polar E. The second letter indicates the precipitation pattern: s represents a dry summer and w for dry winter. The third letter indicates the degree of summer heat: for B climates, h and k signify low and middle latitude climates, respectively; for C and D climates, a, b and c represent hot, warm and cold summer, respectively. Polar E climates concentrate in the high latitudes/altitudes.

Much of the mid-latitude central-western Europe have *marine west coast* climate with precipitation all year round (Cf). The *Mediterranean* climate is characterised by warm-hot dry summers and cool, wet winters (Csa, Csb; Spain, Italy, Greece). *Cold west coast* climate dominate the eastern half of the mid- and high-latitudes with low summer precipitation (Df; Scandinavia, Russia, eastern Europe and the Caucasus). Much of Central Asia is under the influence of cold *interior desert* climate (BWk and BSk). The mechanisms contributing to these climates are provided in Robinson and Henderson-Sellers (1999).

3.10 Summary

This chapter has outlined the emission scenarios and models, including MAGICC6, ClimGen and Mac-PDM.09, used in this thesis for generating precipitation and runoff timeseries. It has also described the identification and quantification of short and long droughts as applied in Chapters 4–6. The next chapter examines the effects of climate change on European meteorological drought characteristics and the associated uncertainties in the projections.

Chapter 4

Projections of European meteorological droughts: robustness and uncertainties

4.1 Introduction

Over the 20th century, higher European latitudes experienced increased wetting, particularly in winter (Lloyd-Hughes and Saunders, 2002; Briffa *et al.*, 2009) while the Mediterranean became drier, especially in summer (Gao *et al.*, 2006; Sousa *et al.*, 2011). However, Bladé *et al.* (2012) found enhanced summer precipitation in the Mediterranean, particularly Italy and the Balkans, associated with high summer (July–August) North Atlantic Oscillation (SNAO) (Folland *et al.*, 2009; Linderholm *et al.*, 2011). They attributed this to a strong upper-level trough over the Balkans that develops in association with the SNAO, which causes mid-level cooling and increased potential instability. Since the 1950s, the area covered by dry (wet) events has increased (decreased) (Bordi *et al.*, 2009). Climate change could shift and widen the precipitation distribution, increasing the risk of both flood and drought events (Gao *et al.*, 2006), and may alter the characteristics of future dry and wet spells in Europe (Heinrich and Gobiet, 2011). The common view is that precipitation will decrease (increase) in southern (northern) Europe.

Warming may increase the drought-affected area globally, including more severe events

(Burke and Brown, 2008). Although there are different classifications of drought (Section 2.2) depending on the nature of the water deficit and the study objective (Wilhite and Glantz, 1985; AMS, 2004), precipitation is the fundamental driver of drought and analysing future precipitation characteristics is crucial in drought risk assessment (Bordi *et al.*, 2009), especially when considering meteorological droughts (Panu and Sharma, 2002). Many studies have focused on the hydrological aspects (such as river discharge and low flow regimes) rather than assessing meteorological events (Vasiliades *et al.*, 2009). Yet, the application of meteorological drought indices require less input data, which in turn limits the additional uncertainties arising from the availability, quality, resolution and parameterisations of data/models. Furthermore, Hisdal *et al.* (2001) found good agreement between precipitation deviations and droughts trends. Therefore, this chapter focuses on meteorological drought assessment, but see Section 5.8 for a comparison with hydrological drought assessment.

Our incomplete understanding of the behavior of the climate system has led to the development of various emission scenarios and GCMs. Studies with equally weighted multi-models generally outperform the single models (Weigel *et al.*, 2010). However, projections for both mean (Kjellström *et al.*, 2011) and extreme (Frei *et al.*, 2006; Beniston *et al.*, 2007; Blenkinsop and Fowler, 2007a;b; Burke and Brown, 2008) precipitation are often uncertain in both the direction and magnitude of change. Changes in the seasonal distribution of precipitation and drought occurrence will significantly affect water resource management (Blenkinsop and Fowler, 2007a). Although some European drought studies (e.g. Dubrovsky *et al.*, 2005; Blenkinsop and Fowler, 2007a;b; Dubrovsky *et al.*, 2008; Vidal and Wade, 2009; Heinrich and Gobiet, 2011) have attempted to address this through a multi-model and multi-scenario analysis, the number of climate models and emission scenarios applied are often limited, and few (e.g. Burke and Brown, 2008) have explored uncertainty in drought projection using large simulation ensembles.

Using the SPI (Section 4.2.2), this chapter examines the effects of climate change on European meteorological drought characteristics for both 3-month (SPI3) and 12-month (SPI12) events, and assesses their robustness based on precipitation scenarios simulated using ten emission scenarios and eighteen GCMs (Sections 4.4–4.5). GCMs and emission scenarios tend to dominate the uncertainty of climate change (Planton *et al.*, 2008),

and therefore projections of drought should incorporate fully these effects. The relative contribution of emission scenario and GCM variance is also quantified (Section 4.6).

4.2 Methodology

4.2.1 Modelling Framework

MAGICC6 and ClimGen simulations of 21st century monthly precipitation timeseries based on 10 emission scenarios (hereafter, scenarios) and 18 GCMs were assessed (see Section 3.5 for details). Consequently, an ensemble of 180 precipitation scenarios were used for the SPI computation (Section 4.2.2.5) and subsequent drought analysis (Section 4.2.3).

4.2.2 Standardized Precipitation Index (SPI)

The Standardized Precipitation Index (SPI) is one of most widely used drought indices in drought assessment. It has been applied to Africa (e.g. Rouault and Richard, 2005; Lyon, 2009; Roudier and Mahe, 2010), Australia (e.g. Khan *et al.*, 2008), Europe (e.g. Bordi *et al.*, 2001; Loukas and Vasiliades, 2004; Vicente-Serrano and López-Moreno, 2005; López-Moreno and Vicente-Serrano, 2008; Bordi *et al.*, 2009; Vasiliades *et al.*, 2009; Koutroulis *et al.*, 2011), Central (e.g. Méndez and Magaña, 2010) and North America (Motha and Baier, 2005; Kangas and Brown, 2007; Weiss *et al.*, 2009; Logan *et al.*, 2010; McCrary and Randall, 2010), the Middle East (e.g. Türke and Tatl, 2009; Raziei *et al.*, 2010) and other regions. SPI is commonly used operationally to monitor the onset and duration of droughts (Hayes *et al.*, 1999) worldwide by organisations or cooperative efforts including the Global Drought Monitor (Benfield UCL Hazard Research Centre), the APEC Climate Center (APCC) Global Drought Monitoring, the North America Drought Monitor (NADM), the U.S. National Drought Mitigation Center (NDMC), the Drought Management Centre for Southeastern Europe (DMCSEE), and the Caribbean Drought and Precipitation Monitoring Network (CDPMN).

The SPI was developed at Colorado State University in 1993 as an alternative to Palmer's index (see Section 2.2.3) that addresses many of the PDSI's weaknesses (Mckee *et al.*, 1993; 1995). It measures meteorological events and is normalised to identify

SPI values	Intensity	Probability %	Cumulative probability
2.0 or more	Extremely wet	2.3	0.9986
1.5 to 1.99	Very wet	4.4	0.9332
1.0 to 1.49	Moderately wet	9.2	0.8413
-0.99 to 0.99	Near normal	68.2	0.6915
-1.0 to -1.49	Moderately dry	9.2	0.1587
-1.5 to -1.99	Severely dry	4.4	0.0668
-2.0 or less	Extremely dry	2.3	0.0228

Table 4.1: SPI intensity and corresponding event probabilities (Mckee *et al.*, 1993; Shen *et al.*, 2008)

both dry and wet periods (Bordi *et al.*, 2009) for any location with a long-term precipitation record (typically $\geq$30 years). Dry (wet) spells, represented by negative (positive) SPI values, are expressed in terms of precipitation deficit (surplus), percent of normal and probability of non-exceedance (Heim Jr., 2002), with one/two/three standard deviations occurring approximately 68%/95%/99% of the time (Hayes *et al.*, 1999; Table 4.1).

A probability density function (PDF; e.g. Pearson Type III or Gamma) is fitted — separately for each month of the lagged moving average precipitation timeseries — to the frequency distribution of precipitation summed over the timescale concerned. Each PDF is then transformed into a standardised Gaussian distribution (Edwards and McKee, 1997). Therefore, a percentile on the fitted distribution corresponds to the same percentile (Z-score) on the standard Gaussian distribution and the SPI value (Wilhite, 2005); the SPI represents a cumulative probability in relation to a reference period for which the probability distribution parameters are estimated. SPI normalises an anomaly both spatially (by considering the precipitation frequency distribution and the accompanying variation at the location) and temporally (as it can be computed at any timescale). The SPI for any given location (and duration) is expected to have a mean of zero and a variance of one, at least during the calibration period. Table 4.1 shows the categories of drought intensities; a drought is generally defined when SPI≤ -1.0 and to end when the SPI becomes positive (Mckee *et al.*, 1993).

Vicente-Serrano *et al.* (2010) proposed the multi-scalar standardised precipitation evapotranspiration index (SPEI), the computation of which is mathematically similar to the SPI. The SPEI uses precipitation and temperature data, and can be compared to the self-calibrated Palmer drought severity index (sc-PDSI) as it is based on a normalisation of the simple water balance developed by Thornthwaite (1948). The SPI, rather than

the SPEI, has been adopted in this thesis as a measure of meteorological drought (which typically refers to rainfall deficit), and also for reasons described in Sections 4.2.2.1 and 4.2.2.2; the effect of temperature and potential evapotranspiration (PET), is explored in Chapter 5.

4.2.2.1 Suitability

Keyantash and Dracup (2002) and Quiring (2009b) assessed the overall utility of meteorological indices using six criteria, *viz*. robustness, tractability, transparency, sophistication, extendability and dimensionality. They found SPI (along with rainfall deciles / percentiles) to be highly valuable for monitoring meteorological drought (see below). The National Meteorological and Hydrological Services (NMHSs) globally have been recommended to characterise meteorological droughts using the SPI (Hayes *et al.*, 2011). The intensity, magnitude and duration of a drought can be determined, along with the historical data-based probability of emerging from a specific drought (Heim Jr., 2002).

For the mountainous Aragon River Basin, central Spanish Pyrenees, (Vicente-Serrano and López-Moreno, 2005) found that short SPI timescales (1–3 months) generally corresponded to river flow droughts, and longer timescales (7–10 months) were useful for analysing droughts in reservoir storage. However, seasonality was found in the suitability of the SPI for monitoring droughts, e.g. river flows in autumn responded well to 1–7 month SPI timescales as both the moisture conditions found at the beginning of the season and the short-scale precipitation conditions govern the hydrological response. On timescales of 9–12 months, SPI corresponds closely to the PDSI (Guttman, 1998; Heim Jr., 2002; Dubrovsky *et al.*, 2008), i.e. precipitation causes much of the variability in the PDSI results (Lloyd-Hughes and Saunders, 2002). Hayes *et al.* (1999) discussed the advantages of SPI over the complex Palmer index (Alley, 1984) (see Section 4.2.2.2); Guttman (1998) and Lloyd-Hughes and Saunders (2002) indicated that SPI provides a better spatial standardisation than the PDSI. SPI also correlates well with fluctuations in shallow groundwater tables in irrigated areas of Australia where rainfall variability is a very influential variable, and can capture major dry periods; therefore the SPI could potentially be adopted for environmental reporting and relating climatic impacts on groundwater levels (Khan *et al.*, 2008).

4.2.2.2 Advantages of the SPI

Lloyd-Hughes and Saunders (2002) found the SPI to be a simple and effective tool for studying European drought. Simplicity is its fundamental strength, with precipitation being the only required input data. Its independence of soil moisture conditions implies that SPI is effective during both winter and summer, nor is it adversely affected by topography. Its variable timescale makes it suitable for assessing various classifications of drought — durations of weeks or months can be defined for meteorological and agricultural applications; durations of years for hydrological and water management purposes (Hayes *et al.*, 1999; Heim Jr., 2002). The standardisation enables comparison across the time period of study, location and climate as both SPI and the lagged moving average precipitation timeseries have the same probability of exceedence (i.e. number of months with values below the threshold level; Steinemann *et al.*, 2005); it is also very practical since events can be associated to a return period (Roudier and Mahe, 2010).

In summary, the SPI is useful for monitoring drought (and wetness) on multiple timescales and comparing climatic conditions of areas governed by different hydrological regimes (Bordi *et al.*, 2009).

4.2.2.3 Limitations of the SPI

Despite its simplicity, SPI excludes other drivers of drought, (e.g. modified evapotranspiration and available energy; Burke, 2011), shows much smaller global land surface areas in drought than other indices that account for atmospheric demand for moisture (Burke and Brown, 2008), and does not consider snowfall. Although hydrological droughts may be represented by the SPI (Nalbantis and Tsakiris, 2008; Tabrizi *et al.*, 2010), drought indicators that include additional processes may be more appropriate for sectoral (e.g. agriculture) impacts assessments (Vidal and Wade, 2009; Burke and Brown, 2010).

Other drawbacks include (Hayes *et al.*, 1999): (1) The identification of a “suitable” theoretical probability distribution for modeling the raw precipitation data prior to standardisation; (2) The quantity and quality of the precipitation data used in the calculation determines its accuracy (which also applies to other indices); (3) Aggregating or averaging precipitation records over space (and time) to obtain mean values may smooth data and

distort the true precipitation distribution (Quiring, 2009b); (4) Since any drought intensity occurs with the same frequency (Table 4.1) for all locations when considered over a long time period, SPI by itself is incapable of identifying the more "drought-prone" regions; (5) Application at short timescales (1–3 months) to regions with low seasonal precipitation may produce misleadingly large positive or negative SPI values; and, (6) The statistical Z-score may not be intuitive to decision-makers. Also, equal categorical intervals have differing probabilities of occurrence, e.g. the probability differential between SPI -1.0 and -1.5 is 9.1%, and between -1.5 and -2.0 is 4.4% (Steinemann *et al.*, 2005).

4.2.2.4 Suitability of Gamma Distribution

Precipitation has a fixed lower boundary (i.e. zero), thus produces a positively skewed distribution (Quiring, 2009a). Significantly skewed precipitation distribution is commonly transformed to a more symmetrical, Gaussian-like distribution by fitting a statistical distribution. This provides a method for estimating the relative frequency (rarity) of a given drought event based on the observations (Husak *et al.*, 2007).

A variety of distributions have been recommended for fitting precipitation (drought) data, including gamma, log-normal, Pearson type III, and Box-Cox (Guttman, 1999; Lloyd-Hughes and Saunders, 2002; Husak *et al.*, 2007); different distributions would yield different SPI values (Quiring, 2009b). Guttman (1999) concluded that the Pearson Type III distribution provides the "best" model for SPI computation. However, it is not suitable for climate change analysis as the distribution is undefined if the future monthly precipitation total is lower than the fitted location parameter — the likelihood of which is high since a strong drying trend has been projected, particularly for the Mediterranean region. Lloyd-Hughes and Saunders (2002) found that the gamma distribution best modeled European monthly precipitation compared to Gaussian and log-normal distributions. This is especially the case for arid regions at short timescales, except for regions south of 45°N that have a more skewed precipitation distribution in arid areas (e.g. eastern Turkey and northwest Spain).

The gamma distribution is popular as it can represent a variety of distribution shapes, from exponential decay (α=1) to near-normal (α=20), using only the shape (α) and scale (β) parameters (Husak *et al.*, 2007). According to central limit theorem, the longer the

length of the timeseries, the distribution of the timeseries mean tends towards a more normal distribution (e.g. as α tends to infinity; Lloyd-Hughes and Saunders, 2002). It is positively skewed and is bounded on the left by zero, which is important since negative precipitation is impossible (Quiring, 2009a).

4.2.2.5 Computation

For a chosen timescale (e.g. 3-month), m, a lagged moving average was computed for the monthly precipitation timeseries (hereafter, "precipitation timeseries"), therefore the value at month i also accounts for conditions in the preceeding i–1 months.

The gamma distribution was then applied, using the $pgamma$ function in R (R Development Core Team, 2012) that gives the distribution function, to model this precipitation timeseries; its PDF is defined as:

$$g(x) = \frac{1}{\beta^{\alpha}\Gamma(\alpha)} x^{\alpha-1} e^{-x/\beta} \qquad \text{for} \quad x > 0 \tag{4.1}$$

where α>0 is a shape parameter, β>0 is a scale parameter, and x>0 is the (projected or present-day) precipitation amount in month *t*. $\Gamma(\alpha)$ is the gamma function and is defined as:

$$\Gamma(\alpha) = \lim_{n\to\infty} \prod_{v=0}^{n-1} \frac{n! n^{y-1}}{y+v} \equiv \int_0^{\infty} y^{\alpha-1} e^{-y} \mathrm{d}y \tag{4.2}$$

The parameters α and β for the calendar month i can be estimated with the following approximations to the maximum likelihood method (Thom, 1958):

$$\hat{\alpha}_i = \frac{1}{4A_i}\left(1 + \sqrt{1 + \frac{4A_i}{3}}\right) \tag{4.3}$$

$$\hat{\beta}_i = \frac{\bar{x}}{\hat{\alpha}_i} \tag{4.4}$$

where, for n observations

$$A_i = \ln(\bar{x_i}) - \frac{\sum \ln(x_i)}{n} \tag{4.5}$$

Integrating the PDF with respect to x and entering the estimates of α_i and β_i produces

an expression for the cumulative probability $G(x)$ of the precipitation amount occurring for a given month and timescale. This cumulative probability distribution is then transformed into the standard normal distribution, using the $qnorm$ function in R, to generate the SPI.

The gamma distribution is undefined for x=0, and $P(x$=0)>0, where $P(x$=0) is the probability of zero precipitation. Abramowitz and Stegun (eds) (1965) and Husak *et al.* (2007) offered approximate conversion for these undefined entries; instead, this study carried out a linear interpolation between the preceding and subsequent SPI values. Where these undefined entries occurred at the start (or end) of the timeseries, the subsequent (or preceding) SPI value was adopted. Cells with >10% of the timeseries that cannot be modelled by the gamma distribution (i.e. >10% of the values of the precipitation timeseries were zero) were excluded as drought analysis for very dry regions would not be so meaningful. For α with values >100, they were adjusted to 100 to avoid very large α and very small β values as the product of α and β gives the mean; such adjustment would have little impact on the gamma distribution as $\alpha\approx$100 is similar to a Gaussian distribution.

4.2.3 Drought Analysis

Drought identification and the parameters (i.e. drought severity and frequencies of DAI25 and DAI50) used and the timescales considered, along with study area/regions are detailed in Sections 3.6–3.9. Both short (SPI3) and long (SPI12) droughts, defined as SPI≤ -1.5 (a *severe*/*extreme* drought, Table 4.1), were studied. Climate change effects were determined by comparing results in 2001–2050 and 2051–2100 to those in 1951–2000. Drought severity was derived for each of the 9140 cells within the study area. Regional severities, DAI25 and DAI50 frequencies (see Section 3.8), based on the PRUDENCE regions and Köppen climates types (see Section 3.9), are presented for analysis in Sections 4.4–4.6.

4.3 Drought Threshold Expressed as Precipitation

Since SPI is standardised (Section 4.2.2.3), it provides no information on the concerned threshold/intensity in absolute precipitation terms, which could be more useful in practical applications. This is shown in Figure 4.1 — for each cell, the precipitation

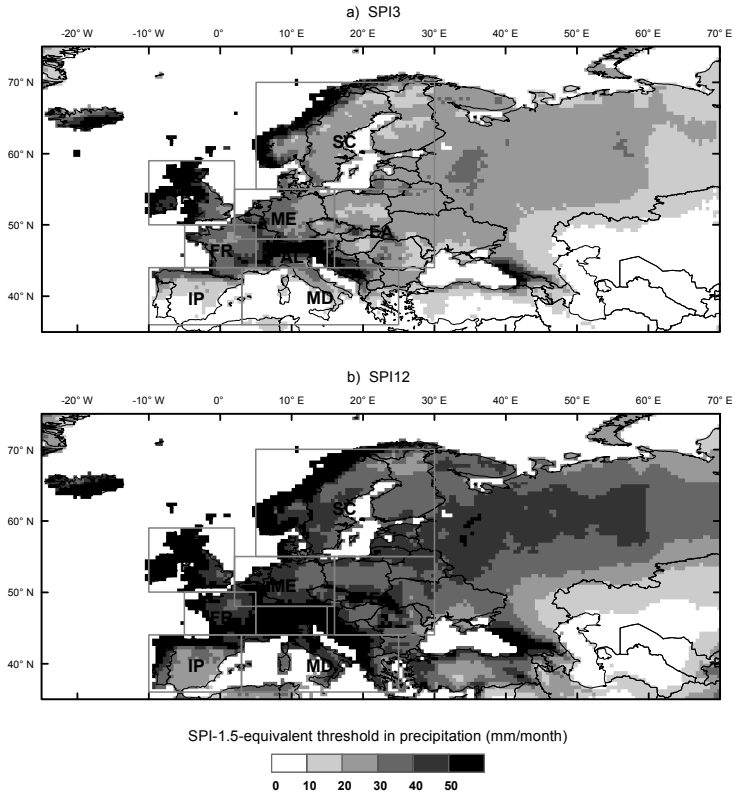

Figure 4.1: Threshold in precipitation (mm/month) that has the same percentile as less than SPI-1.5 during 1951–2000 for (a) SPI3 and (b) SPI12 events.

threshold value is comparable to SPI-1.5 as both have the same percentile exceedence. Similar to the runoff thresholds (Section 3.7.1), the absolute precipitation threshold for each cell was derived by identifying the percentile based on the number of months of the SPI timeseries with values being ≤ -1.5 in the 1951–2000 period. This percentile was then applied to the 1951–2000 lagged moving average precipitation timeseries to extract the threshold in absolute precipitation, i.e. the probability of the precipitation timeseries falling below the identified precipitation threshold is the same as the SPI value being ≤ -1.5 in the 1951–2000 period. Alternatively, absolute precipitation could also be obtained by interpolating the shape and scale parameters of the gamma distribution.

According to Figure 4.1, the 3-month or 12-month lagged moving average precipitation that corresponds with the SPI-1.5 drought definition varies widely across Europe, ranging from under 10 mm to over 50 mm. In general, higher precipitation threshold values occur in northwestern BI, western coast of Norway, AL, and parts of Russia and the Caucasus. Sub-regional variations in Scotland and southeastern England, for example, may require water resource and drought management strategies to be designed for

very different precipitation levels. Therefore, "relative drought conditions" in different regions may correspond with rather different absolute amounts of rainfall; it is also likely to depend on socio-economic factors such as demand and population.

4.4 Future Changes in Drought

This section presents the projected changes in drought parameters under the 21st century climates. Firstly, ECHam5 under RCP6 is used to demonstrate the spatial variations in the simulated changes in drought severity across the study region (Section 4.4.1). ECHAM5 was chosen as according to Reichler and Kim (2008), it simulated the current climate for 14 climate variables very well compared to most other GCMs. Gleckler *et al.* (2008) found ECHAM5 to be superior in many respects in the extra-tropics and has smaller errors than other "typical" models. Pierce *et al.* (2009) assessed the performance of 21 GCMs using 42 metrics based on seasonal temperature and precipitation, the ENSO and Pacific Decadal Oscillation for western U.S., and ECHAM5 was amongst the better performing models. Hurkmans *et al.* (2010) provided a brief discussion on the choice of ECHAM5–MPI-OM over other GCMs by drawing on results from other research (e.g. Covey *et al.*, 2003; van Ulden and van Oldenborgh, 2006; Reichler and Kim, 2008) that compared model performance based on a range of climate variables. RCP6 was selected to represent moderate radiative forcing (see Section 3.4.2). Secondly, the regional changes in drought parameters based on 180 simulations described in Section 4.2.1 are summarised in Section 4.4.2.

4.4.1 Spatial Variations of Changes in Drought Severity

Figures 4.2–4.4 show the present-day SPI12 and seasonal drought severities, along with their percentage changes in the 21st century projected by ECHAM5 under RCP6. The small spatial and seasonal variations in the 1951–2000 values for both SPI12 and SPI3 (Figures 4.2a and 4.3) are due to the standardised nature of the SPI (see Section 4.2.2).

For the 21st century drought severities, Figures 4.2b, 4.2c and 4.4 generally reveal increases in the lower-latitudes and decreases in the high-latitudes. The largest magnitudes of change (in both directions) in 2051–2100 are of course considerably more widespread

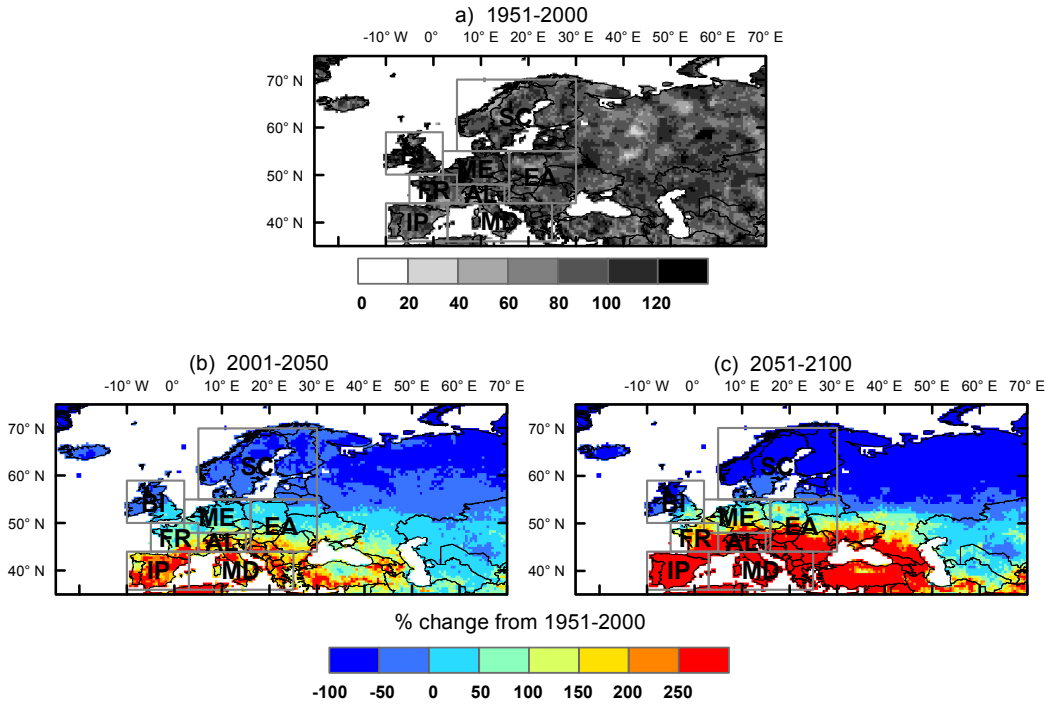

Figure 4.2: SPI12 drought severity (in standard deviation months) in (a) 1951–2000, along with the percentage changes in (b) 2001–2050 and (c) 2051–2100, from 1951–2000, projected by ECHAM5 under RCP6.

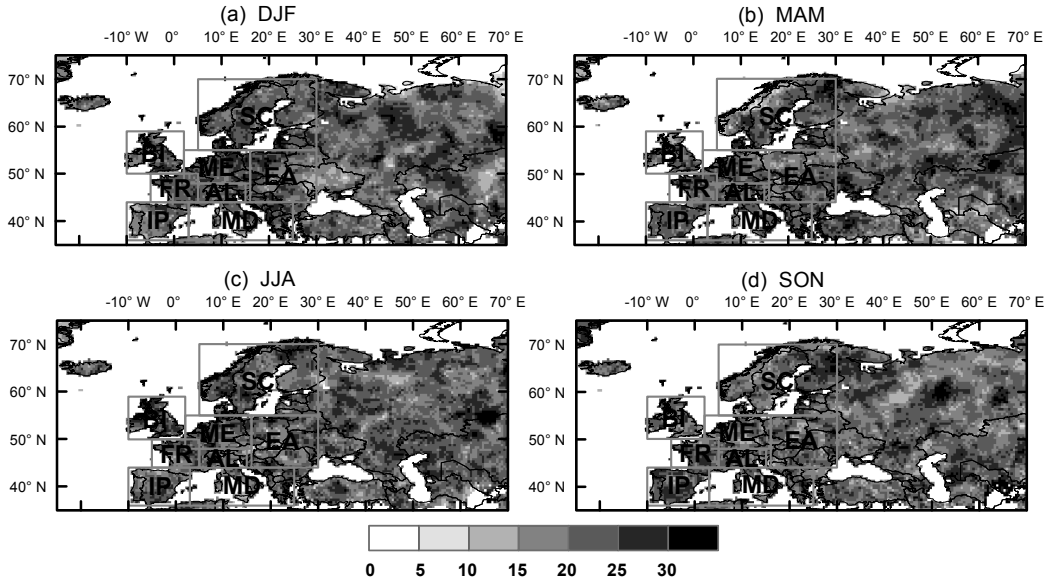

Figure 4.3: Seasonal drought severity (in standard deviation months) in 1951–2000.

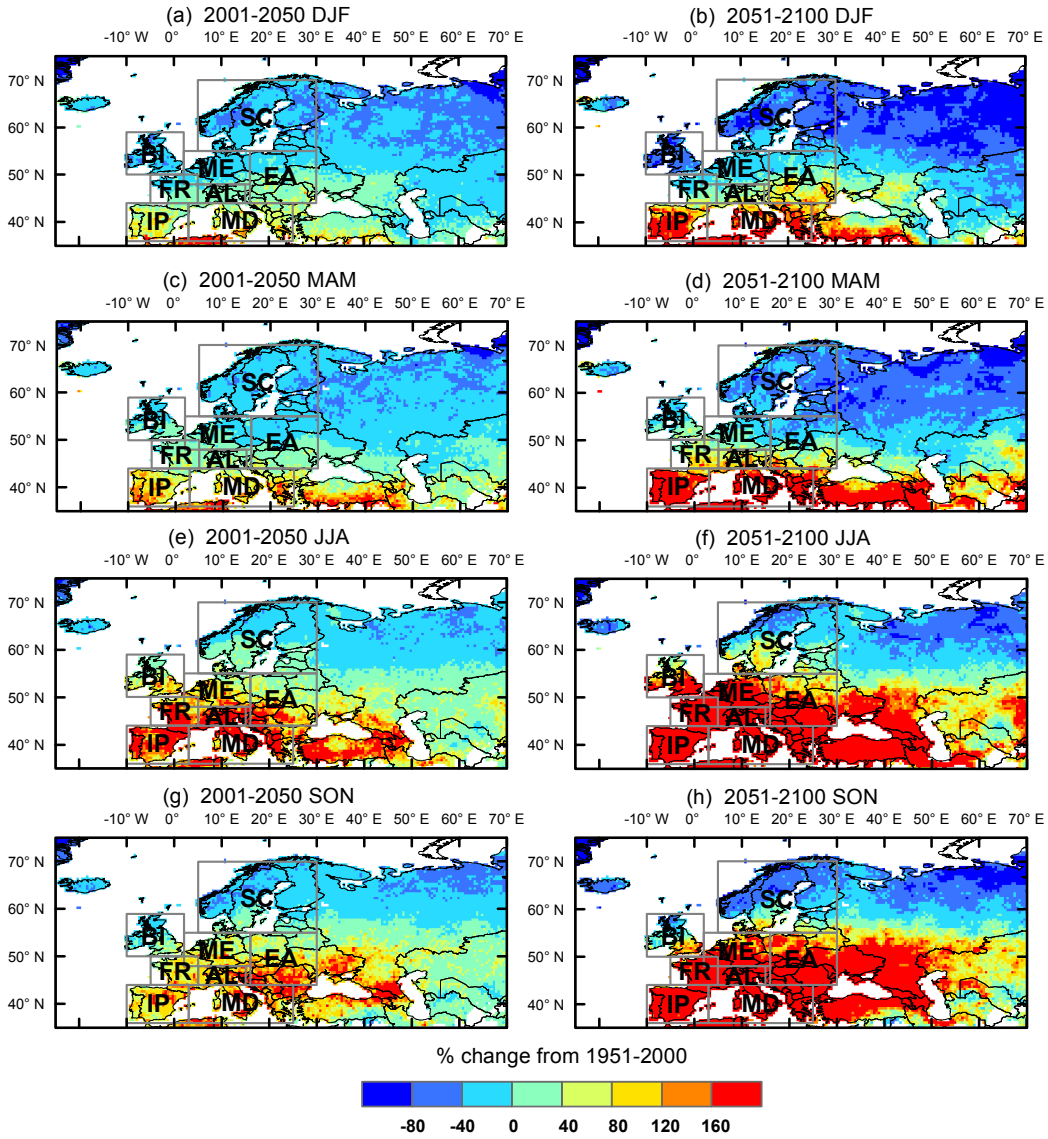

Figure 4.4: Percentage changes in seasonal drought severity in 2001–2050 (left panels) and 2051–2100 (right panels), from 1951–2000, projected by ECHAM5 under RCP6.

than in 2001–2050. Seasonally, the largest decreases occur in the cold seasons whereas the largest increases are found in the warm seasons. Marked increases, by $>$3.5 times for SPI12 and $>$2.6 times for SPI3, in drought severity are simulated for areas around the Mediterranean and Black Sea basins; such increases are projected to occur in 2051–2100 across large parts of this regions even in the cold seasons.

4.4.2 Projections by 18 GCMs under 10 Emission Scenarios

Figure 4.5 shows the level of agreement in the direction of change according to the 180 simulations for PRUDENCE- and Köppen-averaged results. A “robust change” is

defined as occurring when all 180 simulations indicate the same direction of change. A "general positive/negative change" is defined when >90 of the total 180 simulations project an increase/decrease. "Mixed / no change/events" (green) may refer to (1) no identified droughts (notably in frequencies of DAI50, but also in some DAI25 cases), (2) no changes in drought parameters, or (3) when exactly 90 of the 180 simulations project an increase/decrease. The number represents the percentage of total simulations showing increase/decrease. Figure 4.5 does not provide information about the magnitude of change nor about individual simulations. Magnitudes of change — in interquartile ranges (IQRs) and ensemble means (in brackets) — for robust trends are presented in Figures 4.6 and 4.7; IQRs are considered a more representative and robust measure of uncertainty. The discussion in this Section is based on Figures 4.5–4.7; absolute DAI25 frequencies (not shown) quoted below also refer to IQRs.

Figure 4.5 shows that increasing severity and occurrence of large-scale drought are projected for most regions, except for some PRUDENCE (SC) and Köppen (Cfc, Dfc, ET) regions. Overall, robust increases (decreases) in drought conditions are concentrated in southern (northern) Europe; they also tend to vary little with different seasons. Similarly, other studies have shown that the 20th century drying (wetter) trend is likely to continue in western/central Europe (western Russia) (Pal *et al.*, 2004); GCMs and RCMs generally simulate strong increases (decreases) in mean annual precipitation in higher (lower) European latitudes in future (Räisänen *et al.*, 2004; Gao *et al.*, 2006; Beniston *et al.*, 2007; Heinrich and Gobiet, 2011), with uncertain sign of change in the ∼500 km-zone in between (Kjellström *et al.*, 2011). Intensifying wet events in northern Europe, and longer, more frequent, severe and widespread droughts in southern Europe have been projected with high statistical significance and confidence (Heinrich and Gobiet, 2011); much of France, southern England and the western/central Mediterranean could experience the largest increases in maximum dry spell length (Loukas *et al.*, 2008).

Increasing localised precipitation may occur in areas with declining mean precipitation (Buonomo *et al.*, 2007; García-Ruiz *et al.*, 2011), e.g. westward side of mountain chains of western and central Europe due to enhanced westerly winds (Gao *et al.*, 2006). Subsequently, both increasing intense precipitation and more severe "dry and hot" extremes (Kundzewicz *et al.*, 2006), along with increasing drought and flood magnitude,

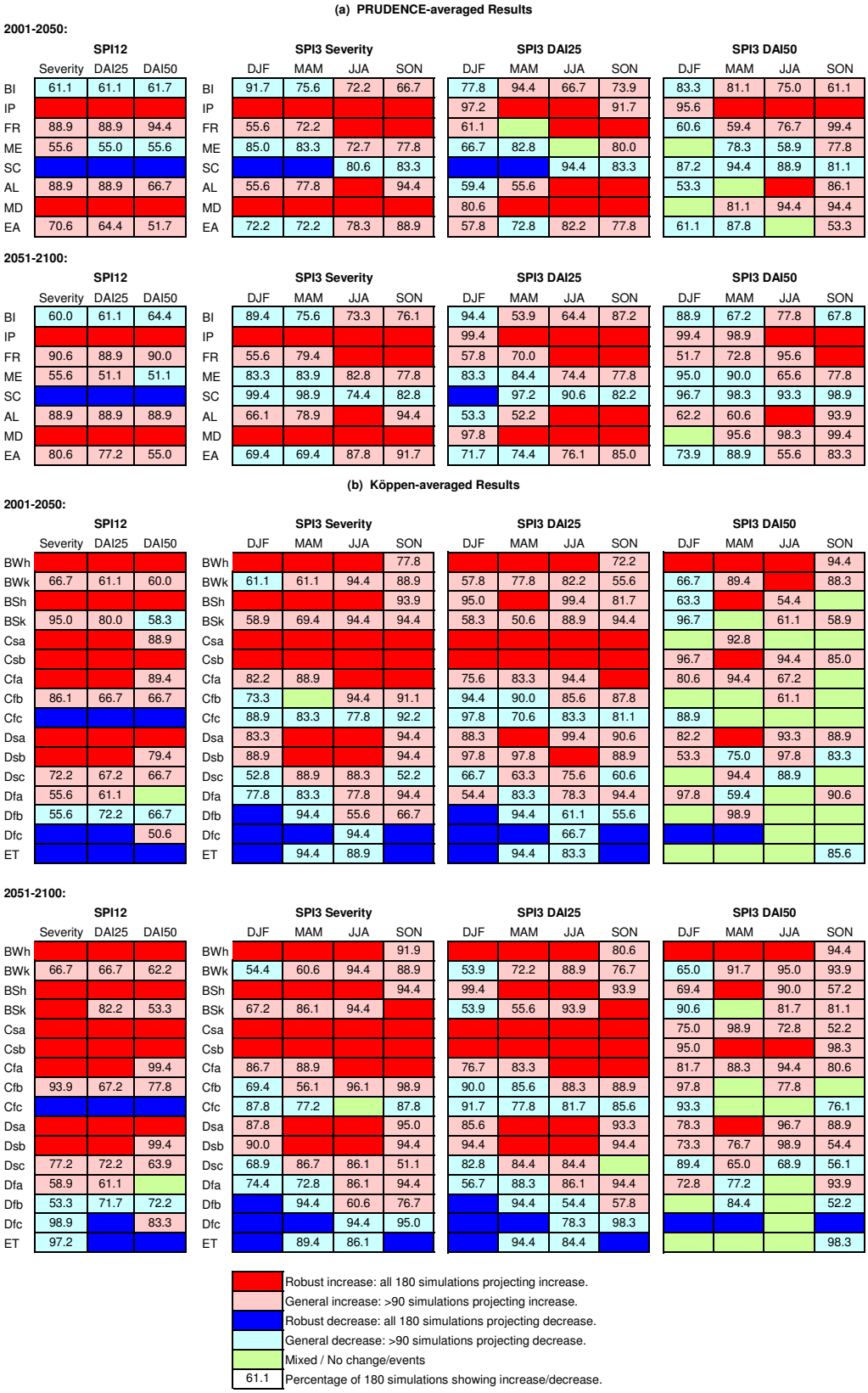

Figure 4.5: Direction of change, from 1951–2000, projected by 18 GCMs under 10 emission scenarios for (a) the PRUDENCE- and (b) Köppen-averaged drought parameters. The number represents the percentage of the total 180 simulations showing positive/negative changes.

(a) SPI12 Results

	2001-2050			2051-2100		
	Severity	DAI25	DAI50	Severity	DAI25	DAI50
BI						
IP	1.9-2.9 (2.4)	2.3-3.2 (2.7)	2.1-4.7 (3.4)	3.4-6.4 (4.8)	3.8-6.1 (5.0)	6.3-15.7 (10.9)
FR						
ME						
SC	0.5-0.7 (0.7)	0.4-0.6 (0.5)	0.7-0.7 (0.7)	0.2-0.5 (0.3)	0.2-0.3 (0.2)	0.7-0.8 (0.7)
AL						
MD	1.6-2.4 (2.0)	1.5-2.6 (2.0)	1.6-2.4 (2.2)	2.7-5.4 (3.7)	2.2-6.7 (4.6)	2.5-6.5 (3.5)
EA						

(b) SPI3 Severity

	2001-2050				2051-2100			
	DJF	MAM	JJA	SON	DJF	MAM	JJA	SON
BI								
IP	1.3-1.6 (1.4)	1.3-1.8 (1.5)	1.6-2.4 (2.0)	1.4-1.7 (1.5)	1.7-2.6 (2.1)	1.8-3.4 (2.4)	2.7-5.4 (3.8)	1.9-3.3 (2.5)
FR			1.4-2.3 (1.7)	1.2-2.1 (1.6)			1.8-5.0 (2.8)	1.6-4.1 (2.6)
ME								
SC	0.7-0.8 (0.7)	0.7-0.8 (0.7)						
AL			1.4-2.3 (1.6)				1.8-4.9 (2.8)	
MD	1.2-1.6 (1.3)	1.3-1.6 (1.4)	1.5-2.2 (1.7)	1.3-1.9 (1.5)	1.5-2.7 (1.8)	1.7-2.8 (2.2)	2.3-4.7 (3.2)	1.9-3.7 (2.6)
EA								

(c) SPI3 DAI25

	2001-2050				2051-2100			
	DJF	MAM	JJA	SON	DJF	MAM	JJA	SON
BI								
IP		1.3-2.0 (1.5)	1.9-3.8 (3.2)			1.9-3.3 (2.4)	4.5-7.9 (6.3)	2.3-3.9 (3.2)
FR			1.6-3.4 (2.5)	1.3-2.3 (1.8)			2.6-6.5 (4.5)	1.9-4.3 (3.0)
ME								
SC	0.5-0.6 (0.5)	0.6-0.8 (0.7)			0.2-0.4 (0.2)			
AL			1.4-2.7 (1.8)	1.4-2.2 (1.8)			2.0-5.3 (3.4)	1.9-4.2 (3.1)
MD		1.7-2.1 (1.9)	2.0-3.2 (2.4)	1.4-2.4 (1.7)		2.2-3.3 (2.6)	3.3-7.5 (5.0)	2.4-5.3 (3.7)
EA								

(d) SPI3 DAI50

	2001-2050				2051-2100			
	DJF	MAM	JJA	SON	DJF	MAM	JJA	SON
BI								
IP		1.4-2.2 (2.0)	7.0-10.0 (8.0)	1.4-1.6 (1.4)			11.0-39.3 (18.0)	2.2-4.0 (3.0)
FR								2.2-5.4 (3.3)
ME								
SC								
AL			1.5-4.1 (2.5)				2.5-15.1 (5.5)	
MD								
EA								

Figure 4.6: Magnitude of change, expressed as ratio to 1951–2000 values, for the interquartile ranges (IQRs) and ensemble means (in brackets) of drought parameters simulated using 18 GCMs under 10 emission scenarios for the PRUDENCE regions. Categories with robust increases (red) and decreases (blue) are shown.

may occur in central Mediterranean and central-western Europe (Pal *et al.*, 2004). This may partly explain the smaller percentage of simulations indicating increases in SPI12 DAI25 frequency than SPI12 severity for Cfb (Figure 4.5b), which covers much of central-western Europe.

Seasonally, Figure 4.5 reveals that robust increases (decreases) for all the drought parameters are more common in summer/autumn (winter/spring). Change magnitudes are often largest in summer, followed by autumn, and smallest in winter; regional variations are more apparent in summer/autumn than in winter/spring (Figures 4.6 and 4.7). Likewise, Frei *et al.* (2006), Beniston *et al.* (2007), Blenkinsop and Fowler (2007b), Ekström

(a) SPI12 Results

	2001-2050			2051-2100		
	Severity	DAI25	DAI50	Severity	DAI25	DAI50
BWh	2.0-2.4 (2.2)	1.6-1.9 (1.8)	2.5-3.5 (3.2)	3.3-5.3 (4.1)	2.6-3.7 (3.1)	4.9-9.4 (6.7)
BWk						
BSh	1.8-2.1 (1.9)	1.9-2.1 (2.0)	1.3-1.6 (1.4)	2.8-4.8 (3.7)	2.6-5.2 (3.7)	2.0-3.6 (2.7)
BSk				1.3-2.5 (1.7)		
Csa	1.8-2.6 (2.1)	3.1-5.2 (4.0)		3.1-5.7 (4.1)	6.7-14.7 (9.6)	2.8-10.5 (5.0)
Csb	1.8-2.6 (2.2)	2.4-3.8 (3.0)	1.6-2.8 (2.0)	3.3-6.1 (4.3)	4.9-8.9 (6.6)	4.0-12.4 (6.6)
Cfa	1.4-2.5 (1.8)	2.1-6.0 (3.5)		2.1-5.2 (3.0)	4.5-14.7 (7.8)	
Cfb						
Cfc	0.7-0.8 (0.7)	0.6-0.8 (0.7)	0.7-0.9 (0.8)	0.4-0.7 (0.6)	0.4-0.5 (0.5)	0.5-0.6 (0.5)
Dsa	1.6-2.2 (1.9)	1.6-2.0 (1.8)	1.8-3.1 (2.3)	2.4-4.7 (3.4)	2.4-4.6 (3.4)	2.9-7.8 (4.7)
Dsb	1.4-2.2 (1.9)	1.6-2.7 (2.3)		2.2-5.0 (3.5)	2.5-5.9 (4.0)	
Dsc						
Dfa						
Dfb						
Dfc	0.4-0.6 (0.5)	0.3-0.5 (0.4)			0.3-0.3 (0.3)	
ET	0.5-0.6 (0.5)	0.4-0.5 (0.5)	0.9-0.9 (0.9)		0.2-0.2 (0.2)	0.9-0.9 (0.9)

(b) SPI3 Severity

	2001-2050				2051-2100			
	DJF	MAM	JJA	SON	DJF	MAM	JJA	SON
BWh	1.6-2.4 (2.0)	1.6-2.1 (1.9)	1.3-1.7 (1.5)		2.4-5.2 (3.6)	2.6-4.5 (3.5)	1.9-3.1 (2.3)	
BWk								
BSh	1.4-1.8 (1.6)	1.7-2.0 (1.8)	1.3-1.6 (1.5)		2.0-3.6 (2.7)	2.6-4.2 (3.3)	1.7-2.9 (2.3)	
BSk								1.3-2.2 (1.5)
Csa	1.3-1.7 (1.5)	1.4-1.7 (1.5)	1.5-2.0 (1.8)	1.3-1.6 (1.4)	1.7-2.9 (2.2)	2.0-3.3 (2.5)	2.2-4.3 (3.1)	1.7-3.0 (2.2)
Csb	1.2-1.5 (1.4)	1.3-1.6 (1.5)	1.7-2.3 (2.0)	1.4-1.9 (1.5)	1.6-2.6 (2.0)	1.8-3.0 (2.2)	2.8-5.3 (3.9)	2.1-3.9 (2.6)
Cfa			1.4-2.3 (1.7)	1.4-2.3 (1.6)			2.1-5.0 (3.0)	2.1-4.9 (3.0)
Cfb								
Cfc								
Dsa		1.4-2.0 (1.6)	1.3-2.0 (1.8)			2.1-3.9 (2.8)	1.9-4.3 (2.9)	
Dsb		1.3-2.0 (1.5)	1.5-2.4 (2.0)			1.9-3.8 (2.6)	2.3-5.2 (3.4)	
Dsc								
Dfa								
Dfb	0.8-0.9 (0.8)				0.6-0.7 (0.6)			
Dfc	0.6-0.7 (0.6)	0.6-0.7 (0.7)		0.7-0.9 (0.8)	0.2-0.4 (0.3)	0.3-0.5 (0.4)		
ET	0.6-0.7 (0.7)			0.7-0.8 (0.7)	0.4-0.6 (0.5)			0.5-0.7 (0.6)

(c) SPI3 DAI25

	2001-2050				2051-2100			
	DJF	MAM	JJA	SON	DJF	MAM	JJA	SON
BWh	1.6-2.3 (1.9)	1.6-2.0 (1.8)	1.2-1.4 (1.3)		2.4-3.8 (3.1)	2.3-3.6 (2.9)	1.6-2.3 (1.8)	
BWk								
BSh		1.8-2.3 (2.0)				3.0-5.1 (3.9)	4.3-8.5 (6.5)	
BSk								1.4-3.3 (1.8)
Csa	1.4-1.9 (1.7)	2.6-3.7 (3.0)	5.0-11.1 (8.5)	1.8-3.0 (2.3)	2.0-5.6 (3.6)	4.3-7.0 (5.6)	11.0-39.0 (24.8)	3.0-11.8 (5.6)
Csb	1.4-2.1 (1.8)	1.6-2.2 (1.9)	2.4-4.4 (3.6)	1.5-2.4 (1.9)	2.2-3.3 (2.8)	2.3-3.7 (2.8)	5.3-9.7 (7.2)	2.8-5.9 (4.0)
Cfa				1.4-3.4 (2.1)			2.9-8.8 (4.8)	2.9-9.3 (4.8)
Cfb								
Cfc								
Dsa		1.5-2.5 (1.9)				2.8-4.7 (3.5)	2.0-4.6 (3.1)	
Dsb			1.7-3.4 (3.0)			2.1-4.7 (3.0)	3.3-6.7 (4.5)	
Dsc								
Dfa								
Dfb	0.8-0.9 (0.8)				0.5-0.8 (0.5)			
Dfc	0.3-0.5 (0.4)	0.4-0.5 (0.5)		0.6-0.8 (0.6)	0.0-0.2 (0.2)	0.0-0.2 (0.1)		
ET	0.0-0.5 (0.3)			0.5-0.7 (0.6)	0.0-0.3 (0.0)			0.3-0.4 (0.3)

(d) SPI3 DAI50

	2001-2050				2051-2100			
	DJF	MAM	JJA	SON	DJF	MAM	JJA	SON
BWh	1.6-2.1 (1.9)	1.5-1.9 (1.7)	1.9-2.5 (2.1)		2.3-5.0 (3.4)	2.3-3.8 (3.1)	2.5-4.9 (3.5)	
BWk			1.0-1.4 (1.2)					
BSh		Inf				Inf		
BSk								
Csa								
Csb		1.5-3.0 (2..0)				3.0-8.5 (4.5)	4.8-34.0 (12.5)	
Cfa								
Cfb								
Cfc								
Dsa		2.0-3.5 (2.0)				3.5-11.6 (6.0)		
Dsb								
Dsc								
Dfa								
Dfb								
Dfc	0.0-0.0 (0.0)	0.0-0.0 (0.0)			0.0-0.0 (0.0)	0.0-0.0 (0.0)		0.0-0.0 (0.0)
ET								

Figure 4.7: Same as Figure 4.6, but for Köppen-averaged drought parameters. "Inf" denotes no drought events in 1951–2000 thus magnitude cannot be mathematically expressed as a ratio.

et al. (2007), Schmidli *et al.* (2007) and Smiatek *et al.* (2009) have projected summer drying and winter wetting, especially in the lower and higher latitudes, respectively.

These seasonal changes are consistent with an area of reduced mean precipitation that migrates northward from southern Mediterranean in winter to cover much of central-western Europe in summer as anti-cyclonic circulation strengthens over the central-southern Europe in winter and northeastern Atlantic in summer (Giorgi *et al.*, 2004; Giorgi and Coppola, 2009). Associated with this is enhanced mean winter precipitation (Schmidli *et al.*, 2007) — by 15–30% in 2071–2100 (from 1961–1990 values; Giorgi *et al.*, 2004), or an average of 2.14%/decade based on 18 GCMs over the 21st century (Giorgi and Bi, 2005) — and also extreme winter precipitation (Frei *et al.*, 2006) over much of western, central and northern Europe (Gibelin and Déqué, 2003), except the central and northern Scandinavian mountains, northwest and eastern Baltic Sea (Ekström *et al.*, 2007). In summer, precipitation slightly declines in northern Europe (Giorgi and Bi, 2005) while southern, western and central Europe experience substantial and widespread reduction (up to 30–45% in 2071–2100 under A2 and B2 emission scenarios, compared to 1961–1990 values) as a ridge forms over western Europe and a trough over eastern Europe that defect Atlantic storms northward (Giorgi *et al.*, 2004; Giorgi and Lionello, 2008). A larger land–sea contrast in lower tropospheric summer warming and an earlier and more rapid decline in soil moisture during spring are primarily responsible for continental and southeastern Europe summer drying (Rowell and Jones, 2006). Warming-induced regional circulation and pressure distribution changes could yield drier, warmer summers, and significantly more intense and persistence summer European droughts, as well as floods, especially in central Mediterranean and central-western Europe (Pal *et al.*, 2004). Spring and autumn have relatively small precipitation changes ($\pm$15% in 2071–2100 under A2 and B2 emsision scenarios, compared to 1961–1990 values; Giorgi *et al.*, 2004).

From 2001–2050 to 2051–2100, positive (negative) changes tend to become more (less) robust with time (Figure 4.5), i.e. greater forcing promotes/exacerbates drought conditions, or reverses changes from negative to positive in some simulations. Both SPI12 and SPI3 timescales reveal similar regional patterns in agreement. Similar to Heinrich and Gobiet (2011), SPI12 results show higher magnitudes of change than SPI3. SPI12 drought severity values are larger than their SPI3 counterparts as drought severity (i.e.

intensity×duration) strongly correlates to duration (Bonacci, 1993; Woo and Tarhule, 1994; Tarhule and Woo, 1997). This, together with the larger changes in SPI12 severity, suggest that longer duration droughts impose a greater drought risk than SPI3, thus are of greater concern.

The DAI50 frequency results are the least robust and are less conclusive than other drought parameters. This, along with their large magnitudes of change, especially in summer (e.g. $\geq$10-fold increase in IP), is related to their relatively rare (mostly $<$5%) present-day occurrence; they tend to occur in $<$20% of the time during 2051–2100. Figure 4.5 indicates greater chances of no changes in DAI50 events or the absence of DAI50 events, hence analysis hereafter focuses on severities and DAI25 frequencies. DAI25 frequencies often have larger increases than changes in severity, which may be complicated by months with temporary above-threshold SPI values occurring within a drought event that negatively contribute to the changes — the effects of including or excluding such "excess periods" are explored in Section 5.6.

The following sections present the results obtained here on a region-by-region basis. Theses are also compared to findings in other studies.

4.4.3 Lower Latitudes

South of 45°N (PRUDENCE: IP and MD; Köppen: BWh, BSh, Csa, Csb, Dsa, Dsb), projections of enhanced drought conditions are typically robust across the 180 simulations (Figure 4.5). The increasing drought conditions obtained here is consistent with the general precipitation reduction simulated for regions from the Mediterranean to Caspian Sea region (Nohara *et al.*, 2006). This also suggests that southern Europe — which already suffers from droughts due to low precipitation and high temperature extremes (Kundzewicz *et al.*, 2006) — might be especially vulnerable to global warming (Giorgi and Lionello, 2008).

4.4.3.1 Mediterranean

For SPI12 severity, magnitudes increase by up to $\sim$3-fold in 2001–2050 and $\sim$6-fold in 2051–2100; DAI25 frequencies have larger increases (Figures 4.6 and 4.7). In absolute terms, 25% of IP and MD being drought-affected occurs in roughly 9% of the time during

1951–2000, but in 25–60% during 2051–2100; Köppen results have similar frequencies. Similarly, other studies have indicated declining precipitation intensity (Beniston *et al.*, 2007) and annual mean precipitation (Buonomo *et al.*, 2007; Lavaysse *et al.*, 2012), by 10–20% or more (Chenoweth *et al.*, 2011; García-Ruiz *et al.*, 2011), due to fewer wet days in southern Europe (Kjellström, 2004), as well as drying of soil moisture (Gibelin and Déqué, 2003; Wang, 2005) and longer hot-and-dry spells (Kundzewicz *et al.*, 2006). Significant and widespread precipitation reduction (e.g. by $>$25%, or $>$125 mm annually, over southwestern Turkey; Evans, 2008) in the Middle East and Turkey occurs due to future decreases in storm track activity in the eastern Mediterranean (Evans, 2010; Hemming *et al.*, 2010; Chenoweth *et al.*, 2011). The projected increases in drought (Sheffield and Wood, 2008b; Sowers *et al.*, 2011; Warren *et al.*, 2012), which fluctuates with precipitation deviations (Hemming *et al.*, 2010), and earlier and longer events (Christensen *et al.*, 2002; Planton *et al.*, 2008), e.g. maximum drought length in Ebro/Gallego (Spain) may be $\sim$30 months longer with enhanced severity (Blenkinsop and Fowler, 2007b), are often consistent across all the models used (Blenkinsop and Fowler, 2007b), drought indices applied (Burke and Brown, 2008) and timescales considered (Loukas *et al.*, 2008), in agreement with the robust changes shown in Figure 4.5.

While precipitation in the southern Mediterranean and the Middle East generally declines across all seasons (Gibelin and Déqué, 2003; Giorgi and Bi, 2005; Kundzewicz *et al.*, 2006; Beniston *et al.*, 2007; Kjellström *et al.*, 2011), it may increase in winter (Gibelin and Déqué, 2003), particularly in northeastern and northwestern Mediterranean coasts (Kjellström *et al.*, 2011) (e.g. northern Balkans; Buonomo *et al.*, 2007; Giorgi and Lionello, 2008), due to extremes (e.g. southern France; Gao *et al.*, 2006) and/or storm activities (Sumner *et al.*, 2003). Such sub-regional variations could explain the less robust (yet with relatively high agreement of $>$80%) winter positive drought trends (Figure 4.5).

Increases in SPI3 drought parameters are typically less than 3-fold in 2001–2050 and 5-fold in 2051–2100; magnitudes of change in summer are considerable in most cases. Csa, Csb and Cfa in particular, have marked increases in summer, especially in 2051–2100, e.g. summer DAI25 frequencies may increase by $\sim$10-fold or more (Figure 4.7) from $\approx$5% of the time during 1951–2000 to 58% of 2051–2100. These results are consistent with the projected increasing summer aridity (Ruosteenoja and Räisänen, 2013) and

drying (Kundzewicz *et al.*, 2006; Blenkinsop and Fowler, 2007b; Ekström *et al.*, 2007), e.g. summer droughts duration may become >30 days longer (Hanson *et al.*, 2007). However, Ruosteenoja and Räisänen (2013) noted that this summer drying may be underestimated as CMIP3 models exclude stomatal resistance with higher CO_2 concentrations (which reduces transpiration, thus further decreases air humidity and cloudiness and increases solar radiation). The drying is associated with precipitation reduction — e.g. by 30% by 2070–2099 (Giorgi and Lionello, 2008; Somot *et al.*, 2008), or −4.25%/decade under SRES A2 (Giorgi and Bi, 2005) — and decreased heavy precipitation (Beniston *et al.*, 2007), along with the northward extension of aridity (Gao and Giorgi, 2008).

4.4.3.2 Western-Central Asia (BWk, BSk)

Similar to the Middle East, literature on Central Asia, particularly those on future climate simulations, is less abundant than for the European Mediterranean due to less research capacity and data availability in this region.

BWk and BSk generally show increases in drought (Figure 4.5), which is in agreement with the projected drying trend and increasing aridity especially in western Turkmenistan Lioubimtseva and Henebry (2009). The relatively low agreement between projections in these results, especially in winter/summer, may be related to the highly uncertain simulated precipitation changes (Lioubimtseva *et al.*, 2005; 2012) — e.g. Lioubimtseva and Henebry (2009) simulated <1 mm/day, and with high temporal and spatial variability — due to the difficulties in climate change modelling in arid zones (Lioubimtseva and Cole, 2006). Furthermore, precipitation trends in this region are complicated by the wetting tendency in both northern (European Russia and Central Siberia) and southern (e.g. Iran) parts of the region, but drying in between (Lioubimtseva and Henebry, 2009). Seasonally, BWk results suggest negative changes in winter drought but positive changes in other seasons (Figure 4.5). These seasonal changes agree with the precipitation projections: increase or vary little in winter, reduce in spring, decline substantially in summer and autumn (Lioubimtseva and Henebry, 2009; Lioubimtseva *et al.*, 2012).

4.4.3.3 France (FR)

France has similar, though less robust, drought changes to the lower latitudes (Figure 4.5). This could be due to the averaging of sub-regional precipitation variations: decreases have been projected in the south and increases northwards (by 25%), with small deviations in the central part and over the Alps (Etchevers *et al.*, 2002). Increases in SPI12 results have relatively high ($\sim$89%) agreement in the projected direction of change across the simulations. This agrees with the longer droughts projected for France (Planton *et al.*, 2008).

For SPI3, winter/spring (mostly winter for FR) results have lower agreement (often $<$60%) than in summer/autumn (typically $\geq$90%), particularly in DAI25 frequencies. This lack of robustness in winter results could be related to the sub-regional variations and uncertainties in the simulated winter precipitation increase (Gao *et al.*, 2006; Planton *et al.*, 2008; Huss, 2011). In summer/autumn, DAI25 frequency increases to $\sim$20% during 2001–2050 (by up to 3.4 times from 1951–2000 value) and 40% during 2051–2100 (6.5 times). These results are consistent with the projected substantial summer precipitation reduction (Räisänen *et al.*, 2004) and increase (by $\sim$50%) in maximum number of consecutive dry days over much of France (Planton *et al.*, 2008).

4.4.4 Higher Latitudes

Of the study region, areas north of 55°N (PRUDENCE: SC; Köppen: Dfc, ET) are the least drought-prone under future climates.

For SPI12, of those cases identified as drought (e.g. DAI25) during 1951–2000, most ($>$50%) remain as drought under climate changes projected for 2001–2050, but $\leq$20% remain as drought (in absolute terms, DAI25 events occur in $<$4% of the time) under the strongest changes projected for 2051–2100 (Figures 4.6 and 4.7). These results follow the projected increasing mean precipitation simulated for Scandinavia and northeastern Europe (Arnell, 1999c; Räisänen *et al.*, 2004; Hanssen-Bauer *et al.*, 2005; Nohara *et al.*, 2006; van Lanen *et al.*, 2007; Wilson *et al.*, 2010) due to more frequent wet days (Buonomo *et al.*, 2007) and increased precipitation intensity (Kjellström, 2004; Alcamo *et al.*, 2007b).

Unlike other regions, negative changes in drought parameters occur throughout the

year, including summer/autumn (Figure 4.5). Agreement is higher in winter/spring (also in autumn), with magnitudes, in both relative and absolute terms, similar to that for SPI12 results; but slightly smaller reductions occur in autumn. Although summer reductions lack absolute robustness, projection agreement is high (>80%). Large parts of EA and southern Russia (Dfb climate) also share similar winter/spring characteristics to the high latitudes, despite lower consistency in simulated direction of change. These seasonal results are consistent with the anticipated precipitation increases that are most pronounced in winter (Räisänen *et al.*, 2004; Hanssen-Bauer *et al.*, 2005; Blenkinsop and Fowler, 2007b) due to more frequent and intense events and extremes (Frei *et al.*, 2006; Giorgi and Coppola, 2009).

In summer, precipitation increases have generally been projected for the high-latitudes of the study region (Kundzewicz *et al.*, 2006; Beniston *et al.*, 2007; Lioubimtseva and Henebry, 2009; Kjellström *et al.*, 2011), e.g. by >25% in 2070s (Alcamo *et al.*, 2007a). Compared to winter/spring results, the less robust summer/autumn regional drought reduction in Figure 4.5 may be related to sub-regional variations and uncertainties in the projected precipitation changes: e.g. increases in northern Scandinavia and decreases or unclear sign of change in the south (Hanssen-Bauer *et al.*, 2005; Frei *et al.*, 2006; Rowell and Jones, 2006; Wong *et al.*, 2011), causing shorter summer droughts to occur in parts of Scandinavia (Hanson *et al.*, 2007). Moreover, in western Russia, dry spell length was found to vary little even with 10–35% increases in summer precipitation, which suggests that the persistence of summer drought is more responsive precipitation reduction than increases (Pal *et al.*, 2004).

4.4.5 The Alps (AL)

The Alpine ridge experiences and separates the competing climate regimes of Mediterranean, Continental, Atlantic and Polar air masses (Beniston, 2005). Recent sub-regional precipitation trends — slight wetting (drying) in northwest (southeast) (European Environment Agency, 2009) — may alter in the future. However, the complex climatic influences, along with topography (Gao *et al.*, 2006), are likely to have contributed to the uncertain trends with larger projection spread in most cases, except the projected changes in summer and autumn which are in more agreement (Figure 4.5).

SPI12 results indicate positive changes with relatively high (∼89%) simulation agreement (Figure 4.5). This agrees with the projected mean precipitation decline found by others (e.g. Beniston, 2005; Smiatek *et al.*, 2009; Kotlarski *et al.*, 2010) that is caused by substantially lower wet-day frequency (Schmidli *et al.*, 2007), such as in southwestern Alps (European Environment Agency, 2009). The strongest drying (by 41%) occurs in the Swiss Alps (Horton *et al.*, 2006), although magnitudes are model-dependent, e.g. for the French Alps (Martin *et al.*, 1996). This may induce earlier and longer droughts (Beniston *et al.*, 2007), e.g. longer droughts in the Brenta region (northern Italy) may have higher maximum severity and frequency (by up to 2–3 events/decade) (Blenkinsop and Fowler, 2007b).

Seasonally, mean precipitation generally increases (decreases) in winter (summer); spring and autumn have less clear trends (Beniston, 2005; Horton *et al.*, 2006), although European Environment Agency (2009) suggested higher autumn precipitation. Figure 4.5 reveals lower agreement (53–79%) in winter/spring, which could be associated with uncertain magnitudes of wetting (Jasper *et al.*, 2004; Beniston, 2005; European Environment Agency, 2009; Smiatek *et al.*, 2009; Kotlarski *et al.*, 2010).

Robust summer/autumn increases have magnitudes almost comparable to that for IP/MD, by up to 2.7 times in 2001–2050 and 5.3 times in 2051–2100 (Figure 4.6); DAI25 events may occur in up to 23% and 46% in the respective periods. These correspond with findings in other studies, that include declining mean summer and autumn precipitation (Beniston, 2005; Smiatek *et al.*, 2009; Kotlarski *et al.*, 2010) due to less frequent wet-days (Calanca, 2007; Schmidli *et al.*, 2007), increasing summer dry periods (Beniston, 2005; Smiatek *et al.*, 2009), particularly in northern Alps where droughts are currently rare (European Environment Agency, 2009), and more frequent (by 15–50%) and severe (by 20%) droughts (Calanca, 2007).

4.4.6 Mid-Europe (ME) and Eastern Europe (EA)

The SPI analysis generally reveals intensifying drought conditions in ME and EA for both long and short events, except for winter/spring (Figure 4.5). These results agree with findings in other studies. For example, Nohara *et al.* (2006) projected lower annual mean precipitation for the Danube basin. Much of central Europe is projected to experience an

increase in the duration of the longest dry period (Kundzewicz *et al.*, 2006). In eastern Europe, more frequent very dry years (Maracchi *et al.*, 2005), strong increases in 100-year droughts in Hungary, Bulgaria, Romania, Ukraine and southern Russia have been simulated (Lehner *et al.*, 2006). The low agreement (<56%) in the projected SPI12 changes for ME (Figure 4.5) follows an unclear sign and magnitude of precipitation change for much of the year (Kjellström *et al.*, 2011), as more frequent/intense heavy precipitation counteracts the declining precipitation in central Europe (McGregor *et al.*, 2005; Kundzewicz *et al.*, 2006).

For SPI3 results, the negative changes in drought parameters in winter for both regions (Figure 4.5) are consistent with the increasing winter (due to more frequent and intense precipitation) and spring precipitation (Räisänen *et al.*, 2004; Giorgi and Coppola, 2009; Ruosteenoja and Räisänen, 2013).

Increasing summer/autumn drought conditions projected for both regions may be associated with modified land-atmosphere feedbacks, which also influences climate change. As warming shifts European climatic regimes northwards, central-eastern Europe becomes a new transitional zone between dry/wet climates, similar to the present-day Mediterranean (Kyselý *et al.*, 2010). Strong land-atmosphere interactions in this zone have been found to increase summer precipitation variability (Seneviratne *et al.*, 2006). A larger land–sea contrast in lower tropospheric summer warming causes an earlier, more rapid decline in soil moisture during spring and a positive summer feedback mechanism (Rowell and Jones, 2006). Both positive (McGregor *et al.*, 2005; Giorgi and Coppola, 2009) and negative (Rowell and Jones, 2006; van Lanen *et al.*, 2007; e.g. Räisänen *et al.* (2004) simulated by up to 70% under SRES A2) precipitation changes have been projected for continental and southeastern Europe. The abundant summer precipitation with more frequent/intense precipitation events in central Europe was found to relate to some feedbacks between convection, radiation and surface fluxes — mechanisms of which are not well identified and may vary among models (Planton *et al.*, 2008), hence the lack of robustness in results obtained here.

4.4.7 British Isles (BI)

Reduction in SPI12 severity and DAI25 frequency are projected, but with low ($<$62%) agreement (Figure 4.5). These are consistent with the uncertain direction of change for mean precipitation in Scotland and northern England, as well as the inconsistent changes in occurrence and severity of longer-duration drought simulated for the UK (Blenkinsop and Fowler, 2007a). Blenkinsop and Fowler (2007a) and Vidal and Wade (2009) reported shorter and less severe long droughts (though with high uncertainty, particularly for southern England; Blenkinsop and Fowler, 2007a). However, Burke *et al.* (2010) found events based on 12-month precipitation accumulations would become slightly more severe; Fowler and Kilsby (2004) simulated increasing drought frequency, duration and severity in most regions by 2070–2100. Longer events could become more frequent in regions that rely on groundwater resources, representing potentially serious challenges for the companies concerned (Blenkinsop and Fowler, 2007a). The low agreement found here (Figure 4.5) could be associated with the averaging of sub-regional spatial variations — increasing drought duration and severity are more likely in southern/southeast England (with frequency to triple by 2070–2100; Fowler and Kilsby, 2004), than in Scotland (Vidal and Wade, 2009; Burke *et al.*, 2010; Burke and Brown, 2010).

Seasonal changes (Figure 4.5) generally follow the simulated mean precipitation increase in winter and decrease in summer (Blenkinsop and Fowler, 2007a). Although studies indicate more frequent short droughts over the UK (Vidal and Wade, 2009; Burke *et al.*, 2010), e.g. by $>$35% under SRES A2 (Fowler and Kilsby, 2004), the direction of change in Scotland and Northern Ireland and some eastern coastal areas is uncertain with increasing winter precipitation (Blenkinsop and Fowler, 2007a). The uncertainty in the projected summer drying is caused by two competing forces: land-sea contrast in the lower tropospheric summer warming produces increased rainfall whereas large-scale atmospheric changes, including remotely forced circulation changes, reduces rainfall (Rowell and Jones, 2006). The simple interpretation of future "wetter winters" and "drier summers" implies the expectation of short summer droughts and no dry winters; however, multi-season to multi-year droughts (as described by SPI12 and SPI24) could occur even with winter wetting (Vidal and Wade, 2009).

4.4.8 Köppen Climate Zones

The 16 Köppen climate zones (Figure 3.2) can be broadly categorised into "high", "moderate" and "low" based on their overall projected magnitudes of change in drought parameters. The "high" category includes BWh, BSh, Csa, Csb, Cfa, Dsa and Dsb. These climates tend to occur in the low-latitudes around the Mediterranean and Black Sea basins, and have robust increases in drought. The "moderate" climates consists of BWk, BSk, Cfb, Dsc, Dfa and Dfb. These mostly correspond to the mid-latitudes and Central Asia, where drought decreases in winter/spring and increases in summer/autumn. The "low" category is characterised by polar climates (Cfc, Dfc and ET) found in the high latitudes and the Alps. These regions generally show reduced drought conditions. Patterns of change for the Köppen climate zones generally correspond with those for the PRUDENCE regions due to the geographic clustering of these climate types in each of the three categories.

4.5 Projection Range

Uncertainties in climate change projections create a significant challenge to how scientific information can be used in practical applications (Blenkinsop and Fowler, 2007a). While Figures 4.6 and 4.7 show the IQRs and mean magnitudes of change of drought parameters from the 180 simulations, Figures 4.8–4.10 and 4.11–4.13 demonstrate both the 1951–2000 values and the full projection range for PRUDENCE- and Köppen-averaged results, respectively. As the Figures suggest, projected drought characteristics and changes are highly influenced by the choice of emission scenario and GCM but they also enable some generalisations to be made.

Greater uncertainty roughly corresponds with greater magnitude of change, i.e. a larger projection range tends to accompany higher warming (e.g. in 2051–2100 and in summer/autumn) for both SPI12 and SPI3. Therefore, regional variations and the associated uncertainties generally increase with time, and are more apparent in the warm seasons, similar to studies for mean precipitation change (e.g. Wang, 2005; Frei *et al.*, 2006; Beniston *et al.*, 2007; Schmidli *et al.*, 2007; Smiatek *et al.*, 2009). Furthermore, low-latitude regions tend to have the largest uncertainties in change magnitude, whereas

the high latitudes show relatively small uncertainties and little seasonality, as warming is greatest in former and smallest in the latter.

In summary, results for 2001–2050 are relatively insensitive to the choice of emission scenario or GCM, whereas the magnitudes, or even direction, of change in 2051–2100 are strongly influenced by the emission scenario or GCM applied. Compared to the warm seasons and warmer regions, results in the cold seasons and colder regions are also less affected by the chosen scenario or GCM.

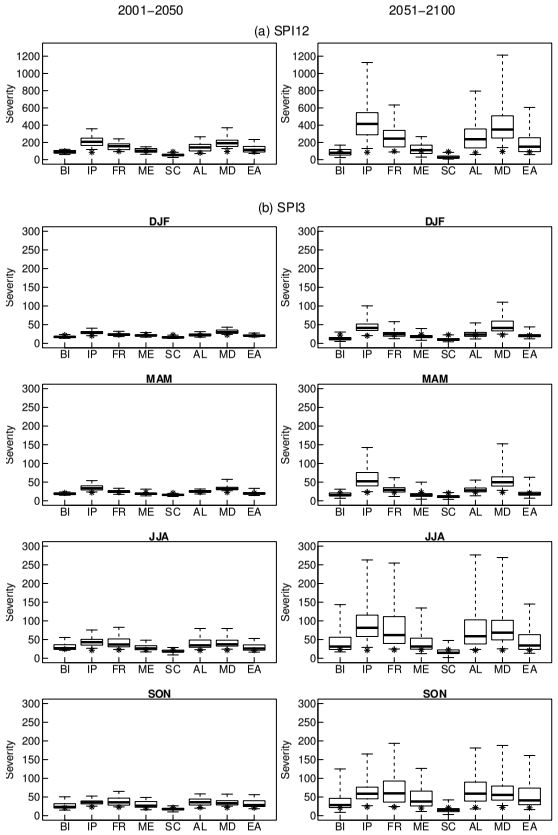

Figure 4.8: PRUDENCE-averaged drought severity based on 180 simulations. The whiskers represent the maximum and minimum data points, the box indicate the interquartile ranges (IQRs) and median values. Asterisks (*) denote 1951–2000 values.

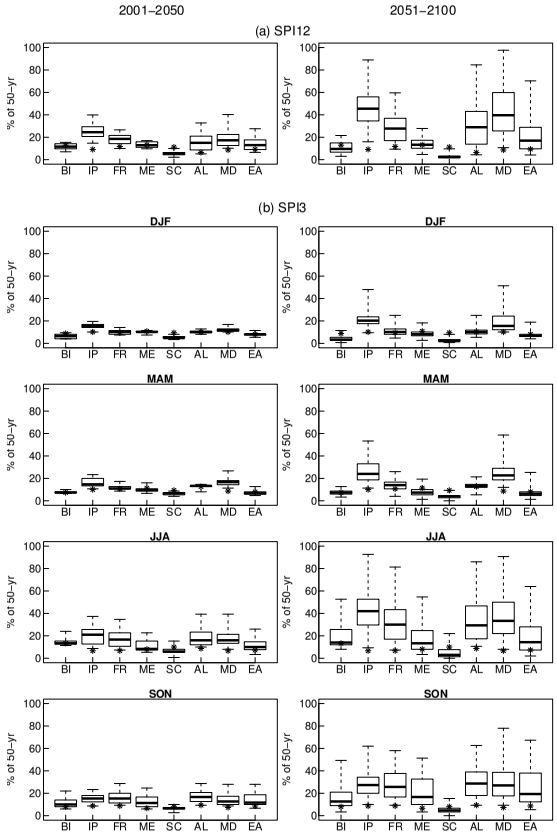

Figure 4.9: Same as Figure 4.8, but for frequency of DAI25.

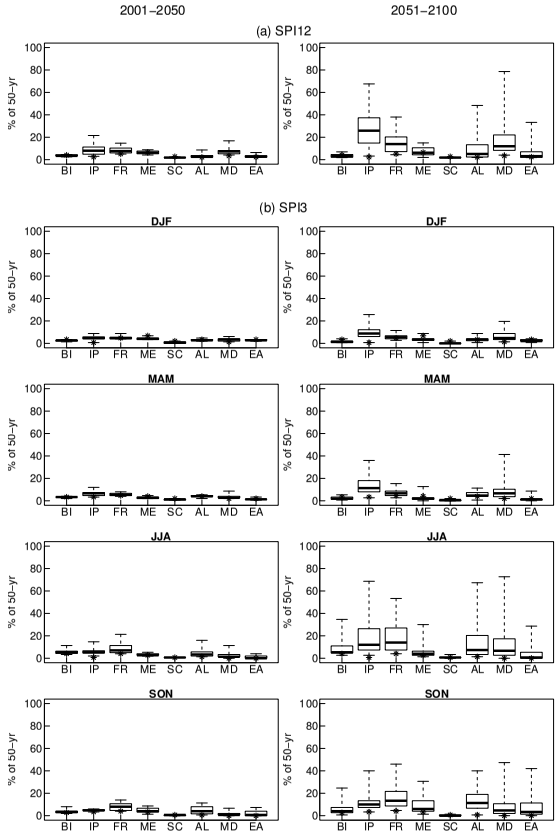

Figure 4.10: Same as Figure 4.8, but for frequency of DAI50.

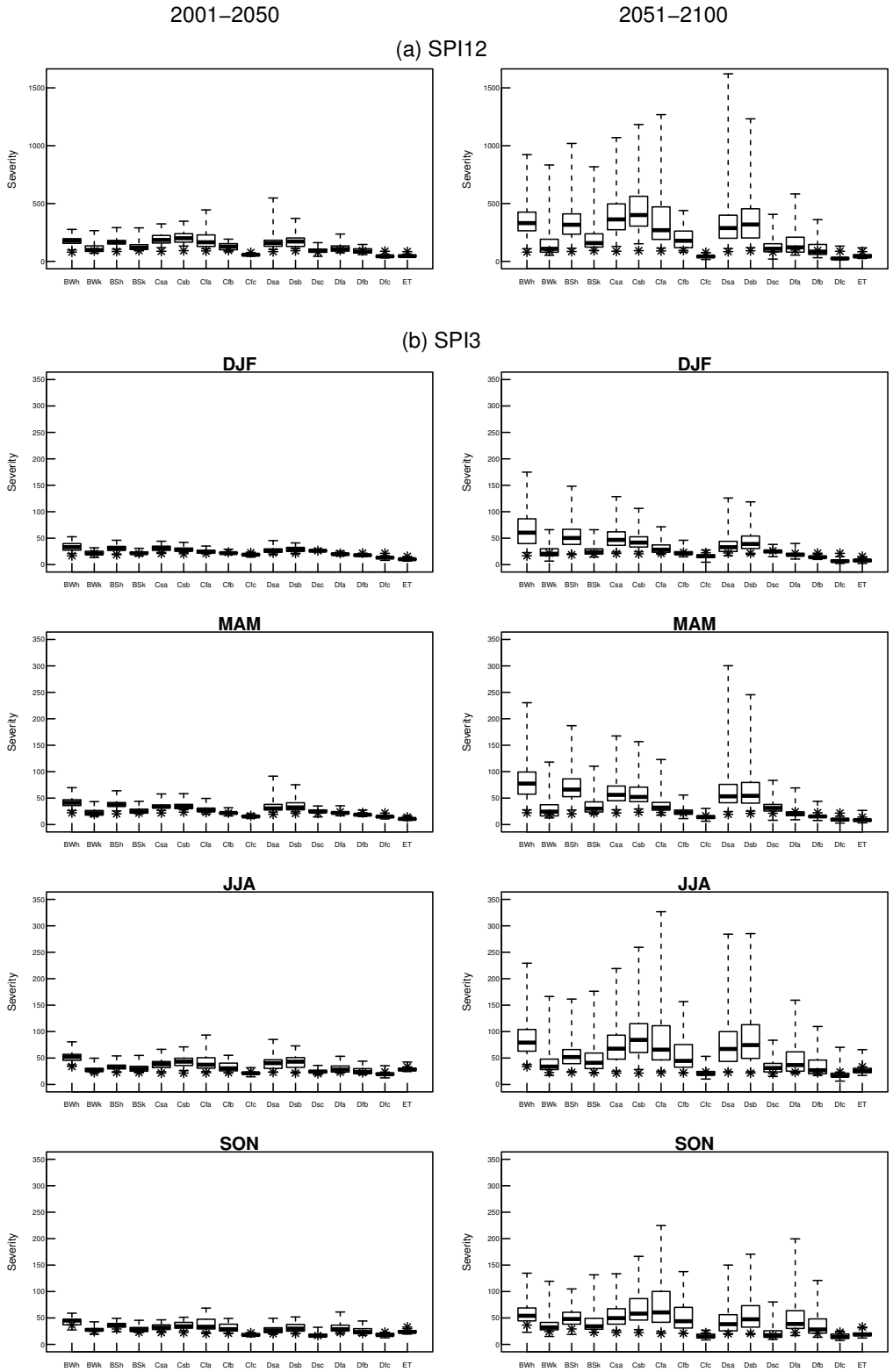

Figure 4.11: Same as Figure 4.8, but for Köppen-averaged severity.

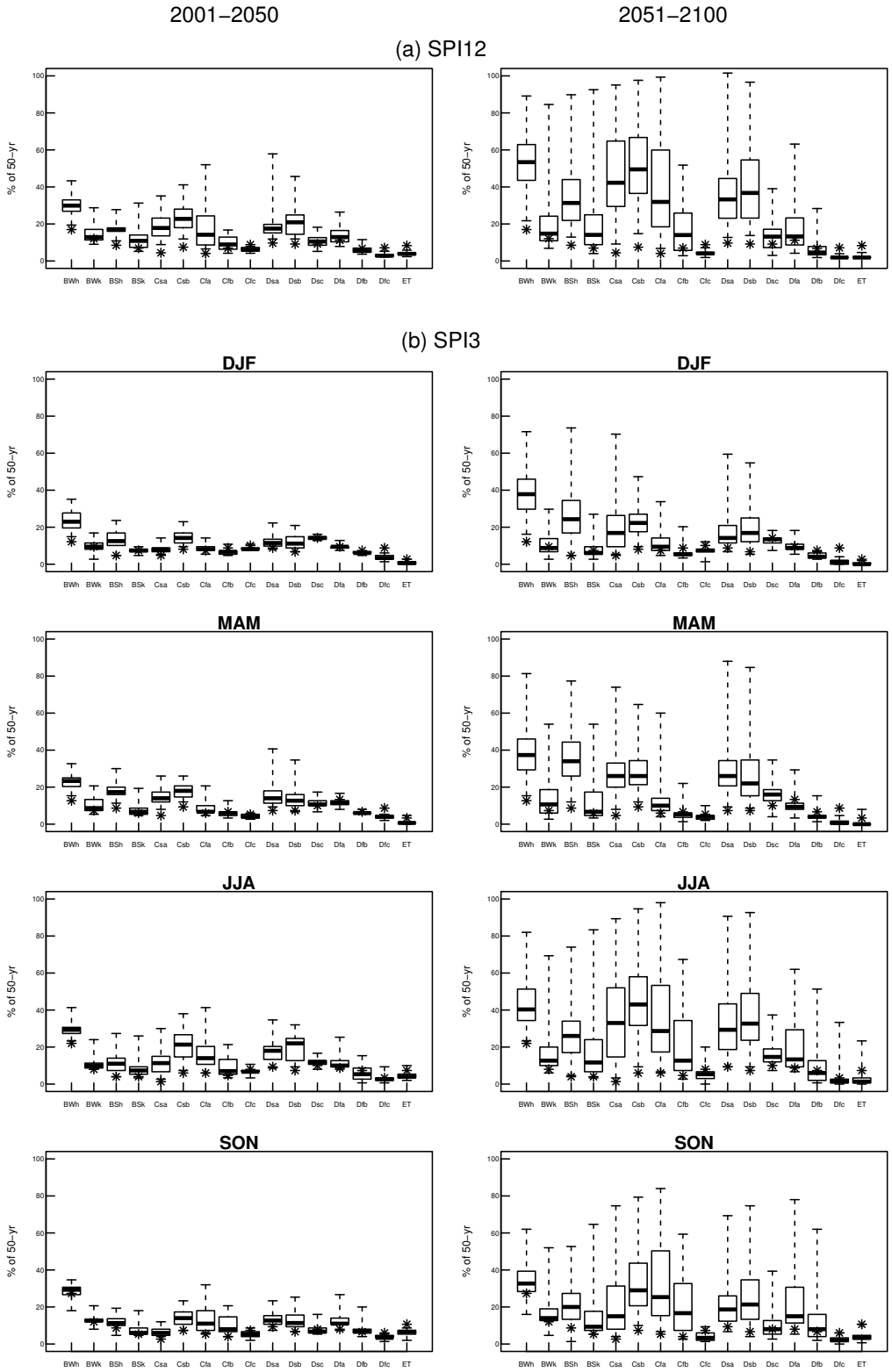

Figure 4.12: Same as Figure 4.9, but for Köppen-averaged DAI25 frequency.

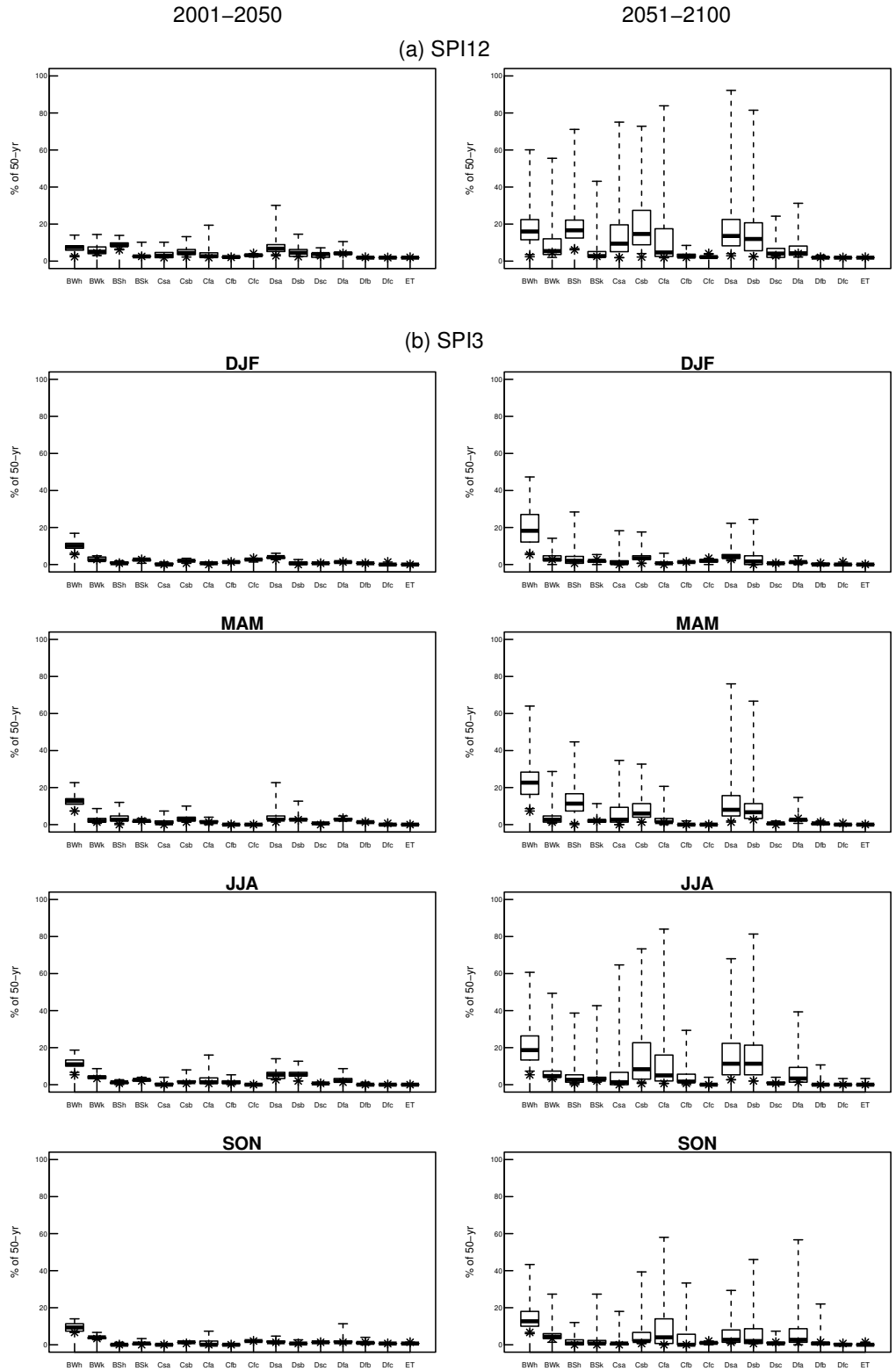

Figure 4.13: Same as Figure 4.10, but for Köppen-averaged DAI50 frequency.

4.6 Sources of Uncertainty

The range of emission scenarios and GCMs applied in the present study has enabled the assessment of their relative contribution in the total variance of the drought projections. Emission scenario uncertainty produces varying degrees of future radiative forcings. GCM uncertainty arises when different GCMs respond differently to the same radiative forcings, producing a range of global temperature warming and a range of geographical and seasonal patterns of precipitation changes.

The overall variance in drought parameters (T^2) was quantified by fitting a linear model to the projections and partitioning the sum of squared deviations (Equation 4.6) into emission scenario uncertainty ($SCEN^2$), GCM uncertainty (GCM^2) and an interaction term (I^2) that arises if scenario and GCM variances are not independent, i.e. the interaction between scenario and GCM. These methods are fairly simple but findings herein are expected to be qualitatively and quantitatively robust. The relative contribution of each of these sources to the projected changes in drought severity are presented in Figures 4.14 and 4.15 for each regional average. Results for DAI25 frequencies (not shown) have very similar regional variations and magnitudes to those for drought severity; those for DAI50 frequencies are excluded due to their relatively rare occurrence under both present-day and future climates.

$$T^2 = SCEN^2 + GCM^2 + I^2 \tag{4.6}$$

Figures 4.14 and 4.15 show that patterns of the relative contribution from these sources of uncertainty vary considerably between 2001–2050 and 2051–2100, and also across the regions. However, different seasons, and both SPI12 and SPI3 results, produce similar patterns.

GCM uncertainty is the dominant source of variance regardless of the region, future period, season and drought parameter. It typically accounts for $>$90% of total variance in 2001–2050, and $>$70% in 2051–2100; it is particularly substantial in BI. Scenario uncertainty is negligible in 2001–2050, but becomes more important in 2051–2100 (5–35% of total variance). In 2051–2100, the scenario contribution roughly reflects the absolute

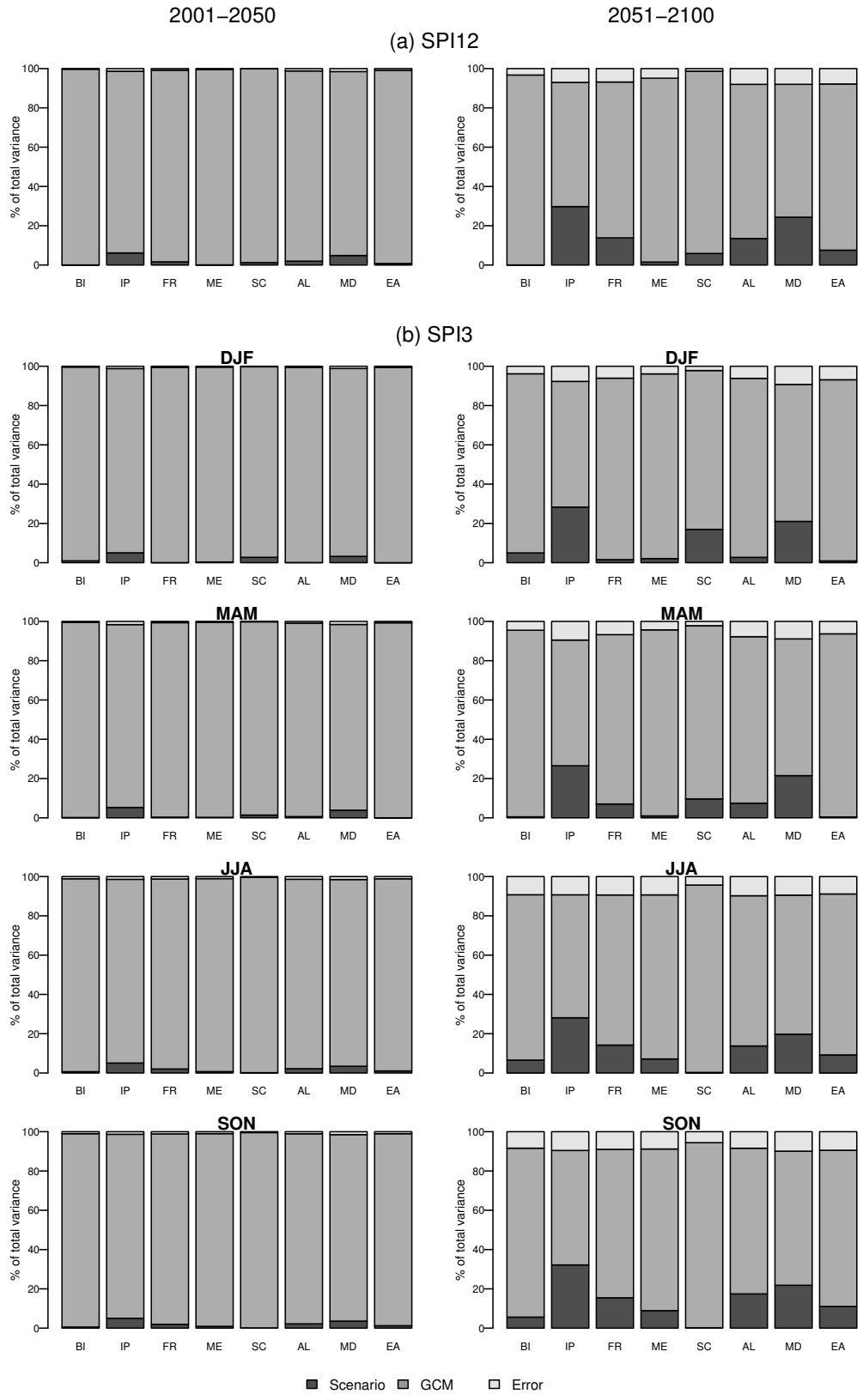

Figure 4.14: Sources of uncertainty in PRUDENCE-averaged drought severities.

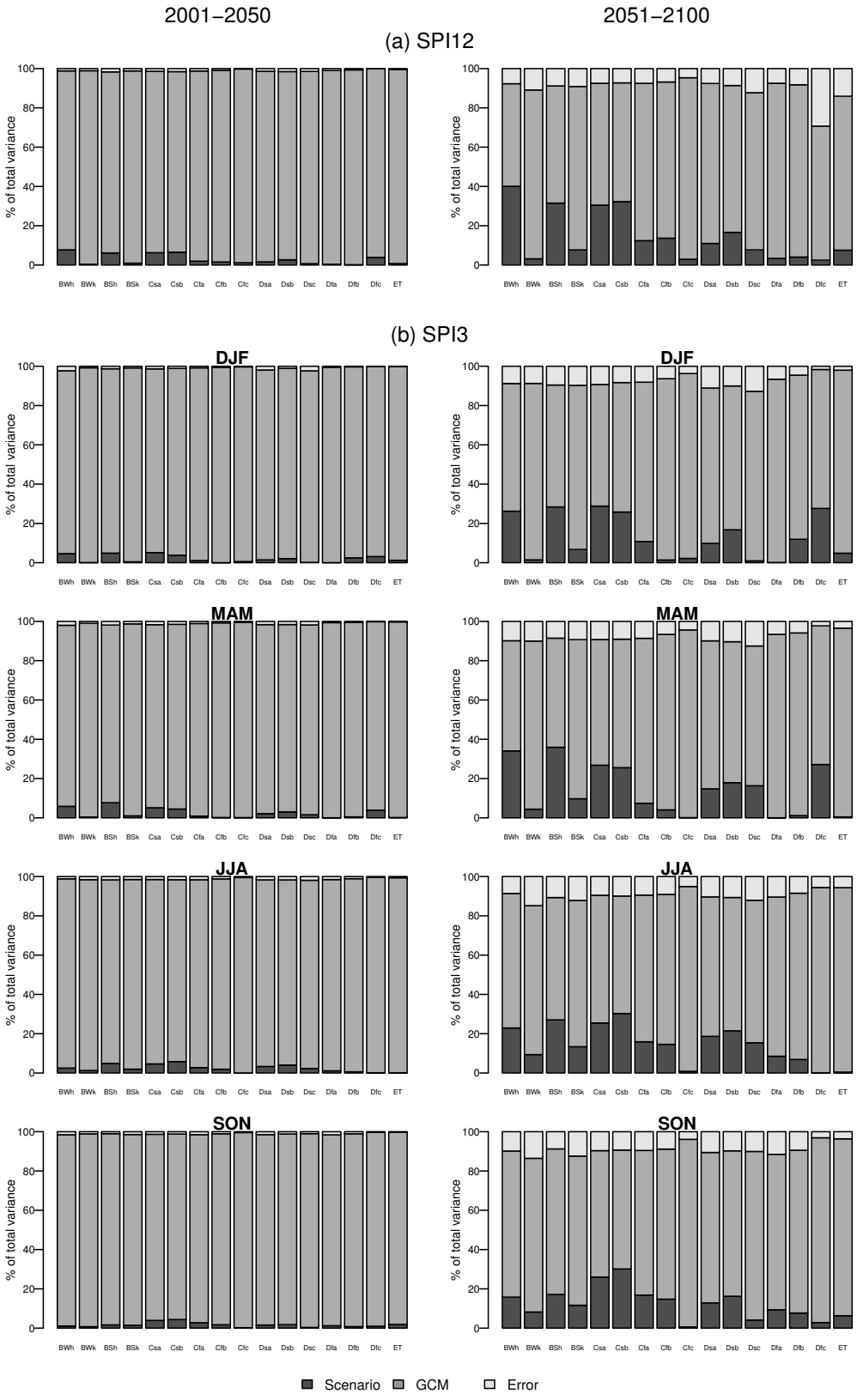

Figure 4.15: Sources of uncertainty in Köppen-averaged severities.

magnitudes of drought severity and DAI25 frequency that correspond to the level of forcing — being largest (∼20–30%) around the Mediterranean basin (PRUDENCE: IP, MD; Köppen: Csa, Csb) and Middle East (Köppen: BWh, BSh, Dsa, Dsb); the relative GCM contribution in these regions is correspondingly lower. Although smaller than for the lower-latitudes, scenario variance is also relatively large (∼10–20%) in the high-latitudes (PRUDENCE: SC; Köppen: Dfc) in winter/spring. These could be related to the relatively robust drying (wetting) trend in the lower (northern) latitudes throughout the year (in winter/spring), thereby results are relatively more dependent on radiative forcing than on the choice of GCM.

An initial study that involved ten carbon cycle models (as mentioned in Section 3.5), in addition to the emission scenarios and GCMs considered in this chapter, also revealed similar relative contributions to those described above: with GCM uncertainty being the greatest source in all cases, scenario uncertainty becoming more important in 2051–2100 compared to 2001–2050, and carbon cycle model uncertainty representing <5% of the total variance in both halves of the 21st century.

Burke and Brown (2010) reported that simulated warming-induced meteorological drought changes for the UK are indistinguishable from natural variability or projection uncertainty. Nevertheless, similar to the present findings, many studies (e.g. Dubrovsky *et al.*, 2005; Lioubimtseva and Cole, 2006; Beniston *et al.*, 2007; Blenkinsop and Fowler, 2007a;b; Buonomo *et al.*, 2007; Giorgi and Lionello, 2008; Vidal and Wade, 2009; Burke *et al.*, 2010; Kyselý *et al.*, 2010) also found climate model (GCM/RCM) uncertainty (particularly GCM and their representation of changes in the large-scale circulation; Kjellström *et al.*, 2011) to dominate in all lead times, especially for precipitation. Variance due to natural internally-generated variability (not explicitly explored here because the ClimGen approach allows this to be controlled for, by constraining the internal variability to follow the sequence of observed precipitation anomalies selected to create the scenario) and emission scenarios in temperature and precipitation projections are more important for the first and last few decades, respectively (Hawkins and Sutton, 2010; Kjellström *et al.*, 2011).

The interaction component typically represents <3% of total uncertainty in 2001–2050 and ∼9% in 2051–2100, suggesting the increasing significance of combined effects

of say, a particular emission scenario and GCM with time. One possible explanation is related to the spatial- and/or temporal-averaging of results for each region and non-linearity introduced by pattern-scaling in ClimGen. In the BI for instance, different combinations of emission scenario and GCM pattern may generate different precipitation decline rates with warming; an overall drying trend occurs if the reduction rate (an exponential function of warming, e.g. for southeastern England), exceeds that of increase (a linear function, e.g. for Scotland); the opposite would indicate an overall wetting. Greater warming could produce a larger discrepancy in the exponential/linear functions. Nevertheless, the fractional contribution of this element remains small.

4.7 Conclusions

This chapter has characterised the spatial and temporal changes in European meteorological drought between 1951–2000 and two future periods, 2001–2050 and 2051–2100. Drought was measured by the SPI, which involves relatively simple calculations and data requirements; drought was defined as SPI≤ -1.5. Precipitation scenarios, simulated by MAGICC6 and ClimGen, based on eighteen GCMs under ten emission scenarios were used. Geographically- and climatically-averaged drought severity (i.e. intensity$\times$duration) and spatial extent for both 3-month and 12-month events were analysed. Since ClimGen incorporates climate change information diagnosed from GCM simulations that were undertaken for CMIP3 (Osborn, 2009), it uses the same sequence of observed variability to generate each series of data, whether for 1951–2000, 2001–2050 or 2051–2100. Therefore, all deviations relative to the baseline can be attributable to anthropogenic climate change and not to internal climate variability.

The projected drought changes generally reflect the precipitation changes simulated in other studies, since SPI is transformed from precipitation accumulated over a given period (Dubrovsky *et al.*, 2008). Results vary substantially depending on the GCM, emission scenario, region and season. Projected changes increase with larger forcing; the agreement between results (robustness) and largest magnitude changes tend to occur in both high- (Scandinavia and Russia) and low-latitudes (the Mediterranean and Black Sea region). The former is projected to become less drought-prone, whereas marked increases in drought severity and DAI25 frequency (typically by 2–3 times in 2001–2050, and 10-fold

or more in 2051–2100 for both SPI3 and SPI12 events) are simulated for the latter. Across much of the study region, increasing forcing promotes/exacerbates drought conditions, or reverses changes from negative to positive in some high-latitude cases. Robust increases (decreases) in drought parameters tend to occur in summer/autumn (winter/spring); negative trends may occur in high latitudes even in summer/autumn. Results averaged across Köppen climate zones demonstrate more robust trends, better reflecting climate change signals, than geographically-averaged results. Sub-regional variations may be considerable, causing inconclusive regional trends (e.g. for the British Isles).

The confidence level of the results depends on the level of uncertainty of the methodologies (Planton *et al.*, 2008). Here, GCM and emission scenario uncertainties were studied. The application of 180 precipitation scenarios has demonstrated the projection range. Despite agreement in the change direction for some regions, their magnitudes are highly uncertain. Uncertainties tend to widen with forcing, therefore are higher in 2051–2100 and summer/autumn. Although emission scenario uncertainty becomes more important post-2050, GCM variance dominates across all dimensions, as commonly found in literature. These results suggest that findings based on a single scenario/model could be highly misleading.

Neither the emission scenarios nor the models were weighted, and each emission scenario and model pattern was assumed to be independent and equally plausible; inter-scenario and inter-model spread were assumed to be representative of the true model uncertainty. This was largely on conceptual grounds (Arnell, 2011) (see in Sections 2.6.6–2.6.10 for discussions on the challenges in weighting models), and equal weighting is the "safer" and more transparent approach for many applications (Weigel *et al.*, 2010). The assumption that all the emission scenarios were equally likely is due to the difficulty in estimating the levels of emissions in future, as well as the incomplete understanding of how the climate system would respond to these emissions.

It is worth noting that increasing drought conditions in regions that already suffer from the hazard maybe of less concern compared to regions that do not currently experience their effects. Since orographically-induced fine scale structures are often absent in GCM-simulated precipitation scenarios (Giorgi and Lionello, 2008), detailed climate change impact studies would require high resolution models with better representation

of topography (Redaud *et al.*, 2002; Räisänen *et al.*, 2004; Gao *et al.*, 2006); inevitably, downscaling could introduce additional uncertainty into the assessment (Planton *et al.*, 2008) and/or represent uncertainty more fully. Local/regional drought impact assessments would require the use of locally appropriate drought indices (Burke and Brown, 2008) and consideration of processes and practices currently excluded from the climate models (e.g. irrigation). The diverse meteorological drought response to climate change found here implies the need for policy-relevant research on climate change impacts and robust adaptation decisions that consider a wide range of expression of modeling uncertainty (Burke and Brown, 2008; Hawkins and Sutton, 2010), or risk-based information (e.g. by considering frequency distributions of climate change impacts) rather than deterministic information (Gosling *et al.*, 2011a).

4.7.1 Limitations

This study is subject to caveats. Results presented here are indicative of plausible climate change impacts on meteorological drought characteristics, and should not be considered as definitive predictions since the primary concern here is to assess changes in a relative sense. Also, the focus on events with SPI≤ -1.5 implies that another threshold would yield different findings. The 1951–2000 baseline was assumed to be representative of future conditions in the absence of climate change (Arnell, 1999c). When fitting the gamma distribution, a linear interpolation of the preceding and subsequent SPI values was applied for undefined entries in months with zero rainfall; an improvement could be made by treating these separately (e.g. Abramowitz and Stegun (eds), 1965; Husak *et al.*, 2007).

Results are also subject to limitations associated with MAGICC6 and ClimGen. For instance, precipitation scenarios are conditional upon MAGICC6-simulated emulations, which may differ from the direct GCM outputs (Li *et al.*, 2009). Also, the pattern-scaling approach in ClimGen assumes a constant spatial pattern of precipitation change over time (Goodess *et al.*, 2003a) that responds linearly (exponentially) to global-mean temperature increase (decrease) (Mitchell, 2003), which may not hold for large changes or where the rate of temperature change slows or even reverses (Arnell, 2011).

Results presented here also under-represent the true uncertainty in drought projections. Amongst others, uncertainty related to climate model physics (Gosling *et al.*,

2011a) and the fitting of a different statistical distribution to the precipitation data have not been explored. Furthermore, results here are SPI-based (limitations of which are discussed in Section 4.2.2.3); using another drought index (e.g. PDSI) could yield different results. Also, SPI may be less appropriate for regions where temperature is more influential than precipitation. Plant response to higher CO_2 levels, which can reduce evapotranspiration and increase soil moisture, and widen global feedbacks onto the climatic drivers of drought, may also influence drought development and have not been accounted for here (Burke, 2011). Lastly, the application of ClimGen has generated gridded outputs at 0.5° resolution due to the pattern-scaling approach, hence downscaling uncertainty has not been explored. Results presented here could be compared to those based on regional climate change simulations (which may be more realistic), such as the CORDEX (Coordinated Regional Climate Downscaling Experiment) initiative from the World Climate Research Program (http://www.meteo.unican.es/en/projects/CORDEX).

This chapter has studied the effects of climate change on meteorological droughts that were defined with precipitation data only. The effects of changes in temperature, and thus potential evapotranspiration on drought are considered in the next chapter, which investigates the future changes in hydrological droughts using hydrological model simulation of runoff.

Chapter 5

Hydrological droughts in Europe under climate change and the uncertainties in the projections

5.1 Introduction

Much of Europe could experience more severe “dry and hot” extremes as climate changes (Kundzewicz *et al.*, 2006). Generally, increasing precipitation and less severe streamflow droughts are projected for northern Europe while the opposite is expected in southern Europe (e.g. Arnell, 1999c; 2003a; Kundzewicz *et al.*, 2006; Lehner *et al.*, 2006; Nohara *et al.*, 2006; Feyen and Dankers, 2009; García-Ruiz *et al.*, 2011; Weiss *et al.*, 2007; Bates *et al.*, 2008; Dai, 2013). Low flows and droughts could negatively impact on agriculture, river navigation, water and energy supplies, exacerbate water stress (Feyen and Dankers, 2009), as well as deteriorate water quality (Blenkinsop and Fowler, 2007b).

Drought risk management requires knowledge and understanding of droughts, their severity and spatial extent (Wong *et al.*, 2011). Hydrological droughts are generally measured by river runoff or streamflows (Panu and Sharma, 2002). Long-term average runoff, which indicates water availability from a resource perspective, is generally equivalent to the difference between precipitation and evapotranspiration (Milly *et al.*, 2005).

Simulation of climate change impacts on drought patterns is inherently uncertain. In addition to uncertainties due to climate and hydrological modelling, uncertainty is also

introduced by the methodology used to characterise drought. In order to study climate change effects on European hydrological droughts (Research Question 1), uncertainties associated with drought definition and quantification need to be considered. This chapter examines the uncertainties introduced by the choice of threshold that identifies drought condition from "normal" climate (Research Question 2) and the definition of when a drought terminates (Research Question 3). In addition, uncertainties arising from drought classification are assessed by comparing hydrological results to those based on a meteorological definition (Chapter 4; Research Question 4). This allows the importance of temperature variations, which in turn modify potential evapotranspiration (PET), to be investigated (Research Question 5). Analysis in this chapter has focused on projections based on eighteen GCMs but only one emission scenario, RCP6, which represents moderate radiative forcing (see Section 3.4.2). This is because findings in Section 4.6 indicate that GCM uncertainty is the dominant source of variance regardless of the region, future period, season and drought parameter, thus is of greater concern compared to emission scenario uncertainty.

In this study, a "category" may refer to a season, region or a 12- or 3-month drought parameter (severity, DAI25 or DAI50). Specific research questions for this chapter include:

1. How might climate change alter European hydrological drought characteristics?
2. Which drought category(-ies) might be more sensitive to droughts during high-flow seasons?
3. As intermittent "wet" conditions may occur within a drought event, which category(-ies) might be more susceptible to a longer drought event being reclassified as a number of mutually dependent minor droughts?
4. Do meteorological and hydrological definitions of drought produce consistent projections of future changes?
5. How does changing temperature, via its influence on PET, impact on the direction and/or magnitude of runoff change?

The chapter is organised as follows. The generation of future climate scenarios is described in Chapter 3. Sections 5.2 and 3.7.1 present the methodology and the runoff

thresholds in absolute values, respectively. Sections 5.5 and 5.6 present the analysis for Research Questions (2) and (3), respectively. Subsequently, hydrological droughts in Europe under future climates are explored in Section 5.7. Section 5.8 discusses the level of consistency in hydrologically- and meteorologically-defined drought results, and the temperature influence is examined in Section 5.8.7. Finally, Section 5.9 presents the concluding remarks and potential for future research.

5.2 Drought Identification

Low flow and *deficit* are commonly used to quantify hydrological droughts (Hisdal *et al.*, 2004). Low flow (e.g. a timeseries of annual minimum *n*-day discharge, mean annual minimum *n*-day discharge or a percentile from the flow duration curve (FDC)) describes the low flow part of the regime (Tallaksen *et al.*, 1997) but does not consider their evolution over time. It is therefore useful for studying the magnitude of a certain drought duration (Clausen and Pearson, 1995). Deficit is commonly obtained by the threshold level method and enables a series of drought events (e.g. duration or deficit volume; Perez *et al.*, 2011) to be derived. Severity of hydrological droughts may also be quantified using the Streamflow Drought Index (SDI; Nalbantis and Tsakiris, 2008), an analogy to SPI, for instance.

This chapter has adopted a methodology similar to that for meteorological drought analysis (Chapter 4). Hydrological droughts were quantified using the threshold approach as it has practical applications when a certain minimum flow is required, e.g. for reservoir design or when permissions for river abstractions are considered (Clausen and Pearson, 1995). The threshold is chosen based on the characteristics of the streamflow regime (Fleig *et al.*, 2006), and a drought occurs when runoff is below a predefined threshold (Perez *et al.*, 2011).

Analysis for both short (3-month) and long (12-month) events were based on a lagged moving average of the runoff timeseries (hereafter, “runoff timeseries”), therefore runoff value for month *t* also accounts for conditions in the preceeding 2 (11) months for 3-month (12-month) events. Deviations between the future periods (2001–2050 and 2051–2100) from the baseline (1951–2000) represent the effects of climate change. Drought parameters examined include severity, DAI25 and DAI50 (see Section 3.8). Even though

absolute deficit volumes may not be comparable across regions as dry regions have lower deficit volumes, their magnitudes of change can be assessed temporally, across seasons (3-month events) and regions.

5.3 Hydrological Drought Thresholds

The methodology for deriving the hydrological drought thresholds in absolute runoff values is described in Section 3.7.1.

5.4 Methodology

The methodology for defining drought fundamentally affects the results and subsequent analysis. This chapter presents a sensitivity analysis on the effects of using different truncation levels and/or drought definitions on the drought parameters. Unless otherwise stated, analyses were carried out for scenarios derived from the 18 GCMs under RCP6 that represents moderate radiative forcing (see Section 3.4.2).

5.4.1 Classification Uncertainties

Research Question 4 in Section 5.1 involves investigating the uncertainties due to two types of drought classification, hydrological and meteorological. To enable their comparison, both SPI and runoff timeseries have the same probability of exceedance (see Section 3.7.1).

Similar to meteorological droughts (Chapter 4), it was only when >3 (or 12) months of runoff timeseries does not fall below the threshold that events were considered separate. This accounts for prolonged dry periods with flow(s) exceeding the threshold level temporarily, therefore a large drought is unlikely to be divided into a number of minor droughts that are mutually dependent (Tallaksen *et al.*, 1997).

Compared to Chapter 4, Mac-PDM.09 yields less grid cells for the same study region, as ClimGen classifies coastal cells as a “land” cell even if the land component represents a very small fraction of the cell. To facilitate comparison between meteorological and hydrological drought characteristics under climate change, those SPI cells that do not exist in the Mac-PDM.09 outputs were excluded, resulting in 8385 cells for 12-month

events. For 3-month events, dry cells with a considerable number of months with zero flow result in the absolute runoff threshold being zero. These cells were excluded because the selection of a non-zero runoff threshold cannot guarantee that the threshold would correspond to the same percentile of exceedence as SPI-1.5; also excluded were two cells with runoff threshold of 0.1 mm — a value so low that makes drought severity difficult to determine as it measures the cumulative departure from the threshold. Hence, short (long) drought analysis involves 7516 (8385) cells of the study region. Alternatively, a higher threshold (lower percentile) can be chosen (e.g. Fleig *et al.*, 2006).

5.4.2 Event Uncertainties

Research Question 3 in Section 5.1 can be addressed by comparing drought results that exclude the excess periods to those that include them (see Section 5.4.1 methodology). Here, excess periods refer to months with temporary above-threshold runoff that occurs within a drought event.

As in Section 5.4.1, fixed runoff thresholds (Section 3.7.1) were used. To generate results that exclude the excess periods, a drought event was defined to start at the point in time when runoff falls below the predefined threshold. However, unlike in Section 5.4.1, the event ends when the threshold is returned to/exceeded even if temporarily (Perez *et al.*, 2011).

5.4.3 Threshold Uncertainties

A threshold may be fixed or varying over the year (Perez *et al.*, 2011). A variable threshold detects streamflow deviations or departures during both high and low flow seasons (Hisdal and Tallaksen, 2000). This may more accurately describe the relative nature of drought so, for example, the January threshold in the Northern Hemisphere extratropics may be higher than that for July, thus identifying droughts that occur in wet periods. It may be used to reflect seasonally-different water demands (Fleig *et al.*, 2006), as both the annual recurring (summer/winter) low-flow period and any deviation from the normal seasonal pattern are important for drought management (Van Loon and Van Lanen, 2012). Streamflow *deficiency* or *anomaly*, rather than streamflow drought, may more appropriately describe periods with discharge below a seasonally-varying threshold

level streamflow (Hisdal and Tallaksen, 2000; Hisdal *et al.*, 2004) as a continuous seasonal low-flow event (e.g. those caused by a delayed onset of the snowmelt flood; Fleig *et al.*, 2006) does not necessarily constitute a drought (Smakhtin, 2001). Nonetheless, deficiencies during high flow seasons could have implications for later drought development (Hisdal and Tallaksen, 2000).

This section describes the methodology of using a monthly variable threshold. To address Research Question 2 in Section 5.1, results produced from this methodology were compared to those from Section 5.4.2. Hence, for both Sections, a drought begins (ends) when runoff timeseries falls below (returns to or exceeds) the threshold value for that particular month, i.e. short periods when runoff exceeds the threshold between two longer periods of drought are not considered to be part of the drought in this comparison.

The range of 70 to 95-percentile are reasonable thresholds to identify low flows for cells with a perennial runoff (e.g. Hisdal *et al.*, 2004; Fleig *et al.*, 2006). Here, the 95-percentile (i.e. that is exceeded by runoff 95% of the time) of the runoff values for each of the twelve months were derived from the 1951–2000 period as it roughly corresponds to the annual SPI-derived fixed threshold in terms of frequency of occurrence. An intermittent or ephemeral runoff implies that the 95-percentile could easily be zero in one or more months, therefore identifying no drought events (Perez *et al.*, 2011). This affects the number of 3-month events; such cells were excluded because droughts in such dry regions are less meaningful, hence this analysis involves 7111 cells of the study region.

5.4.4 Hydrological Droughts in the Future

The effects of both emission scenario and GCM uncertainties were studied for changes in European hydrological droughts. The former involved constructing scenarios by pattern-scaling with the ECHAM5 GCM pattern under six SRES emissions scenarios and four RCPs; the latter used 18 GCMs patterns under RCP6 (see Table 3.1). ECHAM5 was chosen on the basis described in Section 4.4.

5.5 Fixed vs. Seasonally-Varying Thresholds

This section investigates the effects of threshold uncertainties based on the methodology described in Section 5.4.3. It addresses Research Question 2 in Section 5.1, "*Which*

Class	Criteria
Robust increase	All 18 GCMs simulating increase in both definitions.
General increase*	One definition with robust increase; the other definition with 10–17 GCMs simulating increase.
General increase	10–17 GCMs simulating increase in both definitions.
Robust decrease	All 18 GCMs simulating decrease in both definitions.
General decrease*	One definition with robust decrease; the other definition with 10–17 GCMs simulating decrease.
General decrease	10–17 GCMs simulating decrease in both definitions.
Robust opposite	All 18 GCMs simulating increase (or decrease) in one definition and vice versa in the other.
General opposite*	One definition with robust increase (or decrease); the other definition with 10–17 GCMs simulating decrease (or increase).
Mixed	No trend, and/or no change/event in either definition.

Table 5.1: Legend classes of Figures 5.1, 5.5 and 5.16 explained. A (positive or negative) trend is defined as over half of the total 18 GCMs projecting the same direction of change. A robust trend occurs when all 18 GCMs simulate the same direction of change. The letter indicates the definition (I/E = including/excluding excess periods; M/H = meteorological/hydrological events; and F/V = fixed/variable thresholds) with a robust change or a change.

drought category(-ies) might be more sensitive to droughts during high-flow seasons?"

Here, the term "runoff deficit" was adopted as reasoned in Section 5.4.3.

5.5.1 Effects on Direction of Change

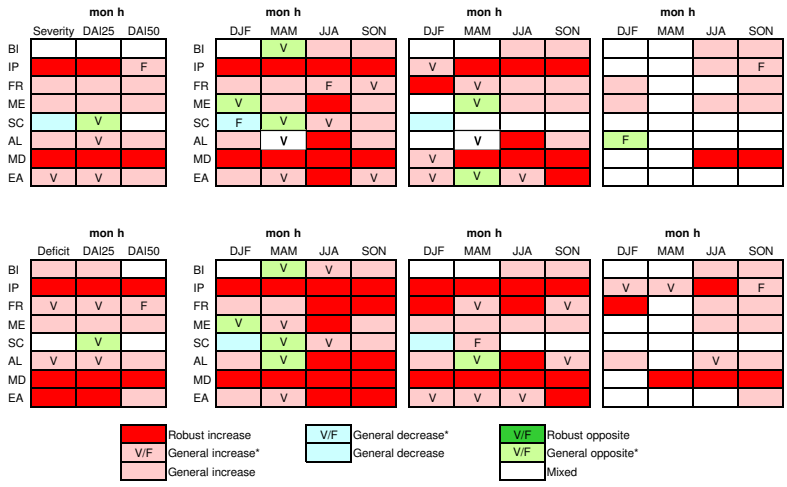

Figure 5.1: Direction of change, from 1951–2000 to (a) 2001–2050 and (b) 2051–2100, in drought metrics based on hydrological deficits that exclude seasonally-excess periods projected by 18 GCMs under RCP6 according to fixed (F) and seasonally-variable (V) thresholds (see Table 5.1).

Compared to fixed thresholds, a seasonally-variable threshold may yield smaller deficits during low-flow seasons as the threshold is relative to the seasonal flow. Meanwhile, a fixed threshold is less likely to capture deficiencies during high-flow seasons; this

effect is considered to outweigh those associated with low-flow seasons (as some of the low-flow season events may be captured by both thresholds). This is reflected in Figure 5.1, which shows the direction of change in the three drought metrics used previously but now determined by hydrological deficits based on fixed and seasonally-variable thresholds for the PRUDENCE regions projected by 18 GCMs under RCP6. Figure 5.1 does not provide information on the magnitude of change nor individual GCM results. The criteria for each legend class in Figure 5.1 are elaborated in Table 5.1.

Figure 5.1 suggests an increasing drying tendency for most drought parameters and more robust (i.e. all 18 GCMs showing the same direction of change) drying in the second half of the century; uncertainty is higher in DAI25 than severity results, and in DAI50 than DAI25 results. A variable threshold yields more robust positive trends in both 12-month and 3-month events. For 3-month results, increases tend to be more robust in summer and autumn for both thresholds but particularly for variable threshold. Contrasting trends — variable threshold indicating positive changes while fixed threshold showing negative changes — tend to occur in spring, namely in AL (both severity and DAI25), and BI and SC (severity), but also in winter in ME (severity). This suggests that spring deficiencies are more common in these regions.

5.5.2 Effects on Magnitude of Change

The effects of fixed/variable thresholds on the magnitude of change were examined for categories where both thresholds demonstrate robust trends. Magnitudes of change of interquartile ranges (IQRs) and ensemble means (in brackets) derived from fixed (top row of each category) and variable (bottom) thresholds are presented in Figure 5.2. Hence, subsequent discussions on the spread of results refer to the IQRs as a more representative and robust measure of uncertainty that is considered appropriate given the number of GCMs used in this thesis.

In addition to more robust increases, a seasonally-variable threshold generates larger increases from 1951–2000 than a fixed threshold for both 12-month and 3-month events. For 12-month events, a variable threshold generates increases roughly twice (or more) of that for fixed threshold. However, in absolute terms, variable thresholds tend to produce lower absolute deficits and less frequent widespread events (12-month DAI25 frequencies

mon h

	Severity	DAI25	DAI50	Severity	DAI25	DAI50
BI						
IP	2.2-3.2 (2.8) 3.9-6.6 (5.5)	2.4-3.1 (2.8) 16.2-26.1 (21.4)	9.7-14.7 (12.4) n/a	4.6-8.2 (7.2) 10.5-20.8 (18.0)	4.3-6.2 (5.3) 38.8-60.7 (50.1)	29.6-54.2 (44.4) n/a
FR						
ME						
SC						
AL						
MD	1.9-3.0 (2.6) 2.9-5.4 (4.3)	2.4-4.8 (3.8) 3.5-6.0 (5.1)	1.7-2.8 (2.3) 8.6-13.5 (11.6)	4.1-8.2 (6.5) 7.5-17.3 (13.3)	6.7-12.8 (10.1) 8.7-23.6 (18.0)	3.4-8.5 (6.9) 17.0-33.5 (30.4)
EA	1.4-3.3 (2.4) 2.0-6.7 (4.5)	1.6-3.4 (2.6) 2.9-11.1 (7.6)		2.6-9.3 (6.7) 5.0-22.9 (15.7)	2.7-8.8 (5.9) 8.1-35.4 (23.0)	

mon h

	DJF	MAM	JJA	SON	DJF	MAM	JJA	SON
BI								
IP	1.8-2.4 (2.1) 2.2-3.0 (2.6)	2.0-3.4 (3.0) 2.2-3.5 (3.1)	2.3-3.5 (2.9) 3.7-6.5 (5.5)	2.1-2.9 (2.4) 3.0-4.9 (3.7)	3.7-6.3 (5.0) 4.4-8.0 (7.0)	4.7-12.4 (9.9) 4.4-9.5 (8.5)	4.5-8.5 (6.6) 10.3-24.6 (18.6)	4.0-6.2 (4.9) 7.9-16.3 (11.8)
FR			1.5-2.7 (2.1) 1.5-3.2 (2.4)	1.5-2.9 (2.1) 2.0-6.4 (4.0)			2.3-6.7 (4.7) 2.7-9.8 (7.3)	2.6-6.6 (4.4) 4.9-23.2 (14.0)
ME			1.5-2.5 (2.0) 1.4-3.1 (2.7)				1.9-4.7 (3.9) 2.4-7.6 (7.2)	
SC								
AL		0.6-0.6 (0.6) 2.1-3.2 (2.8)	1.4-2.7 (2.1) 4.5-9.8 (6.7)	1.6-2.8 (2.3) 3.2-8.7 (6.4)			3.0-7.9 (5.8) 21.3-50.8 (34.3)	3.0-7.5 (5.7) 10.1-40.0 (27.4)
MD	1.7-2.3 (2.0) 2.1-3.3 (2.7)	2.4-3.9 (3.3) 2.6-4.0 (3.6)	2.0-3.0 (2.5) 3.5-6.5 (5.1)	2.0-3.0 (2.5) 3.3-6.2 (4.8)	2.6-4.5 (3.6) 4.3-7.9 (6.1)	4.9-10.5 (8.8) 5.6-10.5 (9.1)	3.7-6.9 (5.7) 8.9-21.2 (16.0)	3.6-6.7 (5.2) 8.8-21.5 (15.3)
EA			1.7-4.6 (3.1) 2.4-7.5 (4.9)	1.5-2.6 (2.1) 2.8-7.6 (5.7)			3.9-20.6 (12.0) 6.2-27.8 (17.4)	2.8-7.3 (5.4) 7.5-31.6 (21.6)

mon h

	DJF	MAM	JJA	SON	DJF	MAM	JJA	SON
BI								
IP	n/a 3.3-4.6 (4.0)	n/a 5.1-8.9 (7.3)	2.1-2.7 (2.4) n/a	1.7-2.1 (1.8) n/a	n/a 6.9-12.4 (9.6)	n/a 9.5-19.0 (15.1)	3.4-4.4 (4.1) n/a	2.3-2.9 (2.5) n/a
FR	1.1-1.7 (1.6) 2.0-3.6 (2.7)		1.3-2.2 (1.7) 1.3-4.7 (3.3)		1.7-6.2 (4.6) 3.2-6.9 (5.9)		1.9-3.9 (3.0) 3.5-15.0 (10.2)	
ME								
SC								
AL		0.4-0.5 (0.5) 5.0-9.5 (7.2)	1.9-3.2 (2.6) 6.1-10.7 (8.4)				3.2-8.8 (6.6) 15.5-43.6 (28.6)	
MD	1.5-3.5 (2.4) 9.3-14.7 (11.8)	1.5-2.9 (2.2) 5.1-6.9 (6.2)	2.4-4.2 (3.4) 9.3-11.7 (12.6)	1.9-2.8 (2.4) 9.3-19.0 (15.3)	3.8-6.8 (5.2) 16.5-30.2 (23.5)	3.5-7.6 (6.5) 9.1-17.6 (14.6)	5.8-8.8 (7.5) 22.2-61.2 (47.6)	3.3-4.2 (3.7) 29.5-66.8 (49.8)
EA				1.7-3.3 (2.5) n/a				3.2-8.7 (5.9) n/a

mon h

	DJF	MAM	JJA	SON	DJF	MAM	JJA	SON
BI								
IP			1.5-3.2 (2.6) n/a				6.8-10.9 (8.8) n/a	
FR	2.0-3.0 (2.7) 2.3-5.0 (3.9)				3.0-5.0 (5.2) 4.0-8.0 (7.1)			
ME								
SC								
AL								
MD		n/a n/a	1.8-2.4 (2.3) n/a	2.0-3.5 (2.8) n/a		n/a n/a	3.6-9.9 (8.2) n/a	4.8-9.9 (7.5) n/a
EA								

Figure 5.2: Magnitude of change, expressed as ratios to 1951–2000 values, for the interquartile ranges (IQRs) and ensemble means (in brackets) of hydrological drought parameters simulated using 18 GCMs under RCP6 for the PRUDENCE regions. Categories with robust positive (red) and contrasting (green) trends are shown; top (bottom) rows representing fixed (variable) thresholds. "n/a" denotes no drought events in 1951–2000 thus the relative magnitude of change cannot be mathematically expressed as a ratio. Categories without robust changes are left blank.

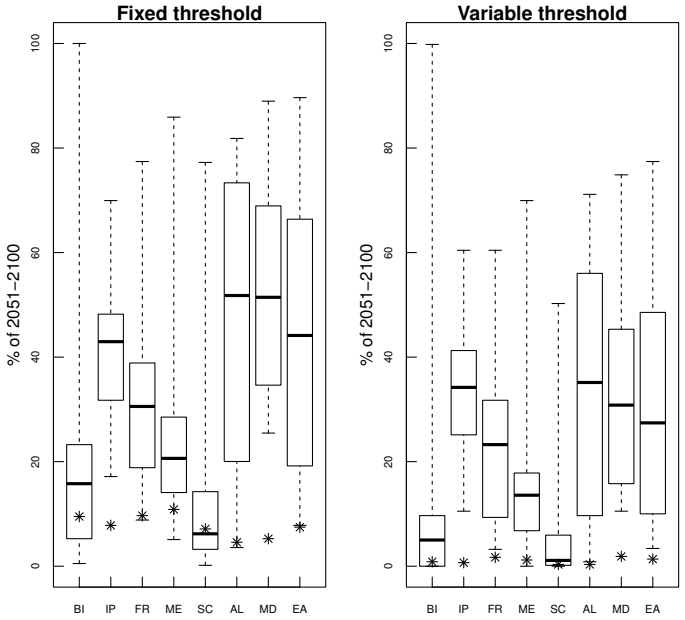

Figure 5.3: Frequency of 12-month DAI25 based on fixed and variable thresholds projected using 18 GCMs under RCP6 for 2051–2100. The whiskers represent the maximum and minimum data points, the box indicate the interquartile ranges and median values. Asterisks (*) denote 1951–2000 values.

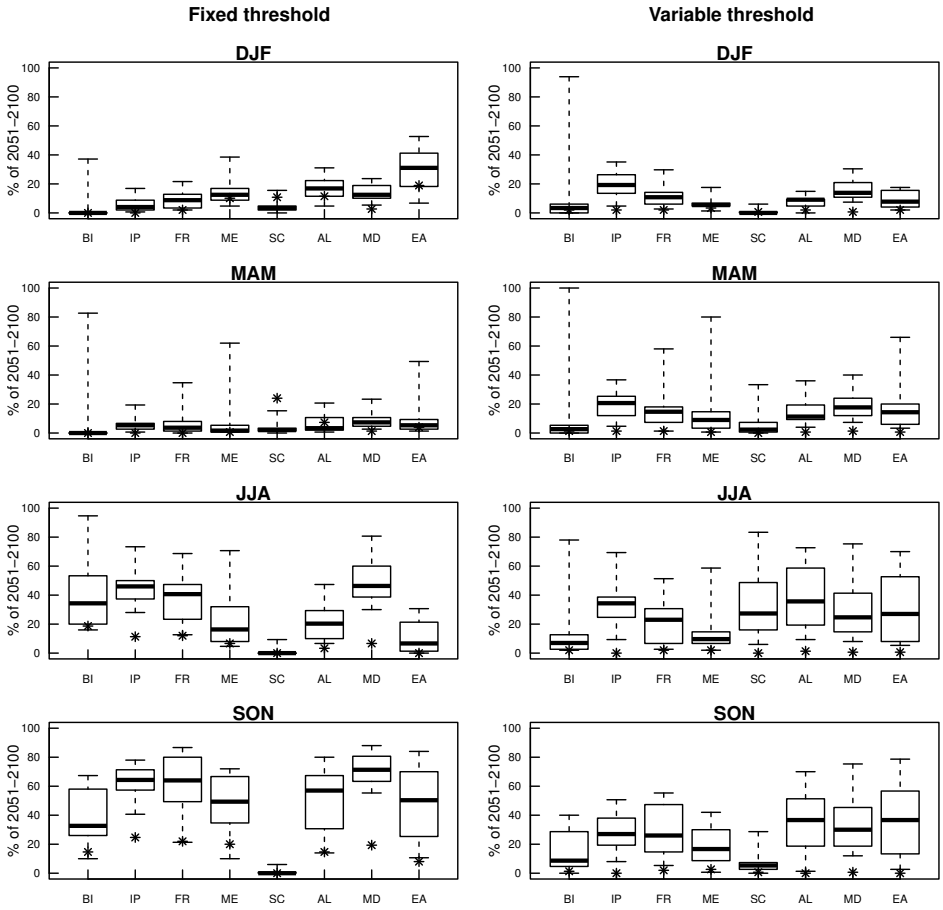

Figure 5.4: Same as Figure 5.3, but for frequency of 3-month DAI25.

in 2051–2100 are illustrated in Figure 5.3) — typically by around 40–50% in 2001–2050 and 25–40% in 2051–2100 for DAI25; 50–70% and 30–50%, respectively, for DAI50 (not shown). Similar patterns also occur in 1951–2000 across all PRUDENCE regions. This implies that a fixed threshold generates larger deficiencies in absolute terms than variable threshold, although the magnitude of change is smaller.

Changes in severity for IP and MD display seasonal differences (Figure 5.2) which are difficult to explain: both thresholds reveal similar increases in winter and spring (by roughly 2–3 times in 2001–2050 and 4–10 times in 2051–2100), and differences between the two thresholds magnify in summer and autumn, to around 3-fold in 2051–2100. Discrepancies in the magnitude of increase are even more considerable for DAI25 frequency. For AL, while a fixed threshold produces summer/autumn increases in severity comparable to those for IP and MD, a seasonally-variable threshold generates substantially larger increases.

Contrary to relative changes but similar to 12-month events, variable threshold tends to yield lower absolute deficits and less frequent widespread events than fixed threshold during summer/autumn across most of the PRUDENCE regions (SC and AL that have relatively high flows during these seasons have the opposite characteristics). This characteristics also occur in high-flow seasons in cold regions, i.e. winter of SC and AL. Figure 5.4 illustrates seasonal DAI25 frequencies in 1951–2000 and 2051–2100.

In spring, a seasonally-variable threshold captures high-flow season deficiencies, hence the larger absolute deficits and more frequent widespread events (Figure 5.4) than fixed thresholds for almost all PRUDENCE regions. This gives rise to the two thresholds producing opposing trends, particularly in SC and AL (Figure 5.1). As an example based on ensemble means of spring severity and frequency of DAI25, AL has the largest discrepancy in magnitude of change: a fixed threshold indicates severity to reduce by 42% (2001–2050) and 25% (2050–2100) while a variable threshold suggests over 2-fold and 9-fold increases, respectively; DAI25 frequency demonstrates similar trends with larger magnitudes.

5.6 Including vs. Excluding Excess Periods

Intermittent "wet" condition with above-threshold runoff (i.e. excess periods) may occur within a drought event. Research Question 3 in Section 5.1, "*Which category(-ies) might be more susceptible to a longer drought event being reclassified as a number of mutually dependent minor droughts?*" is addressed in this section. Uncertainties associated with the termination rule, based on methodologies described in Sections 5.4.1 and 5.4.2, are assessed.

5.6.1 Effects on 1951–2000 Drought Parameters

The meteorological and hydrological results for 1951–2000 that include and exclude excess periods were compared (Table 5.2). Firstly, all the severity and DAI values are positive and negative, respectively: excluding excess periods produces larger severities and smaller DAI values than including excess periods.

Secondly, meteorological severity and frequencies of DAI25 have larger regional percentage differences than their hydrological counterparts. For instance, regional discrepancies in 12-month meteorological and hydrological drought severity are 11–23% and 3–15%, respectively; AL has the smallest (largest) meteorological (hydrological) discrepancy. ME and SC have almost no discrepancy ($<$3%) in frequencies of 12-month hydrological DAI25 whereas meteorological DAI25 differ by 17% and 24%, respectively. This is because precipitation fluctuates more than runoff as precipitation in a particular month tends to be more independent of the conditions in the preceding month.

Thirdly, according to both gridded (not shown) and regional (Table 5.2) results, discrepancies are larger in 12-month than 3-month events for both drought classifications — discrepancies are typically $<$8% (meteorological) and $<$5% (hydrological). Since 12-month events account for a longer duration, the chances of having an excess period are higher than with 3-month events. Percentage differences are higher for IP and AL, based on 12-month meteorological and hydrological definitions, respectively.

Lastly, percentage differences are sometimes much larger for frequencies of widespread events than severities. In a particular month, a cell is either "in drought" or "not in drought" regardless the intensity of the event. Differences for frequency of widespread events are therefore proportional to the total number months in the excess periods. For

	12-months			3-month Severity				3-month DAI25				3-month DAI50			
	Severity	DAI25	DAI50	DJF	MAM	JJA	SON	DJF	MAM	JJA	SON	DJF	MAM	JJA	SON
PRUDENCE-averaged results															
Meteorological:															
BI	18.9	-19.7	-62.5	4.3	0.3	4.3	4.1	-7.7	0.0	-20.0	-16.7	0.0	-20.0	-16.7	0.0
IP	22.5	-29.6	-71.4	1.4	2.2	5.6	2.2	-6.7	-13.3	0.0	-7.7	-100.0	0.0	100.0	-20.0
FR	18.6	-11.6	-50.0	0.3	6.7	1.1	3.0	-14.3	0.0	-10.0	-7.7	-14.3	0.0	-16.7	0.0
ME	13.0	-16.7	-28.9	2.5	4.6	2.9	3.7	-6.3	-5.9	0.0	-20.0	0.0	0.0	0.0	0.0
SC	16.9	-24.2	-68.8	3.5	2.8	3.1	2.2	-7.1	-7.1	-13.3	-8.3	-33.3	0.0	0.0	0.0
AL	11.2	-21.1	-76.9	1.9	4.5	0.7	6.7	-20.0	-5.3	0.0	-21.4	-40.0	-33.3	0.0	0.0
MD	16.2	-21.6	-45.0	2.8	0.2	1.2	2.6	0.0	-7.7	-20.0	-9.1	-50.0	0.0	n/a	n/a
EA	13.1	-12.7	-64.3	1.6	3.4	3.7	3.4	-8.3	-8.3	-9.1	-7.7	0.0	0.0	n/a	n/a
Hydrological:															
BI	8.6	-13.8	-16.7	1.7	0.4	0.0	0.1	n/a	n/a	0.0	-4.3	n/a	n/a	0.0	0.0
IP	5.3	-20.7	-40.0	1.9	0.7	0.3	0.3	n/a	n/a	-10.5	0.0	n/a	n/a	0.0	0.0
FR	4.9	-19.7	-9.1	0.6	4.9	0.5	0.5	0.0	n/a	0.0	-2.9	0.0	n/a	0.0	0.0
ME	4.7	0.0	-31.6	0.4	8.1	1.1	0.6	0.0	0.0	0.0	0.0	0.0	n/a	-33.3	0.0
SC	4.2	-2.3	-100.0	0.7	0.1	0.1	1.2	0.0	0.0	n/a	n/a	0.0	0.0	n/a	n/a
AL	15.0	-28.9	0.0	0.6	0.6	1.8	0.6	-5.6	0.0	0.0	0.0	0.0	n/a	n/a	0.0
MD	4.9	-11.4	-19.0	1.9	2.8	0.2	0.2	0.0	0.0	0.0	0.0	n/a	n/a	0.0	0.0
EA	3.9	-15.4	0.0	1.0	1.4	4.1	0.5	-3.4	0.0	n/a	0.0	-7.7	n/a	n/a	n/a
Köppen-averaged results															
Meteorological:															
BWh	13.5	-11.0	-78.6	0.0	2.0	1.3	1.9	0.0	0.0	0.0	0.0	0.0	0.0	0.0	0.0
BWk	12.8	-16.9	-44.4	5.3	7.1	1.7	7.8	0.0	0.0	-16.7	-33.3	0.0	-50.0	-20.0	-20.0
BSh	18.8	-14.0	-22.2	14.5	20.6	1.2	10.1	-57.1	-15.4	-100.0	-76.9	-100.0	n/a	-100.0	n/a
BSk	14.5	-24.4	-73.3	0.4	2.4	2.0	6.8	-9.1	-11.1	-33.3	0.0	-25.0	-66.7	-33.3	n/a
Csa	17.6	-61.5	-100.0	2.4	2.7	5.4	3.1	-14.3	-14.3	-100.0	-50.0	n/a	n/a	n/a	n/a
Csb	20.6	-25.0	-92.3	0.9	1.3	4.2	2.9	0.0	-7.1	0.0	-9.1	0.0	-50.0	0.0	0.0
Cfa	15.8	-20.8	-100.0	1.8	3.5	1.9	3.3	0.0	-11.1	-11.1	0.0	n/a	0.0	0.0	n/a
Cfb	17.7	-29.3	-91.7	1.8	3.1	4.0	3.3	-23.1	-10.0	-14.3	0.0	-50.0	n/a	-100.0	n/a
Cfc	11.4	-7.7	-70.8	1.6	1.4	0.0	3.8	-13.3	-37.5	-66.7	-36.4	0.0	n/a	n/a	-33.3
Dsa	16.1	-19.3	-64.7	2.1	2.8	2.5	5.0	0.0	0.0	-7.1	-14.3	-25.0	0.0	0.0	0.0
Dsb	12.9	-20.4	-78.6	2.4	2.8	2.8	5.2	0.0	0.0	0.0	0.0	n/a	0.0	0.0	0.0
Dsc	2.0	-20.4	-64.7	3.3	10.9	5.1	3.6	0.0	0.0	0.0	0.0	0.0	n/a	0.0	0.0
Dfa	9.6	-16.7	-45.8	1.5	3.6	4.4	1.0	-7.1	-15.0	-15.4	-25.0	-100.0	-40.0	-50.0	0.0
Dfb	14.9	-27.5	-91.7	2.6	4.3	4.1	2.0	-18.2	-10.0	0.0	-10.0	-100.0	0.0	n/a	0.0
Dfc	14.5	-26.2	-100.0	1.5	3.8	2.9	2.2	-7.7	-7.7	0.0	0.0	-50.0	0.0	n/a	0.0
ET	19.2	-24.5	-91.7	0.5	4.9	10.2	6.0	-25.0	-60.0	-9.1	-18.8	n/a	n/a	n/a	-50
Hydrological:															
BWh	5.3	-1.4	0.0	0.7	0.0	3.9	0.0	n/a	n/a	0.0	0.0	n/a	n/a	0.0	0.0
BWk	4.2	-13.6	-16.7	2232.3	165.7	131.3	136.7	-16.7	0.0	0.0	-25.0	n/a	n/a	n/a	n/a
BSh	2.5	-11.1	0.0	0.4	0.0	0.5	0.3	0.0	0.0	0.0	0.0	0.0	n/a	0.0	0.0
BSk	4.4	-15.2	0.0	577.6	118.1	1116.3	178.0	0.0	n/a	-30.0	-6.3	n/a	n/a	-100.0	-20.0
Csa	3.1	-66.7	n/a	3.0	127.6	0.5	0.6	n/a	n/a	0.0	-2.4	n/a	n/a	-100.0	0.0
Csb	3.7	-15.8	0.0	5.3	3.5	0.5	0.2	n/a	n/a	0.0	0.0	n/a	n/a	0.0	0.0
Cfa	6.3	-22.7	0.0	2.0	1.9	2.0	0.3	-33.3	0.0	0.0	0.0	0.0	n/a	n/a	0.0
Cfb	6.5	-27.1	n/a	0.8	3.6	0.3	0.5	0.0	n/a	0.0	0.0	0.0	n/a	0.0	0.0
Cfc	9.0	-2.3	-57.1	0.9	0.5	0.0	0.2	0.0	0.0	0.0	0.0	n/a	n/a	0.0	0.0
Dsa	8.2	-21.6	-27.3	0.0	0.0	0.0	0.0	0.0	n/a	0.0	-6.7	0.0	n/a	n/a	0.0
Dsb	3.1	-12.5	0.0	0.2	0.0	0.9	0.2	0.0	-100.0	0.0	-5.6	0.0	n/a	n/a	n/a
Dsc	1.9	0.0	0.0	0.0	0.0	n/a	n/a	0.0	-71.3	n/a	n/a	n/a	-78.6	n/a	n/a
Dfa	3.5	-5.6	0.0	5.4	9.9	29.0	11.5	-4.9	-10.0	n/a	-16.7	-6.3	0.0	n/a	n/a
Dfb	2.6	-9.3	0.0	2.3	167.3	42.1	13.4	-5.9	0.0	n/a	n/a	0.0	0.0	n/a	n/a
Dfc	8.6	-14.8	0.0	3.6	7.7	15.6	15.8	0.0	-2.1	n/a	n/a	-50.0	-6.3	n/a	n/a
ET	14.4	-20.6	n/a	0.6	3.1	2.5	11.4	0.0	-7.1	n/a	n/a	n/a	0.0	n/a	n/a

Table 5.2: Percentage difference between regional drought parameters derived from event definitions that include and exclude excess periods for 1951–2000. "n/a" denotes no occurrence of drought events.

severity, small excess volume resulted from short duration and/or small intensities tended to generate small difference between the severity values that include and exclude excess periods; the opposite occurs with large excess volume due to long duration and/or large intensities. Also, disagreement for DAI50 events is also larger than DAI25 due to their less frequent occurrence, so that a small change in number can appear to be a large percentage change.

Similar patterns occur in Köppen-averaged results (Table 5.2). The large percentage differences for BWk and BSk are due to the low severity values that include excess periods ($<$1 mm) and hence a small denominator in the calculation of the percentage. Table 5.2 also shows that for 3-month hydrological severities, cold climates without a dry season are the most sensitive particularly in summer and autumn, which suggests the occurrence of short excess periods in these seasons.

5.6.2 Effects on 21st Century Results

Effects of including and excluding excess periods within drought events were then examined for 21st century hydrological results. Figure 5.5 illustrates the direction of change from 1951–2000, simulated by 18 GCMs, in PRUDENCE-averaged drought parameters for the two event definitions; the legend is elaborated in Table 5.1. Class "Discrepancy" (green) highlights the categories where results based on the two event definitions lack agreement. Overall, the two event definitions nearly always yield the same direction of change, with discrepancies primarily in frequency of DAI50 and winter/spring results. This implies that periods with temporary excursions above the drought threshold are more likely during the high-flow season of winter/spring, and therefore it is for these seasons that the decision to either count such brief periods as part of an ongoing drought or as a non-drought period breaking two separate droughts has the greatest effect on the resultant drought statistics.

The uncertainties introduced by the two event definitions on the magnitude of change from 1951–2000 were further explored with ECHAM5 projections under RCP6 (Table 5.3). This comparison reveals findings similar to 1951–2000 results (Section 5.6.1): with some notable exceptions, regional discrepancies for both 12- and 3-month severity tend to be $<$6%; summer and autumn 3-month values are generally $<$2%. Discrepancies, along

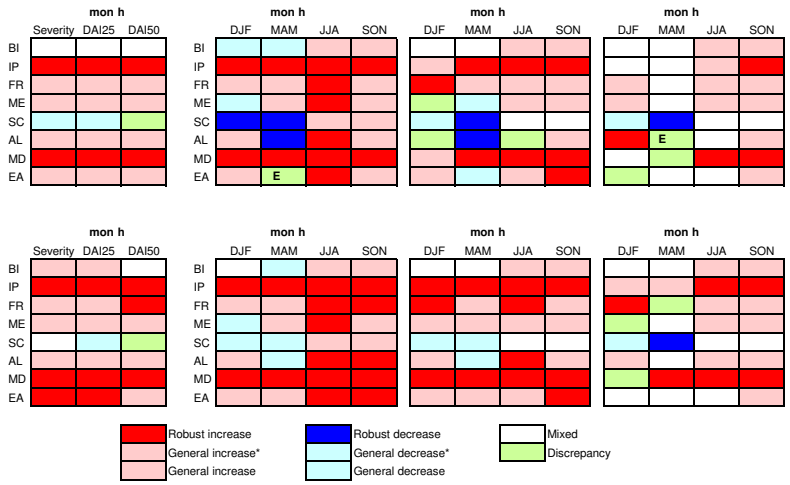

Figure 5.5: PRUDENCE-averaged direction of change from 1951–2000 for hydrological events under a fixed threshold projected by 18 GCMs under RCP6 based on event definitions that include (I) and exclude (E) excess periods. See Table 5.1 for further explanation of the legend classes. The class *Discrepancy* indicates the two event definitions do not share any of the same class above. "I" ("E") represents including (excluding) excess periods with an increasing ("i"), or decreasing ("d"), trend in brackets while the other definition has inconclusive trend.

	12-months			3-month Severity				3-month DAI25				3-month DAI50			
	Severity	DAI25	DAI50	DJF	MAM	JJA	SON	DJF	MAM	JJA	SON	DJF	MAM	JJA	SON
2001–2050:															
BI	11.5	-7.1	-40.0	-39.4	10.8	0.5	1.6	n/a	n/a	0.0	15.4	n/a	n/a	0.0	0.0
IP	1.1	7.6	22.5	5.7	6.3	0.8	0.9	n/a	n/a	-2.7	-2.3	n/a	n/a	-5.9	0.0
FR	-1.9	35.3	-5.4	3.2	20.3	1.1	0.5	0.0	n/a	-5.6	0.0	0.0	n/a	0.0	-5.6
ME	-0.6	-29.4	116.1	-26.2	15.4	1.5	1.1	-33.3	0.0	0.0	-3.8	0.0	n/a	0.0	0.0
SC	2.9	2.4	n/a	-1.2	-0.4	0.4	5.5	0.0	0.0	n/a	n/a	0.0	0.0	n/a	n/a
AL	0.8	21.8	-33.8	3.7	-4.4	1.8	0.8	0.0	0.0	0.0	-3.1	0.0	n/a	n/a	0.0
MD	0.6	1.4	19.0	5.6	4.7	0.7	0.6	-14.3	0.0	0.0	0.0	n/a	n/a	0.0	-3.1
EA	2.4	-7.2	-27.5	8.5	13.2	4.3	0.7	-10.0	0.0	n/a	-3.3	0.0	n/a	n/a	n/a
2051–2100:															
BI	-26.0	7.1	-100.0	-34.8	6.3	0.4	1.1	n/a	n/a	6.4	28.2	n/a	n/a	10.5	25.0
IP	-2.2	19.8	53.7	2.0	5.7	1.0	0.6	n/a	n/a	10.4	0.0	n/a	n/a	-1.6	-2.7
FR	-2.5	33.9	5.8	3.9	2.9	0.4	-0.3	0.0	n/a	-3.2	3.0	0.0	n/a	0.0	-1.6
ME	-2.4	-11.2	46.2	33.9	-3.4	0.0	-0.4	-9.1	-18.7	-2.3	-1.7	-33.3	n/a	58.8	0.0
SC	1.0	28.0	n/a	-0.2	-0.3	0.2	-1.0	0.0	0.0	n/a	n/a	0.0	0.0	n/a	n/a
AL	-5.2	29.1	-20.3	2.9	9.0	-1.0	-0.3	-22.6	-12.5	-4.3	-2.1	-9.1	n/a	n/a	0.0
MD	-0.3	6.4	10.2	1.5	0.1	0.7	0.0	-8.8	-8.3	0.0	0.0	n/a	n/a	-1.3	-2.0
EA	0.3	13.7	-15.4	1.8	3.6	-0.9	0.0	0.8	-14.3	n/a	-1.0	1.1	n/a	n/a	n/a

Table 5.3: Percentage difference between PRUDENCE-averaged magnitude of change from 1951–2000 to either 2001–2050 or 2051–2100, derived from event definitions that include and exclude excess periods as simulated by ECHAM5 under RCP6.

with their regional variations, for frequencies of DAI25/50 (1–35% for DAI25) are larger than for severities. Larger disagreements (by 11–39%) are more common in BI and ME, particularly in winter and spring.

The chance of a larger drought event being divided into a number of mutually dependent minor droughts is reduced as analyses were based on runoff timeseries, i.e. the smoothing has filtered out the short excess periods, as well as minor droughts of short duration and small deficit volume. Alternative to the methodology adopted here, Tallaksen *et al.* (1997) described three pooling procedures that combine mutually dependent events, including the inter-event time and volume criterion method, moving-average procedure and sequent peak algorithm.

5.7 Climate Change and European Hydrological Drought

This subsection examines how European hydrological drought characteristics could vary as climate changes (Research Question 1 in Section 5.1).

5.7.1 Emission Scenario Uncertainties

Figures 5.6 and 5.7 demonstrate the spread of 2051–2100 severity and DAI25 frequency, respectively, associated with the range of emission scenarios (left panels) and GCMs under RCP6 (right). Results for 2001–2050 (not shown) exhibit similar characteristics with smaller magnitudes and uncertainties. In broad terms, both sources of uncertainty resemble similar patterns of change for both 12- and 3-month results. Spread arising from choice of GCM for generating the scenarios is a larger source of uncertainty than that arising from the emission scenarios considered here, particularly in summer and autumn. Similarly, results in Kjellström *et al.* (2011) are less sensitive to emission scenarios until later in the 21st century. Arnell (2003a) found emission scenarios (for a given model) produce similar patterns and magnitudes of change in mean European annual runoff prior to the 2050s, and larger difference in magnitudes of change in the 2080s. Regionally, projections for SC are fairly robust regardless of the season and length of event.

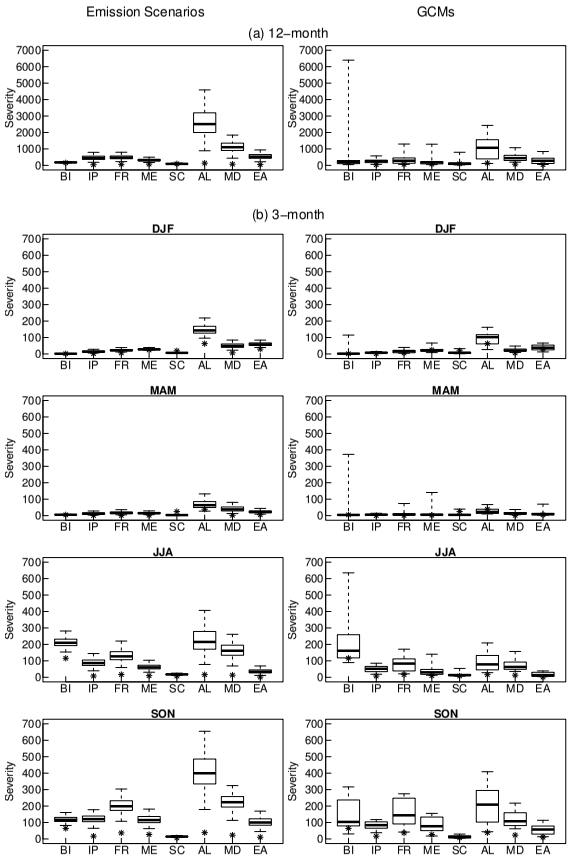

Figure 5.6: Drought severity in 2051–2100 derived from fixed threshold and event definition that excludes excess periods based on ECHAM5 under 10 emission scenarios (left) and 18 GCMs under RCP6 (right). Asterisks (*) denote 1951–2000 values.

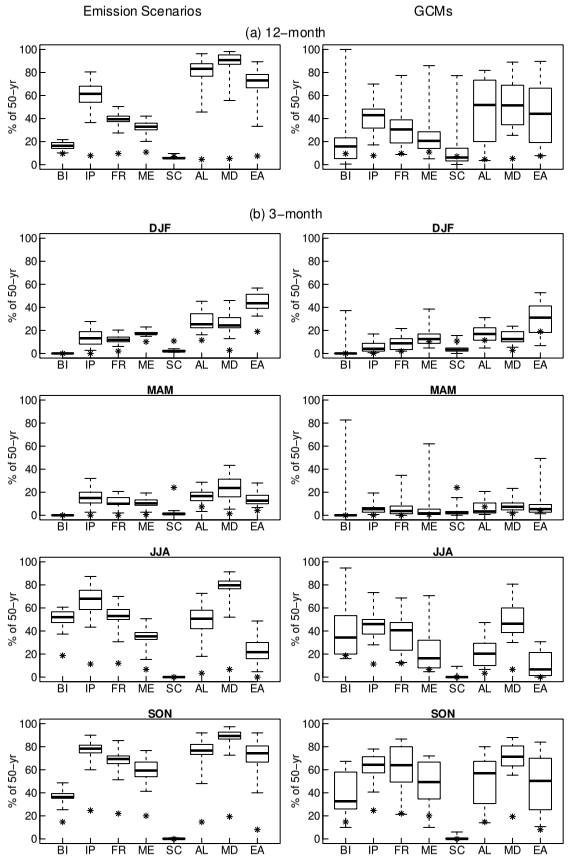

Figure 5.7: Same as Figure 5.6, but for frequency of DAI25.

5.7.2 GCM Uncertainties

Findings in Section 5.6 suggest minor differences between results that include or exclude excess periods. According to Section 5.5, it can be inferred that magnitudes of drying could be larger than those found in this section with the use of seasonally-variable threshold for identifying drought. Section 5.7.1 indicates that emission scenario uncertainties are smaller than GCM spread, hence the following analysis focuses on simulations using 18 GCM patterns scaled to represent the RCP6 scenario.

5.7.3 PRUDENCE-Averaged Results

Figures 5.8, 5.9 and 5.10 show simulations from the 18 GCMs of hydrological drought severity, frequency of DAI25 and DAI50, respectively, for the 21st century alongside their 1951–2000 values. The boxplots display the minimum and maximum data values, first and third quartiles, and the median of the set of 18 results (one from each GCM used). The level of GCM-consistency in the direction of change is illustrated in Figure 5.5, with the legend class as elaborated in Table 5.1. Magnitudes of change for categories with robust trends are presented in Figure 5.11.

Results indicate that climate change projections would generally increase drought conditions across all PRUDENCE regions. Kundzewicz *et al.* (2006) also simulated more severe “dry and hot” extremes for most of Europe, along with considerably longer duration of the longest dry spell in 2070–2099. Uncertainties in projections are higher in 2051–2100 and roughly correspond to the amount of warming. The drying trend is more extensive spatially in 2051–2100 than 2001–2050 for both 12-month and 3-month events. Robust drying occurs in the southern latitudes (IP and MD), and also in summer/autumn, which is in agreement with Feyen and Dankers (2009). The high latitudes (SC) and altitudes (AL) may experience decreasing drought conditions, particularly in winter and spring; however, seasonal changes of permafrost and glacial melt are not represented in Mac-PDM.09.

Regional changes in hydrological drought characteristics are discussed in subsequent sections.

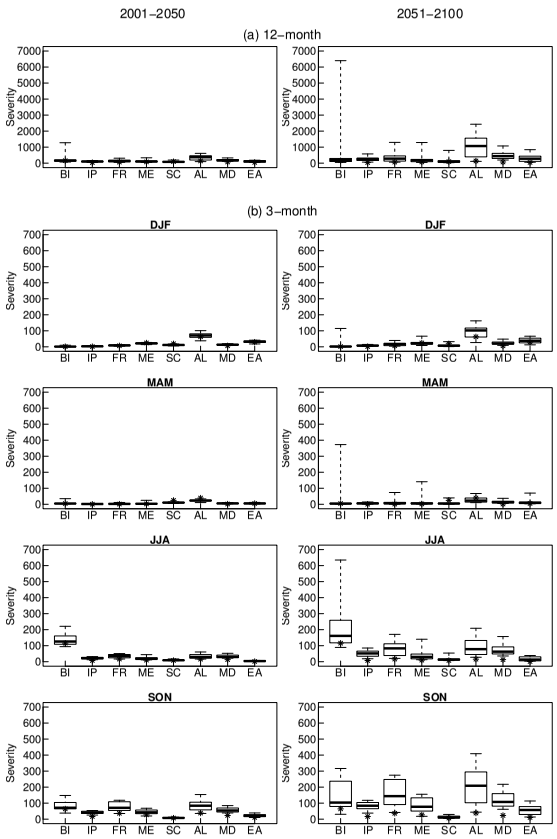

Figure 5.8: PRUDENCE-averaged drought severity derived from fixed threshold and event definition that excludes excess periods projected by 18 GCMs under RCP6. Asterisks (*) denote 1951–2000 values.

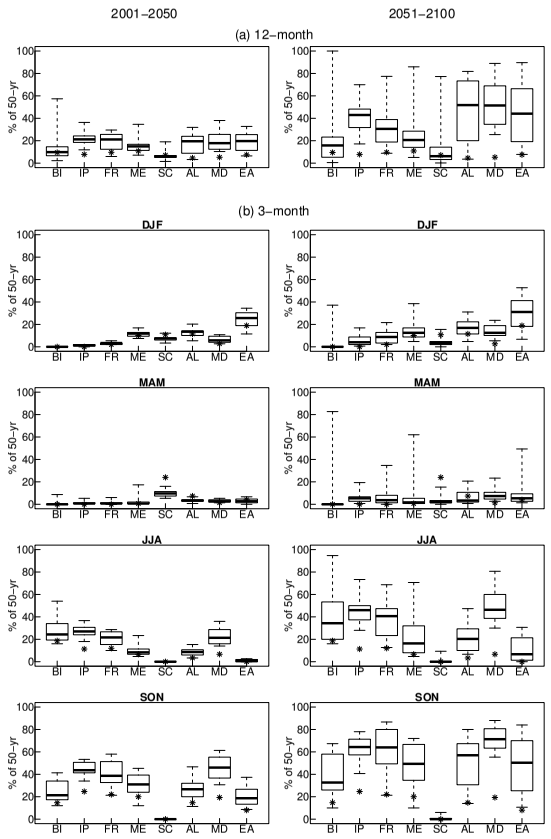

Figure 5.9: Same as Figure 5.8, but for frequency of DAI25.

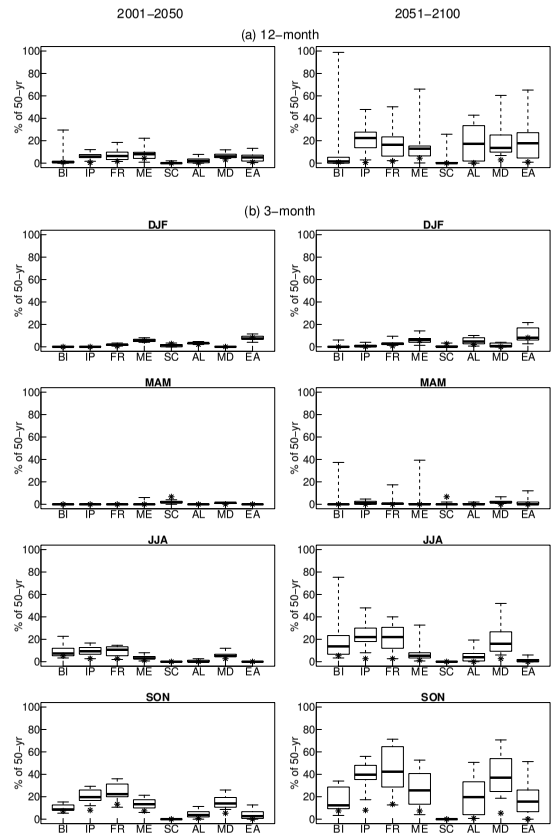

Figure 5.10: Same as Figure 5.8, but for frequency of DAI50.

mon h

	Severity	DAI25	DAI50	Severity	DAI25	DAI50
BI						
IP	2.2-3.2 (2.8)	2.4-3.1 (2.8)	9.7-14.7 (12.4)	4.6-8.2 (7.2)	4.3-6.2 (5.3)	29.6-54.2 (44.4)
FR						4.1-13.8 (10.4)
ME						
SC						
AL						
MD	1.9-3.0 (2.6)	2.4-4.8 (3.8)	1.7-2.8 (2.3)	4.1-8.2 (6.5)	6.7-12.8 (10.1)	3.4-8.5 (6.9)
EA				2.6-9.3 (6.7)	2.7-8.8 (5.9)	

mon h

	DJF	MAM	JJA	SON	DJF	MAM	JJA	SON
BI								
IP	1.8-2.4 (2.1)	2.0-3.4 (3.0)	2.3-3.5 (2.9)	2.1-2.9 (2.4)	3.7-6.3 (5.0)	4.7-12.4 (9.9)	4.5-8.5 (6.6)	4.0-6.2 (4.9)
FR			1.5-2.7 (2.1)				2.3-6.7 (4.7)	2.6-6.6 (4.4)
ME			1.5-2.5 (2.0)				1.9-4.7 (3.9)	
SC	0.5-0.7 (0.6)	0.4-0.5 (0.4)						
AL		0.6-0.6 (0.6)	1.4-2.7 (2.1)				3.0-7.9 (5.8)	3.0-7.5 (5.7)
MD	1.7-2.3 (2.0)	2.4-3.9 (3.3)	2.0-3.0 (2.5)	2.0-3.0 (2.5)	2.6-4.5 (3.6)	4.9-10.5 (8.8)	3.7-6.9 (5.7)	3.6-6.7 (5.2)
EA			1.7-4.6 (3.1)				3.9-20.6 (12.0)	2.8-7.3 (5.4)

mon h

	DJF	MAM	JJA	SON	DJF	MAM	JJA	SON
BI								
IP		n/a	2.1-2.7 (2.4)	1.7-2.1 (1.8)	n/a	n/a	3.4-4.4 (4.1)	2.3-2.9 (2.5)
FR	1.1-1.7 (1.6)				1.7-6.2 (4.6)		1.9-3.9 (3.0)	
ME								
SC		0.3-0.5 (0.4)						
AL		0.4-0.5 (0.5)					3.2-8.8 (6.6)	
MD		1.5-2.9 (2.2)	2.4-4.2 (3.4)	1.9-2.8 (2.4)	3.8-6.8 (5.2)	3.5-7.6 (6.5)	5.8-8.8 (7.5)	3.3-4.2 (3.7)
EA				1.7-3.3 (2.5)				3.2-8.7 (5.9)

mon h

	DJF	MAM	JJA	SON	DJF	MAM	JJA	SON
BI								
IP				1.5-3.2 (2.6)			6.8-10.9 (8.8)	2.1-5.9 (4.9)
FR					3.0-5.0 (5.2)			
ME								
SC		0.2-0.4 (0.3)				0.0-0.0 (0.0)		
AL	1.3-1.7 (1.6)	n/a						
MD			1.8-2.4 (2.3)	2.0-3.5 (2.8)		n/a	3.6-9.9 (8.2)	4.8-9.9 (7.5)
EA								

Figure 5.11: PRUDENCE-averaged magnitude of change, expressed as ratio to 1951–2000 values, for the IQRs and ensemble means (in brackets) of hydrological drought parameters (excluding excess periods) simulated using 18 GCMs under RCP6. Categories with robust positive (red) and negative (blue) trends are shown. "n/a" denotes no drought events in 1951–2000 thus the relative magnitude of change cannot be mathematically expressed as a ratio.

5.7.3.1 Iberian Peninsula (IP) and Mediterranean (MD)

All GCMs project increasing drying for 12-month events over the 21st century for IP and MD (Figure 5.5). These regions have similar magnitudes of increase (Figure 5.11) in 2001–2050, by two to four-fold for severity and DAI25 frequency. Increases in 2051–2100 are considerably greater: by over 4-fold, and up to 8- and 13-fold for severity and DAI25 frequency. In absolute terms, DAI25 occurs 16–25% of the time during 2001–2050 for both regions, and up to 48% of the time during 2051–2100 for IP, and 67% for

MD. The marked increases in DAI50 frequency are due to their rare occurrence (<5%) in 1951–2000; in absolute terms, DAI50 are projected to occur in approximately 5–8% of 2001–2050 and 10–28% of 2051–2100.

These results are consistent with the anticipated runoff decline (Nohara *et al.*, 2006) (which has much less uncertainty than that for precipitation; Gosling *et al.*, 2010) in the southern Europe/Mediterranean, caused by warming, higher evapotranspiration and decreasing annual mean precipitation (see Section 4.4.3). In a global study, Adam *et al.* (2009) projected southern Europe to have one of the strongest areas of runoff declines by 2040. Nohara *et al.* (2006) projected decreasing annual mean precipitation and runoff for the Danube and Euphrates, based on simulations from 19 GCMs. By the 2050s, 30-year average annual runoff in the region south of around 50°N could be 50% lower (Arnell, 1999c).

These changes in runoff could bring about low-flows (Alcamo *et al.*, 2007b) and droughts. By the 2050s, flow below the current 10-year return period minimum annual runoff ("drought" runoff) could be three times more frequent in areas with simulated decreasing average annual runoff (Arnell, 2003a). By 2100, minimum flow in the Iberian Peninsula and southern France could reduce by 20–40% (Feyen and Dankers, 2009). Using the WaterGAP model, Lehner *et al.* (2006) simulated more frequent 100-year hydrological drought in southern (Portugal, Spain, western France, Italy) and most of southeastern Europe while Weiss *et al.* (2007) estimated it to become ten times more frequent in the 2070s over a large part of the northern Mediterranean. More frequent long-duration droughts are expected for southern Europe, despite uncertainties in the magnitude (Blenkinsop and Fowler, 2007b). For the Ebro/Gallego region (Spain), Blenkinsop and Fowler (2007b) projected, with high model consistency, increasing severity and duration of long droughts with maximum drought length to increase by ≈30 months. These could increase the pressure on water resources, particularly groundwater, due to decreases in recharge during the cooler, wetter part of the year (Blenkinsop and Fowler, 2007b). Similarly, water availability for the region south of 47°N could drop by up to 23% by the 2020s and 6–36% by the 2070s (Alcamo *et al.*, 2007b). García-Ruiz *et al.* (2011) has provided a comprehensive review on the projected changes in climate and streamflow regimes for the Mediterranean basin, which generally implies increasing water stress.

Robust increases are projected for both IP and MD across all seasons throughout the 21st century for severity and DAI25 frequency (except winter for 2001–2050; Figure 5.5). Both regions have similar severity and DAI25 frequency increases in 2001–2050 (Figure 5.11), by around two to four-fold. Marked increases, being most (least) pronounced in spring (winter), occur in 2051–2100: by up to seven-fold in winter, twelve-fold in spring, and nine-fold in summer and autumn.

Winter results have the smallest magnitude of increase (Figure 5.11) for both IP and MD. This could reflect the sub-regional precipitation variations (Kundzewicz *et al.*, 2006; Buonomo *et al.*, 2007; García-Ruiz *et al.*, 2011) (see Section 4.4.3), winter discharges to become more irregular (García-Ruiz *et al.*, 2011) and/or the initial melting of long-term storage of frozen precipitation in major streams originating in the Alps (e.g. Danube; van Lanen *et al.*, 2007; Huss, 2011) and other Mediterranean mountain regions such as Sierra Nevada, southern Spain (García-Ruiz *et al.*, 2011) and central Spanish Pyrenees (López-Moreno and García-Ruiz, 2004), despite the lower precipitation (Kjellström *et al.*, 2011). By 2051–2100, further warming and the altered snowmelt hydrology (see Section 2.5) may cause DAI25 to become frequent. Since glacial contribution to runoff is limited to certain basins, these changes are more notable in DAI25 frequency than in severity.

The large summer and autumn increases in drought conditions are related to summer drying (see Section 4.4.3), and intensified summer low flows in the Mediterranean (García-Ruiz *et al.*, 2011); the larger magnitudes of increase in spring may be related to earlier snowmelt.

5.7.3.2 Scandinavia (SC)

Although without robust trends, SC generally shows decreasing 12-month severities and frequencies of widespread events (Figure 5.5). Other studies have also found increasing precipitation (see Section 4.4.4), higher evaporation and runoff (Nohara *et al.*, 2006) that imply decreasing drought conditions.

Higher precipitation offsets the increased temperatures and evapotranspiration (van Lanen *et al.*, 2007) that would otherwise reduce runoff (Arnell, 2003a). Moreover, evapotranspiration variations have only minor influence in snowmelt-dominated regions (Barnett *et al.*, 2005). Therefore, annual discharge increases (van Lanen *et al.*, 2007), e.g. in

Norway (Roald *et al.*, 2004; Hanssen-Bauer *et al.*, 2005) and Denmark (Thodsen, 2007), perhaps by up to 25% by the 2050s (Arnell, 1999c) while total mean annual runoff in the Baltic Sea may vary by between -2% and $+15\%$ (Graham, 2004). This, produces lower severity (Feyen and Dankers, 2009) and intensity (Arnell, 1999c) of streamflow drought in northern and northeastern Europe. Also, changes are not uniform, with increases (decreases) in the northernmost (southernmost) catchments across the Baltic Basin (Graham, 2004; Graham *et al.*, 2007).

Seasonally, severity and DAI25 frequency decrease in winter and/or spring and increase in summer and autumn (Figure 5.5). These changes may be related to the higher precipitation in the cold seasons, warming-induced earlier snowmelt, and the associated higher cold-season runoff and lower warm-season runoff, as found in other studies (see Section 4.4.4). Also, higher evapotranspiration may offset precipitation increase (Feyen and Dankers, 2009). For the Baltic Basin, Graham (2004) and Graham *et al.* (2007) projected winter (summer) flows to increase (reduce) by up to 54% (22%) on average, with greatest uncertainties due to different RCMs in summer and autumn. Nevertheless, warming may not affect the timing of flow in very cold regions (Arnell, 1999c).

Figure 5.11 shows that both severity and DAI25 frequency reduce by up to 50% in winter and 70% in spring. The more robust changes in 2001–2050 suggest that in ClimGen, under a small warming scenario (e.g. in 2001–2050), the overall rate of precipitation reduction in cells with decreasing precipitation (an exponential function of global-mean temperature change; see Section 3.2) may be smaller than the rate of precipitation increase in cells with increasing precipitation (a linear function), thus a regional positive change. As warming continues (e.g. in 2051–2100), particularly in winter (Hanssen-Bauer *et al.*, 2005), the overall rate of precipitation decline may exceed that for precipitation increase, thus a regional negative change. Together with the effect of increased evaporation (van Lanen *et al.*, 2007), which may dominate over the precipitation change signal (Feyen and Dankers, 2009), the sign of hydrological response changes from positive to negative with higher levels of warming (e.g. the British Teme basin; Todd *et al.*, 2011), hence weakening model consensus.

Hydrological indicators may respond differently to the same climatic inputs. This may be due to the physical structure of the river basin (e.g. storage in soils, aquifers,

lakes, bogs, snow pack, glaciers) and/or the relative importance of the seasonal distribution of precipitation and increased evapotranspiration (van Lanen *et al.*, 2007) and reduced snowmelt (Feyen and Dankers, 2009). For example, Wong *et al.* (2011) found that warming is primarily responsible for drought variations in Norway except the south where reduced summer precipitation dominates. In addition, despite the expected higher summer precipitation (Kundzewicz *et al.*, 2006; Kjellström *et al.*, 2011), its sub-regional variations — increases (decreases) in northern (southern) Scandinavia (Hanssen-Bauer *et al.*, 2005; Frei *et al.*, 2006) — and mixed trends in minimum flow and flow deficit in non-frost seasons (Feyen and Dankers, 2009), contribute to the lack of robustness in the summer and autumn results (Figure 5.5). Nevertheless, the increasing summer and autumn severities obtained here are consistent with negative streamflow trends simulated for Norway (Engen-Skaugen *et al.*, 2005; Roald *et al.*, 2006; Beldring *et al.*, 2008) and Denmark (Thodsen, 2007), and the lower minimum flows in the frost-free season in parts of Sweden as reduced and earlier snowmelt (see Section 2.5.2) offsets the precipitation increase (Feyen and Dankers, 2009). The inconsistent changes in DAI25 frequencies found in the present study are also attributable to reduced likelihood of widespread droughts in geographically large regions such as SC.

5.7.3.3 Alps (AL)

AL generally demonstrates increasing drought conditions across all categories, except spring results which show negative changes (Figure 5.5); only spring, summer and autumn have robust changes.

The 12-month drought results obtained here agree with the expected precipitation changes (see Section 4.4.5) and findings from other studies. For example, based on climate-change scenarios from 19 RCMs for 11 mountainous catchments in the Swiss Alps, Horton *et al.* (2006) simulated mean annual runoff to decrease by up to 30% in 2070–2099. For the Kitzbheler Ache catchment in the Austrian Alps, Laghari *et al.* (2012) projected reducing annual snowmelt (by 31–81%) and runoff (by 6–33%), and increasing average annual evapotranspiration (by 6–20%) by 2071–2100 based on 13 regional climate change scenarios under SRES A2 and B2.

Snow cover (e.g. in the French Alps; Martin *et al.*, 1996) is highly sensitive to climate

variations. Each degree (°C) of warming could reduce snowpack duration in alpine catchments by about three weeks (Graham *et al.*, 2007), and alpine river flow is more affected by warming than precipitation and land use changes (Zierl, 2005). Seasonal precipitation variations are more influential in the hydrological regime of lower-altitude catchments (Horton *et al.*, 2006). The alpine flow regime becomes rainfall-dominated instead of rainfall and snowmelt-dominated (Laghari *et al.*, 2012) with warmer, wetter winters and springs (Beniston, 2005; European Environment Agency, 2009; Smiatek *et al.*, 2009; Kotlarski *et al.*, 2010). Snowpack volume in alpine catchments could be 60% lower in 2070–2100 (Graham *et al.*, 2007), runoff deviations caused by glaciers loss (Zemp *et al.*, 2006) and earlier snowmelt described in Section 2.5.2 are reflected in the seasonal results (Figures 5.5 and 5.11).

In spring, both severity and frequency of widespread events are roughly halved in 2001–2050, with high model consistency. These results, some of which also depend on conditions in the preceding winter, are consistent with Janža (2011)'s projected higher winter and lower spring discharges for the Upper Socčva River basin, Solvenia (southeastern Alps).

Consistent with the anticipated drying trend (see Section 4.4.5), increasing drought conditions occur in all other seasons, with more robust changes in summer: by around 3–8 times in 2051–2100 for both severity and DAI25 frequency. Similar to the results here, minimum flow for the region during the frost-free season could be 20–40% lower (Feyen and Dankers, 2009). Runoff contribution to the Po basin from currently glacierized areas could be $>$75% lower by 2080–2100 compared to the 20th century average in August/September (Huss, 2011). By 2071–2100, drought frequency and severity during the Alpine summer growing season (April to August) could increase by 15–50% and 20%, respectively (Calanca, 2007) due to much lower summer flows (Jasper *et al.*, 2004).

5.7.3.4 Mid-Europe (ME) and Eastern Europe (EA)

Both ME and EA show increasing 12-month drought conditions throughout the 21st century (Figure 5.5). EA severity and DAI25 frequency demonstrate robust marked increases (by 2–9-fold) in 2051–2100 (Figure 5.11).

These results are consistent with the declining annual runoff projected for eastern Europe and western Russia over the 21st century (Strzepek and Yates, 1997; Arnell, 2003a; 2004a) despite the annual precipitation increase in Eastern Europe (Hirabayashi *et al.*, 2008), with the largest reduction in southeastern Europe by 2050 (Arnell, 1999c). Average annual water availability in these regions could decline by >25% by 2050 relative to 1961–1990 (Alcamo *et al.*, 2007b). Annual runoff may decrease by 3–24% in Romania, and deviate by −10% to +3% and −20% to +128% in Czech Republic and Ukraine, respectively (Smith and Lazo, 2001). Precipitation reduction over the Mediterranean region to the Caspian Sea region (Nohara *et al.*, 2006) lowers Danube discharge by 21.9%, along with annual maximum, minimum, and mean streamflow (by 13.3%; Nohara *et al.*, 2006) of the Rhine (Hurkmans *et al.*, 2010).

Reducing runoff implies increasing drought conditions in eastern Europe (Hirabayashi *et al.*, 2008): Lehner *et al.* (2006) projected strong increases in 100-year droughts for southeastern Europe (e.g. Hungary, Bulgaria, Romania, Moldova, Ukraine, southern Russia) and Kundzewicz *et al.* (2006) simulated longer duration of the longest dry period for much of central Europe. The Rhine, Danube and Dniepr rivers could experience more frequent drought during 2071–2100 (Hirabayashi *et al.*, 2008); more long droughts are likely in the Meuse/Dommel region (western ME; Blenkinsop and Fowler, 2007b). Even with higher annual precipitation, drought increases in eastern Europe to central Eurasia due to the much higher evapotranspiration (Hirabayashi *et al.*, 2008).

Nonetheless, sub-regional variations have been reported: the Black Forest and the Vogues Mountains (southwestern ME) and the northern tributaries of the Rhine basin (northwestern ME) may experience wetter conditions throughout the year (Hurkmans *et al.*, 2010); Gellens and Roulin (1998) found no clear trends for either streamflow or the number of low flow days for eight Belgian catchments.

In addition to the summer precipitation decline (see Section 4.4.6), runoff variations in the upstream region affect downstream river flows (Nohara *et al.*, 2006), and glacial meltwaters affect both local/regional basins and the hydrological regime of large catchments with glacierisation of <1% (Huss, 2011). The contribution of high summer glacier runoff in lowland areas with low precipitation and high evapotranspiration signifies a non-linear relationship between the relative importance of glacier contribution to runoff (Huss,

2011).

Snowmelt hydrology is important in the water cycle of EA, the margin between maritime and continental climate regimes, and ME, e.g. the Rhine basin is influenced by conditions in the alpine part of the catchment (Hurkmans *et al.*, 2010); 9% of September runoff in 2003 in the lower Danube (0.06% glacierisation) was estimated to be glacier meltwater (Huss, 2011). Warming diminishes the importance of snowfall, leading to a large flow regime (Arnell, 1999c; 2003a). For instance, the "rain-fed/meltwater" Rhine river could become a mainly "rain-fed" river (Pfister *et al.*, 2004). Runoff contributions to the Rhine and Danube basins from currently glacierised areas during 2080–2100 could be $>$75% lower compared to the 20th century average in August/September, although with slower reduction in catchments with a large ice volume (Huss, 2011). Even with small changes in total annual runoff (e.g. a mountainous region of southwestern Bulgaria; Chang *et al.*, 2002), warming significantly changes the spatial distribution and amount of snow cover (Arnell, 1999c), e.g. the alpine glacierised areas may decline by 12% by 2100 (Huss, 2011). These could alter runoff volume and the timing of maximum runoff (Chang *et al.*, 2002; Hirabayashi *et al.*, 2008) and increase the frequency and magnitude of both peak flows and streamflow droughts (Hurkmans *et al.*, 2010; Section 2.5.2). For short events in the Meuse/Dommel region, Blenkinsop and Fowler (2007b) projected increases in maximum severity, frequency (although the spatial pattern of change is variable and GCM-dependent) and duration (most likely to be in the northern Dommel and the southernmost part of the Meuse; despite higher uncertainties); for areas with a shorter winter recharge period (precipitation increase), these short events may become longer.

These changes are generally reflected in the seasonal results obtained here for ME and EA (Figure 5.5), although Mac-PDM.09 accounts for snowmelt but not glacial melt (hence runoff further downstream would not contain a glacial component). For ME, the decreasing drought conditions in winter/spring (also the case for 2001–2050 DAI25 frequency in EA) agree with the simulated increase in winter flows for the Rhine basin, particularly in lowland catchments (by up to 14%; Graham *et al.*, 2007), winter and spring streamflow at the basin outlet (by $\approx$30% by 2100; Hurkmans *et al.*, 2010), and peak flows in the alpine and pre-alpine catchments of the Rhine (by 9–16%; Pfister *et al.*, 2004). The initial melting of long-term storage of glaciers and snow cover (van Lanen *et al.*, 2007;

Huss, 2011) causes spring frequency of DAI25 to reduce in 2001–2050 but increase in 2051–2100 (Figure 5.5).

The summer and autumn results show positive trends. Both regions reveal robust and marked increases in summer severity throughout the century, by factors of up to 2.5 (ME) and 4.6 (EA) in 2001–2050, and 4.7 (ME) and 20.6 (EA) in 2051–2100. EA also demonstrates robust increases in autumn (Figure 5.11), though with a smaller magnitude of around 3–8-fold in 2051–2100. These are consistent with the projected reduction in summer and autumn river flows (by up to 42% for the Rhine basin; Graham *et al.*, 2007) and average summer discharge at the southern basin outlet (by ≈30% by 2100; Hurkmans *et al.*, 2010) and the Meuse river, western ME (Pfister *et al.*, 2004). Using a conceptual eco-hydrologic model, a revised version of the Soil and Water Assessment Tool (SWAT), Eckhardt and Ulbrich (2003) estimated summer mean monthly streamflow for the Dill catchment (southeast of the Rhenish Massif in Germany) to reduce by up to 50% during 2070–2099. Drogue *et al.* (2004) simulated more severe low flows for July–September in the 2050s for a temperate Alzette river basin in the Grand Duchy of Luxembourg.

The stronger and/or more robust drying trends in EA compared to ME across all seasons are associated with warming being most pronounced in winter over eastern Europe (Giorgi *et al.*, 2004; Somot *et al.*, 2008) and therefore much higher evapotranspiration (Hirabayashi *et al.*, 2008).

For mesoscale basins, both changes in the variability of extreme precipitation and land use affect future changes in peak flows. A changing climate may also influence vegetation cover, which can then have a significant impact on hydroclimatological processes, such as surface runoff, infiltration or evapotranspiration (Pfister *et al.*, 2004). Increased economic activity across much of central and eastern Europe and the anticipated strong increases in water use may cause or exacerbate hydrological or operational droughts (Lehner *et al.*, 2006; Alcamo *et al.*, 2007b).

5.7.3.5 France (FR)

Increasing 12-month drought conditions is projected for FR throughout the 21st century (Figure 5.5). The robust and marked increases (by 4–14-fold) in DAI50 frequency, which occur in 7–23% of 2051–2100 (Figure 5.11), are attributable to its low frequency

(2%) in 1951–2000.

These regional results may have masked sub-regional variations in runoff and the type of changes suggested in other studies. Although the high altitude snowpack (>2000 m) is relatively unaffected, the maximum amplitude of the snowpack at low and medium elevations could be 50% lower and its duration shortened by two months, resulting in lower annual discharge (see Section 2.5.2), which also diminishes with evaporation increase (by 20%; Etchevers *et al.*, 2002). Therefore, climate anomalies are more influential in the Pyrenees than the Alps given the lower height and more moderate increase in winter precipitation (Redaud *et al.*, 2002).

Snow processes in the Alps imply low annual evaporation and large runoff, whereas areas with Mediterranean climates (large annual global radiation, low precipitation) have negligible annual runoff (Habets *et al.*, 1999). Topography and snow are important in the hydrological regime of the Rhone and its tributaries (Redaud *et al.*, 2002), which drains from the Alps (Feyen and Dankers, 2009), leading to large spatial variability of evaporation and total runoff (Habets *et al.*, 1999). Changes in mean annual discharge correspond to the precipitation anomaly and display a strong northward gradient (Etchevers *et al.*, 2002): in the north, precipitation increase of 25% combined with the relatively small (13%) evaporation increase raise discharge by 10–30% and 30–50% in the Jura mountains and Saone valley, respectively. Western France could experience significantly more frequent drought (Lehner *et al.*, 2006). However, as for ME/EA above, much of the runoff further downstream from the Alps, for example, would not contain a glacial component as it is not represented in Mac-PDM.09.

Similar to 12-month results, increasing drought conditions are also projected across all seasons, with high model agreement in summer/autumn severities and winter DAI25/DAI50 frequencies particularly for the 2051–2100 results (Figure 5.5). Increases in severity are up to three times in 2001–2050 summer and 7-fold in 2051–2100 summer and autumn (Figure 5.11). In winter, DAI25 is 1.7 times more frequent in 2001–2050 (to 3%) and >6 times in 2051–2100 (to 13%); DAI50 occurs only in 3% during 2051–2100, even with the 3–5-fold increase.

Ducharne *et al.* (2007) simulated enhanced seasonal contrast of discharge at the outlet of the Seine watershed for 2070–2099 compared to 1960–1989. However, the winter

increases projected here contradict the expected higher winter rainfall (e.g. in northern Rhone due to more liquid precipitation; Huss, 2011) that would raise soil water content thus surface runoff and drainage, particularly in the second future period (Redaud *et al.*, 2002). This could partly be explained by the reduced winter accumulations in (especially medium) mountain areas associated with warming and less snowfall notwithstanding the precipitation increase (Redaud *et al.*, 2002), and partly because some of the winter results are influenced by drying in the preceding autumn.

The projected summer and autumn drying trend is consistent with the anticipated warming (that is more considerable in summer than winter), summer rainfall decline, a very low soil water index for May–October (hence a much earlier soil desaturation and harsher low water periods in autumn), earlier snowmelt (by about one month) and a flood peak in May (rather than June), followed by much lower July and August discharge (Etchevers *et al.*, 2002; Redaud *et al.*, 2002). Specifically, runoff contribution to the Rhone basin from currently glacierised areas in 2080–2100 could decrease by 55% from the 20th century average in August/September (Redaud *et al.*, 2002; Huss, 2011). Decreases in Durance discharge (southern Rhone) is most notable in the rainy autumn (also during spring snowmelt season) (Etchevers *et al.*, 2002). For the Adour-Garonne basin (southwestern France), decreasing snow depth and the snow cover duration (by approximately 50% by 2100; Caballero *et al.*, 2007) produce earlier low flows (by one month) and a stronger deficit in the July discharge (Redaud *et al.*, 2002). However, substantial winter recharge preserves groundwater levels (the perched and alluvial groundwater sheet and the unconfined aquifer) and alleviates deficit during the low-flow period (Redaud *et al.*, 2002), thus the slight decrease (averaged 11%$\pm$8% in 2050–2060 compared to 1985–1995) in low-flow during July–October (Caballero *et al.*, 2007). Though, large reduction in autumn discharge occurs when precipitation deficit is larger than groundwater supply (Caballero *et al.*, 2007). It is worth noting that groundwater in Mac-PDM.09 is not stored but routed as “slowflow” that contributes to runoff.

5.7.3.6 British Isles (BI)

An increase of annual river flow in Western Europe suggest fewer and less severe droughts (van Lanen *et al.*, 2007). However, the 12-month drought results produce inconclusive trends in 2001–2050 and positive trends in 2051–2100 for BI (Figure 5.5). Changes in drought found in other studies are location-dependent. For instance, Arnell (2004b) projected average annual runoff to decrease by up to 15% by the 2020s in eastern England and little change in northern and western Britain under the UKCIP02 scenarios; changes are more extreme by the 2080s. Low flows (Q95) could reduce by 20–25%, 30–50% and 50–80% by the 2020s, 2050s and 2080s, respectively (Arnell, 2003b; 2004b). For longer droughts in the Eden region (north-west England), Blenkinsop and Fowler (2007b) projected decreasing maximum drought severity, duration and frequency (by around one event per decade) with increasing winter precipitation, along with fewer long groundwater droughts and more short-term surface water droughts. Central and eastern England catchments may experience the most severe low flow reductions while flooding increases in northern and western England (Sefton and Boorman, 1997). In Wales, Pilling and Jones (2002) found significantly more frequent low flows in the year as a whole in the Upper Wye catchment even though annual discharge shows small changes. Across much of Ireland, particularly eastern and southeastern parts, Charlton *et al.* (2006) simulated a widespread reduction in annual runoff, with the extreme northwest showing a slight increase. Elevation may also affect annual runoff, e.g. Fowler and Kilsby (2007) found a slight increase ($\approx$16% lower) at high (lower) elevation catchments in northwestern England.

Figure 5.5 reveals that droughts generally increase in summer and autumn, and decrease in winter and spring, although lacking robustness. Other studies suggest similar, weak (Prudhomme and Davies, 2008) or enhanced seasonal patterns (e.g. Harper's Brook; Gosling *et al.*, 2011b). Arnell (2004b) simulated modest increase in mean winter flows, particularly in the north and west while the direction of spring changes is GCM-dependent (Prudhomme and Davies, 2008). Using scenarios from HadRM3H, Fowler and Kilsby (2007) projected runoff in northwestern England to increase by up to 20% from 1961–90 levels in winter and reduce in summer by 40–80% (particularly at lower elevations) under SRES A2, along with a lower magnitude of summer Q95 (by 40–80%) and more frequent

low flows below the present Q95; reductions also occur during the recharge periods of autumn and spring. Based on 21 GCMs, summer runoff deviations range from -40% to $+20\%$ with a 2°C warming from the 1961–1990 mean as rainfall and PET changes (Arnell, 2011). Under the UKCIP02 scenarios, Arnell (2004b) simulated mean summer flows and Q95 to decrease from the 1961–1990 mean by approximately 30% and 25%, respectively, by the 2020s, with reductions larger in southern and eastern England. Wilby *et al.* (2006) simulated lower summer and autumn flows for River Kennet, southern England. Flow variability may increase (decrease) in winter and spring (autumn) though the pattern is weak (Prudhomme and Davies, 2008).

The BI results lack model consistency due to several influencing factors. Literature suggests considerable sub-regional variations for this region — wetting (drying) in the north (south) (Blenkinsop and Fowler, 2007b); the averaging of which would induce uncertainties notably in the 12-month, winter and spring results. Furthermore, although warming is likely to substantially increase the magnitude and frequency of temperature-related weather extreme statistics (e.g. heat-waves; Semenov, 2007), the changing relative dominance of precipitation and PET may produce non-linear hydrological response to a linear climate change forcing (Arnell, 2011).

Prudhomme and Davies (2008) expressed that not all their 2080s trends in mean monthly river flow for four British catchments were significant relative to variations from natural variability; and that an even weaker signal exist with lower significance occurred for shorter time horizons (e.g. the 25-years of water management plans in UK). Furthermore, the combined effects of natural climatic variability and human-induced climate change substantially widens the projection range of future monthly and seasonal streamflow or may counteract the climate change signal, which have important implications for the operational management of future water resources (Arnell, 2003b). Based on the UKCIP98 climate change scenarios, Arnell (2003b) found that human-induced climate change has a different seasonal effect on flows than natural multi-decadal variability (positive in winter and negative in summer) in six catchments in Britain. Increased year-to-year climate variability causes slight increases in mean monthly flows (relative to changes resulting from mean climate changes), and slightly greater decreases in low flows, particularly in upland catchments (Arnell, 2003b); 30-year mean monthly runoff could vary from

the 1961–1990 mean by up to l0%; Q95 could deviate by ±5% and and 10% in southern and northern England, respectively (Arnell, 2004b). However, under the UKCIP02 scenarios, Arnell (2004b) found the climate-change signal larger than natural multi-decadal variability in many British catchments, even by the 2020s (Arnell, 2003b). This is because the climate change signal generally begins to exceed that of multi-decadal variability once the increase in global-mean temperature exceeds 1°C above the 1961–1990 mean (Arnell, 2011).

5.7.4 Köppen-Averaged Results

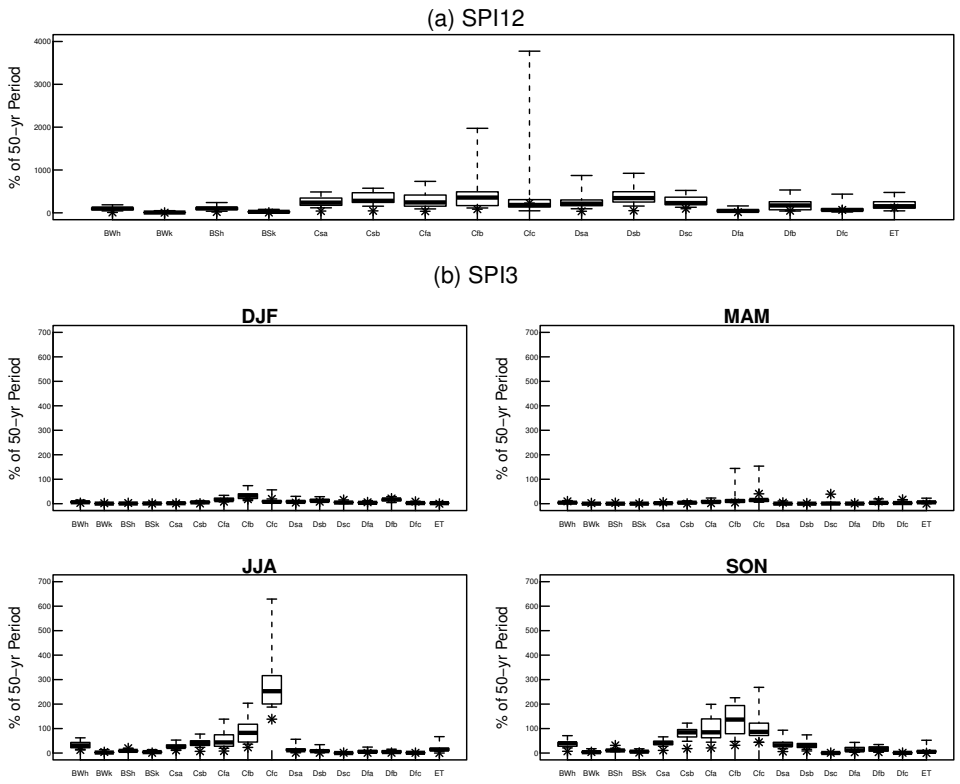

Figure 5.12: Köppen-averaged drought severity based on fixed threshold and event definition that excludes excess periods projected using 18 GCMs under RCP6. Asterisks (*) denote 1951–2000 values.

Köppen climate classifications are described in Section 3.9 (Figure 3.3). Figures 5.12 and 5.13 show simulations of 18 GCMs on 2051–2100 hydrological drought severity, frequency of DAI25 and DAI50, respectively. Results for 2001–2050 are not shown as they show very similar characteristics, with lower magnitudes. Figure 5.14 presents the level of agreement in the Köppen-averaged direction of change simulated by 18 GCMs

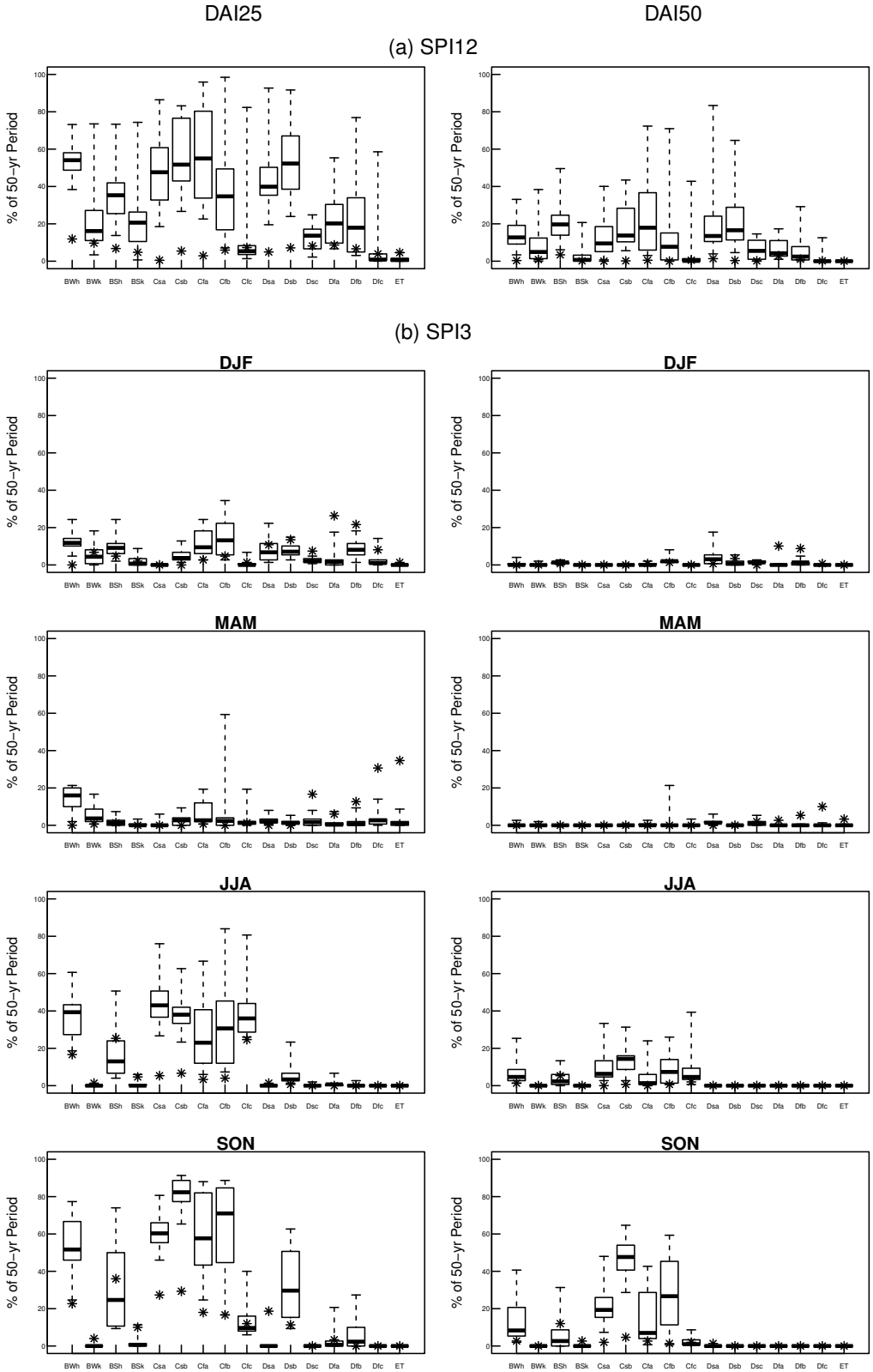

Figure 5.13: Köppen-averaged DAI25 (left panels) and DAI50 (right panels) frequency based on fixed threshold and event definition that excludes excess periods projected using 18 GCMs under RCP6. Asterisks (*) denote 1951–2000 values.

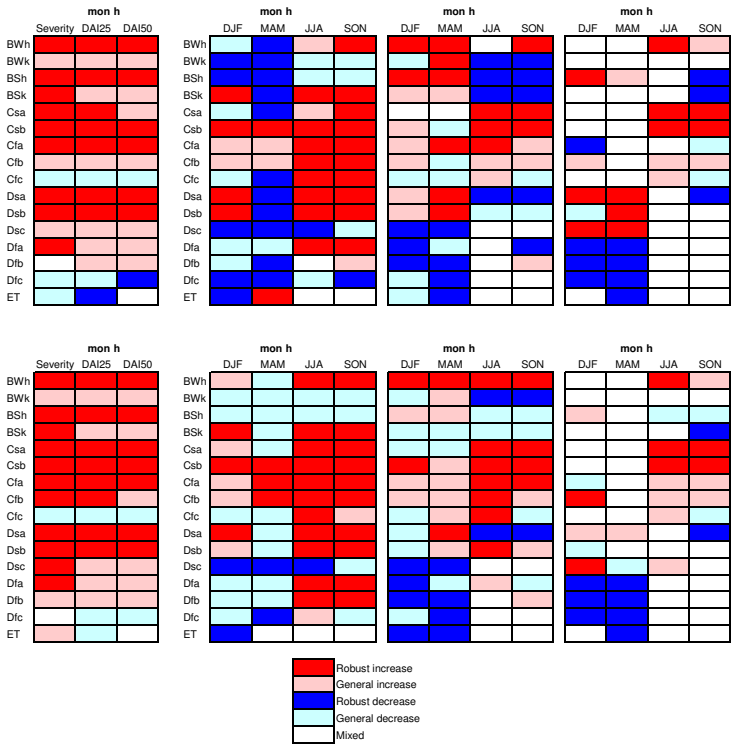

Figure 5.14: Köppen-averaged direction of change from 1951–2000 for hydrological events under fixed threshold projected using 18 GCMs under RCP6 based on event definitions that exclude excess periods.

under RCP6, with the legend elaborated in Table 5.1. For classifications with robust changes, their magnitudes (both IQRs and ensemble mean) are shown in Figure 5.15.

Similar to the PRUDENCE-averaged results (Section 5.7.3), drying is more notable in 2051–2100 than 2001–2050 for both short and long droughts across all climate regimes, particularly in summer and autumn. Decreasing drought conditions are more common in seasonal than annual results, and in 2001–2050 than 2051–2100, in winter and particularly spring due to changes in snow processes (see Section 2.5.2), and/or in cold climates (e.g. Dsc, Dfc). Köppen-averaged results demonstrate much higher consistency between GCM than PRUDENCE-averaged trends even for DAI50 frequencies (Figure 5.5). This may be due to the larger number of Köppen regions with smaller areas (i.e. lower chance of averaging results across cells with opposite signals), which better reflects actual areas of homogeneous climate change signal. Also, Figure 5.14a suggests more robust negative changes in spring severities for arid (B) and cold (D) climates (where snow and snowmelt hydrology are important) than in Figure 5.5a — warming in 2001–2050 implies increased runoff as, in Mac-PDM.09, precipitation falls as rain instead of snow and snowmelt occurs

mon h

	Severity	DAI25	DAI50
BWh	3.4-5.1 (4.4)	2.5-3.0 (2.7)	7.5-10.8 (9.7)
BWk			
BSh	2.1-2.6 (2.3)	2.1-2.7 (2.5)	1.7-2.6 (2.2)
BSk	1.5-2.2 (2.0)		
Csa	2.1-3.1 (2.6)	27.3-38.4 (34.8)	
Csb	2.3-3.4 (2.8)	3.3-5.3 (4.2)	15.5-37.5 (24.9)
Cfa	2.0-3.9 (3.1)	5.2-11.8 (8.9)	2.7-13.5 (9.9)
Cfb	1.2-2.4 (2.0)		
Cfc			
Dsa	2.1-2.9 (2.7)	3.5-4.4 (4.4)	2.2-4.6 (4.4)
Dsb	2.3-3.3 (2.9)	2.7-3.9 (3.5)	3.6-17.1 (12.7)
Dsc			
Dfa	1.3-2.1 (1.8)		
Dfb			
Dfc			0.0-0.2 (0.0)
ET		0.3-0.4 (0.4)	

	Severity	DAI25	DAI50
BWh	8.1-13.4 (12.0)	4.1-4.9 (4.6)	27.8-55.1 (42.5)
BWk			
BSh	4.3-6.7 (5.7)	3.8-6.2 (5.3)	4.1-7.3 (6.1)
BSk	2.7-4.7 (4.4)		
Csa	4.4-8.1 (6.6)	64.8-119.0 (100.0)	n/a
Csb	5.4-9.7 (7.2)	7.9-13.4 (10.1)	62.8-162.8 (115.4)
Cfa	4.2-10.8 (7.8)	12.0-27.1 (19.3)	11.8-69.9 (44.1)
Cfb	2.0-5.8 (5.1)	2.9-8.2 (6.1)	
Cfc			
Dsa	4.6-8.1 (7.5)	7.2-10.2 (9.3)	7.8-17.5 (15.9)
Dsb	5.2-9.7 (8.1)	5.6-9.3 (7.8)	34.1-84.8 (68.5)
Dsc	2.0-3.8 (2.9)		
Dfa	1.6-4.4 (3.4)		
Dfb			
Dfc			
ET			

mon h

	DJF	MAM	JJA	SON
BWh		0.1-0.1 (0.1)		2.3-3.0 (2.7)
BWk	0.2-0.3 (0.3)	0.0-0.0 (0.0)		
BSh	0.1-0.2 (0.1)	0.0-0.0 (0.0)		
BSk	2.1-2.7 (2.5)	0.2-0.2 (0.2)	1.9-2.7 (2.5)	1.7-2.4 (2.1)
Csa		0.1-0.2 (0.2)		1.9-2.3 (2.2)
Csb	3.3-5.0 (4.2)	4.2-6.7 (5.7)	2.2-3.0 (2.7)	2.0-2.7 (2.3)
Cfa			1.8-3.6 (2.7)	1.6-2.8 (2.2)
Cfb			1.4-2.3 (1.9)	1.5-2.6 (2.1)
Cfc		0.4-0.6 (0.5)	1.3-1.6 (1.5)	1.5-2.0 (1.8)
Dsa	1.6-2.1 (1.9)	0.0-0.0 (0.0)	3.6-4.9 (4.6)	2.3-2.9 (2.7)
Dsb	1.4-1.9 (1.7)	0.2-0.4 (0.3)	1.8-2.8 (2.6)	1.2-1.7 (1.6)
Dsc	0.5-0.6 (0.6)	0.2-0.4 (0.3)	0.0-0.0 (0.0)	
Dfa			1.5-3.9 (2.9)	1.3-2.7 (2.0)
Dfb		0.5-0.6 (0.5)		
Dfc	0.5-0.6 (0.6)	0.5-0.6 (0.5)		0.3-0.5 (0.4)
ET	0.2-0.4 (0.3)	1.6-2.2 (2.0)		

	DJF	MAM	JJA	SON
BWh			1.8-3.4 (2.7)	3.9-6.0 (5.5)
BWk				
BSh				
BSk	1.8-3.0 (3.1)		3.3-5.7 (5.4)	2.5-4.6 (3.9)
Csa			2.0-3.0 (2.7)	3.2-4.4 (4.0)
Csb	1.2-2.7 (2.0)	8.6-21.9 (17.4)	4.4-6.9 (6.1)	3.7-5.3 (4.6)
Cfa		2.1-5.3 (4.2)	3.5-9.0 (6.7)	3.1-6.5 (4.8)
Cfb		1.3-3.4 (4.3)	2.0-5.1 (3.7)	2.6-6.1 (4.3)
Cfc			1.5-2.3 (2.0)	
Dsa	1.4-2.5 (2.2)		11.2-17.9 (16.8)	4.5-7.2 (6.2)
Dsb			6.9-13.3 (11.8)	2.7-4.6 (4.0)
Dsc	0.3-0.4 (0.3)	0.0-0.0 (0.0)	0.0-0.1 (0.1)	
Dfa			2.8-12.2 (8.6)	2.3-7.2 (4.9)
Dfb			1.7-8.4 (5.4)	2.2-7.1 (4.7)
Dfc		0.1-0.2 (0.2)		
ET	0.1-0.2 (0.2)			

mon h

	DJF	MAM	JJA	SON
BWh	n/a	n/a		1.2-1.6 (1.4)
BWk		15.8-26.7 (20.7)	0.0-0.0 (0.0)	0.0-0.0 (0.0)
BSh	2.9-4.0 (3.4)	2.6-3.9 (3.1)	0.1-0.4 (0.3)	0.2-0.5 (0.4)
BSk			0.0-0.0 (0.0)	0.0-0.0 (0.0)
Csa			2.9-4.2 (3.9)	1.4-1.6 (1.5)
Csb			2.5-3.1 (2.9)	2.0-2.2 (2.1)
Cfa		4.0-6.8 (5.9)	1.2-3.2 (2.3)	
Cfb				
Cfc				
Dsa		n/a	0.0-0.0 (0.0)	0.0-0.0 (0.0)
Dsb		n/a		
Dsc	0.5-0.6 (0.6)	0.6-0.7 (0.7)		
Dfa	0.1-0.3 (0.2)			0.0-0.2 (0.1)
Dfb	0.5-0.7 (0.6)	0.3-0.5 (0.4)		
Dfc		0.3-0.4 (0.3)		
ET		0.1-0.3 (0.2)		

	DJF	MAM	JJA	SON
BWh	n/a	n/a	1.7-2.6 (2.3)	2.0-2.9 (2.4)
BWk			0.0-0.0 (0.0)	0.0-0.0 (0.0)
BSh				
BSk				
Csa			7.0-9.5 (8.7)	2.0-2.4 (2.2)
Csb	n/a		5.1-6.3 (6.0)	2.7-3.0 (2.8)
Cfa			3.7-12.2 (8.3)	2.5-4.5 (3.4)
Cfb			3.2-11.1 (7.8)	
Cfc			1.2-1.8 (1.6)	
Dsa		n/a	0.0-0.0 (0.0)	0.0-0.0 (0.0)
Dsb			4.0-9.8 (8.2)	
Dsc	0.2-0.4 (0.3)	0.0-0.2 (0.1)		
Dfa	0.0-0.1 (0.1)			
Dfb	0.3-0.5 (0.4)	0.0-0.2 (0.1)		
Dfc		0.0-0.1 (0.1)		
ET	0.0-0.0 (0.1)	0.0-0.1 (0.0)		

mon h

	DJF	MAM	JJA	SON
BWh			1.5-2.0 (1.9)	
BWk				
BSh	3.0-3.8 (3.7)			0.0-0.0 (0.0)
BSk				0.0-0.0 (0.0)
Csa			n/a	1.8-3.3 (3.1)
Csb			2.0-4.8 (3.9)	3.8-6.2 (5.1)
Cfa	0.0-0.0 (0.2)			
Cfb				
Cfc				
Dsa	6.0-10.0 (8.3)	n/a		
Dsb		n/a		
Dsc	n/a	3.4-5.0 (4.2)		
Dfa	0.0-0.0 (0.0)	0.0-0.0 (0.0)		
Dfb	0.2-0.3 (0.3)	0.0-0.0 (0.0)		
Dfc	0.0-0.0 (0.1)	0.2-0.3 (0.2)		
ET		0.0-0.2 (0.2)		

	DJF	MAM	JJA	SON
BWh			2.1-6.5 (6.2)	
BWk				
BSh				
BSk				0.0-0.0 (0.0)
Csa			n/a	7.8-12.9 (11.3)
Csb			13.3-24.0 (21.9)	8.9-11.5 (10.2)
Cfa				
Cfb	1.0-1.5 (1.6)			
Cfc				
Dsa				0.0-0.0 (0.0)
Dsb				
Dsc	n/a			
Dfa	0.0-0.0 (0.0)	0.0-0.0 (0.0)		
Dfb	0.0-0.2 (0.1)	0.0-0.0 (0.0)		
Dfc	0.0-0.0 (0.0)	0.0-0.0 (0.0)		
ET		0.0-0.0 (0.0)		

Figure 5.15: Köppen-averaged magnitude of change, expressed as ratio to 1951–20000 values, for the IQRs and ensemble means (in brackets) of hydrological drought parameters (exclude excess periods) simulated using 18 GCMs under RCP6. Categories with robust trends are shown. "n/a" denotes no drought events in 1951–2000 thus the relative magnitude of change cannot be mathematically expressed as a ratio.

when temperature rises above a threshold.

5.7.4.1 12-month Results

Except for cold regions (Cfc, Dfc and ET), all the Köppen types generally suffer from increasing long drought conditions in both future periods. Robust increases tend to occur in climates with higher temperatures, thus evapotranspiration, and/or dry summers, including hot arid (Bh) zones, temperate and cold climates with dry summer (Cs, Ds), and temperate climate with hot/warm summer and without dry season. For severity, magnitudes of increase are typically around 2–3-fold in 2001–2050 but diverge in 2051–2100, ranging from <5-fold (Dsc) up to 13-fold (BWh) (Figure 5.15). The larger increases (>8-fold) concentrate in the lower latitudes (35–45°N), in agreement with the changes for IP and MD (Section 5.7.3.1).

The majority of the Köppen climates with robust increases in severity also have robust increases in DAI25 frequencies, notably in temperate-based climate types (C) due to their low occurrence (<6%; 0.5% for Csa) in 1951–2000. For Csa, Csb and Cfa, DAI25 is projected to occur 14–34% of the time during 2001–2050 and 33–78% during 2051–2100. Other climates have considerably smaller changes, owing to their frequencies of 5–12% in 1951–2000, although the simulated (absolute) ranges have similar lower bounds and smaller upper bounds (<66%). The more substantial increases in DAI50 frequency is related to their rarity (typically <1%) in 1951–2000. DAI50 occurs in <9% of 2001–2050 and 6–36% of 2051–2100.

Between 1961–1990 and 2021–2050, Hemming *et al.* (2010) simulated decreasing annual precipitation (5–25%) and annual runoff, together with increasing drought index for the region south of the Black Sea; the direction and general magnitude of changes in coastal western areas of Turkey have low uncertainties. Similarly, Arnell (2004a) projected lower average annual runoff by the 2050s in the Middle East, which also suffers from increasing water resource stress throughout the 21st century (Arnell, 1999b). The average annual Tigris-Euphrates river discharge decline is greatest in Turkey at 12% Chenoweth *et al.* (2011). These results, along with the precipitation reduction (see Section 4.4.3), are consistent with the projected robust positive drought trends in hot desert zones (Bh), temperate and cold climates with dry summer (Cs, Ds). However, Abbaspour *et al.*

(2009) projected higher precipitation (up to 40%) and increase in blue water resources (the sum of river discharge and deep groundwater recharge) for northern Iran.

Consistent with the increasing drying projected for BWk here, Agaltseva *et al.* (2011) simulated decreasing Amu Darya River runoff in the medium- and long-term. Although Central Asia could become warmer and probably drier in future, with increasing aridity especially in western Turkmenistan, highly uncertain precipitation projections for arid zones (e.g. Turkmenistan; Lioubimtseva *et al.*, 2012) contribute to the lack of model agreement in BWk results.

Higher precipitation is likely in European Russia/Central Siberia (Lioubimtseva and Henebry, 2009). By 2050s, increased average annual runoff (Arnell, 1999c), water availability and low water stress is simulated for >90% of Russia including the Volga and in southern regions (Alcamo *et al.*, 2007a). However, Hirabayashi *et al.* (2008) projected more frequent drought for the Volga (Dfb) in 2071–2100, which agrees with the Dfb projections obtained here.

5.7.4.2 Temperate climates

Temperate climates (C) occur in much of western and southern Europe, i.e. the PRUDENCE regions except for SC and eastern EA. Projections for temperate climates, particularly for Cfa and Cfb, tend to be more uncertain than for other climates (Figures 5.12 and 5.13). Both these regions with a dry summer (Cs) and those without a dry season (Cf), generally suggest increasing drought conditions in all seasons. Robust severity and DAI25 frequency trends occur predominately in summer and autumn, but also in 2051–2100 spring for severity. These climates have similar severity increases (by 2–3 times) in 2001–2050; in 2051–2100, autumn increases are roughly 3–6 times while 9-fold (Cfa) and 7-fold (Csb) increases are projected in summer. DAI25 is projected to be 2–4 and around 10 times (e.g. Csa, Cfa, Cfb) more frequent in 2001–2050 and 2051–2100, respectively. Changes are larger in summer than autumn. Of the temperate climates, the magnitude of increases for Csa, which prevails in much of the Mediterranean basin, is relatively small (by "only" 3–4 times for severity) compared to Cfa, for instance; Csb also has relatively small increases, particularly in summer.

Figure 5.14 indicates that more severe spring events are projected across much of

western, southern and continental Europe as a whole. Change is most considerable in Csb, with up to 22-fold increase from the very low 1951–2000 values. Although lacking model consistency, the contrasting (negative in 2001–2050, positive in 2051–2100) DAI25 frequency trends in Csb, Cfb, Cfc are due to the initial melting of stored frozen precipitation similar to ME/EA (Section 5.7.3.4). The negative changes in winter droughts for Cfc are consistent with the expected higher winter precipitation (Vidal and Wade, 2009; Burke *et al.*, 2010) and runoff (Arnell, 2004b) in northern parts of BI and higher winter flows in Norway (Roald *et al.*, 2004; Engen-Skaugen *et al.*, 2005; Roald *et al.*, 2006; Beldring *et al.*, 2008).

Csa reveals negative trends in winter/spring drought, possibly related to increases in localised precipitation (Buonomo *et al.*, 2007; García-Ruiz *et al.*, 2011; e.g. westward side of mountain chains of western and central Europe due to enhanced westerly winds), extremes (e.g. southern France; Gao *et al.*, 2006) and/or storm activities (Sumner *et al.*, 2003). These temporary intense events could lead to flooding and/or increased 100-year discharge (e.g. in Spain and southern France, despite the substantial drying on average; Gao *et al.*, 2006).

5.7.4.3 Arid climates

Cold arid (BWk and BSk) climate types characterise Central Asia. The projected drought parameters in these regions have relatively low inter-GCM spread, and widespread droughts are relatively rare (Figures 5.12 and 5.13).

Although increasingly dry conditions (with slightly higher winter rainfall and reductions in spring and summer; see Section 4.4.3) are projected for the Central Asian plains, surface water resources of Central Asia largely originate from mountain glaciers, the accelerated melting of these, higher precipitation (Lioubimtseva and Henebry, 2009) and earlier snowmelt (e.g. in Syr Darya basin; Siegfried *et al.*, 2012). These explain the less severe (by $>$65%) drought in BWk obtained here, notably in 2001–2050 (Figure 5.14), although Mac-PDM.09 incorporates snowmelt but not glacial melt. Both CMIP3 and CMIP5 projections generate a strong decline in glacier extent in Central Asia, the uncertain precipitation projections however imply difficulties in estimating future Central Asian glacier extent, and timing and quantity of water availability downstream (Lutz *et al.*,

2012). These 2051–2100 results therefore become less uncertain as frozen precipitation stores are exhausted.

Robust increases in summer and autumn severity of BSk agree with the warming-induced earlier snowmelt in the Syr Darya basin (eastern half the BWk and BSk zones of Figure 3.3), thus water stress increases in unregulated catchments due to lower water availability for irrigation in the summer (Siegfried *et al.*, 2012). The decreasing DAI25 frequency during these seasons in BSk suggests that only part of the region is affected by snowmelt shifts in snow-/glacier-melt driven rivers — for instance, glacial share in Syr Darya runoff is much smaller than the heavily glaciated headwater catchments near the Tien Shan mountains (Sorg *et al.*, 2012), and some parts may respond more directly to precipitation variations. Furthermore, patterns are complicated by sub-regional precipitation variations (see Section 4.4.3). On the other hand, more severe droughts and more frequent DAI25 in winter/spring in BWk and BSk could be linked to the higher evapotranspiration and larger warming during winter (Lioubimtseva and Cole, 2006; Lioubimtseva and Henebry, 2009).

5.7.4.4 Cold climates

Polar (ET) and cold climates without a dry season (Df) dominate the higher latitudes and continental parts of the study region, whereas cold climates with dry summer (Ds) are found in parts of eastern Turkey, northwestern Iran and Central Asia. Overall, future widespread droughts are uncommon in these climates (Figure 5.13).

All the cold and polar climates tend to experience reducing drought conditions in winter and spring. Model agreement is particularly strong in the frequencies of widespread events, often with marked reductions of $>$50% in 2001–2050 and $>$80% in 2051–2100. For Df and ET climates, frequencies of DAI25 and DAI50 in the 21st century typically reduce to $<$8% and $<$3%, respectively, from up to around 30% (DAI25) and 10% (DAI50) of 1951–2000. These negative drought trends are associated with the increasing precipitation (see Section 4.4.4) and runoff; warming also has less influence on the timing of snowmelt in western Russia (Arnell, 1999c;b).

By the 2050s, larger average annual runoff is generally expected in high latitudes (Arnell, 2004a). In southwestern Russia where water stress in this key agricultural region

is already in the "severe" category due to domestic, industrial and agricultural water use, lower precipitation and warming reduce annual runoff and water availability and produce more frequent extremely low runoff events, similar to eastern Europe and western Russia (Alcamo *et al.*, 2007a). This region corresponds to the Dfa and the southern parts of Dfb zones, which show more severe summer and autumn droughts (by up to 7–8-fold in 2051–2100, and 12-fold in summer for Dfa; Figure 5.15) with high model consistency (Figure 5.14). Regional variations in precipitation and runoff trends may explain the no change in, or higher uncertainties in, the frequencies of widespread events in Df climates.

Climate change and population growth are likely to reduce per capita water resources considerably across much of the Middle East (Chenoweth *et al.*, 2011) though this is not considered here. In the Middle East, precipitation decline (5–25%) is expected throughout December to August (depending on the location), with relatively little change projected across the whole region between September and November; runoff and drought index changes generally show spatial distributions that are comparable to those for precipitation (Hemming *et al.*, 2010). These could exacerbate drought conditions as reflected in the Dsa and Dsb results (Figure 5.14). While autumn severity increases are comparable to other climates, those for summer are particularly substantial — by up to 5-fold in 2001–2050 and 18-fold in 2051–2100. Dsa and Dsb are geographically small regions, and hence have higher chances (up to 10%) of experiencing "widespread" (as a fraction of the small region) droughts. For Dsa, DAI25 occur in 1.3% (summer) and 18.7% (autumn) of 1951–2000 but none are simulated in the 21st century. These robust reductions correspond with the wetting simulated for northern Iran (Abbaspour *et al.*, 2009).

5.7.5 GCM Outlier Effects

These hydrological drought results suggest an anomaly, notably in values for BI in Figures 5.8 and 5.10, and Cfc in Figure 5.12. The IAP/LASG coupled GCM FGOALS_g1.0 (Yu *et al.*, 2010b; 2004) is mostly responsible for this behaviour, which may be attributable to the structure of the GCM and/or the effects of pattern-scaling in ClimGen (Section 3.2). Pattern-scaling is used to construct consistent scenarios representing progressive increases in global-mean temperature. This linear scaling of the magnitude of a spatial pattern of climate change (i.e. the local temperature) by the annual global-mean

temperature may not be appropriate at the largest warming considered here (e.g. SRES A1FI and RCP8.5 scenarios). This is because patterns at the largest warming are extrapolated from values in SRES A2 and A1B, and that the linear relationship may or may not hold.

In terms of the GCM, the Program for Climate Model Diagnosis and Intercomparison (PCMDI) website does not recommend the use of this model's data for mid-high latitude climate studies[1]. Figure 3 in Gleckler *et al.* (2008) suggests that, outside the tropics (20°S to 20°N), FGOALS-g1.0 demonstrates lower than average performance with respect to the reference data. It also shows that performance for temperature at 850 hPa is worse than precipitation, which is reflected in the more notable anomaly in the hydrological (than meteorological) results.

While both the oceanic model and the coupling scheme were improved in version g1.1, version g1.0, which was used in this study, suffers from cold biases at high latitudes and in the tropical Pacific (Yu *et al.*, 2010b), along with the overestimated sea ice extension in both hemispheres and weaker Atlantic meridional overturning circulation (AMOC). Compared to most other CMIP3 GCMs, FGOALS_g1.0 does not perform well in simulating the current climate for 14 climate variables (Reichler and Kim, 2008), such as water vapour (Santer *et al.*, 2009). Pierce *et al.* (2009) assessed the performance of 21 climate models using 42 metrics based on seasonal temperature and precipitation, ENSO, and the Pacific Decadal Oscillation for western U.S. They also found FGOALS_g1.0 to be one of the worst performing models.

Nonetheless, it is worth noting that model skill in simulating climatological means does not necessarily imply an ability to capture either the observed annual cycle or the amplitude and pattern of monthly variability (Santer *et al.*, 2009). Moreover, model agreement with observations does not imply reliability in the simulated future (Stainforth *et al.*, 2007a; Tebaldi and Knutti, 2007; Knutti *et al.*, 2010). The "anomalous" results from FGOALS_g1.0 could be due to the different GCM structure compared to other GCMs, e.g. by including/excluding certain processes or a different representation of these. It is difficult to omit FGOALS_g1.0 from the analysis when GCMs were constructed based on an incomplete understanding of the climate system (see Sections 2.6.9 and 2.6.10).

[1]CMIP3 Climate Model Documentation, References, and Links: http://www-pcmdi.llnl.gov/ipcc/model_documentation/more_info_iap_fgoals.pdf

5.8 Hydrological vs. Meteorological Classifications of Drought

Difficulties in obtaining real-time streamflow data, and computational requirements for characterising hydrological drought (Nalbantis and Tsakiris, 2008), have prompted attempts to characterise them based on precipitation (e.g. via the SPI). Nalbantis and Tsakiris (2008) characterised hydrological drought severity of the Evinos river basin (Greece) by a linear function of SPI with sufficient accuracy. Tabrizi *et al.* (2010) found that SPI12 drought occurrence in Doroodzan Watershed and Reservoir in southwestern Iran (specifically, Jamalbeik rain gauge station) reflects streamflow drought occurrence at the Chamriz hydrometric station. However, streamflow data were necessary for water resources planning and management in Denmark as Hisdal and Tallaksen (2003) found streamflow droughts to be less homogeneous over the region, to display lag and be less frequent and more persistent than precipitation droughts as a result of precipitation deficits, storage conditions and high evaporation losses. Seasonally, Stefan *et al.* (2004) found a lag between precipitation and river discharge anomalies in southern Romania for the period 1931–1999, by 2–3 months in winter and 0–1 months in summer.

This section considers whether meteorological and hydrological classifications produce consistent results, i.e. Research Question 4 in Section 5.1. The effects on the direction of change from 1951–2000 simulated by 18 GCMs under RCP6, based on both meteorological and hydrological classifications is shown in Figure 5.16 (legend is explained in Table 5.1), which provides no information on the magnitude of change nor individual GCMs. For categories with robust trends, their magnitudes of change for the IQRs and ensemble means, derived from meteorological (top row) and hydrological (bottom) definitions are presented in Figure 5.17.

The analysis is based on results that include excess periods as they are included in the meteorological results (Chapter 4), with a fixed threshold. *As per* Section 5.6, the choice of drought definitions that include or exclude excess periods generally has minor effects on both the direction and magnitude of change in hydrological results. However, meteorological results should be interpreted with caution due to the larger difference between values that include and exclude excess periods compared to those for hydrological results (see Table 5.2). The drought parameters used here provide no information on the timing of the events as they describe drought conditions over the 50-year period. For instance,

it would not be possible to determine whether a meteorological drought event coincides with/lags a hydrological event based on drought severity or frequencies of DAI25/DAI50.

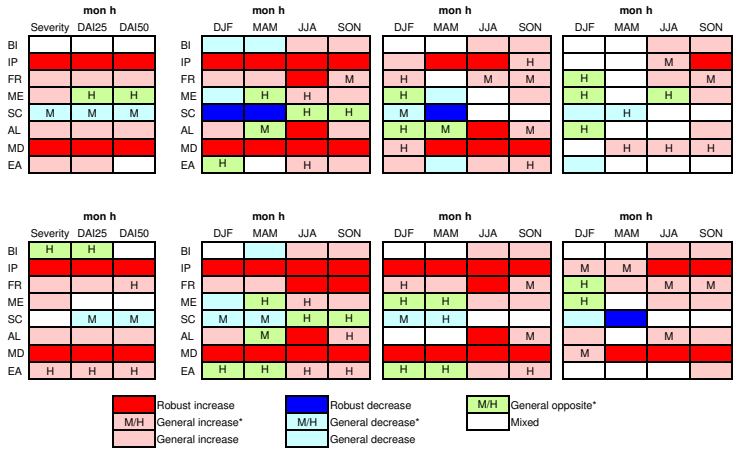

Figure 5.16: Direction of change, relative to 1951–2000, for drought parameters that include excess periods projected by 18 GCMs under RCP6, and consistency between meteorological (M) and hydrological (H) drought classifications.

Similar to the findings in Section 5.7, Figure 5.16 reveals drier conditions for all drought parameters and more robust drying across the PRUDENCE regions in 2051–2100; uncertainty is higher in DAI25 than with severity results, and in DAI50 than DAI25 results. Differences between the magnitude of change for the two drought classifications is relatively small (typically $\leq$50%) in 2001–2050 but maybe $\geq$100% in 2051–2100 owing to the greater warming (Figure 5.17). Hydrological events demonstrate more positive trends than the meteorological droughts for both 12-month and 3-month events, along with larger increases which suggests a role of PET in amplifying the magnitude of change. Similarly, Nohara *et al.* (2006) found larger changes in the ratio of global-mean runoff than precipitation from simulating river discharge for 24 rivers from 19 AOGCMs. Chiew and McMahon (2002) used the conceptual daily rainfall-runoff model, MODHYDROLOG, to assess the effects on surface water fluxes in Australia. They found that rainfall deviations are amplified in runoff, with percentage change in runoff being twice (over four times) of that in rainfall in wet and temperate (ephemeral, with low runoff coefficients) catchments. Wong *et al.* (2011) used the Hydrologiska Byråns Vattenbalansavdelning (HBV) precipitation-runoff model to assess the differences in hydroclimatological summer (15 May–15 October) droughts in Norway. Compared to 1961–1990, they found substantially longer hydrological drought and larger drought-affected areas,

mon h

	Severity	DAI25	DAI50
BI			
IP	1.9-2.7 (2.4) 2.2-3.2 (2.7)	2.2-3.0 (2.7) 2.2-3.1 (2.6)	2.0-4.4 (3.4) 6.5-10.3 (9.0)
FR			
ME			
SC			
AL			
MD	1.6-2.2 (2.1) 2.0-3.1 (2.6)	1.4-2.3 (2.1) 2.6-4.9 (3.9)	1.5-2.3 (2.0) 1.6-2.4 (2.1)
EA			

	Severity	DAI25	DAI50
	3.7-5.9 (5.0) 4.7-8.3 (7.2)	4.1-5.7 (5.0) 3.9-5.3 (4.6)	7.0-14.7 (11.0) 24.2-38.9 (31.6)
	2.6-4.6 (4.1) 4.0-8.2 (6.5)	3.0-5.8 (4.9) 6.9-13.0 (10.0)	2.5-4.9 (4.8) 3.1-8.7 (6.8)

mon h

	DJF	MAM	JJA	SON
BI				
IP	1.4-1.6 (1.4) 1.8-2.4 (2.0)	1.3-1.8 (1.5) 2.0-3.3 (2.9)	1.6-2.3 (2.0) 2.3-3.5 (2.9)	1.3-1.7 (1.5) 2.1-2.9 (2.4)
FR			1.4-2.2 (1.8) 1.5-2.7 (2.0)	
ME				
SC	0.7-0.8 (0.7) 0.5-0.7 (0.6)	0.7-0.8 (0.8) 0.4-0.5 (0.4)		
AL			1.4-2.2 (1.8) 1.4-2.7 (2.1)	
MD	1.2-1.6 (1.4) 1.8-2.3 (2.0)	1.3-1.6 (1.5) 2.3-3.8 (3.3)	1.1-2.2 (1.9) 2.0-3.0 (2.5)	1.3-1.8 (1.6) 2.0-2.9 (2.5)
EA				

	DJF	MAM	JJA	SON
	2.0-2.5 (2.1) 3.6-6.2 (4.9)	1.8-3.4 (2.6) 4.5-11.8 (9.6)	2.8-5.0 (4.0) 4.5-8.4 (6.6)	2.0-3.1 (2.6) 4.0-6.1 (4.9)
			2.0-4.7 (3.5) 2.3-6.7 (4.7)	1.7-4.1 (2.9) 2.6-6.6 (4.4)
			2.1-4.6 (3.6) 3.0-8.0 (5.8)	
	1.5-2.7 (2.0) 2.5-4.5 (3.6)	1.8-2.7 (2.4) 4.9-10.4 (8.8)	1.4-4.7 (3.6) 3.7-6.9 (5.7)	1.9-3.3 (2.9) 3.6-6.7 (5.2)

mon h

	DJF	MAM	JJA	SON
BI				
IP		1.4-2.0 (1.6) n/a	2.0-3.9 (2.9) 1.9-2.5 (2.2)	
FR				
ME				
SC		0.6 0.8 (0.7) 0.3-0.5 (0.4)		
AL			1.4-2.5 (2.1) 1.9-3.2 (2.7)	
MD		1.7-2.0 (1.9) 2.0-3.0 (2.6)	2.0-3.1 (2.6) 2.5-4.2 (3.5)	1.4-2.3 (1.9) 1.9-2.9 (2.4)
EA				

	DJF	MAM	JJA	SON
	1.7-2.4 (2.1) n/a	1.9-3.3 (2.6) n/a	4.7-7.4 (6.2) 3.0-4.0 (3.7)	2.4-3.8 (3.1) 2.4-2.9 (2.6)
			3.1-6.5 (4.6) 2.0-4.1 (3.1)	
			2.5-5.1 (3.9) 3.5-9.4 (6.9)	
	1.2-2.5 (1.8) 4.1-7.1 (5.7)	2.2-3.0 (2.9) 4.0-8.6 (7.1)	3.8-7.4 (5.5) 5.9-8.8 (7.6)	2.5-4.7 (3.8) 3.4-4.2 (3.8)

mon h

	DJF	MAM	JJA	SON
BI				
IP				1.4-1.6 (1.5) 2.1-3.2 (2.6)
FR				
ME				
SC				
AL				
MD				
EA				

	DJF	MAM	JJA	SON
			12.0-32.7 (24.1) 7.0-10.9 (9.0)	2.3-3.8 (3.0) 4.5-6.0 (4.9)
		0.0-0.3 (0.2) 0.0-0.0 (0.0)		
		1.9-4.4 (3.8) n/a	n/a 3.6-10.3 (8.4)	n/a 4.8-10.0 (7.6)

Figure 5.17: Magnitude of change, expressed as ratio to 1951–2000 values, for the IQRs and ensemble means (in brackets) of drought parameters (including excess periods) simulated using 18 GCMs under RCP6 based on meteorological (top row of each category) and hydrological (bottom) classifications. Categories with robust positive (red) and negative (blue) trends are shown. "n/a" denotes no drought events in 1951–2000 thus the relative magnitude of change cannot be mathematically expressed as a ratio.

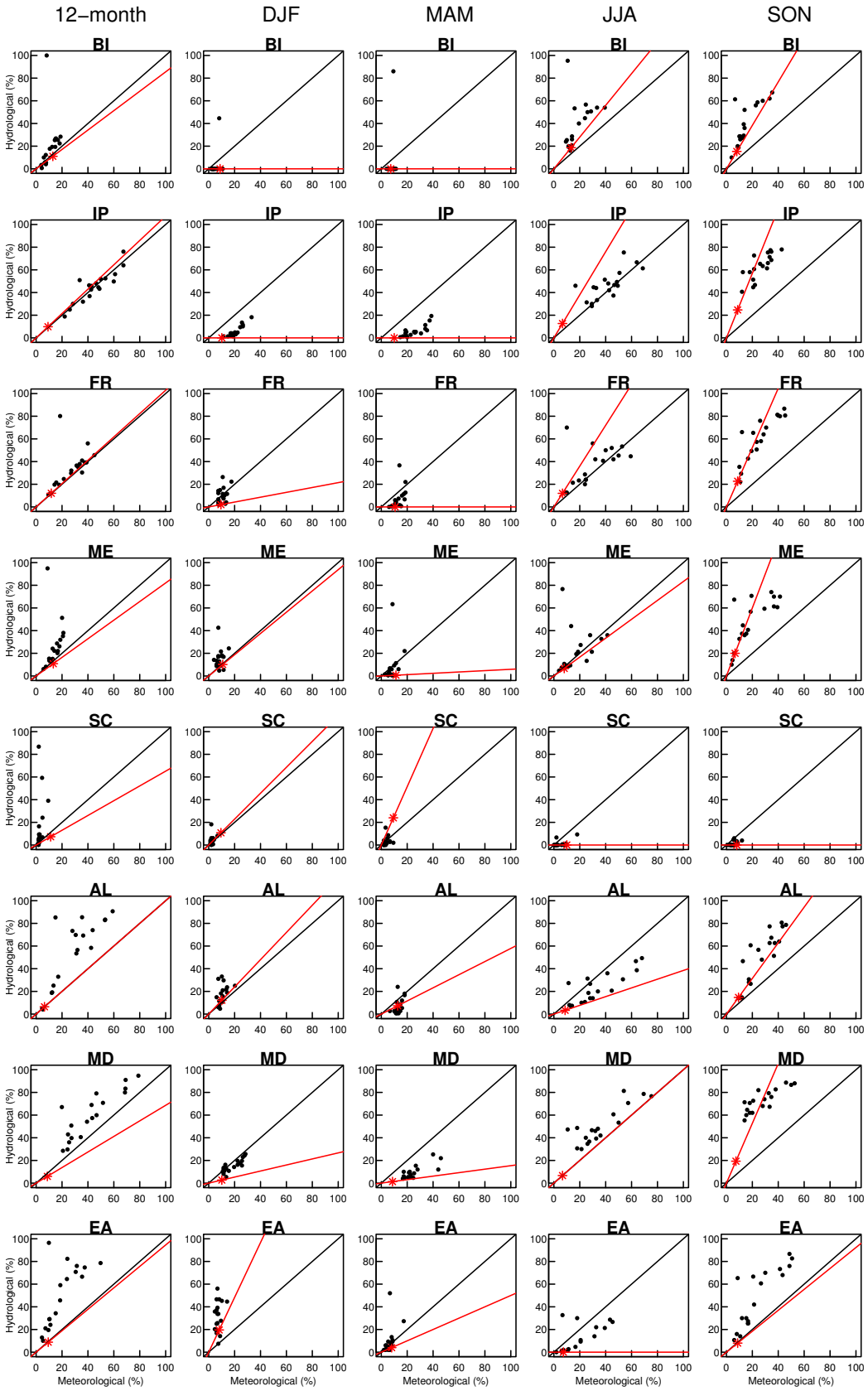

Figure 5.18: Frequencies of meteorological and hydrological DAI25 (include excess periods) for both 12-month and 3-month events in 2051–2100 simulated using 18 GCMs under RCP6. Red asterisks (*) denote 1951–2000 values. Red lines indicate the relative changes in the two drought classifications identical to 1951–2000 values.

especially in the southern and northernmost parts, despite small changes in future meteorological drought characteristics. Further, the changing relative importance of precipitation and PET with warming may produce non-linear hydrological response to a linear climate change forcing, as in the case of British catchments (Arnell, 2011).

Figure 5.18 shows the present-day and 2051–2100 frequencies of 12- and 3-month DAI25 from 18 GCMs based on both classifications. Given the dominance of precipitation effect in both meteorological and hydrological droughts, similar DAI25 frequencies for both classifications are expected; however, they may not necessarily be identical as hydrological events may lag meteorological episodes and/or last longer (see Section 2.2.5), along with the effects of PET in their characteristics. For present-day DAI25 frequencies, the consistency of meteorological and hydrological events depends on the region and season.

In broad terms, projected hydrological DAI25 are more frequent than meteorological ones for both long and short events. The outlier, notably in BI results, is due to the GCM FGOALS_g1.0 (see Section 5.7.5). For 12-month droughts, both drought classifications produce very similar (absolute) frequencies for BI, IP and FR. Seasonally, both definitions suggest that DAI25 will become most frequent in summer and autumn, alongside the largest uncertainties, due to the lower precipitation, higher temperatures and evapotranspiration. Greater frequency of hydrological than meteorological drought tends to occur in summer/autumn (with some exceptions — see Sections 5.8.1–5.8.6), which suggests the greatest importance of increased PET is during the warmer seasons. The opposite appears in winter/spring in BI, IP and MD, which implies that the use of a fixed threshold may not capture hydrological droughts during the cold-seasons that have relatively high precipitation (see Section 5.5). In some cases, the relative changes in DAI25 frequency for the two drought classifications are insensitive to the 1951–2000 values (e.g. FR in autumn); in other cases, the relative changes differ considerably from the present-day values (e.g. EA in autumn).

DAI25 and DAI50 frequencies in 2001–2050 yield very similar characteristics, but with DAI50 frequencies having smaller magnitudes, and severities based on the two definitions are less comparable due to the different units (i.e. meteorological droughts are characterised by SPI whereas hydrological deficits are measured in mm/month), hence

these are not shown. Regional comparisons are presented in Sections 5.8.1–5.8.6).

5.8.1 Iberian Peninsula (IP) and Mediterranean (MD)

IP and MD demonstrate very robust increases in both long and short events throughout the century, with higher uncertainty in winter and spring DAI50 frequencies (Figure 5.16). They also have some of the largest regional increases for both drought classifications (Figure 5.17).

For 12-month severities and DAI25 frequencies, both definitions show up to 3-fold increase in 2001–2050; in absolute terms, occurrence of DAI25 is 15–30%. In 2051–2100, increases are 3–6 and 4–8 times for meteorological and hydrological drought, respectively; increases for MD are considerably more — up to 13-fold for hydrological frequencies, i.e. 77% of 2051–2100. Both definitions suggest DAI50 to affect $\leq$10% of 2001–2050 and up to 35% of 2051–2100. Their marked increases, particularly for IP in 2051–2100, are due to the low 1951–2000 frequencies ($<$4%). For IP in particular, despite the similar absolute DAI50 frequency, hydrological increases are 2–3 times higher than meteorological changes.

Seasonally, 2001–2050 severities commonly increase by under 2- (meteorological) and 3-fold (hydrological). Changes in 2051–2100 diverge with seasons and drought classification: increases in meteorological (hydrological) severities are more pronounced in (summer) spring and summer. As discussed in Section 5.7.3.1, hydrological droughts, particularly in spring, are also influenced by changes in snowmelt hydrology.

DAI25 frequencies reveal characteristics similar to changes in severities, although with smaller classification uncertainties in magnitudes of increase. Both regions have relatively similar winter and spring DAI25 frequencies, with meteorological events being more common: 10–20% (meteorological) and $<$4% (hydrological) of 2001–2050, and 12–33% (meteorological) and $<$19% (hydrological) of 2051–2100. This could be partially explained by the precipitation decrease and relatively small evapotranspiration increase. In summer and autumn, however, hydrological DAI25 are more frequent: in summer, 13–26% (meteorological) and 17–31% (hydrological) of 2001–2050, and 25–49% (meteorological) and 39–59% (hydrological) of 2051–2100; in autumn, 10–17%

(meteorological) and 37–55% (hydrological) of 2001–2050, and 18–34% (meteorological) and 58–81% (hydrological) of 2051–2100. For IP in summer, absolute hydrological droughts are slightly more common than meteorological events; in relative terms, however, increases in hydrological frequencies are slightly smaller as its present-day value is slightly higher than the meteorological counterpart. For MD, hydrological values are higher in both absolute and relative terms.

DAI50 events are less common. In winter and spring, they tend to occur in $<$10% for both drought classifications throughout the 21st century; in summer and autumn, up to 22% (meteorological) and 53% (hydrological) of 2051–2100. The marked relative increases are attributable to the rare occurrence ($<$8%) in 1951–2000.

5.8.2 Scandinavia (SC)

SC generally shows decreasing 12-month drought conditions except hydrological DAI25 for some GCMs (Figure 5.18). The more robust meteorological results are consistent with the higher precipitation expected for northern Europe (see Sections 4.4.4 and 5.7.3.2). Amongst the PRUDENCE regions, SC has some of the lowest DAI25 frequencies and smallest uncertainties according to both drought classifications (Figure 5.18); uncertainties are however higher in 12-month hydrological frequencies.

Seasonally, both meteorological and hydrological definitions reveal decreasing severity and frequency of widespread events in winter and spring. Trends in 2001–2050 have high model consistency; hydrological reductions are larger than their meteorological counterparts, e.g. for severities by 34–63% and 21–32%, respectively. The lack of robustness in 2051–2100 hydrological results may be related to the mechanisms described in Section 5.7.3.2. Summer and autumn severities demonstrate contrasting trends. While the anticipated precipitation increase reduces meteorological severities, increasing hydrological severities are consistent with negative streamflow trends in some parts of SC (Engen-Skaugen *et al.*, 2005; Roald *et al.*, 2006; Thodsen, 2007; Beldring *et al.*, 2008). For both drought classifications, changes for the regionally-averaged frequencies of widespread events are complicated by overall effects of changes in precipitation, evapotranspiration and snow, and their sub-regional variations, as well as the size of this region (Section 5.7.3.2).

5.8.3 Alps (AL)

AL generally demonstrates increasing 12-month meteorological and hydrological drought conditions during 21st century (Figure 5.16). These are related to the expected lower annual mean precipitation and runoff as described Sections 4.4.5 and 5.7.3.3.

Seasonally, spring reveals positive (negative) meteorological (hydrological) trends whilst both definitions show drying trends in summer and autumn (Figure 5.16). The changing snow characteristics alleviates hydrological droughts as detailed in Section 5.7.3.3. While Beniston (2005) and Horton *et al.* (2006) reported inconclusive trends in spring precipitation, the spring meteorological results obtained here indicate a reduction. Strongest GCM agreement occurs in summer throughout the century, and severity and DAI25 frequencies have similar magnitudes of change. In 2001–2050, both drought classifications produce increases of up to 2.5 (meteorological) and 3 (hydrological) times. In 2051–2100, hydrological increases (up to 9-fold) are almost doubled that of meteorological (up to 5-fold). In winter, the projected increasing winter hydrological droughts implies that enhanced PET counteracts higher precipitation; the increasing meteorological severities simulated disagrees with the expected higher precipitation.

Although hydrological events have larger magnitude of change in all seasons, meteorological DAI25 are more (less) abundant than hydrological events in spring and summer (winter and autumn) (Figure 5.18). This may be associated with the delay in hydrological response to meteorological changes. Note that the change in the ratio between the meteorological and hydrological DAI25 frequencies is relative to the present-day ratio.

5.8.4 Mid-Europe (ME) and Eastern Europe (EA)

For 12-month events, both definitions show positive trends for all drought parameters in EA and severities in ME. The mixed direction of change in widespread hydrological droughts in ME (Figure 5.16) may be associated with the unclear sign and magnitude of precipitation change in large parts of the year for much of central Europe (Kjellström *et al.*, 2011).

Positive winter (due to more frequent and intense precipitation) and spring precipitation change over northern-central Europe (Räisänen *et al.*, 2004; Giorgi and Coppola, 2009) reduces meteorological droughts in both regions (Figure 5.16). Meanwhile, greater

warming in winter than spring/summer over eastern (Giorgi *et al.*, 2004) and northern-central Europe (Giorgi and Coppola, 2009) increases evapotranspiration (Hirabayashi *et al.*, 2008) and promotes winter/spring hydrological droughts, notably in EA. The spring results demonstrate that both ME and EA are affected by the altered snowmelt patterns.

In summer and autumn, both drought classifications indicate increasing drought conditions in both regions. Enhanced evapotranspiration, lower precipitation (up to 70% in central Europe; Räisänen *et al.*, 2004) and runoff, as well as a perturbed snowmelt hydrology (Section 5.7.3.4) yield high model agreement in the projected positive hydrological trends. The abundant summer precipitation together with the small and unclear sign of change for autumn precipitation over northern-central Europe (Giorgi and Coppola, 2009) may partially explain the lack of robustness in the projected positive meteorological trends. Autumn DAI25 frequencies for both regions suggest non-linear changes (Figure 5.18).

5.8.5 France (FR)

FR is projected to experience increasing meteorological and hydrological droughts, both long and short, throughout the 21st century. GCM agreement is highest in summer and autumn. In 2051–2100, summer and autumn severities are up to 4–5 (meteorological) and >6 (meteorological) times higher than 1951–2000; the magnitude of increases in summer DAI25 frequencies are reversed for the two drought classifications.

5.8.6 British Isles (BI)

For 12-month results, both drought classifications produce inconclusive trends in 2001–2050. In 2051–2100, hydrological (meteorological) severities and DAI25 frequencies reveal positive (negative) trends, suggesting that higher evapotranspiration counteracts the precipitation increase. The regional results may be complicated by the sub-regional variations in changes in both meteorological (Section 4.4.7) and hydrological (Section 5.7.3.6) events.

Seasonally, droughts remain relatively uncommon in winter and spring (e.g. Figure

5.18) with both drought classifications showing no clear trends, except for the negative severity results. In summer and autumn, both definitions generally show increasing droughts (Figure 5.16) as a result of reduced precipitation during the warmer seasons; higher evapotranspiration and lower runoff also contributed to the increase in hydrological droughts.

5.8.7 Exploring the Effects of PET

A major difference in the two drought classifications explored in this study is that hydrological droughts incorporate temperature effects while SPI is precipitation-only. Changes in hydrological drought over a river basin should be assessed based on changes in both precipitation and evapotranspiration, rather than changes in annual precipitation only (Hirabayashi *et al.*, 2008). PET influence on the direction and/or magnitude of runoff change (Research Question 5 in Section 5.1) was explored by running Mac-PDM.09 with climate projections for ECHAM5 under RCP6 but holding the temperature at present-day (1951–2000) levels. Differences between results from this "constant temperature" (i.e. precipitation changes only) experiment and the "control" run with future temperature scenarios (i.e. with changes in both precipitation and PET, as in Section 5.7) are therefore mostly be attributable to the effects of PET, which is calculated using the Penman-Monteith method in MacPDM.09.

5.8.7.1 Effects on Absolute Drought

Table 5.4 shows the percentage difference between various drought parameters generated from the "constant temperature" and "control" runs for ECHAM5 under RCP6. Overall, "constant temperature" produces considerably lower severity and less frequent widespread events. Across the PRUDENCE regions, constant (i.e. "present-day") temperature yields 59–90% (2001–2050) and 77–99% (2051–2100) less severe 12-month events, and 52–100% less frequent widespread droughts under both future periods. Similar discrepancies are found for 3-month results, with discrepancies larger in 2051–2100 than 2001–2050 due to the larger projected warming. For 3-month results in SC and AL, "constant temperature" tends to produce smaller discrepancies in winter relative to other

	12-months			3-month Severity				3-month DAI25				3-month DAI50			
Region	Severity	DAI25	DAI50	DJF	MAM	JJA	SON	DJF	MAM	JJA	SON	DJF	MAM	JJA	SON
2001–2050:															
BI	-73.8	-100	-100	-64.4	-48.7	-41.7	-53.1	n/a	n/a	-51.1	-54.1	n/a	n/a	-64.7	-23.1
IP	-64.6	-52.2	-68.8	-57.8	-68.8	-53.5	-46.7	-66.7	-75.0	-37.7	-27.5	n/a	n/a	-55.0	-47.7
FR	-90.3	-95.9	-100	-58.0	-95.2	-68.6	-58.1	-40.0	-100	-62.9	-53.1	-100.0	n/a	-80.0	-51.4
ME	-82.5	-90.0	-100	-44.1	-74.0	-70.5	-63.9	-52.6	-100	-78.9	-69.1	-40.0	n/a	-85.7	-62.5
SC	-69.4	-100	n/a	-30.9	61.7	-66.8	-61.4	-44.4	16.7	n/a	n/a	-100.0	-50.0	n/a	n/a
AL	-77.6	-87.2	-100	-26.6	36.7	-64.2	-57.3	-31.8	71.4	-65.0	-50.9	-60.0	n/a	-100	-92.3
MD	-59.1	-69.2	-58.6	-34.3	-65.1	-50.9	-44.4	-50.0	-75.0	-53.7	-37.0	n/a	-50.0	-61.1	-59.0
EA	-84.0	-88.7	-100	-38.5	-55.5	-79.1	-67.6	-50.0	-71.4	-100.0	-78.0	-50.0	n/a	n/a	-100
2051-2100:															
BI	-81.3	-100	-100	-61.2	-71.9	-72.7	-83.4	n/a	n/a	-78.2	-78.3	n/a	n/a	-82.8	-90.5
IP	-81.0	-55.6	-80.9	-83.1	-88.0	-76.7	-68.4	-94.4	-95.5	-51.5	-34.2	-100	-100	-75.4	-56.0
FR	-99.2	-100	-100	-86.1	-99.9	-90.5	-82.2	-100	-100	-85.9	-72.1	-100	-100	-94.0	-78.8
ME	-94.1	-100	-100	-73.4	-93.1	-90.8	-88.0	-72.0	-100	-96.2	-87.5	-92.9	-100	-95.0	-94.5
SC	-86.2	-100	n/a	-60.8	184.4	-89.4	-81.4	-100	0	n/a	n/a	n/a	n/a	n/a	n/a
AL	-91.1	-95.2	-100	-66.5	-48.4	-82.1	-76.0	-66.7	-64.0	-83.1	-66.7	-92.3	-100.0	-100.0	-92.8
MD	-77.4	-70.0	-87.6	-61.3	-84.3	-73.5	-62.9	-54.3	-85.7	-57.6	-31.8	-100.0	-90.0	-85.9	-67.0
EA	-95.7	-98.4	-100	-71.7	-90.3	-91.5	-85.4	-75.4	-88.9	-100	-90.8	-88.5	-100	-100	-1

Table 5.4: Percentage difference between "constant temperature" and "control" runs simulated with ECHAM5 climatology under RCP6.

PRUDENCE regions, and more spring drought (for AL, 2001–2050 only). "Constant temperature" implies no increase in snowmelt (since in Mac-PDM.09, snowmelts only occurs when temperature rises above a threshold) which alleviates drought conditions particularly in spring. Table 5.4 suggests that this effect is larger in SC than AL.

Although precipitation is the predominant driver of the land surface hydrologic system (Adam *et al.*, 2009), these results demonstrate the importance of PET on future changes in hydrological drought. Although the difference between the two runs are mostly attributable to changes in temperature thus PET, the relative contribution from PET and possibly other factors that interact with temperature in MacPDM.09 would be an area for further study. Besides the effects of PET, Gosling and Arnell (2011) found MacPDM.09 simulated runoff to be highly sensitive to the choice of PET calculation method by testing also with the Priestley-Taylor method, and discussed the implications of different PET calculation methods. Both van der Schrier *et al.* (2011) and Sheffield *et al.* (2012) calculated global PDSI values with the Thornthwaite (Thornthwaite, 1948) and Penman-Monteith (Allen *et al.*, 1994a; Ekström *et al.*, 2007) methods. While the former found similar results between the two approaches as precipitation is more important than PET in the simple water balance model of the PDSI algorithm, the latter found diverging results. Results obtained here are therefore likely to differ considerably with a different PET calculation method.

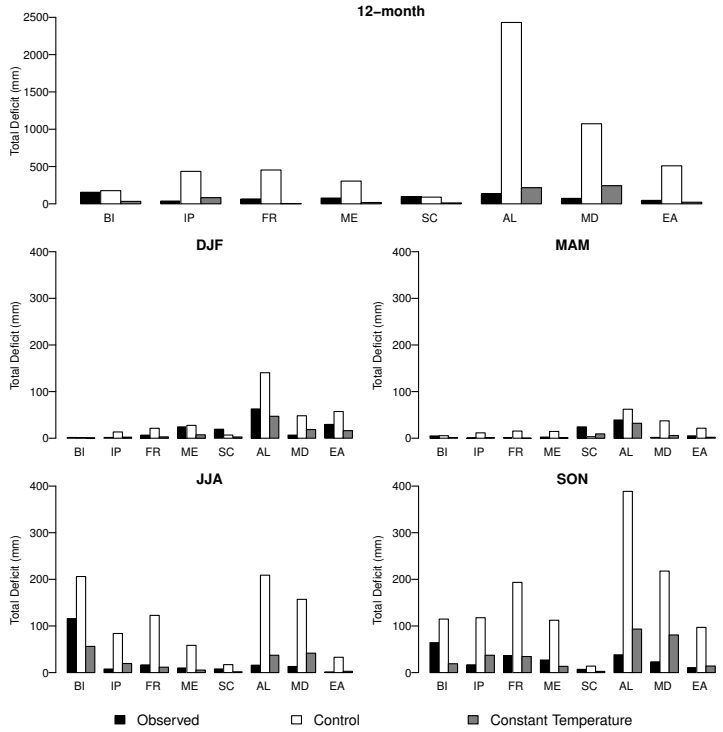

Figure 5.19: Total severity in 1951–2000 and 2051–2100 for "control" and "constant temperature" runs simulated with ECHAM5 climatology under RCP6.

5.8.7.2 Effects on Magnitude of Change

Figure 5.19 illustrates the effects of PET on the magnitude of change from 1951–2000 for total severity in 2051–2100 simulated with ECHAM5 climatology under RCP6. Only IP and MD show positive trends in both experiments in both long and short events, with a considerably lower (>50%) magnitude of increase under "constant temperature". SC shows decreasing 12-month and winter severity, with "constant temperature" producing larger magnitudes. For almost all other categories, PET affects the sign of change except in IP and MD. Taking the AL example, "constant temperature" indicates negative trends in winter and spring and positive in summer and autumn, while "control" shows increases in all seasons. Frequency of DAI25 reveals similar characteristics and is hence not shown.

5.9 Conclusions

This chapter has presented the effects of climate change on hydrological drought characteristics in the 21st century for Europe using gridded ($0.5° \times 0.5°$) monthly runoff output from the hydrological model, Mac-PDM.09. The general methodology adopted in

this chapter follows that applied and detailed in Chapter 4. Future climate scenarios, simulated by MAGICC6 and ClimGen, were used as inputs for Mac-PDM.09. Spatial patterns were presented for PRUDENCE-averaged regions and Köppen-climate regimes, and hydrological drought severity and occurrence of large-scale drought were analysed.

To investigate the robustness of the projected changes in European hydrological droughts, a systematic analysis of the various sources of uncertainty associated with drought modelling was carried out. These include difference due to the choice of drought classification (meteorological vs. hydrological), a fixed or seasonally-varying threshold for determining when drought occurs and termination rule for drought events, along with the spread of results introduced by ten emission scenarios and eighteen GCMs. Specially, this chapter aimed to answer the questions outlined in Section 5.1. Construction of probabilistic scenarios that would be useful in a planning context would require consideration of more than the uncertainties addressed here. Consistency was determined by the level of GCM agreement, with a trend (a robust trend) occurring when $\geq$10 (all 18) GCMs projected the same direction of change. IQRs were used as a more robust measure of model spread. This emphasis on inter-model consistency and the behaviors of the majority of models assumes that GCM agreement in direction of change are more reliable, which may or may not be correct (see discussion in Section 2.7.10).

Drought projections and their future changes generally vary substantially, depending on the GCM, emission scenario, region, season, threshold and the methodology used to define them. Nevertheless, results presented here enable the following generalisations to be made:

- Temporal: Drying intensifies with climate change over the 21st century, with more (less) robust increases (decreases) in 2051–2100 than 2001–2050.

- Regional patterns: Projected changes in both high- (Scandinavia and Russia) and low-latitudes (the Mediterranean and Middle East region) tend to be less sensitive to the various sources of uncertainty investigated. The former is projected to become less drought-prone, especially in winter/spring, while marked increases (typically by 2-3 times in 2001–2050, and up to 10-fold in 2051–2100) are simulated throughout the year for the latter. Winter/spring trends in British Isles and summer/autumn trends in Scandinavia are less conclusive.

- Seasonal patterns: Robust and marked increases, but accompanied by higher uncertainties in magnitudes, are common in summer/autumn, whereas negative trends may occur in winter/spring. Although the largest increases tend to occur in summer/autumn, altered snowmelt processes may cause spring to have the largest magnitude changes in some cases.

- Drought definition: Contrasting trends occur due to choice of different definitions are more common in winter/spring particularly in regions affected by snow and snowmelt. For instance, in spring, the Alps could experience positive meteorological changes but negative trends in hydrological drought. Drought classification uncertainty also leads to opposing changes in summer/autmn in Scandinavia.

- Results averaged climatically according to the Köppen climate classification, rather than geographically, demonstrate higher GCM consistency, thus better reflecting the climate change signal.

- Uncertainties tend to increase over time and with magnitude of warming. They affect frequencies of widespread droughts more than total severity, and DAI50 more than DAI25 results, especially in 2001–2050. The lower agreement in 2001–2050 results for spatially extensive droughts especially DAI50 events, is related to the less substantial near-future warming and/or their rarity especially in larger geographic regions. The effects of emission scenario uncertainty is more important in 2051–2100; however, GCM variance dominates over other sources of uncertainty throughout.

Comparing results derived from fixed and seasonally-variable thresholds identifies categories that are more sensitive to deficiencies during high-flow seasons (Question 2 in Section 5.1), which are less likely to be captured by the fixed threshold. These results suggest that a variable threshold captures these anomalies in regions with higher runoff such as the Alps and Scandinavia especially in the high-flow seasons of winter/spring. A variable threshold also yields considerably larger magnitudes of increase in drying than a fixed threshold that may yield contrasting trends in the wetter seasons.

To identify categories that may be more susceptible to a larger drought event being divided into a number of mutually dependent minor droughts, two drought event termination

rules that either include or exclude "excess" periods (where flows temporarily exceed the threshold level during an event) were applied (Research Question 3 in Section 5.1). For both present-day and 21st century results, discrepancies introduced by the two event definitions (1) affect longer droughts than shorter events; (2) affect frequencies of widespread events more than total severity; and, (3) have negligible effects on hydrological results (although 12-month alpine results have relatively higher discrepancy); however, they have more influence on their meteorological counterparts as precipitation in a particular month has less dependence on conditions of the preceding month.

The level of agreement in results derived from the meteorological and hydrological definitions was assessed. Both classifications generally produced the same direction of change, but hydrological results tended to produce more increases in drought conditions with larger magnitudes than meteorological ones. Disagreement was more common for summer/autumn in Scandinavia, and for winter/spring in Mid-Europe and Eastern Europe as higher PET counteracts precipitation increase; inconsistency also occurred in the alpine spring as earlier snowmelt alleviated hydrological droughts while meteorological events were enhanced by reduced precipitation.

Drought parameters derived from MacPDM.09 were found to be highly sensitive to PET; different results are therefore likely with a different PET calculation method. Higher PET generally implies more droughts in absolute terms, with larger increases. Chiew and McMahon (2002) found that changes in runoff and soil wetness are larger than evapotranspiration changes, hence the relative contribution from PET and possibly other factors that interact with temperature in MacPDM.09 is subject to further study. Winter and 12-month droughts in Scandinavia and British Isles (in 2001–2050) were projected to decrease regardless of PET changes, but higher PET implies smaller reduction. Higher PET also reduced winter droughts in Scandinavia and the Alps due to increased melting of frozen precipitation.

Outcomes in this chapter are conditional upon the limitations of MAGICC6, ClimGen (those associated with pattern-scaling and the underlying GCMs) and Mac-PDM.09 (e.g. hydrological model parameters derived from the recent past are assumed to continue to apply in future climates) as discussed in Section 3. Since Mac-PDM.09 calculates runoff independently for each cell, runoff in cells further downstream from the Alps, for instance,

does not contain the glacial component as it would in reality. Results and uncertainty analysis were primarily based on the use of climate change patterns from 18 GCMs under RCP6 and one hydrological model. These climate scenarios do not account for potential changes in the intensity of rainfall at sub-monthly timescales, for example. As such, results here are likely to underestimate the true uncertainty in future hydrological patterns (Arnell, 2011), thus should be considered illustrative rather than definitive. Nevertheless, this comprehensive sampling of uncertainty highlights the range of outcomes that can occur future drought conditions.

Global and catchment-scale hydrological model output for a given GCM can produce substantially different projections of flow changes (e.g. Gosling *et al.*, 2011b; Haddeland *et al.*, 2011). This variance is relatively small compared to GCM uncertainty (inter-GCM differences; Arnell, 2011; Todd *et al.*, 2011), which is often found to be the largest (Graham *et al.*, 2007; Prudhomme and Davies, 2008; Gosling *et al.*, 2011b; Kjellström *et al.*, 2011), particularly during summer months (Wilby *et al.*, 2006). One major source of GCM uncertainty is related to large-scale atmospheric circulation changes (especially changes in precipitation and windiness) and their representation in GCMs (Räisänen *et al.*, 2004; Kjellström *et al.*, 2011). Models also have difficulties in reproducing higher-order statistics of precipitation (Blenkinsop and Fowler, 2007b).

Discharge is not only affected by hydroclimatological processes (van der Wateren-de Hoog, 1995; Hemming *et al.*, 2010), but also catchment characteristics (Hisdal *et al.*, 2001; Chiew and McMahon, 2002; Gudmundsson *et al.*, 2011), elevation (Chang *et al.*, 2002), water quality and anthropogenic influences (e.g. cover change, adaptation measures and abstractions for irrigation, industrial and/or domestic use) in future. Considerations of these are beyond the scope of this chapter but are important for assessing vulnerability to climate change.

It is worth noting that increasing drought conditions in regions that already suffer from the hazard may be of less concern compared to regions that do not currently experience their effects. Adaptation decisions (e.g. on investment in infrastructure such as reservoirs) will need to be made in the context of high uncertainty. As no one technique is superior than the others (e.g. Blenkinsop and Fowler, 2007b; Prudhomme and Davies, 2008), decision-making should be based on multi-scenario and multi-drought definition

approaches, together with multiple climate and impact models (Feyen and Dankers, 2009) to capture uncertainties due to both hydrological and climate modelling (Prudhomme and Davies, 2008). The choice of drought quantification methodology should be governed by purpose of application. Local practices such as irrigation are excluded in the simulation process used here also need to be considered. Existing literature indicates considerable sub-regional variations (e.g. the northern wetting and southern drying trend in the British Isles) and localised storms (e.g. in the Mediterranean) that are likely to be smoothed by the regional averaging process. For instance, topography can induce fine-scale features in the precipitation change signal (Gao *et al.*, 2006); the hydroclimatological processes that govern hydrological droughts may vary between regions and events (Fleig *et al.*, 2011). Therefore, higher resolution models may be more appropriate for impact assessment studies, especially for mountainous regions (e.g. the Alps), although they also have limitations (see Section 2.6.11).

Since future interannual precipitation variability could enhance or alleviate changes in drought caused by mean precipitation changes, the next chapter explores the spatial and temporal effects of climate-change-induced changes in interannual precipitation variability in projected meteorological and hydrological droughts for the European study region.

Chapter 6

Effects of climate change on the interannual variability of precipitation and impacts on droughts

6.1 Introduction

Global warming will directly influence precipitation patterns (Trenberth, 2006). The non-linear hydrological response (Labat *et al.*, 2004) suggests global energy and hydrologic cycles will intensify as climate changes (Giorgi *et al.*, 2004). Overall, interannual hydroclimate variability (both drying and wetting) could enhance (Christensen and Christensen, 2004; Meehl *et al.*, 2000; Seager *et al.*, 2012) due to larger atmospheric water holding capacity and evaporation over oceans (Giorgi and Bi, 2005; Meehl *et al.*, 2007). The likelihood of extreme events (e.g. low summer precipitation, increased dry spell lengths) is very sensitive to deviations in mean and variability of the probability distribution associated with the variable under consideration, hence they (e.g. precipitation extremes; Kharin and Zwiers, 2005) may fluctuate much more than the mean (Gregory *et al.*, 1997). Therefore, temporal and spatial anomalies of climate variability and its seasonal distribution — rather than changes in the long-term mean values — may be more important in terms of societal consequences (Katz and Brown, 1992; Lioubimtseva and Henebry,

2009).

Regional climate fluctuates on timescales of seasons to decades but, until the last decade, conventional impacts studies have concentrated on mean climate changes. Räisänen (2002), Giorgi *et al.* (2004) and Rowell (2005) explored the impacts of CO_2-doubling/climate change on interannual variability of temperature and precipitation. Arnell (2003a) investigated the implications of perturbed relative climate interannual variability on British river flows, Döll (2002) studied how climate change and variability could affect irrigation water requirements, while Vidal and Wade (2009) studied both shifts in drought index and changes in their characteristics due to GCM-derived perturbed inter-monthly climate variability, and Hulme *et al.* (1999) focused on the multi-decadal (30-year) timescale impacts on runoff. Hydrological impact studies (e.g. Lehner *et al.*, 2006) that exclude changes in interannual or daily variability may be under- or over-estimating future floods, droughts and irrigation water requirements (Bates *et al.*, 2008).

Precipitation variability may be measured in absolute (standard deviation, SD) or relative (coefficient of variation, CV) terms, with the latter being more appropriate for impact studies (e.g. water resource management; Vidale *et al.*, 2007) given that it is dimensionless and thus enables comparison between regions with different amounts of precipitation. Global warming generally increases precipitation SD and CV: larger SD may occur in areas with higher or lower mean annual precipitation; CV increases especially with declining mean precipitation since it is expected to decrease (increase) with more (less) precipitation days (Räisänen, 2002). Consequently, a general decline in mean precipitation across the PRUDENCE regions implies a substantial increase in CV (Vidale *et al.*, 2007).

Changes in variability are an important consideration in a changing climate as they may mask/moderate or exacerbate the direction and/or magnitude of an anthropogenic signal, e.g. the strengthened winter NAO combined with background anthropogenic warming rapidly changed the northern Europe winter climate between 1965 and late 1990s (Hurrell, 1995; Hurrell and van Loon, 1997; Parker *et al.*, 2007). Such changes could have implications for the alpine region, which exhibits the strongest European winter interannual precipitation variability (Bartolini *et al.*, 2009), and Iberian hydroelectric production, which currently varies by a factor of three between wet and dry years (Trigo *et al.*, 2004),

for example. Exacerbated precipitation intensity and variability could raise flooding and drought risks (Bates *et al.*, 2008), e.g. more heatwaves and droughts in Europe (Schär and Jendritzky, 2004). Water availability from surface water sources or shallow groundwater wells depend on both the seasonality and the interannual variability of streamflow while seasonal low flows affect the security of water supply (Bates *et al.*, 2008). Even with a constant total precipitation, warming and enhanced precipitation variability generally increase irrigation water demand during the growing season (Bates *et al.*, 2008), and therefore water stress (Lioubimtseva and Henebry, 2009). A change in interannual climate variability could affect agriculture (e.g. crop yields, crop quality and even crop choice; Skuras and Psaltopoulos, 2012), food production and forestry (Salinger, 2005).

Changes in European precipitation (and temperature) interannual variability have been attributed to the effects of: (1) perturbations in mean seasonal temperature and precipitation, which typically enhances future variance when measured over 30 years; (2) variations in SST anomalies that affect seasonal means; (3) deviations in internal atmospheric variance (Rowell, 2005; Vidale *et al.*, 2007) and, (4) land-atmosphere feedbacks especially in transitional climate zones and mid-latitude areas via soil moisture-temperature/precipitation or vegetation-climate interactions (Seneviratne and Stöckli, 2007).

GCMs can allow interannual variability to change independently of mean precipitation in regions where the temporal distribution becomes more skewed with increases in low or high extremes, or both. Future interannual precipitation variability could enhance or alleviate changes in drought caused by mean precipitation changes, but few studies have explored this area. This chapter therefore takes advantage of ClimGen's scenario generation capacity (see Section 3.2) to assess the spatial and temporal effects of climate-change-induced changes in interannual precipitation variability (hereafter, variability) in the projected meteorological and hydrological droughts for the European study region.

6.2 Methodology

To explore the influence of climate-change-driven perturbed precipitation variability in future meteorological and hydrological drought, results from a "control" and a "fixed variability" experiment (ClimGen Option 4 and 3, respectively; see Section 3.2) are compared. The former accounts for changes in both precipitation mean and variability, as

represented by the coefficient of variation (CV) or equivalently by the shape parameter of a gamma distribution (see Equations 3.6 and 3.7); the latter considers only changes in mean precipitation as the CV is kept roughly constant. In both experiments, ECHAM5 pattern-scaled precipitation deviations for both mean and variability were expressed as a fractional change from present-day precipitation (e.g. a fractional change of 1.2 would be +20%) rather than as an absolute change (e.g. +20 mm/month). ECHAM5 was chosen on the basis described in Section 4.4. The effects on 12-month results for drought severity and DAI25 frequency for 2001–2050 and 2051–2100 under RCP3-PD and RCP8.5 were studied. A drought (both meteorological and hydrological) is defined by a fixed threshold (see Section 5.5).

In the "fixed variability" experiment, ClimGen was run with a scenario generation method that multiplies the observations by ECHAM5-derived mean climate perturbations. Variability, which is inherent in the observed time series, is modified so that CV is roughly constant in both periods, hence precipitation standard deviation changes in proportion to the mean. To avoid precipitation in regions of decreasing mean precipitation reaching zero, the magnitude of mean precipitation varies exponentially (rather than linearly) to global-mean temperature change, thus the rate of change accelerates (decelerates) in regions with higher (lower) mean precipitation (see Equation 3.3). These "fixed variability precipitation" scenarios were then applied in MacPDM.09 to generate "fixed variability runoff".

The "control" results are simply those from Chapters 4 and 5 for meteorological and hydrological droughts, respectively.

6.3 Meteorological and Hydrological Drought Severity

Figures 6.1 and 6.2 present the difference between control and fixed variability meteorological and hydrological drought severity, respectively. Patterns of difference in 2051–2100 under RCP3-PD and in 2001–2050 under RCP8.5 are not shown due to their similarities to Figures 6.1a and 6.2a; these figures therefore demonstrate the smallest (top) and largest (bottom) forcing scenarios examined. Missing data points in Figures 6.1b and 6.2b represent cells with no change in severity, or without drought in 1951–2000 and/or 2051–2100.

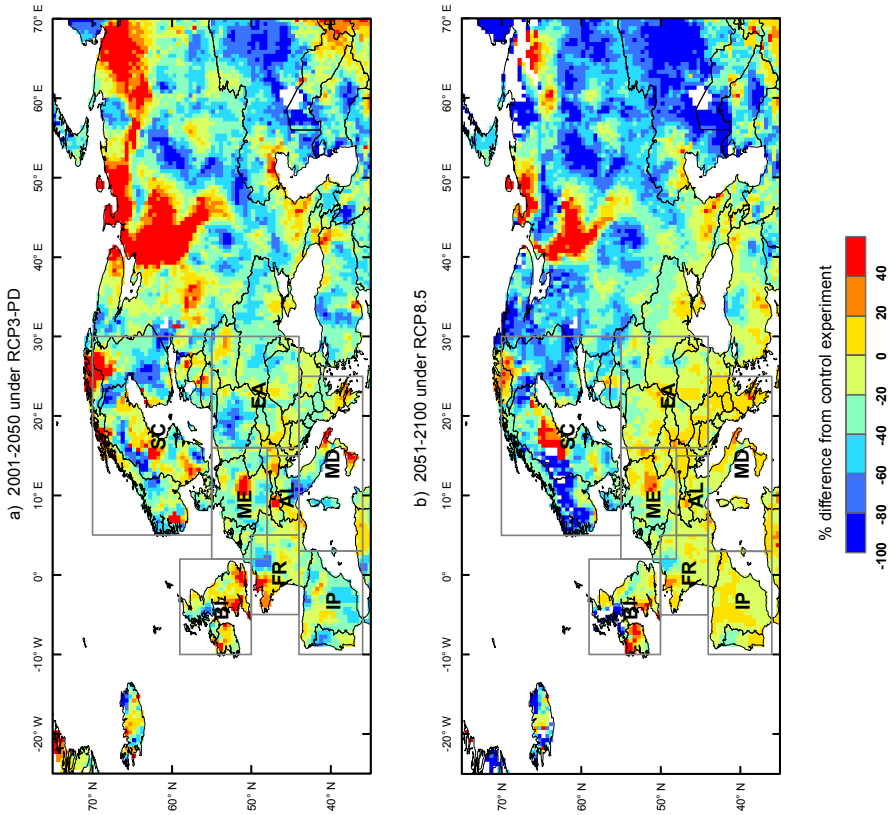

Figure 6.2: Figure 6.1, but for 50-year total hydrological drought severity.

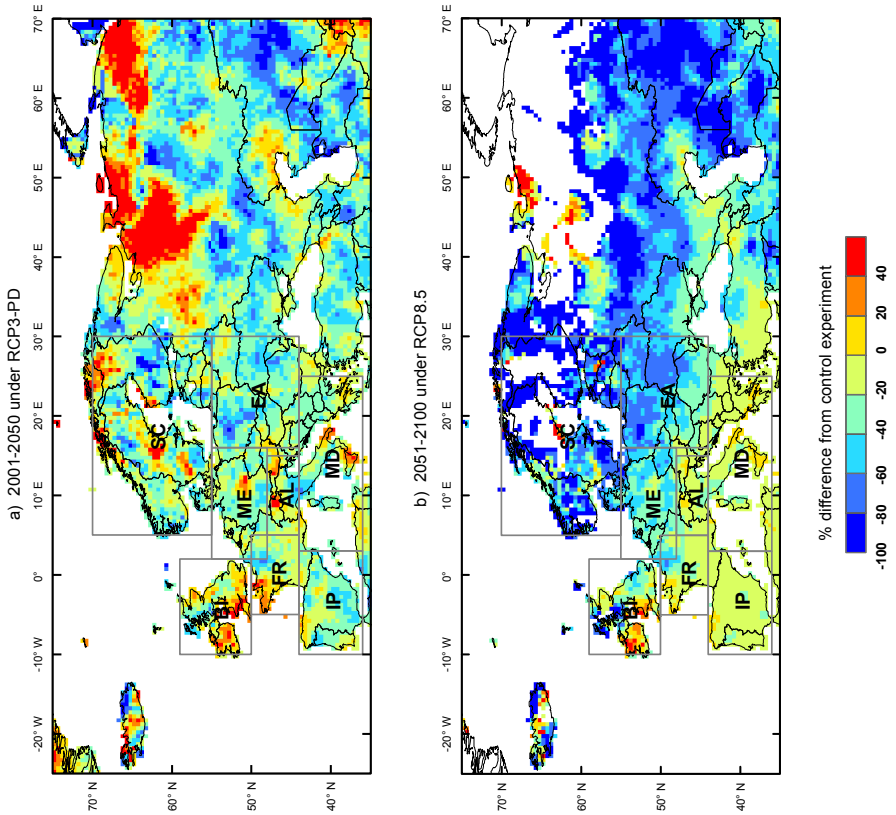

Figure 6.1: Difference between 50-year total meteorological drought severity from fixed variability and control experiments.

Figures 6.1 and 6.2 reveal very similar spatial patterns: across much of the study region, fixed variability severities tend to be lower than control values, i.e. overall, the inclusion of future changes in interannual precipitation variability tend to increase the severity metric of both meteorological and hydrological droughts, relative to the cases where only the mean precipitation changes and the CV of precipitation is hold constant. The opposite trend occurs primarily in parts of Russia/SC (particularly some areas of Sweden), western/southwestern BI, Brittany (FR) and southern Italy where perturbed variability lowers severity. The influence of changed variability on hydrological drought is less geographically structured than for meteorological drought — a characteristic Hulme *et al.* (1999) found in runoff anomalies associated with 30-year climate variability.

Figures 6.1a and 6.2a show similar patterns between the two experiments, with the hydrological results having slightly larger magnitudes, in both positive and negative directions. Figure 6.1b shows relatively small differences (up to -20%) between the two experiments around the Mediterranean basin, which become larger with increasing latitudes (and also in Central Asia); similar characteristics are also present in Figure 6.2b. Figures 6.1b and 6.2b demonstrate differences in severity between meteorological and hydrological droughts. Hydrological results have smaller differences between the two experiments, suggesting that altered variability affects meteorological, more than hydrological, severities, as the SPI-based results more directly reflect precipitation influence; similarly, Lloyd-Hughes and Saunders (2002) found precipitation directly caused much of the variability in their PDSI results. In large parts of the Balkans, IP, central and eastern Europe, variability fluctuations enhance (reduce) meteorological (hydrological) severities, corresponding to lower (higher) 50-year mean precipitation (runoff) (not shown).

In the higher latitudes (except BI) and Central Asia, drought severities, in particular meteorological ones, are considerably lower (up to 100% lower in some areas) when precipitation variability (CV) is held constant compared to the control results. This not only suggests that changes in variability intensifies severity but areas that are “drought-free” (based solely on increased mean precipitation) may become “drought-affected” when changes in variability are also incorporated. Results for the wetting regions, including northern latitudes but also northwestern BI and AL, may also be affected by the methodology used for the generating the magnitude of mean precipitation deviation, see Section

6.5.

As forcing increases (with time and/or under a higher emission scenario), differences in both meteorological and hydrological severity between the two experiments decline in the Mediterranean, Black Sea and Caucasus regions through less intensity (e.g. parts of IP and the Balkans) or reduction in severity (e.g. southern Italy). Since severity is defined as the cumulative deficit over the time period, this weakening effect appears to contradict the expected warming-induced intensification of the hydrological cycle, is attributable to the levelling off of severity in drying regions as precipitation/runoff approaches zero. This also explains the smaller discrepancies in the lower latitudes compared with northern latitudes.

In parts of the Balkans, IP, central and eastern Europe, hydrological severity differences reverse from negative to positive with increasing forcing. Modified variability alleviates, rather than amplifies severity, partly because of more intense precipitation in southern Europe (Kjellström, 2004; Giorgi and Lionello, 2008) associated with the more severe storms (Sumner *et al.*, 2003). Nevertheless, consistent with Figure 6.2, (Arnell, 2003a) found intensified interannual variability reduces Q95 further despite the small impact on mean flows.

6.4 PRUDENCE-Averaged Results

Regional effects of deviations in the interannual variability of precipitation are also examined. Table 6.1 presents the regional changes, from 1951–2000 values, in projected meteorological and hydrological drought parameters from control and fixed variability experiments. For both meteorological and hydrological drought severity and DAI25 frequency, including future changes in interannual variability tends to (1) enhance positive trends (IP, FR, AL, MD, EA), (2) moderate reductions (SC), or (3) reverse reductions in drought so that they become increases (e.g. meteorological drought results for BI and ME). Similar to findings in Section 6.3, changes in meteorological drought are larger than the hydrological drought changes; also their effects generally weaken, except for some scenarios in BI and ME, with increasing forcing. The attenuating effect (reducing differences) with increasing forcing may not reflect the decreasing relative importance of perturbed precipitation variability on severity (as discussed above); nonetheless it is more

	RCP3-PD				RCP8.5			
	2001–2050		2051–2100		2001–2050		2051–2100	
	Control	Fixed	Control	Fixed	Control	Fixed	Control	Fixed
Meteorological Severity:								
BI	1.2	−7.0	0.9	−8.8	6.2	−4.5	42.9	19.7
IP	232.4	154.1	333.5	236.1	311.3	227.0	1171.5	1037.5
FR	84.5	59.5	127.9	92.1	104.0	78.9	393.0	310.0
ME	39.6	8.3	56.8	17.4	49.1	13.0	166.0	71.4
SC	−32.9	−46.4	−44.4	−55.8	−33.6	−49.2	−49.4	−62.6
AL	170.6	130.0	243.6	193.3	228.5	177.6	876.3	740.2
MD	219.2	155.4	312.1	232.4	298.1	224.6	1192.5	1060.8
EA	68.2	17.2	97.5	29.8	87.0	26.1	328.0	146.1
Meteorological DAI25 Frequency:								
BI	−7.9	−30.3	−14.5	−32.9	−7.9	−32.9	−26.3	−48.7
IP	274.1	168.5	357.4	246.3	335.2	235.2	870.4	803.7
FR	85.5	44.9	126.1	75.4	100.0	60.9	320.3	223.2
ME	26.9	−17.9	29.5	−9.0	28.2	−12.8	110.3	14.1
SC	−48.5	−86.4	−65.2	−87.9	−50.0	−87.9	−83.3	−100.0
AL	307.9	205.3	415.8	292.1	407.9	265.8	1210.5	992.1
MD	270.6	154.9	425.5	270.6	364.7	245.1	1027.5	996.1
EA	90.9	0.0	120.0	16.4	116.4	12.7	396.4	125.5
Hydrological Severity:								
BI	−6.9	−5.9	−7.7	−5.8	−4.3	−3.5	51.4	47.7
IP	266.8	177.3	406.8	295.0	392.7	286.7	2047.0	1937.6
FR	146.7	130.1	248.1	207.7	196.5	180.7	1125.0	1046.0
ME	75.5	35.7	122.3	70.7	101.0	58.4	546.4	479.9
SC	−18.3	−33.4	−21.0	−35.0	−18.3	−34.5	42.5	8.8
AL	341.5	313.0	551.7	517.0	517.4	477.0	3267.5	3261.7
MD	334.9	255.0	499.1	407.8	490.5	389.5	2417.8	2411.7
EA	232.3	165.6	372.3	281.0	319.9	236.3	1924.6	1787.1
Hydrological DAI25 Frequency:								
BI	−3.6	16.1	7.1	28.6	0.0	16.1	128.6	133.9
IP	284.8	197.8	367.4	280.4	358.7	291.3	930.4	963.0
FR	150.9	108.8	184.2	157.9	171.9	136.8	421.1	464.9
ME	57.8	37.5	85.9	73.4	85.9	75.0	287.5	315.6
SC	−14.3	−47.6	−11.9	−52.4	−19.0	−47.6	35.7	−42.9
AL	581.5	525.9	896.3	870.4	796.3	729.6	2000.0	2055.6
MD	596.8	500.0	958.1	877.4	754.8	703.2	1764.5	1793.5
EA	240.9	190.9	345.5	288.6	363.6	252.3	1095.5	1127.3

Table 6.1: Percentage changes, from 1951–2000, in meteorological and hydrological drought parameters from two experiments: (1) the "Control", where both the mean and CV of precipitation change (according to the pattern-scaled GCM projections); and, (2) the fixed variability ("Fixed") experiment, where the mean changes but CV is held constant (i.e. the SD changes in proportion to the mean).

indicative in the DAI25 frequencies results.

However, for hydrological DAI25 frequencies in 2051–2100 under RCP8.5, perturbed variability yields slightly smaller increases across all PRUDENCE regions except SC, where the negative trend reverses. As forcing intensifies, wetter-than-average periods associated with variability may also become more frequent and/or widespread, resulting in a smaller proportion of drought-affected areas. Such a pattern also occurs in the BI under all scenarios (see later discussion).

SC tends to have negative drought changes; increased mean precipitation variations alone typically decrease meteorological and hydrological severities and DAI25 frequencies, but perturbed variability lessens the reductions through more frequent and/or longer dry periods. Yet, continued forcing increase reverses the influence of changed variability on hydrological trends for both mean and variability in 2051–2100 under RCP8.5, with altered variability amplifying severity increase and producing more (rather than less) frequent DAI25 events as PET increases.

Based on percent difference in drought parameters between the two experiments in Table 6.1, overall, interannual variability changes are least influential in AL. Although perturbed variability has relatively similar effects in IP, FR, AL and MD, its role in ME and EA is particularly evident in the meteorological results. For meteorological severity in both regions, changes in both mean and variability of precipitation produce increases 2.2–4.8 times larger than with the mean climate alone, compared to 12–51% higher in IP, FR, AL and MD. For EA in 2001–2050 under scenario RCP3-PD, mean precipitation variations produce almost no change in meteorological DAI25 frequency, but the addition of changes in variability almost doubles the frequency. For ME, both experiments project consistent increases but only in 2051–2100 under RCP8.5. Under weaker forcing scenarios, mean changes reduce meteorological DAI25 frequency, but the inclusion of modified variability generates positive changes; perturbed interannual variability does not have such a large impact in the hydrological results. It could be related to the new western/eastern transitional zone in terms of changing precipitation characteristics as climate shifts (Kyselý *et al.*, 2010), and increased summer temperature and precipitation variability due to strong land-atmosphere interactions in central and eastern Europe as climatic regimes shift northwards with increasing GHGs concentrations (Seneviratne *et al.*, 2006).

Except for 2051–2100 under RCP8.5, BI has relatively small changes of regionally-averaged severity due to the averaging of spatial contrast (Figures 6.1 and 6.2) — modified variability enhances (alleviates) severity in western Scotland (Ireland/southwestern England). Both experiments indicate increasing meteorological and hydrological severities only in 2051–2100 under RCP8.5. Under all other scenarios examined, perturbed interannual variability intensifies the severity of meteorological droughts, in contrast to the reductions caused by increased mean precipitation; but changes in interannual variability also amplify hydrological severity reductions.

The results here are broadly consistent with other studies. Dankers and Hiederer (2008) found increasing fluctuations in interannual precipitation variability (CV of the annual precipitation sums) in both northern and southern Europe, and decreases in the areas between. Precipitation intensity and variability falling in drying regions is generally increasing (Dankers and Hiederer, 2008). In southern Europe, precipitation variability increases in both wet/cold season and the dry/warm seasons (Goubanova and Li, 2007) as dry years become drier (Dankers and Hiederer, 2008), and a pronounced increase in negative anomalies (Giorgi and Coppola, 2009) regardless of the magnitude of mean changes (Giorgi and Lionello, 2008). This is in agreement with the enhanced positive changes in drought found here for the Mediterranean regions. Over northern-central Europe, the precipitation probability density functions (PDFs) broaden and flatten, with predominantly increased positive anomalies in winter (as wet years become wetter; Dankers and Hiederer, 2008), and negative in summer (Giorgi and Coppola, 2009). The effects of changes in summer, if greater than those in winter, may partially be responsible for reversing the negative drought changes (from mean precipitation changes alone) in ME obtained here. Similar to mean precipitation, the magnitude of changes in interannual variability generally increases with forcing intensity and is unimportant until the late decades of 21st century — contradicting DAI25 frequency results in the present study; the change signal is also greater in the dry season than the wet season (Giorgi and Lionello, 2008). Greater atmospheric water holding capacity causes higher wet-period precipitation intensities; wet periods are separated by longer dry periods with more frequent extremely hot and dry summers due to feedback interaction with generally drier land areas (Giorgi and Lionello, 2008).

6.5 Control vs. Fixed Variability Experiments

Results from the control and fixed variability experiments differ due to three distinctions in ClimGen Options 4 and 3 methodologies, respectively. These are the (1) modification of observational monthly anomalies that are used to represent future variability, (2) superimposing these modified present-day deviations of precipitation variability onto 21st-century scenarios, and (3) the function used to generate the magnitude of mean precipitation change.

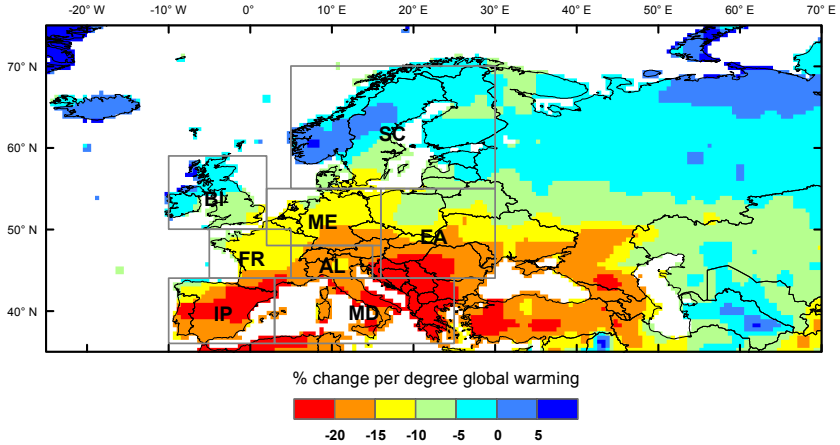

Figure 6.3: ECHAM5-derived shape parameter change pattern (12-month average).

Firstly is the modification of variability, in addition to mean precipitation, in the control but not the fixed variability experiment. The temporal distribution of precipitation may become more (or, in some cases, less) skewed as climate changes. The gamma probability distribution, which best describes variation in precipitation amount over a wet period of a given number of days (Ison *et al.*, 1971; Lloyd-Hughes and Saunders, 2002), contains a shape parameter α and a scale parameter β. α tends to vary with wet-day frequency, therefore measures distribution skewness. Similar to mean precipitation, the projected change in α, as a ratio of the present-day mean, is expressed as a linear or exponential function of the global-mean temperature change. The shape parameter for a particular future scenario can, therefore, be estimated from the global-mean temperature change and a coefficient for each calendar month and each grid cell. The pattern of coefficients has been diagnosed from the CMIP3 GCM simulations and the average of the twelve monthly patterns for the ECHAM5 GCM is shown in Figure 6.3.

For a gamma distribution, given that $\mu = \alpha\beta$ and $\sigma^2 = \alpha\beta^2$, where μ is the mean

and σ^2 is the variance, $CV = 1/\sqrt{\alpha}$. Therefore, the CV of precipitation increases as α decreases, and vice versa. Figure 6.3 shows that a majority of the study region has negative changes with the largest magnitudes in the lower latitudes. This implies that CV increases with global warming, particularly around the Mediterranean and Black Sea regions; CV also increases across much of the high latitudes where declining mean precipitation is expected, consistent with Räisänen (2002) and Vidale *et al.* (2007). As a lower α value implies a more skewed distribution (Goodess *et al.*, 2003a), this explains the worsening drought conditions found in Sections 6.3 and 6.4.

Secondly, there are differences in the way that the observed precipitation variability is superimposed onto the 21st-century scenarios between the two ClimGen methods that might make a very small contribution to the difference between the two experiments. Specifically, the fractional deviations in the fixed variability experiment (ClimGen Option 3; o'_{imy} in Equation 3.3) always have a mean of one, whereas the transformed fractional deviations in the control experiment (ClimGen Option 4; $\tilde{o}_{imy}$ in Equations 3.6 and 3.7) may have a mean that differs slightly from one. Nonetheless, this influence is negligible due to the long baseline period (1951–2000) chosen, which is considered representative of the fluctuations in the timeseries.

Lastly, in regions with declining mean precipitation, the magnitude of mean precipitation in both experiments, and the precipitation distribution shape in the control run, varies exponentially with global-mean temperature change in both experiments. In regions where mean precipitation increases, however, the relationship is linear (exponential) in the control (fixed variability) experiment. Although, results in wetting regions may also be affected by this effect (which becomes apparent with global-mean temperature of $+3^{\circ}$C or above, e.g. in 2051–2100 under RCP8.5), it is relatively unimportant since drought, i.e. regions with precipitation decline, is the primary concern here.

This subsection has discussed the three differences in ClimGen options that explain the differences in the results from the two experiments, i.e. to differentiate the effect of changes in interannual variability and mean. The latter two also lead to non-identical changes in mean precipitation for reasons discussed above. For instance, the 50-year-mean precipitation from the two experiments deviate by -4% to $+8$% in 96% of the study region under lower forcing scenarios, and 90% of the region in 2051–2100 under

RCP8.5. Nonetheless, these inconsistencies are small compared to 50-year mean control precipitation changes from 1951–2000 mean (-80% to $+40\%$ in $\approx 91\%$ of all cells).

6.6 Conclusions

This chapter has examined the effects of climate-change-altered interannual variability on indices of European meteorological and hydrological droughts. This was achieved by comparing results from a "control" and a "fixed variability" experiment generated with ClimGen Options 4 and 3, respectively, for both 2001–2050 and 2051–2100 under RCP3-PD and RCP8.5. The former experiment accounts for both changes in the mean and variability of precipitation (i.e. results from Chapters 4 and 5 for meteorological and hydrological droughts, respectively) while the latter considers only changes in mean precipitation. Differences in the results between the two experiments are predominantly attributable to the perturbed precipitation variability.

Overall for both meteorological and hydrological drought severity and DAI25 frequency, perturbed variability tends to (1) enhance drought conditions, particularly in Mid-Europe and Eastern Europe, (2) moderate reductions in drought conditions (Scandinavia), or (3) reverse reductions in drought conditions (e.g. meteorological results for British Isles and Mid-Europe). Therefore, studies that omit precipitation variability fluctuations may under- or over-estimate drought (but more often underestimate for the study region) and their trends, or may derive conflicting trends to those that take into account both perturbed mean and variability, e.g. meteorological DAI25 frequency in Mid-Europe. A drought-free zone (e.g. in the northern latitudes) according to mean changes only may become drought-affected when modified variability is considered. The British Isles has relatively small changes due to the averaging of sub-regional spatial variations (e.g. deviations in variability enhance drought severity in western Scotland but reduce it in western/southwestern parts of the region), and does not demonstrate clear positive change until very large forcing scenarios.

These results suggest that small changes in mean precipitation could produce large effects on drought results, especially those meteorologically defined. The impact of perturbed interannual variability is more reflected in meteorological than hydrological drought results due to the use of the precipitation-only SPI index. Although severity

results do not reflect the relative importance of modified variability particularly in drying regions, their effects generally weaken, except for some cases in British Isles and Mid-Europe, with increasing forcing as DAI25 frequency results suggest. Under very high forcing, wetter-than-average periods associated with positive precipitation anomalies may also become more frequent and/or widespread, producing slightly smaller increases in hydrological DAI25 frequency; meteorological DAI25 frequencies do not share this characteristic though.

6.6.1 Limitations

Although a range of forcing has been represented by a high (RCP8.5) and a low (RCP3-PD) emission scenario, results here are based on ECHAM5 only. The effects of perturbations in the interannual variability of precipitation simulated using other GCMs may lead to different results, thus is an area for further research. In addition, analysis here was carried out for 12-month drought results; the seasonal effects of changes in interannual precipitation variability therefore warrants further investigation as studies have shown seasonality in the changes in interannual variability of precipitation, with the largest increase in summer, and smaller changes in spring and autumn (Giorgi *et al.*, 2004; Rowell, 2005; Vidale *et al.*, 2007; Giorgi and Coppola, 2009).

Using ClimGen, this study has used the statistical properties of precipitation derived from the observations combined with information from GCM simulations to generate future scenarios, i.e. the effects of the changes in interannual variability of precipitation on drought parameters have been studied by examining the simulated changes in the shape parameter of the gamma distribution. The detailed study of individual drivers of interannual precipitation variability and their changes, such as the NAO (van Loon and Rogers, 1978; Hurrell, 1995; Rodó *et al.*, 1997; Haylock and Goodess, 2004; López-Moreno and Vicente-Serrano, 2008), is beyond the scope of the current study. Also, this study has considered the changes in precipitation variability on the interannual timescale only; changes on other timescales (e.g. inter-decadal; Arnell, 1999c; Hulme *et al.*, 1999) may modify the results further. The effects of perturbations in interannual variability has been assessed for precipitation only; changes in temperature variability may also have an impact

on the projected drought results. In summer, for instance, the increasing interannual variance of precipitation has been found to couple with those for temperature over much of Europe, regardless of the direction of precipitation change (Giorgi and Bi, 2005; Giorgi and Coppola, 2009). These have not been explored here.

The next chapter examines the runoff sensitivity to climatic changes for the European study region using the elasticity approach, and assesses the applicability of such an approach for estimating runoff under a perturbed climate.

Chapter 7

Runoff sensitivity under present-day and future climates: the application of runoff elasticity

7.1 Introduction

Our incomplete understanding of the behaviour of the climate system has led to the development of a wide range of emission scenarios, climate and impact models to support climate change decision making. Despite advances in our scientific understanding and model development, conventional cause-effect analysis (Bruckner *et al.*, 1999) is highly sensitive to the choice of input data and models. Climate and hydrological models may be physically sound, but their use in climate change and hydrological impacts studies are subject to a wide range of sources of uncertainties that range from the choice of emission scenarios, models and model calibration methodologies (which itself is time and resource intensive; Schaake, 1990; Sankarasubramanian *et al.*, 2001), to the difficulties in the interpretation of multi-model results, as described in Section 2.6. This cascade of uncertainty produces a range of possible outcomes (Schneider, 1983). The effects of application of a range of emission scenarios and GCMs have been explored in Chapters 4 and 5 for the case of European drought characteristics under future climates. In addition, decision makers tasked with climate change adaptation planning and policy formulation often have

time and/or resource constraints, making assessments based on a physical model a less appropriate support tool in practical applications. Assessing the sensitivity of a system to a particular trigger offers an alternative (empirical) approach in climate change vulnerability and adaptation assessments, and can provide some indication of the urgency of the issue, i.e. how close the system moves toward critical thresholds (Weiss and Alcamo, 2011), without the level of complexity associated with physical modelling.

Runoff sensitivity to climatic (e.g. precipitation) changes has been estimated using various approaches on both global (Chiew *et al.*, 2006) and regional scales, including U.S. (Sankarasubramanian *et al.*, 2001; Sankarasubramanian and Vogel, 2003; Fu *et al.*, 2007a;b; Renner and Bernhofer, 2012), Australia (Chiew and McMahon, 2002; Chiew, 2006; Department of Water, 2010; Yu *et al.*, 2010a) and China (Fu *et al.*, 2007c; Zheng *et al.*, 2009; Liu and Cui, 2011; Sun *et al.*, 2013); only a few studies have focused on the European region (e.g. Arnell, 1992; Weiss and Alcamo, 2011).

This chapter seeks to evaluate the spatial and temporal variations of runoff sensitivity for the European study region. Elasticity can be used to measure the sensitivity/response of a system to a certain trigger. Section 7.2 provides an overview of the climate elasticity of runoff and the datasets used in this study. Section 7.3 presents the elasticity estimates for the European study region and their changes in a changing climate. Section 7.4 explores the applicability of elasticity values for estimating runoff under a perturbed climate. Section 7.5 presents the concluding remarks. The specific research questions addressed in the chapter are:

1. How does runoff sensitivity to changes in climatic factors vary across the study region under present-day climate?

2. To what extent does climate change alter runoff sensitivity?

3. Can a simple non-parametric estimator be applied as an initial screening tool, prior to the adoption of a physical model-based approach, for estimating runoff change? Specifically, does future runoff estimated with the non-parametric estimator, determined only using 20th century data, agree with those simulated by Mac-PDM.09?

7.2 Climate Elasticity of Runoff

Schaake and Chunzhen (1989) and Schaake (1990) adapted the concept of elasticity (ε), widely used in economics, to estimate the sensitivity of streamflow to climate deviations. ε expresses the ratio of the percent change in one variable to the percent change in another variable (Liu and Cui, 2011) — e.g. precipitation elasticity of streamflow $\varepsilon_p(P, Q)$ represents the proportional change in streamflow Q to the change in precipitation P; alternatively, potential evapotranspiration (PET), instead of precipitation, data may be used for $\varepsilon_{PET}(PET, Q)$. It indicates the hydro-climatic status of the respective basins and the expected proportional sensitivity of climatic changes (Renner and Bernhofer, 2012). Dooge (1992) and Dooge *et al.* (1999) termed it the sensitivity factor. ε_p>1 indicates that a 1% precipitation change can cause a >1% streamflow change (Sankarasubramanian *et al.*, 2001).

7.2.1 Elasticity Estimation Approaches

Runoff deviations under a perturbed climate may be estimated by a physical model-based approach, i.e. using a hydrological model (e.g. Nash and Gleick, 1991; Chiew and McMahon, 2002; Legesse *et al.*, 2010). However, this process can be complex, and time- and resource-intensive.

Alternatively, an empirical approach may offer the advantage of simplicity as it determines streamflow response to climate variations using long-term meteorological and hydrological observations (Risbey and Entekhabi, 1996), which may be more readily available than a physical model. According to Schaake (1990), $\varepsilon_p(P, Q)$, a random variable dependent on P and Q, is defined as:

$$\varepsilon_p(P, Q) = \frac{dQ/Q}{dP/P} = \frac{dQ}{dP}\frac{P}{Q} \tag{7.1}$$

Sankarasubramanian *et al.* (2001) compared the performance of various model structures in estimating elasticity at the mean values of precipitation (μ_P) and streamflow (μ_Q) (Equation 7.2), and recommended the estimator, Equation 7.3, for general usage.

$$\varepsilon_P(\mu_P, \mu_Q) = \frac{dQ}{dP} \mid_{P=\mu_P} \frac{\mu_P}{\mu_Q} \tag{7.2}$$

$$\varepsilon_p(P,Q) = median\left(\frac{Q_t - \bar{Q}}{P_t - \bar{P}}\frac{\bar{P}}{\bar{Q}}\right) \tag{7.3}$$

Equation 7.3 represents the median of annual estimates of climate elasticity over the study period at the specific site; t is time (year), $\bar{P}$ and $\bar{Q}$, are the long-term sample means of precipitation and streamflow, respectively. P_t and Q_t are the annual-mean precipitation and runoff in year t. The use of annual data implies that Equation 7.3 only estimates long-term runoff sensitivity to long-term precipitation changes (Chiew *et al.*, 2006). To capture the full range of observed variability, longer records are generally recommended for estimating elasticity. With potential changes in climate and variability, however, the most recent 30–50 years, or dry or wet periods that are similar to future projections, may be more suitable (Fu *et al.*, 2011).

Sankarasubramanian and Vogel (2003), Chiew (2006) and Liu and Cui (2011) and others have investigated the effects of climate change on annual streamflow based on Equation 7.3. This estimator was tested via Monte Carlo experiments for three basins in the U.S.; it was found to have low bias and was equally or more robust than watershed model-based approaches for evaluating the streamflow sensitivity (Sankarasubramanian *et al.*, 2001). It enables spatial and temporal comparisons of streamflow response to climate change/variability in different scales of the same basins. Liu *et al.* (2012) quantified the impacts of climatic variation and human activities on streamflow changes by first estimating the contribution of streamflow deviations associated with changes in precipitation and potential evapotranspiration (PET) using the climate elasticity method, and then attributed the remaining streamflow variation to human or other influence.

Given the time and resource constraints in water resource management and planning, the relatively simple data requirements and calculations of Equation 7.3 imply that it could potentially be a useful scoping tool to identify areas that warrant in-depth modelling studies. Hence, the application of Equation 7.3 has been explored in this chapter.

Runoff sensitivity may also be obtained from the response surface method (e.g. New, 2002; Weiss and Alcamo, 2011), the Budyko framework (e.g. Renner and Bernhofer, 2012; Sun *et al.*, 2013; Liang and Liu, 2013), or the ArcGIS Geostatistical Analyst (e.g. Fu *et al.*, 2007a;c; Yu *et al.*, 2010a), amongst others (e.g. Dooge, 1992; Vogel *et al.*, 1999; Harman *et al.*, 2011).

7.2.2 Limitations of the Non-Parametric Estimator

Despite the simplicity of Equation 7.3, a numerical drawback is that $\varepsilon_p(P, Q)$ approaches infinity when P_t approaches $\bar{P}$ (Sankarasubramanian *et al.*, 2001). Fu *et al.* (2007b) excluded precipitation changes of $<$10% to overcome this numeric instability, however such an approach has not been adopted here due to the selection of median elasticity values (Equation 7.3).

Since Equation 7.3 is only a function of precipitation, it does not account for the effects of other factors such as temperature (Fu *et al.*, 2007b), hence PET, which also can also alter runoff characteristics (Gedney *et al.*, 2006). For instance, the 20th-century global runoff was found to increase by 4% with a 1°C warming (Labat *et al.*, 2004); the potential changes in future precipitation and temperature distributions could modify future flow regimes, as simulated for Central European basins (Weiss and Alcamo, 2011). Fu *et al.* (2007b) thus extended Equation 7.3 into a two-parameter index, by using the ArcGIS Geostatistical Analyst package and historical records to construct the streamflow-precipitation-temperature relationship. This incorporates the effects of the temperature from the temperature-precipitation plane into the calculation of climate elasticity of streamflow. Furthermore, Equation 7.3 excludes potential changes in rainfall distribution and frequency, land surface processes and surface-atmosphere feedbacks in an enhanced greenhouse environment (Chiew *et al.*, 2006).

7.2.3 Datasets

The calculation of climate elasticity of runoff (Equation 7.3) is based on annual streamflow (Q_t) and annual climate variables such as precipitation (P_t) and PET (PET_t). This involves using the observed (1951–2000) monthly CRU TS 3.0 precipitation timeseries extracted using ClimGen (see Section 3.2), Mac-PDM.09-simulated monthly runoff timeseries and monthly PET timeseries extracted from Mac-PDM.09 for the period 1951–2000 (see Section 3.3). The Mac-PDM.09 simulation was forced by the same CRU TS3.0 observed climate variations.

To analyse the changes in runoff sensitivity under a changed climate, future elasticity values were computed with 21st-century monthly precipitation (from ClimGen) and runoff (from Mac-PDM.09) data projected by ECHAM5 under a low (RCP3-PD) and

high (RCP8.5) emission scenario. ECHAM5 was chosen on the basis described in Section 4.4. This approach enables an assessment of how well elasticity values estimated using 1951–2000 runoff (from Mac-PDM.09) reproduces the Mac-PDM.09-generated future runoff simulated using GCMs and emission scenarios. However, it will likely give an upper bound for the performance of Equation 7.3 because the runoff used to fit the elasticity equation is from the same model that is used to test its performance. Lower performance would be expected if real-world datasets were used for elasticity estimation, because real-world observations will not be perfect.

7.3 Elasticity Estimates

7.3.1 Calendar vs. Hydrological Year

According to Fu *et al.* (2011), an inappropriate accumulation of annual values of streamflow and precipitation may over- or underestimate elasticity. Consequently, timeseries with the strongest precipitation-streamflow relationship should be used, and that the hydrological year (October–September) would be preferable. Elasticities for snowmelt-dominated mountain and high-latitude catchments (e.g. Spokane River basin; Fu *et al.*, 2011) with topographically driven thresholds related to snow loss that are relatively weak in 20th-century records, may become more sensitive to the time periods of annual accumulations and the precipitation-streamflow relationship (Fu *et al.*, 2007b). The initial step in elasticity estimation therefore is to determine whether to use calendar- or hydrological-year results for subsequent analysis.

The strength of the precipitation-runoff relationship was assessed using Pearson's correlation coefficients for 1951–2000 annual timeseries computed with both calendar and hydrological years. The spatial distribution of the correlation coefficients (not shown), however, revealed little difference between the January–December and October–September results.

Subsequently, precipitation and PET elasticity of runoff (hereafter, ε_{ppt} and ε_{PET}, respectively) for both calendar and hydrological years were estimated with Equation 7.3, as shown in Figures 7.1 and 7.2. Monthly precipitation, PET and runoff data for 1951–2000 were used (see Section 7.2.3). The gridded ε_{ppt} and ε_{PET} values (as in Figures

	ε_{ppt}		ε_{PET}	
	Calendar	Hydrological	Calendar	Hydrological
PRUDENCE regions:				
BI	1.48	1.39	-0.20	-0.05
IP	1.86	2.21	-2.23	-1.09
FR	1.73	1.95	-0.42	0.07
ME	1.67	1.92	-0.82	0.17
SC	1.14	1.33	0.08	0.18
AL	1.50	1.63	-2.44	-0.96
MD	1.62	1.91	-2.82	-3.11
EA	1.48	1.68	-2.59	-0.86
Köppen climates:				
BSh	1.65	1.80	-4.92	-2.84
BSk	1.60	1.67	-6.25	-6.14
BWh	1.51	1.74	-3.02	-4.85
BWk	1.54	1.58	-6.56	-6.06
Csa	1.74	2.01	-3.11	-3.67
Csb	1.71	2.10	-1.07	-0.74
Cfa	1.56	1.81	-3.73	-2.66
Cfb	1.62	1.77	-1.45	-0.35
Cfc	1.16	1.28	0.68	0.75
Dsa	1.05	1.25	-3.48	-3.00
Dsb	1.27	1.51	-3.09	-2.70
Dsc	1.05	1.18	-0.30	-0.41
Dfa	1.35	1.73	-6.18	-6.88
Dfb	1.40	1.64	-4.24	-5.08
Dfc	1.28	1.51	-1.19	-0.91
ET	0.88	1.04	0.19	0.30

Table 7.1: ε_{ppt} and ε_{PET} estimated with annual climatic and runoff values based on the calendar and hydrological years.

7.1 and 7.2) were then averaged based on the PRUDENCE regions and Köppen climates types (see Section 3.9). These are presented in Table 7.1.

Hydrological-year ε_{ppt} (Figure 7.1b) tend to be more spatially-coherent, and both gridded and regional (Table 7.1) hydrological-year ε_{ppt} tend to have larger magnitudes, suggesting a more sensitive relationship. For regional averages, the hydrological year yields higher ε_{ppt} values in all PRUDENCE regions except the British Isles, and in every one of the Köppen regions. For example, regional calendar- and hydrological-year ε_{ppt} for IP, FR, ME, MD are 1.48–1.86 and 1.91–2.2, respectively. These results seem to support (Fu *et al.*, 2011)'s argument for using hydrological year. Moreover, the splitting of high European winter precipitation between two calendar years may produce misleading results (Trigo *et al.*, 2004). Therefore, the remaining chapter focuses on hydrological-year results.

ε_{PET} results are less conclusive and are discussed later in this subsection and Section 7.3.3.

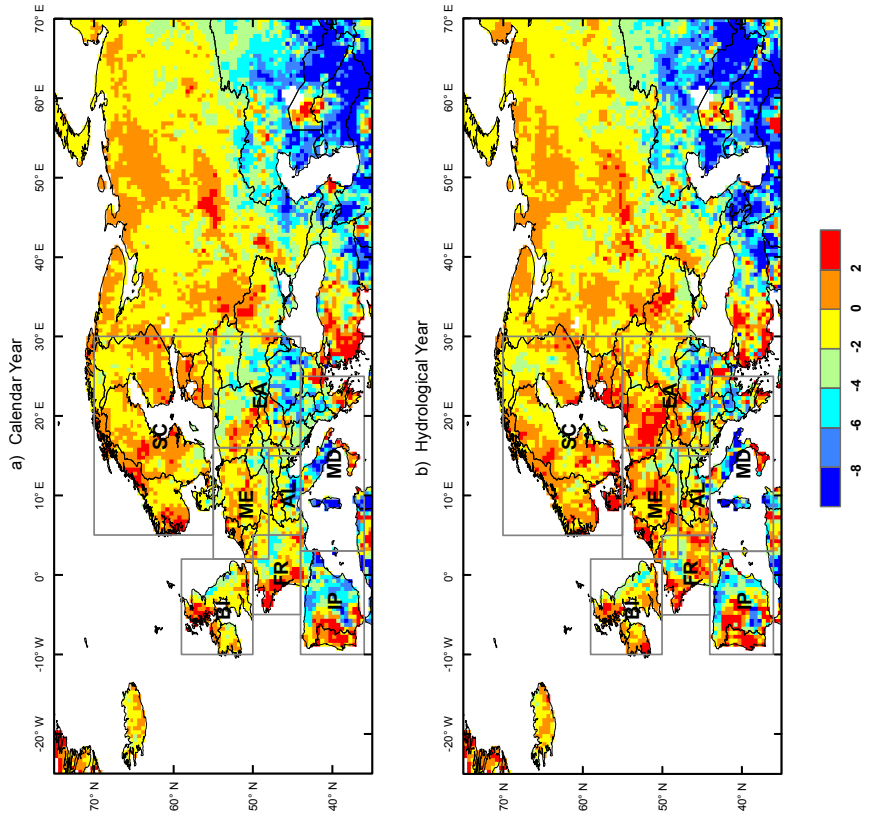

Figure 7.2: PET elasticity of runoff.

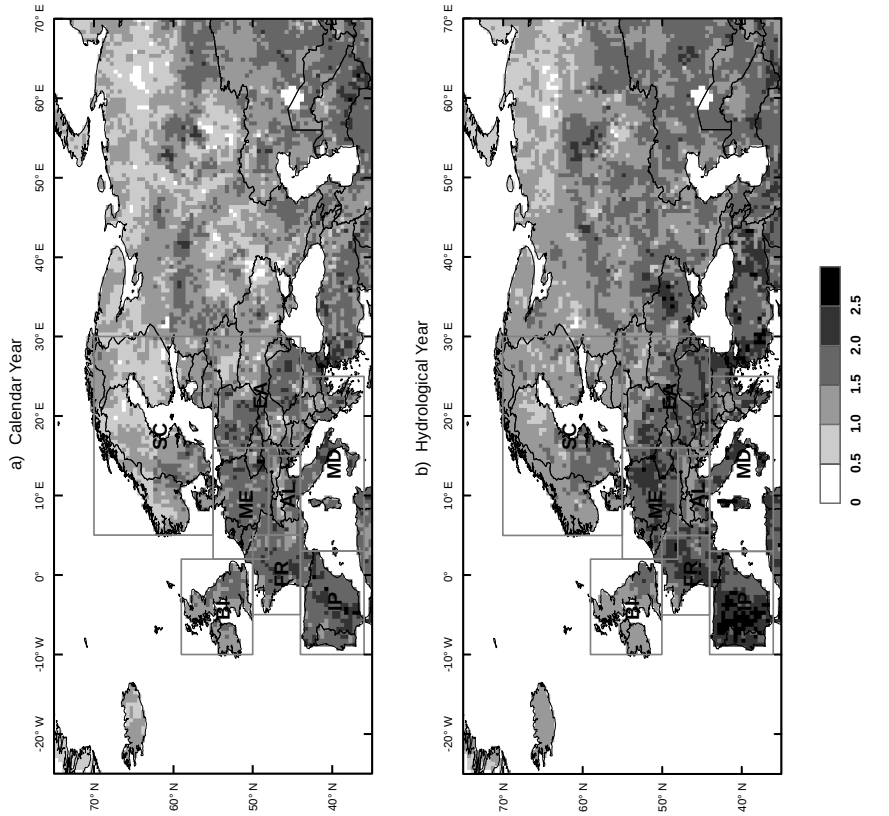

Figure 7.1: Precipitation elasticity of runoff.

7.3.2 Relationship with Runoff Ratio

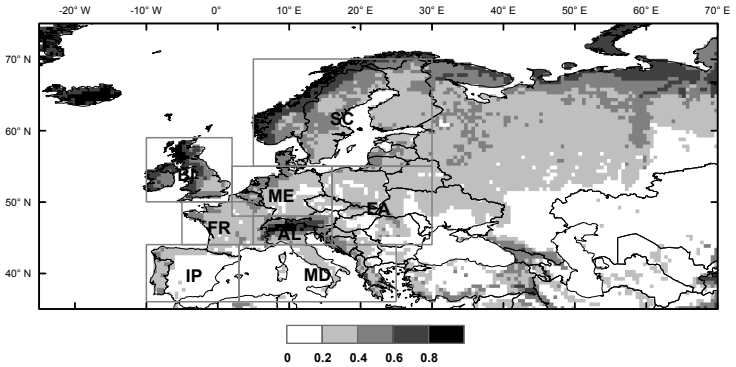

Figure 7.3: Mean runoff ratio for 1951–2000 based on October-September annual precipitation and runoff.

Figure 7.3 shows the mean runoff ratio (runoff/precipitation) derived from 1951–2000 annual (October-September) precipitation and runoff. It implies that runoff ratio negatively correlates to ε_{ppt} (Figure 7.1b) as areas with higher ε_{ppt} tend to have lower runoff ratios, and vice versa. This relationship is explored further below.

The runoff ratio, α, is defined as:

$$\alpha = \bar{Q}/\bar{P} \tag{7.4}$$

where $\bar{Q}$ and $\bar{P}$ are the long-term means of runoff and precipitation, respectively. Re-arranging Equation 7.4 gives:

$$\bar{Q} = \alpha\bar{P} \tag{7.5}$$

On longer timescales, continental river runoff is approximately equal to the difference between land precipitation and evapotranspiration (Gedney *et al.*, 2006). Therefore, assuming that soil moisture and groundwater storage ΔS in the present-day does not vary significantly over the long-term, i.e. ΔS=0, the long-term mean runoff, $\bar{Q}$, is:

$$\bar{Q} = \bar{P} - \overline{AET} \tag{7.6}$$

where $\overline{AET}$ is the long-term mean actual evapotranspiration (AET).

For any particular year, t,

$$Q_t = P_t - AET_t - \Delta S_t \tag{7.7}$$

Equation 7.3 states that:

$$\varepsilon = median(\varepsilon_t) \tag{7.8}$$

where ε_t is:

$$\varepsilon_t = \frac{Q_t - \bar{Q}}{P_t - \bar{P}} \frac{\bar{P}}{\bar{Q}} \tag{7.9}$$

If for year, t, where AET_t and S_t vary,

$$\Delta AET_t = AET_t - \overline{AET} \tag{7.10}$$

substituting Equation 7.6, and then 7.5, into Equation 7.10 gives:

$$\Delta AET_t = AET_t - \bar{P} + \alpha\bar{P} \tag{7.11}$$

substituting Equations 7.7 for Q_t, 7.5 for $\bar{Q}$, and 7.11 for $\alpha\bar{P}$ into Equation 7.9 gives:

$$\varepsilon_t = \frac{1}{\alpha} \cdot \frac{P_t - \bar{P} - (\Delta AET_t + \Delta S_t)}{P_t - \bar{P}} \tag{7.12}$$

Since $P_t - \bar{P} = \Delta P_t$, Equation 7.12 becomes:

$$\varepsilon_{ppt} = \frac{1}{\alpha} \cdot \frac{\Delta P - (\Delta AET_t + \Delta S_t)}{\Delta P} \tag{7.13}$$

If $\Delta AET_t + \Delta S_t = 0$, i.e. only precipitation changes from one year to another, Equation 7.13 simplifies to:

$$\varepsilon_{ppt} = 1/\alpha \tag{7.14}$$

Sankarasubramanian and Vogel (2003) also found the upper bound of ε_{ppt} to be roughly the inverse of runoff ratio.

Figure 7.4 presents the difference between ε_{ppt} and the inverse of runoff ratio ($1/\alpha$). It shows that for the entire study region, ε_{ppt} is smaller than $1/\alpha$, which occurs if $\Delta AET_t +$

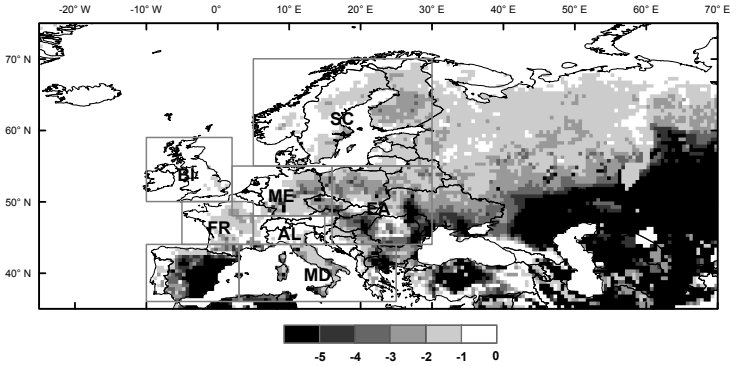

Figure 7.4: Difference between ε_{ppt} and the inverse of 1951–2000 mean runoff ratio.

$\Delta S_t > 0$ when ΔP_t>0 (Equation 7.13). Therefore, in years where ΔP>0 (i.e. a year with positive annual mean precipitation anomaly), the increase of AET and/or ΔS implies a smaller runoff increase than would occur if only precipitation changes; drier years (ΔP<0) imply a smaller runoff decrease as AET and/or ΔS reduces. Although the annual PET does not vary with changes in precipitation alone, changes in water made available by precipitation directly influence AET (Jeton *et al.*, 1996). Since AET cannot exceed PET:

$$AET = \beta PET \tag{7.15}$$

where 0≤β≤1, a wetter year implies that more moisture is available for evaporation ($\beta \rightarrow 1$) or soil moisture storage increases. Figure 7.4 shows that larger differences tend to occur in the lower latitudes (particularly eastern IP and Central Asia), and vice versa. This suggests that AET increases in the lower latitudes are higher than in the northern latitudes.

Although not found here, according to Equation 7.13, $\varepsilon_{ppt} > 1/\alpha$ occurs only if $\Delta AET_t + \Delta S_t < 0$ when ΔP_t>0 (and vice versa). This suggests that AET and/or ΔS decreases in a year where ΔP>0. This may occur with lower PET, which also implies lower AET, but would be unusual as soil moisture storage and β would be expected to be higher in a wetter year.

7.3.3 Spatial Variations in Elasticity

This subsection addresses Research Question 1 in Section 7.1, "*How does runoff sensitivity to changes in climatic factors vary across the study region under present-day climate?*".

7.3.3.1 Precipitation Elasticity of Runoff (ε_{ppt})

According to Figure 7.1, a majority of the study region has ε_{ppt} 1.0–2.5, i.e. a 1% precipitation increase yields a 1.0–2.5% rise in runoff. These results are consistent with Equation 7.3-based estimates of 1.0–3.0 for 500 catchments across the globe (Chiew *et al.*, 2006). This estimator, along with other approaches mentioned in Section 7.2.1, show regional variations in ε_{ppt}: 1.0–2.5 for the U.S. (Sankarasubramanian *et al.*, 2001; Sankarasubramanian and Vogel, 2003; Fu *et al.*, 2007a), 2.0–4.0 for Australia (Chiew and McMahon, 2002; Chiew, 2006; Yu *et al.*, 2010a), 1.3–3.0 for the UK (Arnell, 1992), 1.0–2.1 for the Chinese Yellow River (Zheng *et al.*, 2009; Liu and Cui, 2011) and Poyang Lake Basins (Sun *et al.*, 2013), and 3.0–4.0 for the Meki River Basin in Ethiopia (Legesse *et al.*, 2010). Although not found in the present study, increased precipitation may produce negative climate elasticity as a small precipitation increase (decrease) combined with a large temperature increase (decrease) may generate lower annual streamflow (Fu *et al.*, 2007b).

$\varepsilon_{ppt}>1.5$ occurs across much of western continental Europe and Central Asia/Middle East; large parts of IP has $\varepsilon_{ppt}>2.5$ (Figure 7.1). The lowest values tend to occur in regions north of 60°N and parts of Russia; in some of these areas, ε_{ppt} is <1, so that the relative runoff changes by less than precipitation. According to Jeton *et al.* (1996), the amplified runoff response arises due to the relatively smaller changes in AET compared to the mean precipitation perturbations, given that hydrological models such as Mac-PDM.09 represent annual runoff as roughly the difference between precipitation and AET. This is shown by Equation 7.13, as $\varepsilon_{ppt}>1$ implies that relative AET deviation is smaller than the relative mean precipitation change. This occurs when much of the additional precipitation during a wetter year falls (1) during the cold-season months and AET is limited by energy more than moisture, or (2) during intense precipitation events when a greater proportion runs off rather than increasing soil moisture storage and thus the later

supply of water for AET. $\varepsilon_{ppt}<1$ suggests that relative AET changes exceed precipitation changes, which occurs when much of the water is stored as snow until late spring when more energy is available (i.e. PET increases). This explains the concentration of areas with $\varepsilon_{ppt}<1$ in parts of Russia and Scandinavia, as shown in Figure 7.1.

In agreement with the negative correlation between ε_{ppt} and runoff ratio found in Section 7.3.2, many studies (e.g. Arnell, 1992; New, 2002; Zheng *et al.*, 2009; Liu and Cui, 2011) generally reveal higher (lower) sensitivities in more (less) arid regions or dry (wet) years, although Jeton *et al.* (1996) found larger annual streamflow changes to mean precipitation variations under wetter climates in the north-central Sierra Nevada, California and Nevada. Globally, $\varepsilon_{ppt}>2.0$ occurs in arid and semi-arid regions with lower runoff coefficients, including southeastern Australia, southern and western Africa, mid-western and Southwestern U.S.; $\varepsilon_{ppt}<2.0$ occurs in catchments with high mean annual runoff ratio and very high humidity index (precipitation/PET, both long-term mean), as well as in cold climates that has large snow storage, such as southwestern South America, the mid- and high-latitudes of the Northern Hemisphere such as northwestern U.S. (Sankarasubramanian *et al.*, 2001; Chiew *et al.*, 2006).

Elasticity may also vary with the direction of precipitation change, even with constant temperature (Fu *et al.*, 2007b). For four catchments in southwestern Cape, South Africa, New (2002) found greater (smaller) streamflow response for progressively larger precipitation increases (decreases). Moreover, as found in the Murray-Darling Basin (Fu *et al.*, 2011), precipitation variations alone may not cause directional or large-magnitude runoff changes (Jeton *et al.*, 1996), which depend also on basin-scale effects of climate, soil and vegetation (Wigley and Jones, 1985; Gedney *et al.*, 2006; Liu and Cui, 2011).

7.3.3.2 PET Elasticity of Runoff (ε_{PET})

Figure 7.2 shows that a 1% PET increase produces runoff change between -8% and $+2\%$ across much of the study region, which is consistent with other studies. For instance, New (2002) found low ε_{PET} of 0.2–0.4 in four mountainous catchments in southwestern Cape, South Africa, which increased under wet conditions (i.e. decreased PET). In China, ε_{PET} ranges from -2.1 to -10.2 in Poyang Lake Basin (Sun *et al.*, 2013) and between -1.0 and -4.5 in the Yellow River Basin (Zheng *et al.*, 2009; Liu and Cui, 2011).

Overall, ε_{PET} is larger than ε_{ppt} (typically $\leq$2.5), which appears to suggest that runoff in the study region is more responsive to PET than precipitation changes. While all ε_{ppt} values are positive, ε_{PET} are both positive and negative. PET is expected to negatively correlate with runoff as lower PET tends to offset the effects of any precipitation decline or enhance the effects of precipitation increases, hence higher runoff (Wigley and Jones, 1985). Positive ε_{PET} values, i.e. PET increases with runoff increase as reflected in Figure 7.2, imply greater effect of precipitation increase than PET increase.

Large positive ε_{PET} values ($+$2%) particularly concentrate in parts of western Iberian Peninsula, Scotland, western Eastern Europe (e.g. Poland), western Turkey, parts of Scandinavia, eastern Ukraine and southern Russia. This suggests that annual precipitation and PET values are positively correlated in these regions during 1951–2000, and runoff increases even in years with positive PET anomalies as the effect of precipitation increase is larger than PET. Such a relationship may also occur in future climates as runoff is determined by AET (see Section 7.3.3.1). The largest negative ε_{PET} ($-$8%) occurs in Central Asia/Middle East, but is also found in Romania, and parts of Italy that have the lowest runoff ratios ($<$0.2).

7.3.3.3 Regional ε_{ppt} and ε_{PET}

Table 7.1 shows that in all PRUDENCE regions except MD, precipitation changes affect runoff more than PET changes. Runoff in IP and SC is the most (ε_{ppt} 2.2) and least (ε_{ppt} 1.3) sensitive to precipitation changes, respectively. Along with one of the largest ε_{ppt} (1.9) alongside FR and ME, MD also has the highest ε_{PET} (3.1), suggesting high sensitivity changes to PET changes.

Taking averages according to Köppen climates, ε_{PET} values (negative 3.1–6.6) are larger than ε_{ppt} (1.3–2.1) in the lower latitudes (all arid (B) climates, temperate climates with hot summers (Csa, Cfa), cold climates with/without dry season and with hot/warm summer (Dfa, Dfb, Dsa, Dsb)), suggesting that runoff around the Mediterranean, Black Sea and Caspian Sea is more sensitive to PET than precipitation. In climates with lower temperatures (Csb, Cfb, Cfc, Dfc, Dsc, ET), PET influence is negligible (ε_{PET} 0–1). For ε_{ppt}, Csa and Csb have the highest values (2.0 and 2.1, respectively) while ET and Dsc have the lowest (1.0 and 1.2, respectively). Cfb, which covers much of mid-latitude

Europe, along with Cfa and Dfa that surround the Black Sea, also have relatively high ε_{ppt} of 1.7–1.8.

While temperature strongly influences the seasonal runoff distribution and snow accumulation and ablation processes (Jeton *et al.*, 1996), precipitation predominantly drives the land surface hydrologic system, thus directly and indirectly affect annual mean streamflow (Arnell, 1992; Risbey and Entekhabi, 1996; Adam *et al.*, 2009; Liang and Liu, 2013). Therefore, precipitation variations are regarded as more important than PET changes in determining runoff changes. Hence, ε_{ppt} is considered a more important indicator than ε_{PET}, and the remaining chapter focuses on ε_{ppt}.

7.3.4 ε_{ppt} under Climate Change

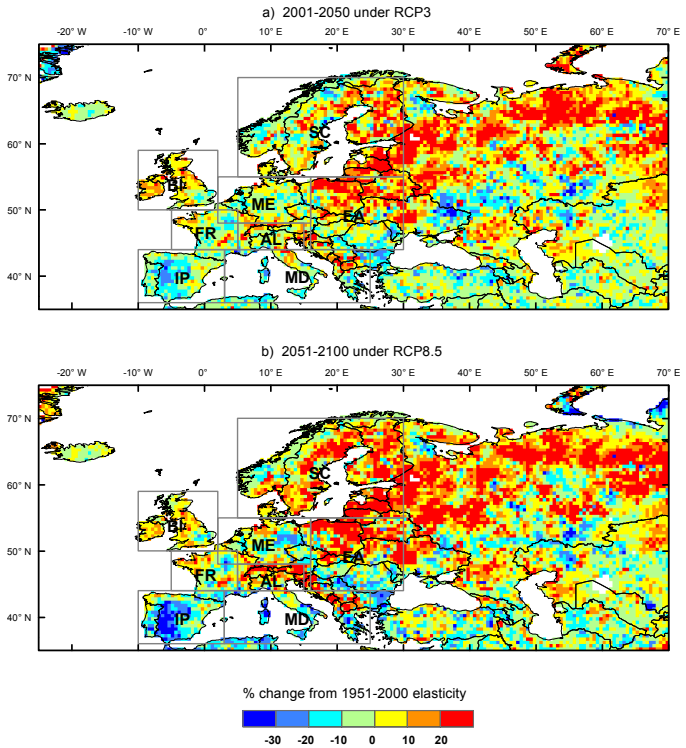

Figure 7.5: Changes in ε_{ppt} based on ECHAM5.

Most studies investigate climate elasticity of streamflow using 20th century data, e.g. for the U.S. (e.g. Sankarasubramanian *et al.*, 2001; Fu *et al.*, 2007b) and China (e.g. Fu *et al.*, 2007c; Zheng *et al.*, 2009; Liu and Cui, 2011; Sun *et al.*, 2013), but few have explored how elasticity could shift as climate changes. This study thus explores the European hydrological response to both present-day and future climates.

To examine the potential changes in ε_{ppt} under climate change (i.e. Research Question

2 in Section 7.1), Equation 7.3 was applied to 2001–2050 and 2051–2100 monthly precipitation and runoff timeseries based on ECHAM5 under RCP3 and RCP8.5 (see Section 7.2.3). Percentage changes in ε_{ppt} relative to the 1951–2000 values (Figure 7.1b) were derived (Figure 7.5). Patterns of change in 2051–2100 under RCP3 and in 2001–2050 under RCP8.5 (not shown) are similar to Figure 7.5a.

Figure 7.5 shows similar spatial patterns of ε_{ppt} changes from 1951–2000 in the two future periods under both emission scenarios. While changes of $\pm$20% in the 21st century scatter across the study region, stronger positive trends ($>$20%) predominantly occur in the band northern EA—eastern SC—northern Russia. These trends are more widespread in 2051–2100 under RCP8.5, for which they also extend into the Alps and along the east coast of the Adriatic Sea. Under present-day conditions, frozen precipitation in these regions implies a smaller runoff response to precipitation fluctuations ($\varepsilon_{ppt}<$1.5, Figure 7.1b). As more precipitation falls as rain instead of snow with warming, runoff responds more quickly to precipitation variations, yielding a higher runoff sensitivity to precipitation. Future ε_{ppt} decreases by $>$20% in IP where 1951–2000 ε_{ppt} is $>$2.0. This reduction could be related to the increasing importance of future PET, causing less of the precipitation changes to be reflected in runoff deviations. Another explanation is related to soil moisture storage changes: initial drier soil conditions (due to increased PET with warming) imply that in a year with positive precipitation anomaly, a greater proportion of the added moisture infiltrates into the soil until it becomes saturated, thus a smaller proportion contributes to runoff.

Generally, Figure 7.5 suggests that areas with some of the lowest (highest) present-day sensitivities of runoff to precipitation change, $\varepsilon_{ppt}<$1.5 ($>$2.0), have some of the largest (smallest) increases in the 21st century. This suggests reducing geographical variations in ε_{ppt} values.

7.4 Runoff Estimated by Elasticity

As mentioned above, streamflow sensitivities have been dervived in a number of studies but few have used elasticity values to estimate runoff. Chiew (2006) compared streamflow estimated by Equation 7.3 with a simple lumped conceptual daily rainfall-runoff model SIMHYD. In a report by the Government of Western Australia (Department of

Water, 2010), runoff changes in southwest Western Australia under a perturbed climate were determined using elasticities derived with 20th-century data. Since few studies have validated the use of elasticity values in estimating runoff changes, this section examines whether the application of an elasticity function could reproduce Mac-PDM.09-simulated runoff for the European study region (Research Question 3 in Section 7.1).

Using ε_{ppt} values derived in Section 7.3.3.1, runoff was estimated with Equation 7.16:

$$Q_{fut} = \bar{Q} + \varepsilon_{ppt}\bar{Q} \cdot \frac{P_{fut} - \bar{P}}{\bar{P}} \tag{7.16}$$

where Q_{fut} represents the elasticity-estimated 50-year mean runoff under climate change, $\bar{Q}$ is the 1951–2000 runoff mean based on Mac-PDM.09 output, ε_{ppt} denotes the precipitation elasticity of runoff, P_{fut} is the 50-year mean precipitation in the 21st century, and $\bar{P}$ is the 1951–2000 mean. The 21st-century precipitation data were based on ECHAM5 under RCP3 and RCP8.5 (see Section 7.2.3).

These elasticity-estimated runoff values, presented in Section 7.4.1, were then compared to Mac-PDM.09 simulations for the 21st century (Section 7.4.2).

7.4.1 ε_{ppt}-estimated Runoff

Figure 7.6 shows the percentage changes in 21st century using ε_{ppt}-estimated runoff based on the 1951–2000 mean. Similar to Figure 7.5, changes in 2051–2100 under RCP3 and in 2001–2050 under RCP8.5 are not shown due to their similarities to Figure 7.6a.

Northern and southern latitudes have the largest positive and negative trends of ε_{ppt}-estimated runoff change, respectively. In absolute terms, the former have the highest future 50-year mean runoff (e.g. Norway and western BI have $>$50 mm/month) while the latter have the lowest values (e.g. much of IP, Central Asia/Middle East have $<$10 mm/month). AL also has $>$50 mm/month of long-term mean runoff, but a moderate decrease of 10–30%.

ε_{ppt}-estimated values are generally $>$10% higher (lower) than 1951–2000 mean in areas north of 60°N (south of 45°N and west of the Caspian Sea). The most extreme warming scenario (Figure 7.6b) reveals runoff $>$30% higher in the northern latitudes, and $>$50% lower in the lower latitudes, particularly in IP and around the Mediterranean basin where the predicted reduction exceeds 70%.

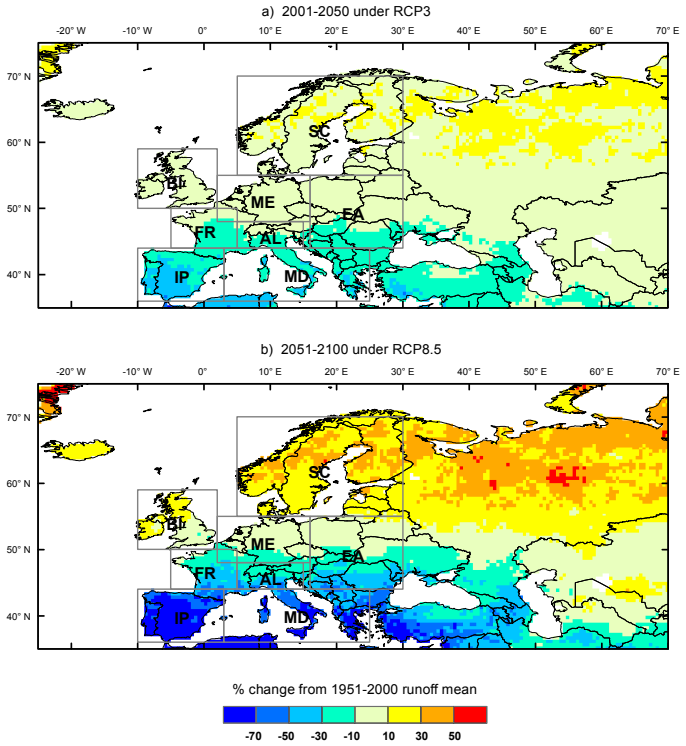

Figure 7.6: Changes in ε_{ppt}-estimated runoff, from 1951–2000 mean, based on ECHAM5.

For Figure 7.6b, ε_{ppt} produces negative runoff estimates in 1.3% of the study region, primarily in south-central IP and parts of southwestern Turkey (not shown). These roughly correspond to the regions with the highest present-day elasticity ($\geq$2.5) combined with large precipitation declines (by 34–59%) from 1951–2000 (other scenarios have $<$27% reduction). When estimating runoff with ε_{ppt}, large precipitation decrease and/or high ε_{ppt} values may reduce runoff by $>$100%. Although these cases could be set to zero, caution is needed anyway when estimating runoff change with elasticity values under large warming scenarios, as these changes may lie outside the range of the present-day annual variations used for elasticity estimation.

7.4.2 Comparison with Mac-PDM.09-simulated Runoff

This section examines the level of agreement between elasticity and hydrological modelling output by comparing the 21st century runoff estimated by ε_{ppt} (Section 7.4.1) and Mac-PDM.09 under a "control" and "constant-temperature" experiment. Climate scenarios under RCP3 and RCP8.5 based on ECHAM5 were used.

The "control" experiment involves using 21st-century ClimGen climate projections as input into Mac-PDM.09, i.e. the approach adopted in Chapter 5. Runoff/runoff change

estimated by elasticity and Mac-PDM.09 are hereafter termed “estimated” and “control” runoff/runoff change, respectively.

As Equation 7.3 only considers one climate variable, ε_{ppt}-estimated runoff might be more comparable to Mac-PDM.09 simulations generated with 21st century precipitation and 1951–2000 temperature — the “constant-temperature” experiment. Similarly, runoff/runoff change from this experiment is referred as “constant-temperature” runoff/runoff change, hereafter.

“Control” and “constant-temperature” runoff changes from 1951–2000 mean values are presented in Figures 7.7 and 7.9, respectively. As for Figures 7.5 and 7.6, only results for the most extreme (small and large) climate change scenarios are shown.

7.4.2.1 Control Runoff Comparison

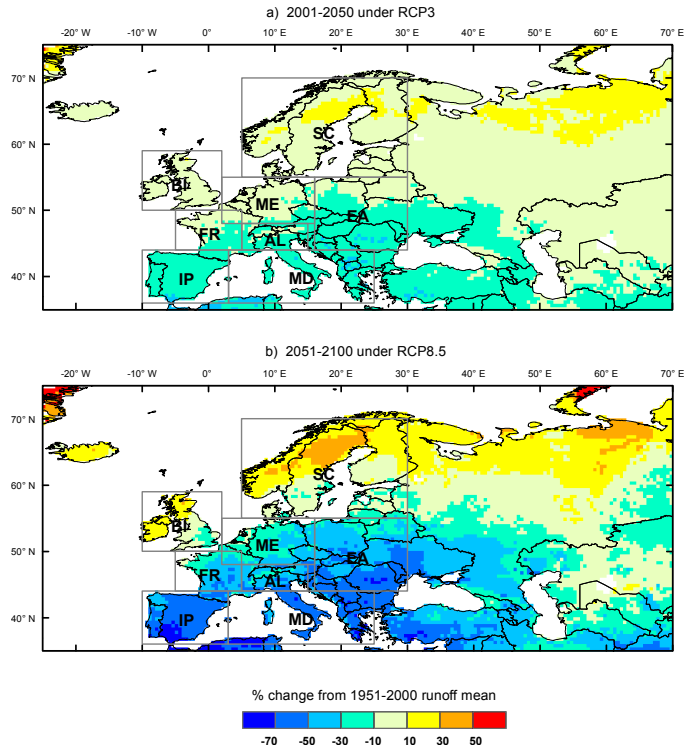

Figure 7.7: Changes in Mac-PDM.09-simulated runoff, from 1951–2000 mean, based on ECHAM5.

Under the smaller warming scenario, both the elasticity and modelling approaches (Figures 7.6a and 7.7a, respectively) produce similar spatial patterns of runoff change as

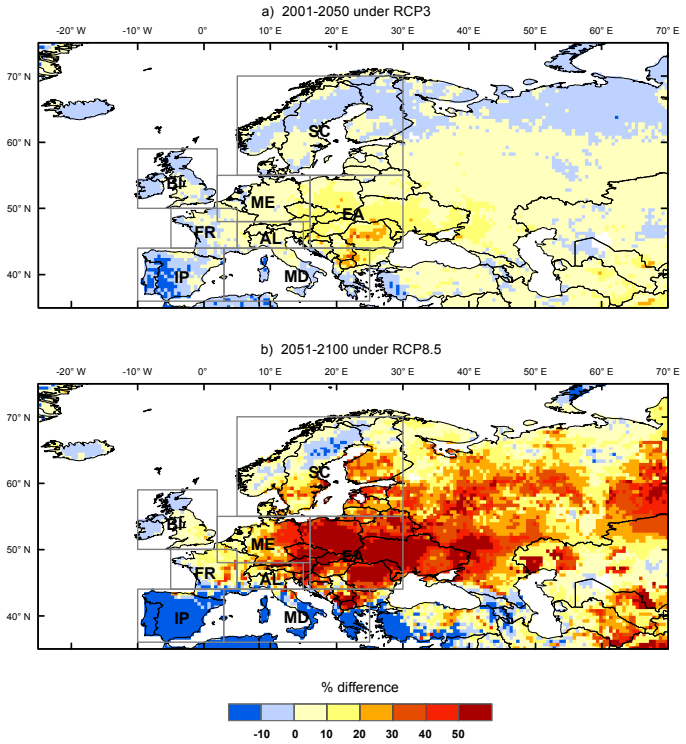

Figure 7.8: Percentage difference of ε_{ppt}-estimated runoff from Mac-PDM.09-simulated runoff, based on ECHAM5.

discussed in Section 7.4.1. The control experiment yields larger reductions across 45–55°N as the anticipated higher PET is accounted for in Mac-PDM.09 but not in the elasticity results. Reductions of 30–50% in southeastern Europe are slightly more common in simulated than estimated changes, suggesting the importance of PET; other potential explanations include elasticity estimates based on present-day values, or the elasticity concept itself, may be inappropriate for deriving long-term changes. For southwestern IP, however, reductions of this magnitude are more widespread in estimated than simulated results. Larger magnitudes of change occur in 2051–2100 under RCP8.5, with both approaches indicating 2051–2100 runoff to be $>$10% higher than 1951–2000 mean in areas north of 60°N, and $>$30% lower south of 45°N. Reductions of $>$70% are common around the Mediterranean basin, particularly in the elasticity-based estimates.

Overall, simulated trends tend to be more negative than elasticity-estimated changes. ε_{ppt} values only consider precipitation and not temperature/PET effects, therefore they may overestimate runoff by excluding losses from increased PET, which reduces (enhances) the magnitude of simulated runoff increase (reduction) notably in the high- (mid-) latitudes. This is reflected in Figure 7.8, which shows the discrepancies between estimated

and simulated 21st century runoff based on ECHAM5; discrepancy is considerable under the largest warming scenario. Exceptions include the relatively unaffected northwestern study region due to lower PET, and around the Mediterranean basin where estimated runoff is lower than simulated.

In the lower latitudes, PET is expected to increase with climate change, thus the runoff simulated by Mac-PDM.09 during the control experiment, for which changes in PET are allowed, is expected to be lower (greater reduction) than values estimated only from precipitation change; it is worth noting that it is AET, rather than PET, that determines the runoff. However, consistent with the Department of Water (2010) report and Chiew (2006), contrasting trends are found around the Mediterranean basin, which coincides with some of the highest elasticity values. On an annual basis, Department of Water (2010) found estimated reductions up to 28% larger than the modelled changes. According to Chiew (2006), which found a reasonable agreement between ε_{ppt} estimated by Equation 7.3 and a rainfall-runoff model, their model-simulated values tended to be larger in catchments with low runoff coefficients. Chiew (2006) related this to the highly non-linear rainfall-runoff relationship in ephemeral catchments with low runoff coefficients, and that the use of the median value in Equation 7.3 excluded the occasional high runoff values. Such attribution may partially explain the lower estimated runoff (larger reductions) around the Mediterranean basin found here.

Another possible explanation is associated with the use of elasticity as a factor for runoff change — given the very low 1951–2000 runoff values, upon which elasticity estimation and subsequent runoff computation are based, even a large multiplier (i.e. elasticity) might not produce large runoff values.

7.4.2.2 "Constant-Temperature" Runoff Comparison

Figure 7.9 illustrates the changes in runoff under the constant-temperature experiment. Compared to the control experiment trends (Figure 7.7), changes are considerably more positive (smaller reductions or greater increases), particularly under RCP8.5, due to higher precipitation as PET does not increase with the use of present-day temperature, hence there is no increase in PET-induced runoff loss.

Even under the smaller warming scenario (Figure 7.9a), $>$30% runoff increase is

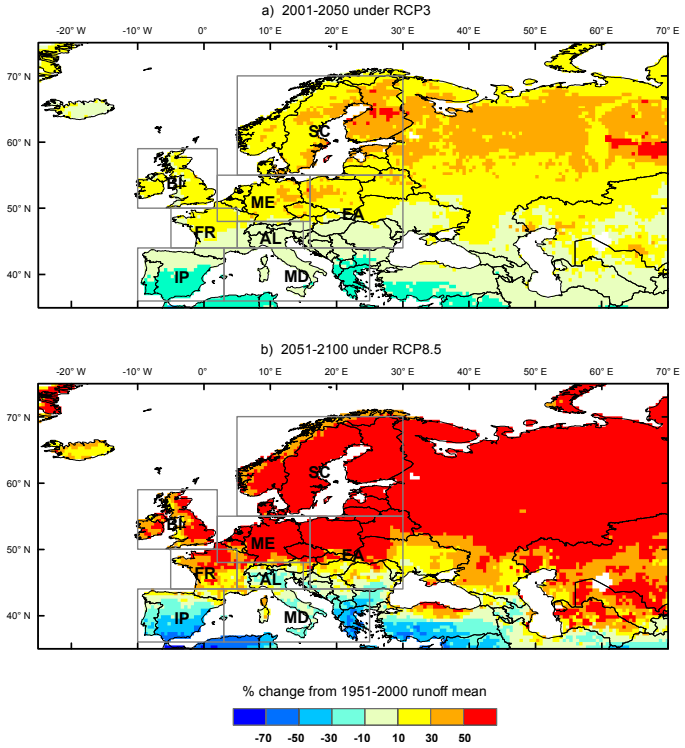

Figure 7.9: Changes in Mac-PDM.09-simulated runoff with present-day temperature, from 1951–2000 mean, based on ECHAM5.

widespread in areas north of 60°N and in parts of central/eastern Europe — these trends are comparable to the ε_{ppt}-estimated 2051–2100 trends under the larger warming RCP8.5 scenario (Figure 7.6b). Absolute constant-temperature runoff (not shown) is typically 20% higher than estimated runoff, and 20–40% higher in the band stretching from western IP, FR, ME, northwestern EA to eastern SC and northern Russia. Discrepancies between ε_{ppt}-estimated runoff and constant-temperature runoff are therefore larger than with the control results.

7.4.2.3 Elasticity vs. Simulated Runoff

The discrepancy between Mac-PDM.09-simulated and ε_{ppt}-estimated runoff was studied further by examining two cells of the study region based on the difference between the 50-year averages of the annual mean runoff in 2051–2100 under RCP8.5 derived from two experiments: one simulated using Mac-PDM.09 (blue solid symbols in Figure 7.10) and the other, estimated using elasticity approach (orange solid symbols in Figure 7.10).

For the "well-performing" cell (centred at 38.75°N,−1.25°E, eastern Spain), both experiments indicate, with a future reduction in precipitation, a decrease in future annual

mean runoff, with a relatively small difference (by 10.9%) between the two values. For the "poorly-performing" cell (centred at 57.75°N,67.25°E, eastern Russia), with a future increase in precipitation, the ε_{ppt}-estimated runoff changes by $+33.4\%$ while the Mac-PDM.09-simulated runoff shows a -12.8% change, suggesting the influence of PET on the direction of change.

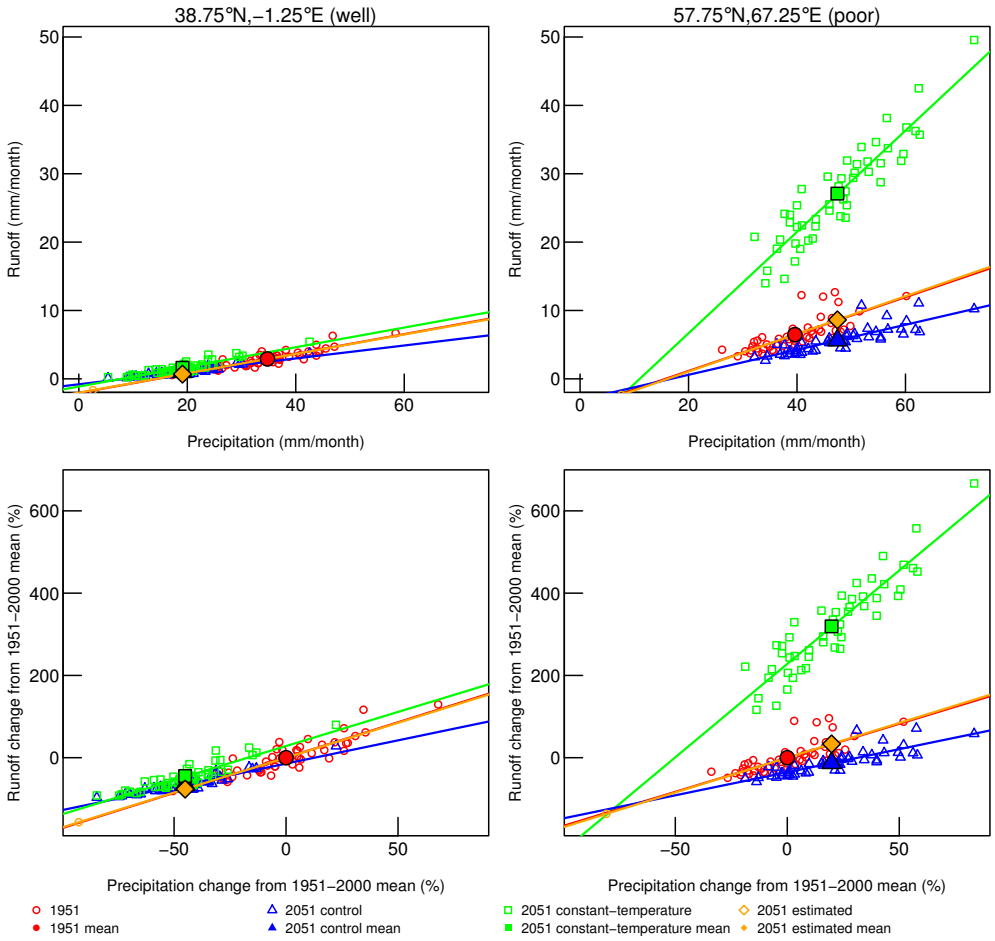

Figure 7.10: Annual (Oct-Sep) mean precipitation plotted against runoff for 1951–2000 (indicated as "1951"; red) and 2051–2100 (indicated as "2051"; projected by ECHAM5 under the RCP8.5) for a well-performing (left) and a poorly-performed (right) cell. Future runoff values are from the control (blue) and constant-temperature (green) experiments, as well as those estimated using ε_{ppt} (orange). Linear regressions based on the present-day values and these experiments, along with their respective 50-year averages (solid symbols), are also shown. Only the 50-year mean is estimated using ε_{ppt} (orange). Top (bottom) panels present the absolute values (relative changes).

Figure 7.10 shows the hydrological-year annual mean precipitation plotted against runoff for both 1951–2000 (indicated as "1951" in the key; see Section 7.2.3 for the datasets used) and 2051–2100 (indicated as "2051"). The 21st-century runoff values projected by ECHAM5 under the RCP8.5 scenario were from the three experiments: (1) control (indicated as "control"; see the beginning of this Section); (2) constant-temperature

(indicated as "constant-temperature"); and, (3) ε_{ppt} (indicated as "estimated"; see Section 7.4.1). The left (right) panels present values for the well-performing (poorly-performed) cell. The top panels show the absolute precipitation and runoff values; the bottom panels show their percentage changes relative to the 1951–2000 values. Also shown are linear regressions based on their respective annual means for both the 1951–2000 and the three future experiments, along with their 50-year averages (indicated as "1951 mean" and "2051 mean", respectively). It is worth noting that neither precipitation nor runoff can be negative; the top left panel of Figure 7.10 suggests that for that particular cell, precipitation of around 10 mm/month or lower implies zero runoff using the elasticity relationship.

Figure 7.10 reveals that both cells show almost identical linear regressions based on 1951–2000 (red) and ε_{ppt}-estimated (orange) runoff. This demonstrates that both simple linear regression derived from present-day precipitation and runoff values and Equation 7.3 would give similar estimates of the sensitivity of runoff to precipitation changes, given that ε_{ppt} are based on the median ratios of present-day precipitation and runoff deviations. The more apparent distinction between the values from the control (blue) and constant-temperature (green) experiments implies the larger role of PET in the poorly-performing cell, which has a larger mean PET increase of $+48.7\%$ (compared to $+30.7\%$ for the well-performing cell).

Outliers (e.g. high runoff values) are more likely to affect simulated than ε_{ppt}-estimated results. Despite the more diverging mean estimated, simulated and constant-temperature runoff in the poorly-performed cell, both cells have very similar ε_{ppt} — 1.70 (well-performed) and 1.69 (poorly-performed). If precipitation declines by 50% in both cells, the "poorly-performed" cell in Figure 7.10 may actually have a smaller discrepancy between the estimated (orange) and simulated (blue) runoff — results may differ since the regression lines for this cell were fitted to a wetter, rather than a drier, scenario.

In summary, effects of outliers in the simulated output, the direction and magnitude of precipitation change all determine the capability of ε_{ppt} in reproducing mean Mac-PDM.09-simulated runoff.

7.5 Conclusions

This chapter has examined the sensitivity of runoff to precipitation and PET changes for the European study region by assessing the elasticity of runoff to climatic factors. Elasticity was computed with a non-parametric estimator, Equation 7.3 (Sankarasubramanian *et al.*, 2001), using 1951–2000 monthly timeseries of CRU TS 3.0 precipitation, and MacPDM.09-simulated PET and runoff.

Across much of the study region, small climate perturbations produce much larger runoff changes: a 1% precipitation increase yields $+1.0\%$ to $+2.5\%$ runoff change, whereas a 1% PET increase yields -8% to $+2\%$ runoff change. In agreement with Fu *et al.* (2011), elasticities based on means over the hydrological, rather than calendar, year were considered more appropriate. Positive ε_{PET} (e.g. in western Iberian Peninsula and Poland), also reported by New (2002) for South African catchments, suggests increasing runoff in years with positive PET anomalies due to a larger relative increase in precipitation than PET, hence the effect of the positive precipitation anomaly counteracts that of the PET. Although ε_{PET} values are larger than ε_{ppt}, ε_{ppt} is considered more important as precipitation change is primarily responsible for runoff variations, except perhaps in snow-dominated regions where temperature deviations can affect the seasonal distribution of runoff (which is not considered here). Nevertheless, regional elasticities provide some indication of the importance of PET in the Mediterranean, Black Sea and Caspian Sea regions. The sensitivity criteria adopted by Weiss and Alcamo (2011) also highlight the importance of evapotranspiration in the water balance of southern European basins that may dampen the effects of increasing precipitation.

As demonstrated in Section 7.3.2 and in agreement with other studies, ε_{ppt} is roughly equivalent to the inverse of the runoff ratio; lower- (higher-) latitude runoff are more (less) sensitive to precipitation perturbations.

Using WaterGAP, Weiss and Alcamo (2011) assessed the sensitivity of water availability and vulnerability of eighteen European river basins to climate change based on six RCMs under SRES A1B. They found sensitivity to climate change increases with latitude as warming-induced earlier snowmelt de-stabilises Nordic flow regime (see Section 2.5). This contradiction with results presented here arises from the different methodologies: in

Weiss and Alcamo (2011), the number of days below freezing, the degree of water limitation of evapotranspiration, and the degree of change in the timing and magnitude of future temperature and precipitation, and their combined effects, determine the overall sensitivity of a basin; the present study has used Mac-PDM.09 outputs to assess runoff sensitivity specifically in relation to annual precipitation or PET variations, which excludes sensitivity in runoff timing that is important in snow-dominated regions (Jeton *et al.*, 1996).

Areas with lower runoff responses, $\varepsilon_{ppt}<1.5$, under present-day climates may experience some of the largest increases (by $\approx$20%) in sensitivity under 21st-century climates, while areas with high elasticity ($\varepsilon_{ppt}<2.0$) may see the reverse, thus reducing the range of elasticity as climate changes. This occurs as warming increases the proportion of rainfall compared to snowfall (positive trends) in the northern latitudes and increases the influence of PET in Iberian Peninsula (negative trends).

Since the non-parametric estimator, Equation 7.3, could be useful for estimating runoff under future climates, this study has attempted to validate ε_{ppt}-estimated runoff against Mac-PDM.09-simulated values.

For the climate change scenarios examined, the ability of ε_{ppt} in reproducing Mac-PDM.09 simulations decreases with time/increasing climate change, thus the index's performance deteriorates under larger temperature changes (Fu *et al.*, 2007b). Under the smaller climate change scenario, runoff generated with ε_{ppt} and Mac-PDM.09 generally differs slightly ($\pm$10%) across the study region; both indicate increases (reductions by 10–30%) in high latitudes (south of 50°N). ε_{ppt}, which excludes temperature/PET changes, overestimates runoff in central/eastern and southeastern Europe. This suggests the role of PET in these regions, or the application of ε_{ppt} may be inappropriate for longer-term changes. In western Iberian Peninsula and parts of the Mediterranean, larger runoff decline (30–50%) is more common in estimated than simulated cases despite increasing PET. This is due to the combination of the use of median value of Equation 7.3 (Chiew, 2006), and the low 1951–2000 runoff values. The negative ε_{ppt}-estimated runoff also contributes to the larger estimated reductions. Although these negative values, which occur if climate variations and/or sensitivity exceeds some threshold levels, could simply be replaced by zeros, Equation 7.3 should be applied cautiously especially in areas with large precipitation decrease and/or high ε_{ppt} values.

Under the highest warming scenario examined, small discrepancies ($\pm$10%) are restricted to the British Isles and northwestern parts of the high-latitudes, suggesting that for these regions, runoff estimation is less sensitive to the choice of ε_{ppt} or Mac-PDM.09 approach, or the magnitude of climate change. Estimated runoff is $>$30% larger than model output in the region extending eastwards from Germany to Russia and parts of Central Asia, and 10–60% lower around the Mediterranean basin, thus results in these regions are more sensitive to the estimation approach used.

The elasticity of runoff such as ε_{ppt} is shown to produce mean annual runoff estimates comparable to complex hydrological model Mac-PDM.09 for large parts of the European study region, except for the Mediterranean regions, eastern and southeastern Europe. However, this is expected to a certain degree, as the function is derived from the Mac-PDM.09-simulated runoff for 1951–2000. In agreement with Chiew *et al.* (2006) and Department of Water (2010), this study concludes that ε_{ppt} is particularly useful for estimate runoff changes in large-scale or scoping studies given the relatively simple data requirement (i.e. historic precipitation and runoff data), and the complication of selecting and calibrating of hydrological model(s) such that many of the associated uncertainties are avoided. However, the capability of ε_{ppt} in reproducing mean Mac-PDM.09-simulated runoff diminishes with seasonal results as found in Department of Water (2010), increasing climate change, and is influenced by effects of outliers in simulated output, direction and magnitude of precipitation change. Therefore, it may be more appropriate to use physical models to assess future runoff changes, especially for regions and/or timescales where larger climate change is anticipated (e.g. southern Europe).

7.5.1 Limitations

This study has a number of caveats. Limitations of Equation 7.3-related are outlined in Section 7.2.2. Results here are based on a 50-year period; using another timeframe may produce different results (Fu *et al.*, 2011), although the magnitude of discrepancy is subject to further investigation. Also, the future runoff sensitivity was based on ECHAM5, thus simulations using another GCM may generate different results. The approach of deriving the elasticity values using present-day Mac-PDM.09 output and subsequently assessing the performance against Mac-PDM.09 simulations for the 21st-century will likely

give an upper bound on the performance; using observed runoff to compute the elasticity values and then testing the performance against Mac-PDM.09 (or other hydrological models) may indicate lower performance. Moreover, ε_{ppt}-estimated runoff has only been validated against Mac-PDM.09 output; performance of the estimator may or may not vary with a different hydrological model.

Runoff sensitivity has been estimated with a one-parameter estimator (i.e. the factor is being considered in isolation), and only long-term precipitation/runoff changes have been considered here. However, runoff fluctuations are not merely a function of precipitation and runoff, which may interact with other natural or human factors. Temperature changes, for instance, could amplify or suppress runoff variations (Fu *et al.*, 2007b), such as in snowmelt-dominated regions (Wilson *et al.*, 2010; Wong *et al.*, 2011). Nonetheless, results here are considered less affected by this due to the use of annual averages.

There are also interactions between the climate, vegetation, soil and hydrological processes (Liu and Cui, 2011). El Niño/La Niña climatic variability (Fu *et al.*, 2007c) and catchment characteristics (Renner and Bernhofer, 2012; Liang and Liu, 2013), particularly at monthly scales (Arnell, 1992), further complicate magnitudes and patterns of streamflow response to climatic changes. In the Upper Loire basin, France, although an annual precipitation increase (decrease) of $\sim$10% increases discharge by $\sim$10–20% (20–40%) annually, the discharge amount per unit area, dry and wet periods (with the former effect being larger) also affects the magnitude of change (van der Wateren-de Hoog, 1995). At basin scale, altitude (consequently, average temperature) might be important (Jeton *et al.*, 1996). Nevertheless, direct and indirect human activities may be the predominant factor, as in the Chinese Miyun Reservoir Basin (Liu *et al.*, 2012) and the Ethiopian Meki Basin (Legesse *et al.*, 2010); land-use change and abstractions in headwaters of Yellow River Basin accounted for $>$70% of the streamflow reduction in the 1990s (Zheng *et al.*, 2009).

While precipitation is important in determining runoff sensitivity, its interaction with other influences (natural or human) should also be considered, depending on the study aims. For instance, Liu *et al.* (2012) assessed streamflow sensitivity to aridity index, which accounts for both precipitation and PET, for two Chinese basins. In addition, trends of sensitivity of water availability and vulnerability (which considers the system's response) may be different (Weiss and Alcamo, 2011). In practice, besides the chosen

criteria, advancing technologies or economies may alter vulnerability thresholds, thereby changing the sensitivity of a basin. Therefore, it is important to have clearly defined study objectives when assessing the sensitivity of runoff or a basin water availability to account for the major (including local) contributing factors.

The next chapter highlights the main results, their policy implications and knowledge gaps.

Chapter 8

Summary and Outlook

This thesis aimed to examine the effects of climate change on European drought characteristics, as well as the associated uncertainties in the methodologies for drought quantification and climate change projection, through a multi-scenario and multi-model approach. In this study, droughts are characterised by drought severity, and their spatial extent are quantified using the Drought Area Index (DAI) — the frequencies of DAI25 and DAI50 denote the percentage of the 50-year period during which $\geq$25% and $\geq$50% of the region is drought-affected, respectively. This chapter highlights the main results, their policy implications and knowledge gaps.

This thesis builds on existing literature by systematically analysing some of the uncertainties in drought projections under a changing climate. As discussed in Section 1.1, few studies have examined the climate-change-induced changes in drought using a large ensemble of simulations; the meteorological drought analysis in Chapter 4 is based on simulations projected by ten emission scenarios and 18 general circulation models (GCMs). Also, the uncertainties associated with the definitional issues of drought have not been well studied; these are presented in Chapter 5. There is limited literature covering the effects of changes in interannual precipitation variability on future drought variations; this is explored in Chapter 6. Furthermore, few studies have examined the runoff sensitivity to climatic changes especially for Europe, and the applicability of such an approach for estimating runoff under a perturbed climate has barely been explored. These are assessed in Chapter 7.

8.1 Key Findings

Across much of the European study region, climate change is projected to increase drought severity and frequencies of DAI25 and DAI50, with reductions in these drought parameters in the high-latitudes (Scandinavia and Russia), especially in winter and spring but in some cases, also in summer/autumn (see Chapters 4 and 5). These results are consistent with the general simulated trends of wetting in the northern Europe, as well as the drying and increasing drought conditions projected for the lower latitudes, despite of the different definitions of dryness/drought applied. For both meteorological and hydrological droughts, the northern and southern latitudes of the study region tend to have the largest magnitudes of change. Marked increases in both 3-month and 12-month drought severity and frequency of DAI25 events (by 2–3 times in 2001–2050, and up to 10-fold in 2051–2100) are simulated for the Mediterranean and Middle East/Central Asia regions. Contrasting sub-regional variations can lead to small or unclear overall signs of regional-mean change (e.g. for the British Isles, with drought conditions decreasing in the north and worsening in the south).

Results obtained in both Chapters 4 and 5 indicate that the projected changes in all the meteorological and hydrological drought parameters vary substantially depending on the GCM, emission scenario, region and season. Agreement on the direction of change is generally higher: (1) in both high and lower latitudes; (2) in 2051–2100 than in 2001–2050; (3) with robust increases (decreases) in drought tending to occur in summer and autumn (winter and spring). Despite consensus in the sign of change for some regions (e.g. the Mediterranean regions often have robust and marked increases in drought conditions in summer and autumn), their magnitudes are highly uncertain — such uncertainties tend to increase with time and with magnitude of warming. Results averaged across Köppen climate zones demonstrate more robust trends, better reflecting climate change signals, than geographically-averaged results.

Uncertainties have differential impacts on different drought parameters, affecting the frequency of widespread drought, more than total severity (see Chapters 4 and 5). Although the influence of different emission scenarios becomes more important post-2050, GCM variance dominates regardless of the region, season, future period, timescale, drought

parameter studied (see Section 4.6), as commonly found in the literature. Different definitions of drought — including the choice of threshold that identifies drought condition from "normal" climate, the definition of when a drought terminates and drought classification — can result in contrasting trends, and this behaviour is common in winter/spring, particularly in regions affected by snow and snowmelt (see Chapter 5). For instance, in spring, the Alps could experience increasing meteorological drought conditions (due to reduced precipitation) but reductions in hydrological droughts (with earlier snowmelt). Different drought classifications and their effects also lead to opposing changes in summer/autmn in Scandinavia. Nevertheless, results according to both meteorological and hydrological drought definitions generally indicate the same direction of change, but hydrological results tend to produce more positive changes in drought conditions and also with larger magnitudes than meteorological ones (see Section 5.8).

Drought parameters derived from MacPDM.09 were found to be highly sensitive to potential evapotranspiration (PET); different results are therefore likely with a different PET calculation method (see Section 5.8.7). Higher PET generally implies more drought conditions in absolute terms, with larger increases. Winter and 12-month droughts in Scandinavia and British Isles (in 2001–2050) were projected to decrease regardless of PET changes, but higher PET implies smaller reduction. Higher PET also reduced winter droughts in Scandinavia and the Alps due to increased melting of frozen precipitation. In the Norwegian Arctic (Svalbard region), although measured annual precipitation has increased in recent decades, the fraction of annual precipitation falling as snow has decreased (Forland and Hanssen-Bauer, 2003), due to the more efficient rainfall processes compared to snow falling. This suggests that as the climate warms, more rainfall may occur with more frequent and intense events and extremes (Kjellström, 2004; Frei *et al.*, 2006; Buonomo *et al.*, 2007; Alcamo *et al.*, 2007b; Giorgi and Coppola, 2009).

Perturbations to the interannual variability of precipitation due to climate change tends to (1) enhance drought conditions, particularly in Mid-Europe and Eastern Europe, (2) moderate reductions in drought conditions (Scandinavia), or (3) reverse reductions in drought conditions (e.g. meteorological results for British Isles and Mid-Europe); these effects are more apparent in meteorological than hydrological drought results (see Chapter

6). Therefore, studies that do not consider changes in precipitation variability may underestimate (or in a few cases, over-estimate) drought conditions, or may yield opposite trends to those that take into account both perturbed mean and variability. A drought-free area (e.g. parts of the northern latitudes) according to changes in mean precipitation only may become drought-affected when modified variability is considered.

Although variations in interannual variability of precipitation plays a role in altering drought characteristics, the predominant driver is mean precipitation changes. Therefore, the long-term mean sensitivity of runoff to precipitation and PET changes across the European study region was studied by assessing the elasticity of runoff to climatic factors using a non-parametric estimator ε (see Chapter 7). A 1% precipitation increase is found to yield a $+1.0\%$ to $+2.5\%$ runoff change. Although the PET elasticity of runoff ε_{PET} was also studied, the precipitation elasticity of runoff ε_{ppt} was considered more important in causing runoff variations, except perhaps in snow-dominated regions where temperature deviations can affect the seasonal distribution of runoff. ε_{ppt} is roughly equivalent to the inverse of the runoff ratio; lower- (higher-) latitude runoff are more (less) sensitive to precipitation perturbations. Areas with lower runoff responses, $\varepsilon_{ppt}<1.5$, under present-day climates may experience some of the largest increases (by $\approx$20%) in sensitivity under 21st-century climates, while areas with high elasticity ($\varepsilon_{ppt}<2.0$) may see the reverse, thus reducing the range of elasticity values as climate changes. This occurs as warming increases the proportion of rainfall compared to snowfall (positive trends) in the northern latitudes and increases the influence of temperature in Iberian Peninsula (negative trends). The performance of ε_{ppt} in reproducing Mac-PDM.09 runoff simulations deteriorates with time/increasing climate change. Therefore, it may be more appropriate to use physical models to assess future runoff changes, especially for regions and/or timescales where larger climate change is anticipated (e.g. southern Europe).

8.2 Policy Implications

This study seeks to develop an improved understanding of potential changes in drought under future climates, which could facilitate the development and implementation of more effective drought management and climate change adaptation measures.

The diverse meteorological and hydrological drought response to climate change simulated in this study implies that findings based on a single scenario/model could be highly misleading. Substantial research and considerable improvements in climate models are needed before climate projections can be applied directly and effectively in adaptation planning and design, e.g. water management (Kundzewicz and Stakhiv, 2010), as suggested by the range of projected changes in drought characteristics found in this thesis. Uncertainties in climate change projections or the risk information supplied to decision-makers are unlikely to decrease in the near future (Knutti, 2008; Todd *et al.*, 2011). Even with a perfect climate model, future changes in non-climatic pressures such as demographic and economic development, natural forcings (solar and volcanic activity), and natural internal variability mean that climate change and hydrological projections would remain highly uncertain, especially at the regional scale (Wilby, 2010). Therefore, policy-relevant research on climate change impacts and robust adaptation decisions should be based on a multi-scenario and multi-model approach; they also need to consider a wide range of expressions of modeling uncertainty (Burke and Brown, 2008; Hawkins and Sutton, 2010), or risk-based information (e.g. by considering frequency distributions of climate change impacts) rather than deterministic information (Gosling *et al.*, 2011a).

Although the degree of uncertainty in future projections of river flow, for example, may create challenges in the development of appropriate adaptation measures (Todd *et al.*, 2011), many organisations have experience in working in the face of various kinds of uncertainty (Stainforth *et al.*, 2007a). Over-interpretation and over-confidence in the results could undermine the credibility of climate science to inform policy (Stainforth *et al.*, 2007a; Knutti, 2008); information can be misleading if the climate projections, their uncertainties and caveats are not adequately quantified and communicated (Valle *et al.*, 2009) — e.g. probability density functions (PDFs) may provide a false sense of security (Parker, 2010b); the end-user may assume that the newest models provide the best information, and that the model spread provides some estimate of uncertainty (Knutti, 2008).

Despite the limitations, climate models simulate numerous processes and feedbacks; large ensembles, as applied in this study, enhance our understanding of the range of possible model behaviour in response to different emission scenarios (Stainforth *et al.*, 2007b).

They can also help to identify the areas where results depend strongly on model assumptions, thus provide guidance for future model development (Knutti, 2008). Much resource has been allocated to climate research and model development, such as the variables and spatial/temporal scales of interest, but these should be shaped by the needs of the end-users and policy-makers if the goal is to benefit society (Knutti, 2008). More emphasis is needed on extracting the data and information that is decision- and policy-relevant, and to explore how to make the best use of the model results so that they add value to decision making (Knutti, 2008), e.g. by working with stakeholders and to provide guidance on how to use/interprete the data and information. Each simulation presents a "what-if" scenario; appropriate interpretation and accurate communication of such information and uncertainties, even in qualitative terms, is therefore crucial and can have substantial value in the design of robust adaptation strategies that reduce vulnerability to both climate variability and change (Pappenberger and Beven, 2006; Stainforth *et al.*, 2007a;b).

8.3 Limitations and Further Work

Specific limitations and areas for further research are presented in the relevant chapters. This subsection outlines some of the limitations of the study approach adopted in this thesis and provides some general directions for future work.

Analysis in this thesis has focused on relative drought. Given that drought is a phenomenon relative to the local conditions that can occur in virtually all climate regimes, including in cold regions (van Lanen *et al.*, 2007; Vidal and Wade, 2009), it needs to be considered in a relative, rather than an absolute, sense (Mpelasoka *et al.*, 2008). Nevertheless, the application of a fixed absolute drought threshold (say, 20 mm of precipitation) for the entire study region would allow the identification of the more "drought-prone" areas (e.g. the Mediterranean regions are more likely to suffer from drought than the higher latitudes). Therefore, an absolute drought analysis could provide useful information for large-scale management practices and could aid resource allocation. Also, the projected changes in drought characteristics presented here, as well as the SPI computation, are based on the reference period of 1951–2000; the choice of another baseline (e.g. 1961–1990) could lead to different results.

A caveat of this study is the separate characterisation of drought severity and spatial

extent. This could be improved in future work by assessing the spatio-temporal characteristics of droughts simultaneously through a severity–area–duration analysis, which relates the area of each drought to its severity (Andreadis *et al.*, 2005; Sheffield *et al.*, 2009). Alternatively, Perez *et al.* (2011) presented two methodologies (non-contiguous and contiguous drought area analyses) for analysing the spatio-temporal development and characteristics of large-scale hydrological droughts using gridded timeseries of hydrometeorological data.

In this thesis, future changes in drought characteristics have been assessed on a continental scale and from the natural science perspective, i.e. the societal aspects have not been examined. This study could therefore be extended to investigate the effects of climate change in relation to specific impact sectors such as agriculture, using locally appropriate drought indices (Burke and Brown, 2008) such as those covered in Section 2.2. Such analysis may need to be carried out on a local or regional scale (e.g. for specific basin(s)), with the aid of higher resolution models that have better representation of topography (Redaud *et al.*, 2002; Räisänen *et al.*, 2004; Gao *et al.*, 2006); processes and practices that are often excluded from the climate models (e.g. irrigation) may also need to be considered. The application of multiple hydrological/impact models may also provide an indication of another dimension of uncertainty (Haddeland *et al.*, 2011).

Some of the analyses presented in this thesis have only been carried out using geographically-averaged results based on the sub-regions of the PRUDENCE project. Yet, findings presented here suggest that results averaged climatically according to the Köppen climate classification may better reflect the climate change signal. Therefore, regional analyses based on climatic conditions could be an interesting area of study.

Although this thesis has explored the effects of several sources of uncertainty on drought projections under future climates, results obtained here under-represent the true uncertainty as other sources of uncertainty have not been examined. For example, meteorological droughts have only been represented by the precipitation-only Standardised Precipitation Index (SPI); the application of another meteorological drought index may produce different results.

An initial study indicated that carbon cycle models represented less than 5% of total variance that also encompassed GCM and emission scenario uncertainties. However, this

source of uncertainty has been estimated to be ∼40% of that of the physical climate properties (e.g. equilibrium climate sensitivity and global heat capacity; Huntingford *et al.*, 2009), thus could be explored further in the meteorological and hydrological drought analyses.

The application of ClimGen has generated gridded outputs at 0.5° resolution, hence downscaling uncertainty has not been investigated in this thesis. Hence, results presented in this thesis could be compared to those based on regional climate change simulations such as the CORDEX (Coordinated Regional Climate Downscaling Experiment) initiative from the World Climate Research Program (http://www.meteo.unican.es/en/projects/CORDEX).

Several sources of uncertainty associated with hydrological modelling have not been studied in this thesis. These include suppressed plant transpiration due to CO_2-induced stomatal closure (which could increase runoff) (Gedney *et al.*, 2006), which implies an underestimation of future increases in runoff and an overestimation of decreases — Betts *et al.* (2007) found that a CO_2 doubling on plant transpiration increases simulated global mean runoff by 6% relative to pre-industrial levels. In addition, modified land-atmosphere feedbacks may influence climate change (e.g. precipitation variability in central-eastern Europe; Räisänen *et al.*, 2004; Rowell and Jones, 2006; Seneviratne *et al.*, 2006; van Lanen *et al.*, 2007; Kyselý *et al.*, 2010). Mechanisms of feedbacks between convection, radiation and surface fluxes, for instance, are not well identified and may vary among models (Planton *et al.*, 2008). Also, these may not be represented in hydrological models, thus contributes to another source of uncertainty. Furthermore, the representation of evapotranspiration, snow accumulation and melt, storage and the parametrisation of storage processes (e.g. land and aquifer characteristics) are important aspects in hydrological modelling (Van Loon *et al.*, 2012) that have not been explored in this thesis.

Drought analyses carried out here have been based on the monthly precipitation and runoff timeseries. However, the daily resolution is important in operational monitoring of drought development and decision-making in agriculture and water resource management (Lu, 2011), especially on a local or regional scale, as a drought-affected region may return to normal condition with only one day of intense rainfall. The consideration of hydrological variables at the daily time step would also be more suitable for detailed monitoring of drought development and propagation in the subsurface components of the hydrological

cycle. Droughts can be quantified on a daily time scale using the Effective Drought Index (EDI; Byun and Wilhite, 1999), for instance. The EDI is a standardised index that calculates daily water accumulation with a weighting function of time passage using daily rain and snowfall data from timeseries of 30 years or more. Alternatively, a daily SPI has been developed to overcome the difficulties with the standard SPI using only monthly values (Wanders *et al.*, 2010). SPI values are calculated for each day separately based on a moving monthly time frame (i.e. 30-day backwards moving average), using the parameters α and β that are estimated for each day are based on the previous 30 days. Downscaling or generating rainfall or runoff at the daily time step may introduce another source of uncertainty though.

While the ability of land surface models (LSMs) and/or global hydrological models (GHMs) in reproducing large-scale historic runoff, hydrological extremes and other variables have been assessed in several studies (e.g. Haddeland *et al.*, 2011; Prudhomme *et al.*, 2011; Gudmundsson *et al.*, 2012b; Van Loon *et al.*, 2012), few climate change impact studies based on multiple impact models exist. Since only Mac-PDM.09 has been applied in this thesis, similar to Hagemann *et al.* (2012), the effects of different GHMs on projected changes in drought characteristics could be further investigated.

Another area of further research could be to compare the hydrological drought results to those derived from the Palmer Drought Severity Index (PDSI), as well as the standardised precipitation evapotranspiration index (SPEI), for instance, as both of these methods account for temperature effects. Moreover, both meteorological and hydrological drought events have been defined based on the threshold of SPI-1.5; this study could be extended by studying the changes in drought for a more extreme SPI category (e.g. SPI-2.0) and compare with the results obtained here.

In addition to the scientific/technical element of drought analysis, it is equally, if not more, important to develop efficient linkages with practitioners engaged in drought monitoring, forecasting and management operations, as well as the policy domain (Panu and Sharma, 2002; Kampragoua *et al.*, 2011), as discussed in Section 8.2. Given that the uncertainties associated with future drought projections are unlikely to be constrained in the near term, it is worth exploring how the findings in this study could contribute to the development and implementation of drought risk assessment and management practices, as

well as societal vulnerability assessments, to reduce the adverse impacts of droughts under a changing climate. Working closely with stakeholders, such as policymakers, water resource managers and others, would help to determine how this study could be further developed to address the drought/water resource issues within an integrated framework, based on their needs.

References

Abbaspour, K., M. Faramarzi, S. Ghasemi, and H. Yang (2009), Assessing the impact of climate change on water resources in Iran, *Water Resources Research*, *45*(10), W10,434.

Abramowitz, M., and I. Stegun (eds) (1965), *Handbook of Mathematical Functions with Formulas, Graphs, and Mathematical Tables*, Dover Publications, New York.

Adam, J., A. Hamlet, and D. Lettenmaier (2009), Implications of global climate change for snowmelt hydrology in the twenty-first century, *Hydrological Processes*, *23*(7), 962–972.

Agaltseva, N., M. Bolgov, T. Spektorman, M. Trubetskova, and V. Chub (2011), Estimating hydrological characteristics in the Amu Darya River basin under climate change conditions, *Russian Meteorology and Hydrology*, *36*(10), 681–689.

Alcamo, J., N. Dronin, M. Endejan, G. Golubev, and A. Kirilenko (2007a), A new assessment of climate change impacts on food production shortfalls and water availability in Russia, *Global Environmental Change*, *17*(3-4), 429–444.

Alcamo, J., M. Flörke, and M. Märker (2007b), Future long-term changes in global water resources driven by socio-economic and climatic changes, *Hydrological Sciences Journal*, *52*(2), 247–275.

Alexander, L., and J. Arblaster (2009), Assessing trends in observed and modelled climate extremes over Australia in relation to future projections, *International Journal of Climatology*, *29*(3), 417–435.

Alexander, L., X. Zhang, T. Peterson, J. Caesar, B. Gleason, A. Klein Tank, M. Haylock, D. Collins, B. Trewin, F. Rahimzadeh, A. Tagipour, K. Rupa Kumar, J. Revadekar, G. Griffiths, L. Vincent, D. Stephenson, J. Burn, E. Aguilar, M. Brunet, M. Taylor, M. New, P. Zhai, M. Rusticucci, and J. Vazquez-Aguirre (2006), Global observed changes in daily climate extremes of temperature and precipitation, *Journal of Geophysical Research*, *111*, D05,109.

Allen, C., A. Macalady, H. Chenchouni, D. Bachelet, N. McDowell, M. Vennetier, T. Kitzberger, A. Rigling, D. Breshears, E. T. Hogg, P. Gonzalez, R. Fensham, Z. Zhang, J. Castro, N. Demidova, J.-H. Lim, G. Allard, S. Running, A. Semerci, and N. Cobb (2010), A global overview of drought and heat-induced tree mortality reveals emerging climate change risks for forests, *Forest Ecology and Management*, *259*(4), 660–684.

Allen, M., and W. Ingram (2002), Constraints on future changes in climate and the hydrologic cycle, *Nature*, *419*(6903), 224–232.

Allen, R., M. Smith, A. Perrier, and L. Pereira (1994a), An update for the calculation of reference evapotranspiration, *ICID Bulletin*, *43*(2), 35–92.

Allen, R., M. Smith, A. Perrier, and L. Pereira (1994b), An update for the definition of reference evapotranspiration, *ICID Bulletin*, *43*, 1–34.

Alley, R., J. Marotzke, W. Nordhaus, J. Overpeck, D. Peteet, R. Pielke, R. Pierrehumbert, P. Rhines, T. Stocker, L. Talley, and J. Wallace (2003), Abrupt climate change, *Science*, *299*(5615), 2005–2010.

Alley, W. (1984), The Palmer Drought Severity Index: Limitations and Assumptions, *Journal of Climate and Applied Meteorology*, *23*(7), 1100–1109.

Alston, M., and J. Kent (2004), *Social Impacts of Drought: A report to NSW Agriculture*, Tech. rep., Centre for Rural Social Research, Charles Sturt University, Wagga Wagga.

AMS (2004), American Meteorological Society (AMS) Statement on meteorological drought, *Bulletin of the American Meteorological Society*, *85*, 771–773.

Andreadis, K., E. Clark, A. Wood, A. Hamlet, and D. Lettenmaier (2005), Twentieth-Century Drought in the Conterminous United States, *Journal of Hydrometeorology*, *6*(6), 985–1001.

Archer, S., and K. Predick (2008), Climate change and ecosystems of the Southwestern United States, *Rangelands*, *30*(3), 23–28.

Arnell, N. (1992), Factors controlling the effects of climate change on river flow regimes in a humid temperate environment, *Journal of Hydrology*, *132*(1-4), 321–342.

Arnell, N. (1999a), A simple water balance model for the simulation of streamflow over a large geographic domain, *Journal of Hydrology*, *217*(3-4), 314–335.

Arnell, N. (1999b), Climate change and global water resources, *Global Environmental Change*, *9*(Supplement 1), S31–S49.

Arnell, N. (1999c), The effect of climate change on hydrological regimes in Europe - a continental perspective, *Global Environmental Change*, *9*(1), 5–23.

Arnell, N. (2003a), Effects of IPCC SRES emissions scenarios on river runoff: a global perspective, *Hydrology and Earth System Sciences*, *7*(5), 619–641.

Arnell, N. (2003b), Relative effects of multi-decadal climatic variability and changes in the mean and variability of climate due to global warming: future streamflows in Britain, *Journal of Hydrology*, *270*(3-4), 195–213.

Arnell, N. (2004a), Climate change and global water resources: SRES emissions and socio-economic scenarios, *Global Environmental Change*, *14*(1), 31–52.

Arnell, N. (2006), Climate Change and Water Resources: A Global Perspective, in: *Avoiding Dangerous Climate Change* (Schellnhuber, J., W. Cramer, N. Nakicenovic, T. Wigley, and G. Yohe, eds.), chap. 17, p. 460, Cambridge University Press, Cambridge, UK.

Arnell, N. (2011), Uncertainty in the relationship between climate forcing and hydrological response in UK catchments, *Hydrology and Earth System Sciences*, *15*(3), 897–912.

Arnell, N. W. (2004b), Climate-change impacts on river flows in Britain: the UKCIPO2 scenarios, *Water and Environment Journal*, *18*(2), 112–117.

Barnett, T., J. Adam, and D. Lettenmaier (2005), Potential impacts of a warming climate on water availability in snow-dominated regions., *Nature*, *438*(7066), 303–309.

Bartolini, E., P. Claps, and P. D'Odorico (2009), Interannual variability of winter precipitation in the European Alps: relations with the North Atlantic Oscillation., *Hydrology and Earth System Sciences*, *13*(1), 17–25.

Bates, B., Z. Kundzewicz, S. Wu, and J. Palutikof (2008), *Climate Change and Water. Technical Paper of the Intergovernmental Panel on Climate Change*, Tech. rep., IPCC Secretariat, Geneva.

Beldring, S., T. Engen-Skaugen, E. Fø rland, and L. Roald (2008), Climate change impacts on hydrological processes in Norway based on two methods for transferring regional climate model results to meteorological station sites, *Tellus A*, *60*(3), 439–450.

Beniston, M. (2005), Mountain Climates and Climatic Change: An Overview of Processes Focusing on the European Alps, *Pure and Applied Geophysics*, *162*(8-9), 1587–1606.

Beniston, M., D. Stephenson, O. Christensen, C. Ferro, C. Frei, S. Goyette, K. Halsnaes, T. Holt, K. Jylhä, B. Koffi, J. Palutikof, R. Schöll, T. Semmler, and K. Woth (2007), Future extreme events in European climate: an exploration of regional climate model projections, *Climatic Change*, *81*(S1), 71–95.

Berger, J. (2006), The case for objective Bayesian analysis, *Bayesian Analysis*, *1*(3), 385–402.

Berger, J., V. De Oliveira, and B. Sansó (2001), Objective Bayesian Analysis of Spatially Correlated Data, *Journal of the American Statistical Association*, *96*(456), 1361–1374.

Bergman, K., P. Sabol, and D. Miskus (1988), Experimental indices for monitoring global drought conditions, in: *13th Annual Climate Diagnostics Workshop*, pp. 190–197, Cambridge, MA, US Dept. of Commerce.

Berrang-Ford, L., J. Ford, and J. Paterson (2011), Are we adapting to climate change?, *Global Environmental Change*, *21*(1), 25–33.

Betts, R., O. Boucher, M. Collins, P. Cox, P. Falloon, N. Gedney, D. Hemming, C. Huntingford, C. Jones, D. Sexton, and M. Webb (2007), Projected increase in continental runoff due to plant responses to increasing carbon dioxide., *Nature*, *448*(7157), 1037–1041.

Bigler, C., O. Bräker, H. Bugmann, M. Dobbertin, and A. Rigling (2006), Drought as an Inciting Mortality Factor in Scots Pine Stands of the Valais, Switzerland, *Ecosystems*, *9*(3), 330–343.

Bladé, I., B. Liebmann, D. Fortuny, and G. Oldenborgh (2012), Observed and simulated impacts of the summer NAO in Europe: implications for projected drying in the Mediterranean region, *Climate Dynamics*, *39*(3-4), 709–727.

Blenkinsop, S., and H. Fowler (2007a), Changes in drought frequency, severity and duration for the British Isles projected by the PRUDENCE regional climate models, *Journal of Hydrology*, *342*(1-2), 50–71.

Blenkinsop, S., and H. Fowler (2007b), Changes in European drought characteristics projected by the PRUDENCE regional climate models, *International Journal of Climatology*, *27*(12), 1595–1610.

Bonacci, O. (1993), Hydrological identification of drought, *Hydrological Processes*, *7*(3), 249–262.

Bond, G., B. Kromer, J. Beer, R. Muscheler, M. Evans, W. Showers, S. Hoffmann, R. Lotti-Bond, I. Hajdas, and G. Bonani (2001), Persistent solar influence on North Atlantic climate during the Holocene, *Science*, *294*(5549), 2130–2136.

Bordi, I., K. Fraedrich, and A. Sutera (2009), Observed drought and wetness trends in Europe: an update, *Hydrology and Earth System Sciences*, *13*, 1519–1530.

Bordi, I., S. Frigio, P. Parenti, A. Speranza, and A. Sutera (2001), The analysis of the Standardized Precipitation Index in the Mediterranean area: large-scale patterns, *Annali di Geofisica*, *44*(5-6), 979–993.

Bradley, R. (2000), 1000 Years of Climate Change, *Science*, *288*(5470), 1353–1355.

Brekke, L., M. Dettinger, E. Maurer, and M. Anderson (2008), Significance of model credibility in estimating climate projection distributions for regional hydroclimatological risk assessments, *Climatic Change*, *89*(3-4), 371–394.

Briffa, K., P. Jones, and M. Hulme (1994), Summer moisture variability across Europe, 18921991: An analysis based on the palmer drought severity index, *International Journal of Climatology*, *14*(5), 475–506.

Briffa, K., G. van der Schrier, and P. Jones (2009), Wet and dry summers in Europe since 1750: evidence of increasing drought, *International Journal of Climatology*, *29*(13), 1894–1905.

Bruckner, T., G. Petschel-Held, F. Tóth, H.-M. Füssel, C. Helm, M. Leimbach, and H.-J. Schellnhuber (1999), Climate change decision-support and the tolerable windows approach, *Environmental Modeling and Assessment*, *4*(4), 217–234.

Buonomo, E., R. Jones, C. Huntingford, and J. Hannaford (2007), On the robustness of changes in extreme precipitation over Europe from two high resolution climate change simulations, *Quarterly Journal of the Royal Meteorological Society*, *133*(622), 65–81.

Bureau of Reclamation, U. D. o. t. I. (2011), *SECURE Water Act Section 9503(c) Reclamation Climate Change and Water*, Tech. rep., Report to Congress.

Burke, E. (2011), Understanding the sensitivity of different drought metrics to the drivers of drought under increased atmospheric CO2, *Journal of Hydrometeorology*, *12*(6), 1378–1394.

Burke, E., and S. Brown (2008), Evaluating Uncertainties in the Projection of Future Drought, *Journal of Hydrometeorology*, *9*(2), 292–299.

Burke, E., and S. Brown (2010), Regional drought over the UK and changes in the future, *Journal of Hydrology*, *394*(3-4), 471–485.

Burke, E., R. Perry, and S. Brown (2010), An extreme value analysis of UK drought and projections of change in the future, *Journal of Hydrology*, *388*(1-2), 131–143.

Burke, E. J., S. J. Brown, and N. Christidis (2006), Modeling the Recent Evolution of Global Drought and Projections for the Twenty-First Century with the Hadley Centre Climate Model, *Journal of Hydrometeorology*, *7*(5), 1113–1125.

Buser, C., H. Künsch, D. Lüthi, M. Wild, and C. Schär (2009), Bayesian multi-model projection of climate: bias assumptions and interannual variability, *Climate Dynamics*, *33*(6), 849–868.

Byun, H.-R., and D. Wilhite (1999), Objective Quantification of Drought Severity and Duration, *Journal of Climate*, *12*(9), 2747–2756.

Caballero, Y., S. Voirin-Morel, F. Habets, J. Noilhan, P. LeMoigne, A. Lehenaff, and A. Boone (2007), Hydrological sensitivity of the Adour-Garonne river basin to climate change, *Water Resources Research*, *43*(7), W07,448.

Cai, W., T. Cowan, P. Briggs, and M. Raupach (2009), Rising temperature depletes soil moisture and exacerbates severe drought conditions across southeast Australia, *Geophysical Research Letters*, *36*(21), L21,709.

Calanca, P. (2007), Climate change and drought occurrence in the Alpine region: How severe are becoming the extremes?, *Global and Planetary Change*, *57*(1-2), 151–160.

CCSP (2008), *Climate Models: An Assessment of Strengths and Limitations. A Report by the U.S. Climate Change Science Program and the Subcommittee on Global Change Research*, Tech. Rep. July, Department of Energy, Office of Biological and Environmental Research, Washington, D.C., USA.

Chang, H., C. Knight, M. Staneva, and D. Kostov (2002), Water resource impacts of climate change in southwestern Bulgaria, *GeoJournal*, *57*(3), 159–168.

Charles, S., B. Bates, P. Whetton, and J. Hughes (1999), Validation of downscaling models for changed climate conditions: case study of southwestern Australia, *Climate Research*, *12*(1), 1–14.

Charlton, R., R. Fealy, S. Moore, J. Sweeney, and C. Murphy (2006), Assessing the Impact of Climate Change on Water Supply and Flood Hazard in Ireland Using Statistical Downscaling and Hydrological Modelling Techniques, *Climatic Change*, *74*(4), 475–491.

Chen, H., and J. Sun (2009), How the best models project the future precipitation change in China, *Advances in Atmospheric Sciences*, *26*(4), 773–782.

Chen, J., F. Brissette, and R. Leconte (2011), Uncertainty of downscaling method in quantifying the impact of climate change on hydrology, *Journal of Hydrology*, *401*(3-4), 190–202.

Cheng, Y., U. Lohmann, J. Zhang, Y. Luo, Z. Liu, and G. Lesins (2005), Contribution of Changes in Sea Surface Temperature and Aerosol Loading to the Decreasing Precipitation Trend in Southern China, *Journal of Climate*, *18*(9), 1381–1390.

Chenoweth, J., P. Hadjinicolaou, A. Bruggeman, J. Lelieveld, Z. Levin, M. Lange, E. Xoplaki, and M. Hadjikakou (2011), Impact of climate change on the water resources of the eastern Mediterranean and Middle East region: Modeled 21st century changes and implications, *Water Resources Research*, *47*(6), W06,506.

Chiew, F. (2006), Estimation of rainfall elasticity of streamflow in Australia, *Hydrological Sciences Journal*, *51*(4), 613–625.

Chiew, F., and T. McMahon (2002), Modelling the impacts of climate change on Australian streamflow, *Hydrological Processes*, *16*(6), 1235–1245.

Chiew, F., M. Peel, T. McMahon, and L. Siriwardena (2006), Precipitation elasticity of streamflow in catchments across the world, *IAHS-AISH publication*, *388*, 256–262.

Chiew, F., J. Teng, J. Vaze, and D. Kirono (2009), Influence of global climate model selection on runoff impact assessment, *Journal of Hydrology*, *379*(1-2), 172–180.

Christensen, J., T. Carter, and F. Giorgi (2002), PRUDENCE employs new methods to assess European climate change, *Eos, Transactions American Geophysical Union*, *83*(13), 147.

Christensen, J., T. Carter, M. Rummukainen, and G. Amanatidis (2007), Evaluating the performance and utility of regional climate models: the PRUDENCE project, *Climatic Change*, *81*(S1), 1–6.

Christensen, J., and O. Christensen (2007), A summary of the PRUDENCE model projections of changes in European climate by the end of this century, *Climatic Change*, *81*(S1), 7–30.

Christensen, O., and J. Christensen (2004), Intensification of extreme European summer precipitation in a warmer climate, *Global and Planetary Change*, *44*(1-4), 107–117.

Ciais, P., M. Reichstein, N. Viovy, A. Granier, J. Ogée, V. Allard, M. Aubinet, N. Buchmann, C. Bernhofer, A. Carrara, F. Chevallier, N. De Noblet, A. Friend, P. Friedlingstein, T. Grünwald, B. Heinesch, P. Keronen, A. Knohl, G. Krinner, D. Loustau, G. Manca, G. Matteucci, F. Miglietta, J. Ourcival, D. Papale, K. Pilegaard, S. Rambal, G. Seufert, J. Soussana, M. Sanz, E. Schulze, T. Vesala, and R. Valentini (2005), Europe-wide reduction in primary productivity caused by the heat and drought in 2003, *Nature*, *437*(7058), 529–533.

Clarke, L., J. Edmonds, H. Jacoby, H. Pitcher, J. Reilly, and R. Richels (2007), Scenarios of Greenhouse Gas Emissions and Atmospheric Concentrations, in: *Synthesis and Assessment Product 2.1 by the U.S. Climate Change Science Program and the Subcommittee on Global Change Research*, chap. Sub-report, p. 154, Department of Energy, Office of Biological & Environmental Research, Washington, 7 DC., USA.

Clausen, B., and C. Pearson (1995), Regional frequency analysis of annual maximum streamflow drought, *Journal of Hydrology*, *173*(1-4), 111–130.

Collier, P., G. Conway, and T. Venables (2008), Climate change and Africa, *Oxford Review of Economic Policy*, *24*(2), 337–353.

Collins, M. (2004), El Niño- or La Niña-like climate change?, *Climate Dynamics*, *24*(1), 89–104.

Collins, M., and M. Allen (2002), Assessing the Relative Roles of Initial and Boundary Conditions in Interannual to Decadal Climate Predictability, *Journal of Climate*, *15*(21), 3104–3109.

Cook, E., D. Meko, and C. Stockton (1997), A New Assessment of Possible Solar and Lunar Forcing of the Bidecadal Drought Rhythm in the Western United States, *Journal of Climate*, *10*(6), 1343–1356.

Cook, E., C. Woodhouse, C. Eakin, D. Meko, and D. Stahle (2004), Long-term aridity changes in the western United States, *Science*, *306*(5698), 1015–1018.

Corso-Perez, G., H. Lanen, N. Bertrand, C. Chen, D. Clark, S. Folwell, S. Gosling, N. Hanasaki, J. Heinke, and F. Voss (2011), *Drought at the global scale in the 21st Century. Technical Report No 43. WATCH deliverables D 4.3.1.*, Tech. rep.

Covey, C., K. AchutaRao, U. Cubasch, P. Jones, S. Lambert, M. Mann, T. Phillips, and K. Taylor (2003), An overview of results from the Coupled Model Intercomparison Project, *Global and Planetary Change*, *37*(1-2), 103–133.

Crowley, T., and K.-Y. Kim (1996), Comparison of proxy records of climate change and solar forcing, *Geophysical Research Letters*, *23*(4), 359–362.

Cullen, H., A. Kaplan, P. Arkin, and P. DeMenocal (2002), Impact of the North Atlantic Oscillation on Middle Eastern Climate and Streamflow, *Climatic Change*, *55*(3), 315–338.

Dai, A. (2011), Drought under global warming: a review, *Wiley Interdisciplinary Reviews: Climate Change*, *2*(1), 45–65.

Dai, A. (2013), Increasing drought under global warming in observations and models, *Nature Climate Change*, *3*(1), 52–58.

Dai, A., K. Trenberth, and T. Qian (2004), A Global Dataset of Palmer Drought Severity Index for 18702002: Relationship with Soil Moisture and Effects of Surface Warming, *Journal of Hydrometeorology*, *5*(6), 1117–1130.

Dankers, R., and R. Hiederer (2008), *Extreme Temperatures and Precipitation in Europe: Analysis of a High-Resolution Climate Change Scenario. JRC Scientific and Technical Reports*, Tech. rep., European Commission Joint Research Centre, Institute for Environment and Sustainabilit, EUR 23291 EN - 2008.

Das, H. (2003), Agrometeorology Related to Extreme Events, in: *Agrometeorology Related to Extreme Events* (Das, H., T. Adamenko, K. Anaman, R. Gommes, and G. Johnson, eds.), 201, pp. 7–34.

Department of Water (2010), *The effects of climate change on streamflow in south-west Western Australia: Projections for 2050.*, Tech. rep., Government of Western Australia. Surface water hydrology series. Report no. HY34. Perth, Western Australia, Available at http://www.water.wa.gov.au/PublicationStore/first/95412.pdf.

Déqué, M., D. Rowell, D. Lüthi, F. Giorgi, J. Christensen, B. Rockel, D. Jacob, E. Kjellström, M. Castro, and B. Hurk (2007), An intercomparison of regional climate simulations for Europe: assessing uncertainties in model projections, *Climatic Change*, *81*(S1), 53–70.

Deser, C., A. Phillips, V. Bourdette, and H. Teng (2012), Uncertainty in climate change projections: the role of internal variability, *Climate Dynamics*, *38*(3-4), 527–546.

Dickinson, R. (2013), Modeling Evapotranspiration for Three-Dimensional Global Climate Models, in: *Climate Processes and Climate Sensitivity* (Hansen, J., and T. Takahashi, eds.), pp. 58–72, American Geophysical Union, Washington, D.C.

Ding, Y., M. Hayes, and M. Widhalm (2011), Measuring economic impacts of drought: a review and discussion, *Disaster Prevention and Management*, *20*(4), 434–446.

Ding, Y., G. Ren, Z. Zhao, Y. Xu, Y. Luo, Q. Li, and J. Zhang (2007), Detection, causes and projection of climate change over China: An overview of recent progress, *Advances in Atmospheric Sciences*, *24*(6), 954–971.

Döll, P. (2002), Impact of Climate Change and Variability on Irrigation Requirements: A Global Perspective, *Climatic Change*, *54*(3), 269–293.

Dooge, J. (1992), Sensitivity of Runoff to Climate Change: A Hortonian Approach, *Bulletin of the American Meteorological Society*, *73*(12), 2013–2024.

Dooge, J., M. Bruen, and B. Parmentier (1999), A simple model for estimating the sensitivity of runoff to long-term changes in precipitation without a change in vegetation, *Advances in Water Resources*, *23*(2), 153–163.

Dore, M. (2005), Climate change and changes in global precipitation patterns: what do we know?, *Environment international*, *31*(8), 1167–81.

Douville, H., F. Chauvin, S. Planton, J.-F. Royer, D. Salas-Mélia, and S. Tyteca (2002), Sensitivity of the hydrological cycle to increasing amounts of greenhouse gases and aerosols, *Climate Dynamics*, *20*(1), 45–68.

Dracup, J., K. Lee, and E. Paulson Jr. (1980), On the Definition of Droughts, *Water Resources Research*, *16*(2), 297–302.

Drogue, G., L. Pfister, T. Leviandier, A. El Idrissi, J.-F. Iffly, P. Matgen, J. Humbert, and L. Hoffmann (2004), Simulating the spatio-temporal variability of streamflow response to climate change scenarios in a mesoscale basin, *Journal of Hydrology*, *293*(1-4), 255–269.

Dubrovsky, M., I. Nemesova, and J. Kalvova (2005), Uncertainties in climate change scenarios for the Czech Republic, *Climate Research*, *29*(2), 139–156.

Dubrovsky, M., M. Svoboda, M. Trnka, M. Hayes, D. Wilhite, Z. Zalud, and P. Hlavinka (2008), Application of relative drought indices in assessing climate-change impacts on drought conditions in Czechia, *Theoretical and Applied Climatology*, *96*(1-2), 155–171.

Ducharne, A., C. Baubion, N. Beaudoin, M. Benoit, G. Billen, N. Brisson, J. Garnier, H. Kieken, S. Lebonvallet, E. Ledoux, B. Mary, C. Mignolet, X. Poux, E. Sauboua, C. Schott, S. Théry, and P. Viennot (2007), Long term prospective of the Seine River system: confronting climatic and direct anthropogenic changes., *The Science of the total environment*, *375*(1-3), 292–311.

Easterling, D., J. Evans, P. Groisman, T. Karl, K. Kunkel, and P. Ambenje (2000), Observed Variability and Trends in Extreme Climate Events: A Brief Review, *Bulletin of the American Meteorological Society*, *81*(3), 417–425.

Eckhardt, K., and U. Ulbrich (2003), Potential impacts of climate change on groundwater recharge and streamflow in a central European low mountain range, *Journal of Hydrology*, *284*(1-4), 244–252.

Edwards, D., and T. McKee (1997), *Characteristics of 20th century drought in the United States at multiple time scales*, Tech. rep., Climatology Report Number 97-2. Colorado State University, Fort Collins, CO.

Ekström, M., P. Jones, H. Fowler, G. Lenderink, T. Buishand, and D. Conway (2007), Regional climate model data used within the SWURVE project 1: projected changes in seasonal patterns and estimation of PET, *Hydrology and Earth System Sciences*, *11*(3), 1069–1083.

Ellis, A. W., G. B. Goodrich, and G. M. Garfin (2009), A hydroclimatic index for examining patterns of drought in the Colorado River Basin, *International Journal of Climatology*, *30*(2), 236–255.

Eltahir, E., and P.-F. Yeh (1999), On the asymmetric response of aquifer water level to floods and droughts in Illinois, *Water Resources Research*, *35*(4), 1199–1217.

Engen-Skaugen, T., L. Roald, S. Beldring, E. Fø rland, O. Tveito, K. Engeland, and R. Benestad (2005), *Climate Change Impacts on Water Balance in Norway*, Tech. rep., Met. Report No. 1/2005, Climate, Oslo.

Etchevers, P., C. Golaz, F. Habets, and J. Noilhan (2002), Impact of a climate change on the Rhone river catchment hydrology, *Journal of Geophysical Research*, *107*(D16), 4293.

European Environment Agency (2009), *Regional climate change and adaptation: The Alps facing the challenge of changing water resources*, Tech. rep., EEA Report No 8/2009, Copenhagen.

Evans, J. (2008), 21st century climate change in the Middle East, *Climatic Change*, *92*(3), 417–432.

Evans, J. (2010), Global warming impact on the dominant precipitation processes in the Middle East, *Theoretical and Applied Climatology*, *99*(3-4), 389–402.

Fang, K., X. Gou, F. Chen, M. Yang, J. Li, M. He, Y. Zhang, Q. Tian, and J. Peng (2009), Drought variations in the eastern part of northwest China over the past two centuries: evidence from tree rings, *Climate Research*, *38*, 129–135.

Feyen, L., and R. Dankers (2009), Impact of global warming on streamflow drought in Europe, *Journal of Geophysical Research*, *114*, D17,116.

Findell, K., and T. Delworth (2010), Impact of Common Sea Surface Temperature Anomalies on Global Drought and Pluvial Frequency, *Journal of Climate*, *23*(3), 485–503.

Fink, A., T. Brücher, A. Krüger, G. Leckebusch, J. Pinto, and U. Ulbrich (2004), The 2003 European summer heatwaves and drought - synoptic diagnosis and impacts, *Weather*, *59*(8), 209–216.

Fleig, A., L. Tallaksen, H. Hisdal, and S. Demuth (2006), A global evaluation of streamflow drought characteristics, *Hydrology and Earth System Sciences*, *10*(4), 535–552.

Fleig, A., L. Tallaksen, H. Hisdal, and D. Hannah (2011), Regional hydrological drought in north-western Europe: linking a new Regional Drought Area Index with weather types, *Hydrological Processes*, *25*(7), 1163–1179.

Foley, A. (2010), Uncertainty in regional climate modelling: A review, *Progress in Physical Geography*, *34*(5), 647–670.

Folland, C., J. Knight, H. Linderholm, D. Fereday, S. Ineson, and J. Hurrell (2009), The Summer North Atlantic Oscillation: Past, Present, and Future, *Journal of Climate*, *22*(5), 1082–1103.

Forland, E., and I. Hanssen-Bauer (2003), Past and future climate variations in the Norwegian Arctic: overview and novel analyses, *Polar Research*, *22*(2), 113–124.

Fowler, H., and C. Kilsby (2004), Future increases in UK water resource drought projected by a regional climate model, in: *Proceedings of the BHS International Conference on Hydrology: Science and Practice for the 21st Century, Volume 1*, pp. 15–21, London, 12-16 July 2004.

Fowler, H., and C. Kilsby (2007), Using regional climate model data to simulate historical and future river flows in northwest England, *Climatic Change*, *80*(3-4), 337–367.

Fowler, H., and R. Wilby (2007), Beyond the downscaling comparison study, *International Journal of Climatology*, *27*(12), 1543–1545.

Frederick, K., and D. Major (1997), Climate Change and Water Resources, *Climatic Change*, *37*(1), 7–23.

Frei, C., R. Schöll, S. Fukutome, J. Schmidli, and P. L. Vidale (2006), Future change of precipitation extremes in Europe: Intercomparison of scenarios from regional climate models, *Journal of Geophysical Research*, *111*, D06,105.

Frich, P., L. Alexander, P. Della-Marta, B. Gleason, M. Haylock, A. Klein Tank, and T. Peterson (2002), Observed coherent changes in climatic extremes during the second half of the twentieth century, *Climate Research*, *19*, 193–212.

Frieler, K., M. Meinshausen, T. Schneider von Deimling, T. Andrews, and P. Forster (2011), Changes in global-mean precipitation in response to warming, greenhouse gas forcing and black carbon, *Geophysical Research Letters*, *38*(4), L04,702.

Fu, G., M. Barber, and S. Chen (2007a), Impacts of Climate Change on Regional Hydrological Regimes in the Spokane River Watershed, *Journal of Hydrologic Engineering*, *12*(5), 452–461.

Fu, G., S. Charles, and F. Chiew (2007b), A two-parameter climate elasticity of streamflow index to assess climate change effects on annual streamflow, *Water Resources Research*, *43*, W11,419.

Fu, G., S. Charles, N. Viney, S. Chen, and J. Wu (2007c), Impacts of climate variability on stream-flow in the Yellow River, *Hydrological Processes*, *21*(25), 3431–3439.

Fu, G., F. Chiew, S. Charles, and F. Mpelasoka (2011), Assessing precipitation elasticity of streamflow based on the strength of the precipitation-streamflow relationship, in: *MODSIM2011, 19th International Congress on Modelling and Simulation. Modelling and Simulation Society of Australia and New Zealand, 12-16 December 2011* (Chan, F., D. Marinova, and R. Anderssen, eds.), pp. 1652–1658, ISBN: 978-0-9872143-1-7, Perth, Western Australia.

Fujino, J., R. Nair, M. Kainuma, T. Masui, and Y. Matsuoka (2006), Multi-gas mitigation analysis on stabilization scenarios using AIM global model. Multigas Mitigation and Climate Policy, *Energy Journal*, *3*(Special Issue), 343–354.

Fung, F., A. Lopez, and M. New (2011), Water availability in +2C and +4C worlds, *Philosophical transactions. Series A, Mathematical, physical, and engineering sciences*, *369*(1934), 99–116.

Gallagher, J., P. Biscoe, and B. Hunter (1976), Effects of drought on grain growth, *Nature*, *264*(5586), 541–542.

Gao, X., and F. Giorgi (2008), Increased aridity in the Mediterranean region under greenhouse gas forcing estimated from high resolution simulations with a regional climate model, *Global and Planetary Change*, *62*(3-4), 195–209.

Gao, X., J. Pal, and F. Giorgi (2006), Projected changes in mean and extreme precipitation over the Mediterranean region from a high resolution double nested RCM simulation, *Geophysical Research Letters*, *33*(3), L03,706.

García-Ruiz, J., J. López-Moreno, S. Vicente-Serrano, T. LasantaMartínez, and S. Beguería (2011), Mediterranean water resources in a global change scenario, *Earth-Science Reviews*, *105*(3-4), 121–139.

Gedney, N., P. Cox, R. Betts, O. Boucher, C. Huntingford, and P. Stott (2006), Detection of a direct carbon dioxide effect in continental river runoff records, *Nature*, *439*(7078), 835–8.

Gellens, D., and E. Roulin (1998), Streamflow response of Belgian catchments to IPCC climate change scenarios, *Journal of Hydrology*, *210*(1-4), 242–258.

Gibbs, W., and J. Maher. (1967), Rainfall deciles as drought indicators, *Bureau of Meteorology Bulletin*, *48*, Commonwealth of Australia, Melbourne.

Gibelin, A.-L., and M. Déqué (2003), Anthropogenic climate change over the Mediterranean region simulated by a global variable resolution model, *Climate Dynamics*, *20*(4), 327–339.

Giorgi, F., and X. Bi (2005), Regional changes in surface climate interannual variability for the 21st century from ensembles of global model simulations, *Geophysical Research Letters*, *32*(13), L13,701.

Giorgi, F., X. Bi, and J. Pal (2004), Mean, interannual variability and trends in a regional climate change experiment over Europe. II: climate change scenarios (2071-2100), *Climate Dynamics*, *23*(7), 839–858.

Giorgi, F., and E. Coppola (2009), Projections of twenty-first century climate over Europe, *EPJ Web of Conferences*, *1*(ERCA 2008 - From the Human Dimensions of Global Environmental Change to the Observation of the Earth from Space), 29–46.

Giorgi, F., and P. Lionello (2008), Climate change projections for the Mediterranean region, *Global and Planetary Change*, *63*(2-3), 90–104.

Gleckler, P., K. Taylor, and C. Doutriaux (2008), Performance metrics for climate models, *Journal of Geophysical Research*, *113*, D06,104.

Gobron, N., B. Pinty, F. Mélin, M. Taberner, M. Verstraete, A. Belward, T. Lavergne, and J.-L. Widlowski (2005), The state of vegetation in Europe following the 2003 drought, *International Journal of Remote Sensing*, *26*(9), 2013–2020.

Goodess, C., C. Hanson, M. Hulme, and T. Osborn (2003a), Representing Climate and Extreme Weather Events in Integrated Assessment Models: A Review of Existing Methods and Options for Development, *Integrated Assessment*, *4*(3), 145–171.

Goodess, C., T. Osborn, and M. Hulme (2003b), *The identification and evaluation of suitable scenario development methods for the estimation of future probabilities of extreme weather events*, Tech. rep., Tyndall Centre for Climate Change Research, UEA, Norwich, UK.

Gosling, S., and N. Arnell (2011), Simulating current global river runoff with a global hydrological model: model revisions, validation, and sensitivity analysis, *Hydrological Processes*, *25*(7), 1129–1145.

Gosling, S., D. Bretherton, K. Haines, and N. Arnell (2010), Global hydrology modelling and uncertainty: running multiple ensembles with a campus grid., *Philosophical transactions. Series A, Mathematical, physical, and engineering sciences*, *368*(1926), 4005–4021.

Gosling, S., G. McGregor, and J. Lowe (2011a), The benefits of quantifying climate model uncertainty in climate change impacts assessment: an example with heat-related mortality change estimates, *Climatic Change*, *112*(2), 217–231.

Gosling, S., R. Taylor, N. Arnell, and M. Todd (2011b), A comparative analysis of projected impacts of climate change on river runoff from global and catchment-scale hydrological models, *Hydrology and Earth System Sciences*, *15*, 279–294.

Goubanova, K., and L. Li (2007), Extremes in temperature and precipitation around the Mediterranean basin in an ensemble of future climate scenario simulations, *Global and Planetary Change*, *57*(1-2), 27–42.

Graham, L. (2004), Climate Change Effects on River Flow to the Baltic Sea, *AMBIO: A Journal of the Human Environment*, *33*(4), 235–241.

Graham, L., S. Hagemann, S. Jaun, and M. Beniston (2007), On interpreting hydrological change from regional climate models, *Climatic Change*, *81*(S1), 97–122.

Greatbatch, R. (2000), The North Atlantic Oscillation, *Stochastic Environmental Research and Risk Assessment*, *14*(4-5), 213–242.

Gregory, J., J. Mitchell, and A. Brady (1997), Summer Drought in Northern Midlatitudes in a Time-Dependent CO2 Climate Experiment, *Journal of Climate*, *10*(4), 662–686.

Grimm, A. (2010), Interannual climate variability in South America: impacts on seasonal precipitation, extreme events, and possible effects of climate change, *Stochastic Environmental Research and Risk Assessment*, *25*(4), 537–554.

Gudmundsson, L., L. Tallaksen, and K. Stahl (2011), Spatial cross-correlation patterns of European low, mean and high flows, *Hydrological Processes*, *25*(7), 1034–1045.

Gudmundsson, L., L. Tallaksen, K. Stahl, D. Clark, E. Dumont, S. Hagemann, N. Bertrand, D. Gerten, J. Heinke, N. Hanasaki, F. Voss, and S. Koirala (2012a), Comparing Large-Scale Hydrological Model Simulations to Observed Runoff Percentiles in Europe, *Journal of Hydrometeorology*, *13*(2), 604–620.

Gudmundsson, L., T. Wagener, L. Tallaksen, and K. Engeland (2012b), Evaluation of nine large-scale hydrological models with respect to the seasonal runoff climatology in Europe, *Water Resources Research*, *48*(11), W11,504.

Gutowski, W., G. Hegerl, G. Holland, T. Knutson, L. Mearns, R. Stouffer, P. Webster, M. Wehner, and F. Zwiers (2008), Causes of Observed Changes in Extremes and Projections of Future Changes, in: *Weather and Climate Extremes in a Changing Climate. Regions of Focus: North America, Hawaii, Caribbean, and U.S. Pacific Islands* (Karl, T., G. Meehl, C. Miller, S. Hassol, A. Waple, and W. Murray, eds.), chap. 3, p. 180, A Report by the U.S. Climate Change Science Program and the Subcommittee on Global Change Research, Washington, DC.

Guttman, N. (1998), Comparing the Palmer Drought Index and the Standardized Precipitation Index, *Journal of the American Water Resources Association*, *34*(1), 113–121.

Guttman, N. (1999), Accepting the Standardized Precipitation Index: A Calculation Algorithm, *JAWRA Journal of the American Water Resources Association*, *35*(2), 311–322.

Gutzler, D., and T. Robbins (2011), Climate variability and projected change in the western United States: regional downscaling and drought statistics, *Climate Dynamics*, *37*(5-6), 835–849.

Habets, F., P. Etchevers, C. Golaz, E. Leblois, E. Ledoux, E. Martin, J. Noilhan, and C. Ottlé (1999), Simulation of the water budget and the river flows of the Rhone basin, *Journal of Geophysical Research*, *104*(D24), 31,145.

Haddeland, I., D. Clark, W. Franssen, F. Ludwig, F. Voß, N. Arnell, N. Bertrand, M. Best, S. Folwell, D. Gerten, S. Gomes, S. Gosling, S. Hagemann, N. Hanasaki, R. Harding, J. Heinke, P. Kabat, S. Koirala, T. Oki, J. Polcher, T. Stacke, P. Viterbo, G. Weedon, and P. Yeh (2011), Multimodel Estimate of the Global Terrestrial Water Balance: Setup and First Results, *Journal of Hydrometeorology*, *12*(5), 869–884.

Hagemann, S., K. Arpe, and E. Roeckner (2006), Evaluation of the Hydrological Cycle in the ECHAM5 Model, *Journal of Climate*, *19*(16), 3810–3827.

Hagemann, S., C. Chen, D. B. Clark, S. Folwell, S. N. Gosling, I. Haddeland, N. Hanasaki, J. Heinke, F. Ludwig, F. Voß, and A. J. Wiltshire (2012), Climate change impact on available water resources obtained using multiple global climate and hydrology models, *Earth System Dynamics Discussions*, *3*(2), 1321–1345.

Hagemann, S., C. Chen, J. Haerter, J. Heinke, D. Gerten, and C. Piani (2011), Impact of a Statistical Bias Correction on the Projected Hydrological Changes Obtained from Three GCMs and Two Hydrology Models, *Journal of Hydrometeorology*, *12*(4), 556–578.

Haigh, J. D. (1999), A GCM study of climate change in response to the 11-year solar cycle, *Quarterly Journal of the Royal Meteorological Society*, *125*(555), 871–892.

Hansen, J., A. Lacis, R. Ruedy, and M. Sato (1992), Potential climate impact of Mount Pinatubo eruption, *Geophysical Research Letters*, *19*(2), 215–218.

Hansen, J., M. Sato, R. Ruedy, A. Lacis, K. Asamoah, K. Beckford, S. Borenstein, E. Brown, B. Cairns, B. Carlson, B. Curran, S. de Castro, L. Druyan, P. Etwarrow, T. Ferede, M. Fox, D. Gaffen, J. Glascoe, H. Gordon, S. Hollandsworth, X. Jiang, C. Johnson, N. Lawrence, J. Lean, J. Lerner, K. Lo, J. Logan, A. Luckett, M. McCormick, R. McPeters, R. Miller, P. Minnis, I. Ramberran, G. Russell, P. Russell, P. Stone, I. Tegen, S. Thomas, L. Thomason, A. Thompson, J. Wilder, R. Willson, and J. Zawodny (1997), Forcings and chaos in interannual to decadal climate change, *Journal of Geophysical Research*, *102*(D22), 25,679–25,720.

Hanson, C., J. Palutikof, M. Livermore, L. Barring, M. Bindi, J. Corte-Real, R. Durao, C. Giannakopoulos, P. Good, T. Holt, Z. Kundzewicz, G. Leckebusch, M. Moriondo, M. Radziejewski, J. Santos, P. Schlyter, M. Schwarb, I. Stjernquist, and U. Ulbrich (2007), Modelling the impact of climate extremes: an overview of the MICE project, *Climatic Change*, *81*(S1), 163–177.

Hanssen-Bauer, I., C. Achberger, R. Benestad, D. Chen, and E. Fø rland (2005), Review: statistical downscaling of climate scenarios over Scandinavia, *Climate Research*, *29*, 255–268.

Harman, C., P. Troch, and M. Sivapalan (2011), Functional model of water balance variability at the catchment scale: 2. Elasticity of fast and slow runoff components to precipitation change in the continental United States, *Water Resources Research*, *47*(2), W02,523.

Harris, G., M. Collins, D. Sexton, J. Murphy, and B. Booth (2010), Probabilistic projections for 21st century European climate, *Natural Hazards and Earth System Science*, *10*(9), 2009–2020.

Harris, I., P. Jones, T. Osborn, and D. Lister (2013), Updated high-resolution grids of monthly climatic observations - the CRU TS3.10 Dataset, *International Journal of Climatology*, p. in press.

Hawkins, E., and R. Sutton (2010), The potential to narrow uncertainty in projections of regional precipitation change, *Climate Dynamics*, *37*(1-2), 407–418.

Hayes, M. (1998), Drought Indices, National Drought Mitigation Center, Lincoln, Nebraska.

Hayes, M., C. Alvord, and J. Lowrey (2007), Intermountain West Climate Summary July 2007 Climate Summary, *Intermountain West Climate Summary*, *3*(6), 2–6.

Hayes, M., M. Svoboda, N. Wall, and M. Widhalm (2011), The Lincoln Declaration on Drought Indices: Universal Meteorological Drought Index Recommended, *Bulletin of the American Meteorological Society*, *92*(4), 485–488.

Hayes, M., M. Svoboda, D. Wilhite, and O. Vanyarkho (1999), Monitoring the 1996 Drought Using the Standardized Precipitation Index, *Bulletin of the American Meteorological Society*, *80*(3), 429–438.

Haylock, M., G. Cawley, C. Harpham, R. Wilby, and C. Goodess (2006), Downscaling heavy precipitation over the United Kingdom: a comparison of dynamical and statistical methods and their future scenarios, *International Journal of Climatology*, *26*(10), 1397–1415.

Haylock, M. R., and C. M. Goodess (2004), Interannual variability of European extreme winter rainfall and links with mean large-scale circulation, *International Journal of Climatology*, *24*(6), 759–776.

Heddinghaus, T., and P. Sabol (1991), A review of the Palmer Drought Severity Index and where do we go from here?, in: *7th Conf. on Appl. Climatol.*, pp. 242–246, American Meteorological Society, 10-13 September 1991, Boston.

Hegerl, G., E. Black, R. Allan, W. Ingram, D. Polson, K. Trenberth, R. Chadwick, P. Arkin, B. Sarojini, A. Becker, E. Blyth, A. Dai, P. Durack, D. Easterling, H. Fowler,

E. Kendon, G. Huffman, C. Liu, R. Marsh, M. New, T. Osborn, N. Skliris, P. Stott, P.-L. Vidale, S. Wijffels, L. Wilcox, K. Willett, and X. Zhang (2013), Quantifying changes in the global water cycle, *Bulletin of the American Meteorological Society*, (under review).

Hegerl, G., F. Zwiers, P. Braconnot, N. Gillett, Y. Luo, J. Marengo Orsini, N. Nicholls, J. Penner, and P. Stott (2007), Understanding and Attributing Climate Change, in: *Climate Change 2007: The Physical Science Basis. Contribution of Working Group I to the Fourth Assessment Report of the Intergovernmental Panel on Climate Change* (Solomon, S., D. Qin, M. Manning, Z. Chen, M. Marquis, K. Averyt, M. Tignor, and H. Miller, eds.), Cambridge University Press, Cambridge, United Kingdom and New York, NY, USA.

Heim Jr., R. (2002), A Review of Twentieth-Century Drought Indices Used in the United States, *Bulletin of the American Meteorological Society*, *83*(8), 1149–1165.

Heinrich, G., and A. Gobiet (2011), The future of dry and wet spells in Europe: A comprehensive study based on the ENSEMBLES regional climate models, *International Journal of Climatology*, *32*(13), 1951–1970.

Helama, S., J. Merilainen, and H. Tuomenvirta (2009), Multicentennial megadrought in northern Europe coincided with a global El Nino-Southern Oscillation drought pattern during the Medieval Climate Anomaly, *Geology*, *37*(2), 175–178.

Held, I., and B. Soden (2000), Water vapor feedback and global warming, *Annual Review of Energy and the Environment*, *25*, 441–475.

Held, I., and B. Soden (2006), Robust Responses of the Hydrological Cycle to Global Warming, *Journal of Climate*, *19*(21), 5686–5699.

Hemming, D., C. Buontempo, E. Burke, M. Collins, and N. Kaye (2010), How uncertain are climate model projections of water availability indicators across the Middle East?, *Philosophical Transactions of the Royal Society A: Mathematical, Physical and Engineering Sciences*, *368*(1931), 5117–5135.

Henderson-Sellers, A., and P. Robinson (1986), *Contemporary Climatology*, Longman Scientific and Technical, Harlow, England.

Herweijer, C., R. Seager, E. Cook, and J. Emile-Geay (2007), North American Droughts of the Last Millennium from a Gridded Network of Tree-Ring Data, *Journal of Climate*, *20*(7), 1353–1376.

Hewitson, B., and R. Crane (1996), Climate downscaling: techniques and application, *Climate Research*, *7*(2), 85–95.

Hewitson, B., and R. Crane (2006), Consensus between GCM climate change projections with empirical downscaling: Precipitation downscaling over South Africa, *International Journal of Climatology*, *26*(10), 1315–1337.

Hijioka, Y., Y. Matsuoka, H. Nishimoto, M. Masui, and M. Kainuma (2008), Global GHG emissions scenarios under GHG concentration stabilization targets, *Journal of Global Environmental Engineering*, *13*, 97–108.

Hirabayashi, Y., S. Kanae, S. Emori, T. Oki, and M. Kimoto (2008), Global projections of changing risks of floods and droughts in a changing climate, *Hydrological Sciences Journal*, *53*(4), 754–772.

Hisdal, H., B. Clausen, A. Gustard, E. Peters, and L. Tallaksen (2004), Event Definitions and Indices, in: *Hydrological Drought Processes and Estimation Methods for Streamflow and Groundwater* (Tallaksen, L., and H. van Lanen, eds.), pp. 139–198, Developments inWater Science, 48, Elsevier Science B.V., Amsterdam.

Hisdal, H., K. Stahl, L. Tallaksen, and S. Demuth (2001), Have streamflow droughts in Europe become more severe or frequent?, *International Journal of Climatology*, *21*(3), 317–333.

Hisdal, H., and L. Tallaksen (2000), *Drought Event Definition*, Tech. rep., ARIDE Technical Report no. 6. University of Oslo, Oslo, Norway.

Hisdal, H., and L. Tallaksen (2003), Estimation of regional meteorological and hydrological drought characteristics: a case study for Denmark, *Journal of Hydrology*, *281*(3), 230–247.

Hoerling, M., and A. Kumar (2003), The perfect ocean for drought., *Science*, *299*(5607), 691–694.

Horton, P., B. Schaefli, A. Mezghani, B. Hingray, and A. Musy (2006), Assessment of climate-change impacts on alpine discharge regimes with climate model uncertainty, *Hydrological Processes*, *20*(10), 2091–2109.

Hu, Z.-Z., and B. Huang (2009), Interferential Impact of ENSO and PDO on Dry and Wet Conditions in the U.S. Great Plains, *Journal of Climate*, *22*(22), 6047–6065.

Hulme, M., E. Barrow, N. Arnell, P. Harrison, T. Johns, and T. Downing (1999), Relative impacts of human-induced climate change and natural climate variability, *Nature*, *397*(6721), 688–691.

Hunt, B. (2009), Multi-annual dry episodes in Australian climatic variability, *International Journal of Climatology*, *29*(12), 1715–1730.

Huntingford, C., J. Lowe, B. Booth, C. Jones, G. Harris, L. Gohar, and P. Meir (2009), Contributions of carbon cycle uncertainty to future climate projection spread, *Tellus B*, *61*(2), 355–360.

Huntington, T. (2006), Evidence for intensification of the global water cycle: Review and synthesis, *Journal of Hydrology*, *319*(14), 83–95.

Hurkmans, R., W. Terink, R. Uijlenhoet, P. Torfs, D. Jacob, and P. Troch (2010), Changes in Streamflow Dynamics in the Rhine Basin under Three High-Resolution Regional Climate Scenarios, *Journal of Climate*, *23*(3), 679–699.

Hurrell, J. (1995), Decadal Trends in the North Atlantic Oscillation: Regional Temperatures and Precipitation, *Science*, *269*(5224), 676–679.

Hurrell, J., and H. van Loon (1997), Decadal trends in the North Atlantic Oscillation: regional temperatures and precipitation, *Climatic Change*, *36*(3-4), 301–326.

Husak, G., J. Michaelsen, and C. Funk (2007), Use of the gamma distribution to represent monthly rainfall in Africa for drought monitoring applications, *International Journal of Climatology*, *27*(7), 935–944.

Huss, M. (2011), Present and future contribution of glacier storage change to runoff from macroscale drainage basins in Europe, *Water Resources Research*, *47*(7), W07,511.

Iglesias, A., L. Garrote, F. Flores, and M. Moneo (2006), Challenges to Manage the Risk of Water Scarcity and Climate Change in the Mediterranean, *Water Resources Management*, *21*(5), 775–788.

Iizumi, T., M. Nishimori, K. Dairaku, S. Adachi, and M. Yokozawa (2011), Evaluation and intercomparison of downscaled daily precipitation indices over Japan in present-day climate: Strengths and weaknesses of dynamical and bias correction-type statistical downscaling methods, *Journal of Geophysical Research*, *116*, D01,111.

IPCC (2012), Managing the Risks of Extreme Events and Disasters to Advance Climate Change Adaptation, in: *A Special Report of Working Groups I and II of the Intergovernmental Panel on Climate Change* (Field, C., V. Barros, T. Stocker, D. Qin, D. Dokken, K. Ebi, M. Mastrandrea, K. Mach, G.-K. Plattner, S. Allen, M. Tignor, and P. Midgley, eds.), p. 582, Cambridge University Press, Cambridge, UK and New York, NY, USA.

Ison, N., A. Feyerherm, and L. Bark (1971), Wet Period Precipitation and the Gamma Distribution, *Journal of Applied Meteorology*, *10*(4), 658–665.

Jacob, D., L. Bärring, O. Christensen, J. Christensen, M. D. Castro, M. Déqué, F. Giorgi, S. Hagemann, M. Hirschi, R. Jones, E. Kjellström, G. Lenderink, B. Rockel, E. Sánchez, C. Schär, S. Seneviratne, S. Somot, A. V. Ulden, and B. V. D. Hurk (2007), An inter-comparison of regional climate models for Europe : model performance in present-day climate, *Climatic change*, *81*(S1), 31–52.

Janža, M. (2011), Impact assessment of projected climate change on the hydrological regime in the SE Alps, Upper Soča River basin, Slovenia, *Natural Hazards*, pp. 1–19.

Jasper, K., P. Calanca, D. Gyalistras, and J. Fuhrer (2004), Differential impacts of climate change on the hydrology of two alpine river basins, *Climate Research*, *26*(2), 113–129.

Jeton, A., M. Dettinger, and J. Smith (1996), *Potential Effects of Climate Change on Streamflow: Eastern and Western Slopes of the Sierra Nevada, California and Nevada*, Tech. rep., U.S. Geological Survey, Water Resources Investigations Report 954260.

Kampragoua, E., S. Apostolakia, E. Manolia, J. Froebrichb, and D. Assimacopoulos (2011), Towards the harmonization of water-related policies for managing drought risks across the EU, *Environmental Science & Policy*, *14*(7), 815–824.

Kangas, R., and T. Brown (2007), Characteristics of US drought and pluvials from a high-resolution spatial dataset, *International Journal of Climatology*, *27*(10), 1303–1325.

Karl, T. (1986), The Sensitivity of the Palmer Drought Severity Index and Palmer's Z-Index to their Calibration Coefficients Including Potential Evapotranspiration, *Journal of Climate and Applied Meteorology*, *25*(1), 77–86.

Katz, R., and B. Brown (1992), Extreme events in a changing climate: Variability is more important than averages, *Climatic Change*, *21*(3), 289–302.

Kelly, P., P. Jones, and J. Pengqun (1996), The spatial response of the climate system to explosive volcanic eruptions, *International Journal of Climatology*, *16*(5), 537–550.

Kelly, P., and T. Wigley (1992), Solar cycle length, greenhouse forcing and global climate, *Nature*, *360*(6402), 328–330.

Kendon, E. J., D. P. Rowell, R. G. Jones, and E. Buonomo (2008), Robustness of Future Changes in Local Precipitation Extremes, *Journal of Climate*, *21*(17), 4280–4297.

Keyantash, J., and J. Dracup (2002), The Quantification of Drought: An Evaluation of Drought Indices, *Bulletin of the American Meteorological Society*, *83*(8), 1167–1180.

Keyantash, J., and J. Dracup (2004), An aggregate drought index: Assessing drought severity based on fluctuations in the hydrologic cycle and surface water storage, *Water Resources Research*, *40*(9), W09,304.

Khan, S., H. Gabriel, and T. Rana (2008), Standard precipitation index to track drought and assess impact of rainfall on watertables in irrigation areas, *Irrigation and Drainage Systems*, *22*(2), 159–177.

Kharin, V., and F. Zwiers (2005), Estimating Extremes in Transient Climate Change Simulations, *Journal of Climate*, *18*(8), 1156–1173.

Kiem, A., and D. Verdon-Kidd (2010), Towards understanding hydroclimatic change in Victoria, Australia preliminary insights into the "Big Dry", *Hydrology and Earth System Sciences*, *14*(3), 433–445.

Kingston, D., M. Todd, R. Taylor, J. Thompson, and N. Arnell (2009), Uncertainty in the estimation of potential evapotranspiration under climate change, *Geophysical Research Letters*, *36*(20), L20,403.

Kirono, D., D. Kent, K. Hennessy, and F. Mpelasoka (2011), Characteristics of Australian droughts under enhanced greenhouse conditions: Results from 14 global climate models, *Journal of Arid Environments*, *75*(6), 566–575.

Kjellström, E. (2004), Recent and Future Signatures of Climate Change in Europe, *AMBIO: A Journal of the Human Environment*, *33*(4), 193–198.

Kjellström, E., G. Nikulin, U. Hansson, G. Strandberg, and A. Ullerstig (2011), 21st century changes in the European climate: uncertainties derived from an ensemble of regional climate model simulations, *Tellus A*, *63*(1), 24–40.

Knutti, R. (2008), Should we believe model predictions of future climate change?, *Philosophical transactions. Series A, Mathematical, physical, and engineering sciences*, *366*(1885), 4647–4664.

Knutti, R., R. Furrer, C. Tebaldi, J. Cermak, and G. Meehl (2010), Challenges in combining projections from multiple climate models, *Journal of Climate*, *23*(10), 2739–2758.

Kotlarski, S., T. Bosshard, E. Fischer, D. Lüthi, and C. Schär (2010), Climate scenarios for the European Alps and extreme events, Climate Change Scenario Workshop, 2 March 2010, Zurich, Switzerland.

Koutroulis, A., A.-E. Vrohidou, and I. Tsanis (2011), Spatiotemporal Characteristics of Meteorological Drought for the Island of Crete, *Journal of Hydrometeorology*, *12*(2), 206–226.

Kuhlmann, J., and J. Quaas (2010), How can aerosols affect the Asian summer monsoon? Assessment during three consecutive pre-monsoon seasons from CALIPSO satellite data, *Atmospheric Chemistry and Physics Discussions*, *10*(2), 4887–4926.

Kundzewicz, Z., M. Radziejewski, and I. Pinskwar (2006), Precipitation extremes in the changing climate of Europe, *Climate Research*, *31*(1), 51–58.

Kundzewicz, Z., and E. Stakhiv (2010), Are climate models ready for prime time in water resources management applications, or is more research needed?, *Hydrological Sciences Journal*, *55*(7), 1085 – 1089.

Kyselý, J., L. Gaál, R. Beranová, and E. Plavcová (2010), Climate change scenarios of precipitation extremes in Central Europe from ENSEMBLES regional climate models, *Theoretical and Applied Climatology*, *104*(3-4), 529–542.

Labat, D., Y. Goddéris, J. Probst, and J. Guyot (2004), Evidence for global runoff increase related to climate warming, *Advances in Water Resources*, *27*(6), 631–642.

Laghari, A., D. Vanham, and W. Rauch (2012), To what extent does climate change result in a shift in Alpine hydrology? A case study in the Austrian Alps, *Hydrological Sciences Journal*, *57*(1), 103–117.

Lau, K., M. Kim, and K. Kim (2006), Asian summer monsoon anomalies induced by aerosol direct forcing: the role of the Tibetan Plateau, *Climate Dynamics*, *26*(7-8), 855–864.

Lau, K.-M., and K.-M. Kim (2006), Observational relationships between aerosol and Asian monsoon rainfall, and circulation, *Geophysical Research Letters*, *33*, L21,810.

Lavaysse, C., M. Vrac, P. Drobinski, M. Lengaigne, and T. Vischel (2012), Statistical downscaling of the French Mediterranean climate: assessment for present and projection in an anthropogenic scenario, *Natural Hazards and Earth System Science*, *12*(3), 651–670.

Le Houérou, H. (1996), Climate change, drought and desertification, *Journal of Arid Environments*, *34*(2), 133–185.

Lean, J., J. Beer, and R. Bradley (1995), Reconstruction of solar irradiance since 1610: Implications for climate change, *Geophysical Research Letters*, *22*(23), 3195–3198.

Legesse, D., T. Abiye, C. Vallet-Coulomb, and H. Abate (2010), Streamflow sensitivity to climate and land cover changes: Meki River, Ethiopia, *Hydrology and Earth System Sciences*, *14*, 2277–2287.

Lehner, B., P. Döll, J. Alcamo, T. Henrichs, and F. Kaspar (2006), Estimating the Impact of Global Change on Flood and Drought Risks in Europe: A Continental, Integrated Analysis, *Climatic Change*, *75*(3), 273–299.

Lei, Y., and A. Duan (2011), Prolonged dry episodes and drought over China, *International Journal of Climatology*, *31*(12), 1831–1840.

Li, H., A. Dai, T. Zhou, and J. Lu (2010), Responses of East Asian summer monsoon to historical SST and atmospheric forcing during 19502000, *Climate Dynamics*, *34*, 501–514.

Li, J., F. Chen, E. Cook, X. Gou, and Y. Zhang (2007a), Drought reconstruction for North Central China from tree rings: the value of the Palmer drought severity index, *International Journal of Climatology*, *27*(7), 903–909.

Li, L., B. Wang, and T. Zhou (2007b), Contributions of natural and anthropogenic forcings to the summer cooling over eastern China: An AGCM study, *Geophysical Research Letters*, *34*, 1–5.

Li, Y., W. Ye, M. Wang, and X. Yan (2009), Climate change and drought: a risk assessment of crop-yield impacts, *Climate Research*, *39*(1), 31–46.

Liang, L., and Q. Liu (2013), Streamflow sensitivity analysis to climate change for a large water-limited basin, *Hydrological Processes*, p. in press.

Liang, S., S. Ge, L. Wan, and J. Zhang (2010), Can climate change cause the Yellow River to dry up?, *Water Resources Research*, *46*, W02,505.

Liepert, B., and M. Previdi (2012), Inter-model variability and biases of the global water cycle in CMIP3 coupled climate models, *Environmental Research Letters*, *7*(1), 14,006.

Linderholm, H., T. Ou, J.-H. Jeong, C. Folland, D. Gong, H. Liu, Y. Liu, and D. Chen (2011), Interannual teleconnections between the summer North Atlantic Oscillation and the East Asian summer monsoon, *Journal of Geophysical Research*, *116*(D13), D13,107.

Lioubimtseva, E., and R. Cole (2006), Uncertainties of Climate Change in Arid Environments of Central Asia, *Reviews in Fisheries Science*, *14*(1-2), 29–49.

Lioubimtseva, E., R. Cole, J. Adams, and G. Kapustin (2005), Impacts of climate and land-cover changes in arid lands of Central Asia, *Journal of Arid Environments*, *62*(2), 285–308.

Lioubimtseva, E., and G. Henebry (2009), Climate and environmental change in arid Central Asia: Impacts, vulnerability, and adaptations, *Journal of Arid Environments*, *73*(11), 963–977.

Lioubimtseva, E., J. Kariyeva, and G. Henebry (2012), Climate Change in Turkmenistan, in: *The Handbook of Environmental Chemistry*, The Handbook of Environmental Chemistry, pp. 1–19, Springer Berlin / Heidelberg.

Liu, Q., and B. Cui (2011), Impacts of climate change/variability on the streamflow in the Yellow River Basin, China, *Ecological Modelling*, *222*(2), 268–274.

Liu, X., W. Liu, and J. Xia (2012), Comparison of the streamflow sensitivity to aridity index between the Danjiangkou Reservoir basin and Miyun Reservoir basin, China, *Theoretical and Applied Climatology*.

Liu, Y., J. Stanturf, and S. Goodrick (2010), Trends in global wildfire potential in a changing climate, *Forest Ecology and Management*, *259*(4), 685–697.

Liu, Y., J. Sun, and B. Yang (2009), The effects of black carbon and sulphate aerosols in China regions on East Asia monsoons, *Tellus, Series B: Chemical and Physical Meteorology*, *61*(4), 642–656.

Lloyd-Hughes, B., and M. Saunders (2002), A drought climatology for Europe, *International Journal of Climatology*, *22*(13), 1571–1592.

Lockwood, J. (1999), Is Potential Evapotranspiration and Its Relationship with Actual Evapotranspiration Sensitive to Elevated Atmospheric CO2 Levels?, *Climatic Change*, *41*(2), 193–212.

Lockwood, M. (2012), Solar Influence on Global and Regional Climates, *Surveys in Geophysics*, *33*(3-4), 503–534.

Logan, K., N. Brunsell, A. Jones, and J. Feddema (2010), Assessing spatiotemporal variability of drought in the U.S. central plains, *Journal of Arid Environments*, *74*(2), 247–255.

Lopez, A., F. Fung, M. New, G. Watts, A. Weston, and R. Wilby (2009), From climate model ensembles to climate change impacts and adaptation: A case study of water resource management in the southwest of England, *Water Resources Research*, *45*(8), W08,419.

López-Moreno, J., and J. García-Ruiz (2004), Influence of snow accumulation and snowmelt on streamflow in the central Spanish Pyrenees, *Hydrological Sciences Journal*, *49*(5), 787l–802.

López-Moreno, J., and S. Vicente-Serrano (2008), Positive and Negative Phases of the Wintertime North Atlantic Oscillation and Drought Occurrence over Europe: A Multitemporal-Scale Approach, *Journal of Climate*, *21*(6), 1220–1243.

Loukas, A., and L. Vasiliades (2004), Probabilistic analysis of drought spatiotemporal characteristics inThessaly region, Greece, *Natural Hazards and Earth System Sciences*, *4*(5/6), 719–731.

Loukas, A., L. Vasiliades, and J. Tzabiras (2008), Climate change effects on drought severity, *Advances in Geosciences*, *17*, 23–29.

Lu, E. (2011), A Method for Monitoring Meteorological Drought at Daily Scale, in: *36th NOAA Annual Climate Diagnostics and Prediction Workshop*, p. 7, Science and Technology Infusion Climate Bulletin. NOAAs National Weather Service, Fort Worth, TX, 3-6 October 2011.

Lu, J., G. Sun, S. McNulty, and D. Amatya (2005), A comparison of six potential evapotranspiration methods for regional use in the southeastern United States, *Journal of the American Water Resources Association*, *41*(3), 621–633.

Lutz, A., W. Immerzeel, A. Gobiet, F. Pellicciotti, and M. Bierkens (2012), New climate change scenarios reveal uncertain future for Central Asian glaciers, *Hydrology and Earth System Sciences Discussions*, *9*, 12,691–12,727.

Lyon, B. (2009), Southern Africa Summer Drought and Heat Waves: Observations and Coupled Model Behavior, *Journal of Climate*, *22*(22), 6033–6046.

Maracchi, G., O. Sirotenko, and M. Bindi (2005), Impacts of Present and Future Climate Variability on Agriculture and Forestry in the Temperate Regions: Europe, *Climatic Change*, *70*(1-2), 117–135.

Maraun, D., F. Wetterhall, A. M. Ireson, R. E. Chandler, E. J. Kendon, M. Widmann, S. Brienen, H. W. Rust, T. Sauter, M. Themel, V. K. C. Venema, K. P. Chun, C. M. Goodess, R. G. Jones, C. Onof, M. Vrac, and I. Thiele-Eich (2010), Precipitation downscaling under climate change: Recent developments to bridge the gap between dynamical models and the end user, *Rev. Geophys.*, *48*(3), RG3003.

Marsh, T., G. Cole, and R. Wilby (2007), Major droughts in England and Wales, 18002006, *Weather*, *62*(4), 87–93.

Martin, E., B. Timbal, and E. Brun (1996), Downscaling of general circulation model outputs: simulation of the snow climatology of the French Alps and sensitivity to climate change, *Climate Dynamics*, *13*(1), 45–46.

McAlpine, C., J. Syktus, J. Ryan, R. Deo, G. Mckeon, H. Mcgowan, and S. R. Phinn (2009), A continent under stress: interactions, feedbacks and risks associated with impact of modified land cover on Australia's climate, *Global Change Biology*, *15*(9), 2206–2223.

McCrary, R., and D. Randall (2010), Great Plains Drought in Simulations of the Twentieth Century, *Journal of Climate*, *23*(8), 2178–2196.

McGregor, G., C. Ferro, and D. Stephenson (2005), Projected Changes in Extreme Weather and Climate Events in Europe, in: *Extreme Weather Events and Public Health Responses SE - 2* (Kirch, W., R. Bertollini, and B. Menne, eds.), pp. 13–23, Springer Berlin Heidelberg.

Mckee, T., N. Doesken, and J. Kleist (1993), The relationship of drought frequency and duration to time scales, in: *Preprints, 8th Conference on Applied Climatology*, January, pp. 179–184, 17-22 January, Anaheim, CA.

Mckee, T., N. Doesken, and J. Kleist (1995), Drought monitoring with multiple time scales, in: *Preprints, 9th Conference on Applied Climatology*, pp. 233–236, 15-20 January 1995, AMS, Dallas, TX.

McKenney, M., and N. Rosenberg (1993), Sensitivity of some potential evapotranspiration estimation methods to climate change, *Agricultural and Forest Meteorology*, *64*(1-2), 81–110.

Mearns, L., I. Bogardi, F. Giorgi, I. Matyasovszky, and M. Palecki (1999), Comparison of climate change scenarios generated from regional climate model experiments and statistical downscaling, *Journal of Geophysical Research*, *104*(D6), 6603–6621.

Mechler, R., S. Hochrainer, A. Aaheim, H. Salen, and A. Wreford (2010), Modelling economic impacts and adaptation to extreme events: Insights from European case studies, *Mitigation and Adaptation Strategies for Global Change*, *15*(7), 737–762.

Meehl, G., C. Covey, K. Taylor, T. Delworth, R. Stouffer, M. Latif, B. McAvaney, and J. B. Mitchell (2007), THE WCRP CMIP3 Multimodel Dataset: A New Era in Climate Change Research, *Bulletin of the American Meteorological Society*, *88*(9), 1383–1394.

Meehl, G., F. Zwiers, J. Evans, T. Knutson, L. Mearns, and P. Whetton (2000), Trends in Extreme Weather and Climate Events: Issues Related to Modeling Extremes in Projections of Future Climate Change, *Bulletin of the American Meteorological Society*, *81*(3), 427–436.

Meinshausen, M., S. Raper, and T. Wigley (2008), Emulating IPCC AR4 atmosphere-ocean and carbon cycle models for projecting global-mean, hemispheric and land/ocean temperatures: MAGICC 6.0, *Atmospheric Chemistry and Physics Discussions*, *8*(2), 6153–6272.

Meinshausen, M., S. Raper, and T. Wigley (2011a), Emulating coupled atmosphere-ocean and carbon cycle models with a simpler model, MAGICC6 Part 1: Model description and calibration, *Atmospheric Chemistry and Physics*, *11*(4), 1417–1456.

Meinshausen, M., T. Wigley, and S. Raper (2011b), Emulating atmosphere-ocean and carbon cycle models with a simpler model, MAGICC6 Part 2: Applications, *Atmospheric Chemistry and Physics*, *11*(4), 1457–1471.

Méndez, M., and V. Magaña (2010), Regional Aspects of Prolonged Meteorological Droughts over Mexico and Central America, *Journal of Climate*, *23*(5), 1175–1188.

Mendicino, G., A. Senatore, and P. Versace (2008), A Groundwater Resource Index (GRI) for drought monitoring and forecasting in a mediterranean climate, *Journal of Hydrology*, *357*(3-4), 282–302.

Miller, W., T. Piechota, S. Gangopadhyay, and T. Pruitt (2011), Development of streamflow projections under changing climate conditions over Colorado River Basin headwaters, *Hydrology and Earth System Sciences Discussions*, *15*, 2145–2164.

Milly, P., K. Dunne, and A. Vecchia (2005), Global pattern of trends in streamflow and water availability in a changing climate., *Nature*, *438*(7066), 347–50.

Mishra, A., and V. Singh (2010), A review of drought concepts, *Journal of Hydrology*, *391*(1-2), 202–216.

Mishra, A., and V. Singh (2011), Drought modeling A review, *Journal of Hydrology*, *403*(1-2), 157–175.

Mitchell, T. (2003), Pattern Scaling: An Examination of the Accuracy of the Technique for Describing Future Climates, *Climatic Change*, *60*(3), 217–242.

Mitchell, T., T. Carter, P. Jones, M. Hulme, and M. New (2004), *A comprehensive set of high-resolution grids of monthly climate for Europe and the globe : the observed record (1901-2000) and 16 scenarios (2001-2100)*, Tech. Rep. July, Tyndall Centre for Climate Change Research, Norwich, UK.

Mitchell, T., and P. Jones (2005), An improved method of constructing a database of monthly climate observations and associated high-resolution grids, *International Journal of Climatology*, *25*(6), 693–712.

Moberg, A., P. Jones, D. Lister, A. Walther, M. Brunet, J. Jacobeit, L. Alexander, P. Della-Marta, J. Luterbacher, P. Yiou, D. Chen, A. Klein Tank, O. Saladié, J. Sigró, E. Aguilar, H. Alexandersson, C. Almarza, I. Auer, M. Barriendos, M. Begert, H. Bergström, R. Böhm, C. Butler, J. Caesar, A. Drebs, D. Founda, F.-W. Gerstengarbe, G. Micela, M. Maugeri, H. Österle, K. Pandzic, M. Petrakis, L. Srnec, R. Tolasz, H. Tuomenvirta, P. Werner, H. Linderholm, A. Philipp, H. Wanner, and E. Xoplaki (2006), Indices for daily temperature and precipitation extremes in Europe analyzed for the period 19012000, *Journal of Geophysical Research*, *111*(D22), D22,106.

Moser, D., N. Sauberer, and W. Willner (2011), *Generalisation of drought effects on ecosystem goods and services over the Alps*, Tech. rep., Alp-Water-Scarce Internal Project Report.

Moss, R., J. Edmonds, K. Hibbard, M. Manning, S. Rose, D. van Vuuren, T. Carter, S. Emori, M. Kainuma, T. Kram, G. Meehl, J. Mitchell, N. Nakicenovic, K. Riahi, S. Smith, R. Stouffer, A. Thomson, J. Weyant, and T. Wilbanks (2010), The next generation of scenarios for climate change research and assessment, *Nature*, *463*(7282), 747–756.

Motha, R., and W. Baier (2005), Impacts of Present and Future Climate Change and Climate Variability on Agriculture in the Temperate Regions: North America, *Climatic Change*, *70*(1), 137–164.

Mpelasoka, F., K. Hennessy, R. Jones, and B. Bates (2008), Comparison of suitable drought indices for climate change impacts assessment over Australia towards resource, *International Journal of Climatology*, *28*(10), 1283–1292.

Murphy, J. (1999), An Evaluation of Statistical and Dynamical Techniques for Downscaling Local Climate, *Journal of Climate*, *12*(8), 2256–2284.

Murphy, J. (2000), Predictions of climate change over Europe using statistical and dynamical downscaling techniques, *International Journal of Climatology*, *20*(5), 489–501.

Murphy, J., D. Sexton, G. Jenkins, P. Boorman, B. Booth, C. Brown, R. Clark, M. Collins, G. Harris, E. Kendon, R. Betts, S. Brown, K. Humphrey, M. McCarthy, R. McDonald, A. Stephens, C. Wallace, R. Warren, R. Wilby, and R. Wood (2009), *Climate change projections. UK Climate Projections Science Report*, Tech. rep., Met Office Hadley Centre, Exeter.

Nakicenovich, N., and R. Swart (2000), *Special Report on Emissions Scenarios*, Cambridge University Press., Cambridge, UK.

Nalbantis, I., and G. Tsakiris (2008), Assessment of Hydrological Drought Revisited, *Water Resources Management*, *23*(5), 881–897.

Nash, L., and P. Gleick (1991), Sensitivity of streamflow in the Colorado Basin to climatic changes, *Journal of Hydrology*, *125*(3-4), 221–241.

New, M. (2002), Climate change and water resources in the southwestern Cape, South Africa, *South African Journal Of Science*, *98*(7-8), 369–376.

New, M., A. Lopez, S. Dessai, and R. Wilby (2007), Challenges in using probabilistic climate change information for impact assessments: an example from the water sector, *Philosophical Transactions of the Royal Society A: Mathematical, Physical and Engineering Sciences*, *365*(1857), 2117–2131.

Nicholls, N. (2004), The Changing Nature of Australian Droughts, *Climatic Change*, *63*(3), 323–336.

Nohara, D., A. Kitoh, M. Hosaka, and T. Oki (2006), Impact of Climate Change on River Discharge Projected by Multimodel Ensemble, *Journal of Hydrometeorology*, *7*(5), 1076–1089.

Osborn, T. (2009), *A user guide for ClimGen : a flexible tool for generating monthly climate data sets and scenarios ClimGen version 1-02*, February, Climatic Research Unit, School of Environmental Sciences, University of East Anglia, Norwich.

Overpeck, J., K. Hughen, D. Hardy, R. Bradley, R. Case, M. Douglas, B. Finney, K. Gajewski, G. Jacoby, A. Jennings, S. Lamoureux, A. Lasca, G. MacDonald, J. Moore, M. Retelle, S. Smith, A. Wolfe, and G. Zielinski (1997), Arctic Environmental Change of the Last Four Centuries, *Science*, *278*(5341), 1251–1256.

Overpeck, J., and B. Udall (2010), Dry Times Ahead, *Science*, *328*(5986), 1642–1643.

Paeth, H., N. Hall, M. Gaertner, M. Alonso, S. Moumouni, J. Polcher, P. M. Ruti, A. H. Fink, M. Gosset, T. Lebel, A. T. Gaye, D. P. Rowell, W. Moufouma-Okia, D. Jacob, B. Rockel, F. Giorgi, and M. Rummukainen (2011), Progress in regional downscaling of west African precipitation, *Atmospheric Science Letters*, *12*(1), 75–82.

Pal, J., F. Giorgi, and X. Bi (2004), Consistency of recent European summer precipitation trends and extremes with future regional climate projections, *Geophysical Research Letters*, *31*(13), L13,202.

Palmer, W. (1965), *Meteorological drought. Research Paper No. 45.*, U.S. Weather Bureau.

Palmer, W. (1968), Keeping track of crop moisture conditions, nationwide: The new crop moisture index, *Weatherwise*, *21*(4), 156–161.

Panu, U., and T. Sharma (2002), Challenges in drought research: some perspectives and future directions, *Hydrological Sciences Journal*, *47*(1), 19–30.

Pappenberger, F., and K. Beven (2006), Ignorance is bliss: Or seven reasons not to use uncertainty analysis, *Water Resources Research*, *42*(5), W05,302.

Parker, D., C. Folland, A. Scaife, J. Knight, A. Colman, P. Baines, and B. Dong (2007), Decadal to multidecadal variability and the climate change background, *Journal of Geophysical Research*, *112*(D18), D18,115.

Parker, W. (2010a), Predicting weather and climate: Uncertainty, ensembles and probability, *Studies In History and Philosophy of Science Part B: Studies In History and Philosophy of Modern Physics*, *41*(3), 263–272.

Parker, W. (2010b), Whose Probabilities? Predicting Climate Change with Ensembles of Models, *Philosophy of Science*, *77*(5), 985–997.

Paulo, A., and L. Pereira (2006), Drought Concepts and Characterization, *Water International*, *31*(1), 37–49.

Pausas, J. (2004), Changes in Fire and Climate in the Eastern Iberian Peninsula (Mediterranean Basin), *Climatic Change*, *63*(3), 337–350.

Peel, M., B. Finlayson, and T. McMahon (2007), Updated world map of the Köppen-Geiger climate classification, *Hydrology and Earth System Sciences*, *11*(5), 1633–1644.

Perez, G. C., M. van Huijgevoort, F. Voß, and H. van Lanen (2011), On the spatio-temporal analysis of hydrological droughts from global hydrological models, *Hydrology and Earth System Sciences*, *8*(1), 619–652.

Perry, A. (1976), The long drought of 1975-76, *Weather*, *31*(10), 328–336.

Peters, E., G. Bier, H. van Lanen, and P. Torfs (2006), Propagation and spatial distribution of drought in a groundwater catchment, *Journal of Hydrology*, *321*(1-4), 257–275.

Peters, E., P. Torfs, H. van Lanen, and G. Bier (2003), Propagation of drought through groundwatera new approach using linear reservoir theory, *Hydrological Processes*, *17*(15), 3023–3040.

Peters, E., and H. van Lanen (2003), Propagation of drought in groundwater in semi-arid and sub-humid climatic regimes, *Hydrology of the Mediterranean and Semi-Arid Regions, vol. 278IAHS*, *278IAHS*, 312–317.

Peters, E., H. van Lanen, P. Torfs, and G. Bier (2005), Drought in groundwaterdrought distribution and performance indicators, *Journal of Hydrology*, *306*(1-4), 302–317.

Pfister, L., J. Kwadijk, A. Musy, A. Bronstert, and L. Hoffmann (2004), Climate change, land use change and runoff prediction in the RhineMeuse basins, *River Research and Applications*, *20*(3), 229–241.

Piao, S., P. Ciais, Y. Huang, Z. Shen, S. Peng, J. Li, L. Zhou, H. Liu, Y. Ma, Y. Ding, P. Friedlingstein, C. Liu, K. Tan, Y. Yu, T. Zhang, and J. Fang (2010), The impacts of climate change on water resources and agriculture in China, *Nature*, *467*(7311), 43–51.

Pierce, D., T. Barnett, B. Santer, and P. Gleckler (2009), Selecting global climate models for regional climate change studies, *Proceedings of the National Academy of Sciences*, *106*(21), 8441–8446.

Pilling, C., and J. Jones (2002), The impact of future climate change on seasonal discharge, hydrological processes and extreme flows in the Upper Wye experimental catchment, Mid-Wales, *Hydrological Processes*, *16*(6), 1201–1213.

Planton, S., M. Déqué, F. Chauvin, and L. Terray (2008), Expected impacts of climate change on extreme climate events, *Comptes Rendus Geosciences*, *340*(9-10), 564–574.

Potter, N., F. Chiew, and A. Frost (2010), An assessment of the severity of recent reductions in rainfall and runoff in the MurrayDarling Basin, *Journal of Hydrology*, *381*(1-2), 52–64.

Prudhomme, C., and H. Davies (2008), Assessing uncertainties in climate change impact analyses on the river flow regimes in the UK. Part 2: future climate, *Climatic Change*, *93*(1-2), 197–222.

Prudhomme, C., S. Parry, J. Hannaford, D. Clark, S. Hagemann, and F. Voss (2011), How well do large-scale models reproduce regional hydrological extremes in Europe?, *Journal of Hydrometeorology*, *12*(6), 1181–1204.

Quevauviller, P. (2011), Adapting to climate change: reducing water-related risks in Europe EU policy and research considerations, *Environmental Science & Policy*, *14*(7), 722–729.

Quiring, S. (2009a), Developing Objective Operational Definitions for Monitoring Drought, *Journal of Applied Meteorology and Climatology*, *48*(6), 1217–1229.

Quiring, S. (2009b), Monitoring Drought: An Evaluation of Meteorological Drought Indices, *Geography Compass*, *3*(1), 64–88.

R Development Core Team (2012), *R: A Language and Environment for Statistical Computing*, R Foundation for Statistical Computing, Vienna, Austria.

Räisänen, J. (2001), CO2 -Induced Climate Change in CMIP2 Experiments: Quantification of Agreement and Role of Internal Variability, *Journal of Climate*, *14*(9), 2088–2104.

Räisänen, J. (2002), CO2 - Induced Changes in Interannual Temperature and Precipitation Variability in 19 CMIP2 Experiments, *Journal of Climate*, *15*(17), 2395–2411.

Räisänen, J., U. Hansson, A. Ullerstig, R. Döscher, L. Graham, C. Jones, H. Meier, P. Samuelsson, and U. Willén (2004), European climate in the late twenty-first century: regional simulations with two driving global models and two forcing scenarios, *Climate Dynamics*, *22*(1), 13–31.

Raje, D., and P. Mujumdar (2010), Hydrologic drought prediction under climate change: Uncertainty modeling with Dempster-Shafer and Bayesian approaches, *Advances in Water Resources*, *33*(9), 1176–1186.

Ramanathan, V., and Y. Feng (2009), Air pollution, greenhouse gases and climate change: Global and regional perspectives, *Atmospheric Environment*, *43*(1), 37–50.

Rampino, M., and S. Self (1992), Volcanic winter and accelerated glaciation following the Toba super-eruption, *Nature*, *359*(6390), 50–52.

Ratcliffe, R., M. Miles, B. Rydz, and E. Shaw (1978), Meteorological Aspects of the 1975-76 Drought [and Discussion], *Proceedings of the Royal Society A: Mathematical, Physical and Engineering Sciences*, *363*(1712), 3–20.

Raziei, T., I. Bordi, L. Pereira, and A. Sutera (2010), Space-time variability of hydrological drought and wetness in Iran using NCEP/NCAR and GPCC datasets, *Hydrology and Earth System Sciences*, *14*, 1919–1930.

Redaud, J., J. Noilhan, M. Gillet, M. Huc, and G. Begni. (2002), *Climate Change and Its Impact on the Water Regime in France*, Tech. rep., MEDIAS/GB/db/2002/162. Ministère de l'Ecologie et du Dévelopment Durable. Toulouse. Available at http://www.uicnmed.org/web2007/CDCambio_climatico/contenido/E/PDF/CC_e2a.pdf.

Reichler, T., and J. Kim (2008), How Well Do Coupled Models Simulate Today's Climate?, *Bulletin of the American Meteorological Society*, *89*(3), 303–311.

Renner, M., and C. Bernhofer (2012), Applying simple water-energy balance frameworks to predict the climate sensitivity of streamflow over the continental United States, *Hydrology and Earth System Sciences*, *16*(8), 2531–2546.

Riahi, K., A. Grubler, and N. Nakicenovic (2007), Scenarios of long-term socio-economic and environmental development under climate stabilization, *Technological Forecasting and Social Change*, *74*(7), 887–935.

Rind, D., R. Goldberg, J. Hansen, C. Rosenzweig, and R. Ruedy (1990), Potential evapotranspiration and the likelihood of future drought, *Journal of Geophysical Research: Atmospheres*, *95*(D7), 9983–10,004.

Risbey, J., and D. Entekhabi (1996), Observed Sacramento Basin streamflow response to precipitation and temperature changes and its relevance to climate impact studies, *Journal of Hydrology*, *184*(3-4), 209–223.

Roald, L., S. Beldring, T. Engen-Skaugen, E. Fø rland, and R. Benestad (2006), *Climate Change Impacts on Streamflow in Norway*, Tech. rep., Norwegian Water Resources and Energy Directorate, Report A1-2006.

Roald, L., S. Beldring, and T. Skaugen (2004), Scenarios of annual and seasonal runoff in Norway, in: *XXIII Nordic Hydrological Conference Selected Articles NHP Report 48, vol. I* (Järvet, A., ed.), pp. 71–76.

Robinson, P., and A. Henderson-Sellers (1999), *Contemporary Climatology*, 2nd edn., Longman Press, Singapore.

Robock, A. (2000), Volcanic eruptions and climate, *Reviews of Geophysics*, *38*(2), 191–219.

Rodó, X., E. Baert, and F. Comín (1997), Variations in seasonal rainfall in Southern Europe during the present century: relationships with the North Atlantic Oscillation and the El Niño-Southern Oscillation, *Climate Dynamics*, *13*(4), 275–284.

Rogelj, J., M. Meinshausen, and R. Knutti (2012), Global warming under old and new scenarios using IPCC climate sensitivity range estimates, *Nature Climate Change*, *2*(4), 248–253.

Rouault, M., and Y. Richard (2005), Intensity and spatial extent of droughts in southern Africa, *Geophysical Research Letters*, *32*, L15,702.

Roudier, P., and G. Mahe (2010), Study of water stress and droughts with indicators using daily data on the Bani river (Niger basin, Mali), *International Journal of Climatology*, *30*(11), 1689–1705.

Rowell, D. (2005), A scenario of European climate change for the late twenty-first century: seasonal means and interannual variability, *Climate Dynamics*, *25*(7-8), 837–849.

Rowell, D. (2006), A Demonstration of the Uncertainty in Projections of UK Climate Change Resulting from Regional Model Formulation, *Climatic Change*, *79*(3-4), 243–257.

Rowell, D., and R. Jones (2006), Causes and uncertainty of future summer drying over Europe, *Climate Dynamics*, *27*(2-3), 281–299.

Ruosteenoja, K., and P. Räisänen (2013), Seasonal Changes in Solar Radiation and Relative Humidity in Europe in Response to Global Warming, *Journal of Climate*, *26*(8), 2467–2481.

Salinger, M. (2005), Climate Variability and Change: Past, Present and Future An Overview, *Climatic Change*, *70*(1-2), 9–29.

Sankarasubramanian, A., and R. Vogel (2003), Hydroclimatology of the continental United States, *Geophysical Research Letters*, *30*(7), 1363.

Sankarasubramanian, A., R. Vogel, and J. Limbrunner (2001), Climate elasticity of streamflow in the United States, *Water Resources Research*, *37*(6), 1771.

Santer, B., K. Taylor, P. Gleckler, C. Bonfils, T. Barnett, D. Pierce, T. Wigley, C. Mears, F. Wentz, W. Brüggemann, N. Gillett, S. Klein, S. Solomon, P. Stott, and M. Wehner (2009), Incorporating model quality information in climate change detection and attribution studies., *Proceedings of the National Academy of Sciences of the United States of America*, *106*(35), 14,778–83.

Santer, B., T. Wigley, M. Schlesinger, and J. Mitchell (1990), *Developing climate scenarios from equilibrium GCM results*, Tech. rep., MPI Report Number 47, Hamburg.

Schaake, J. (1990), From climate to flow, in: *Climate Change and U.S. Water Resources* (Waggoner, P., ed.), chap. 8, pp. 177–206, John Wiley and Sons, New York.

Schaake, J., and L. Chunzhen (1989), Development and application of simple water balance models to understand the relationship between climate and water resources, in: *New directions for surface water modelling, Proceedings of the Baltimore Symposium*, IAHS Publ. no.181.

Schär, C., and G. Jendritzky (2004), Hot news from summer 2003, *Nature*, *432*, 559–560.

Schmidli, J., C. Goodess, C. Frei, M. Haylock, Y. Hundecha, J. Ribalaygua, and T. Schmith (2007), Statistical and dynamical downscaling of precipitation: An evaluation and comparison of scenarios for the European Alps, *Journal of Geophysical Research*, *112*, D04,105.

Schneider, S. (1983), CO2, Climate and Society: A Brief Overview, in: *Social Science Research and Climate Changee: An Interdisciplinary Appraisal* (Chen, R., E. Boulding, and S. Schneider, eds.), pp. 9–15, Springer Netherlands, Boston.

Schubert, S., D. Gutzler, H. Wang, A. Dai, T. Delworth, C. Deser, K. Findell, R. Fu, W. Higgins, M. Hoerling, B. Kirtman, R. Koster, A. Kumar, D. Legler, D. Lettenmaier, B. Lyon, V. Magana, K. Mo, S. Nigam, P. Pegion, A. Phillips, R. Pulwarty, D. Rind, A. Ruiz-Barradas, J. Schemm, R. Seager, R. Stewart, M. Suarez, J. Syktus, M. Ting, C. Wang, S. Weaver, and N. Zeng (2009), A U.S. CLIVAR Project to Assess and Compare the Responses of Global Climate Models to Drought-Related SST Forcing Patterns: Overview and Results, *Journal of Climate*, *22*(19), 5251–5272.

Seager, R., N. Naik, and L. Vogel (2012), Does Global Warming Cause Intensified Interannual Hydroclimate Variability?, *Journal of Climate*, *25*(9), 3355–3372.

Sefton, C., and D. Boorman (1997), A regional investigation of climate change impacts on UK streamflows, *Journal of Hydrology*, *195*(1-4), 26–44.

Semenov, M. (2007), Development of high-resolution UKCIP02-based climate change scenarios in the UK, *Agricultural and Forest Meteorology*, *144*(1-2), 127–138.

Seneviratne, S., D. Lüthi, M. Litschi, and C. Schär (2006), Land-atmosphere coupling and climate change in Europe, *Nature*, *443*(7108), 205–209.

Seneviratne, S., N. Nicholls, D. Easterling, C. Goodess, S. Kanae, J. Kossin, Y. Luo, J. Marengo, K. McInnes, M. Rahimi, M. Reichstein, A. Sorteberg, C. Vera, and X. Zhang (2012), Changes in climate extremes and their impacts on the natural physical environment, in: *Managing the Risks of Extreme Events and Disasters to Advance Climate Change* (Field, C., V. Barros, T. Stocker, D. Qin, D. Dokken, K. Ebi, M. Mastrandrea, K. Mach, G.-K. Plattner, S. Allen, M. Tignor, and P. Midgley, eds.), a special edn., pp. 109–230, Cambridge University Press, Cambridge, UK, and New York, NY, USA.

Seneviratne, S., and R. Stöckli (2007), The Role of Land-Atmosphere Interactions for Climate Variability in Europe, in: *Climate Variability and Extremes during the Past 100 Years* (Brönnimann, S., J. Luterbacher, T. Ewen, H. Diaz, R. Stolarski, and U. Neu, eds.), *Advances in Global Change Research*, vol. 33, pp. 179–193, Springer Netherlands.

Shanahan, T., J. Overpeck, K. Anchukaitis, J. Beck, J. Cole, D. Dettman, J. Peck, C. Scholz, and J. King (2009), Atlantic forcing of persistent drought in West Africa, *Science*, *324*(5925), 377–380.

Sheffield, J., K. Andreadis, E. Wood, and D. Lettenmaier (2009), Global and Continental Drought in the Second Half of the Twentieth Century: Severity-Area-Duration Analysis and Temporal Variability of Large-Scale Events, *Journal of Climate*, *22*(8), 1962–1981.

Sheffield, J., and E. Wood (2008a), Global Trends and Variability in Soil Moisture and Drought Characteristics, 1950-2000, from Observation-Driven Simulations of the Terrestrial Hydrologic Cycle, *Journal of Climate*, *21*(3), 432–458.

Sheffield, J., and E. Wood (2008b), Projected changes in drought occurrence under future global warming from multi-model, multi-scenario, IPCC AR4 simulations, *Climate Dynamics*, *31*(1), 79–105.

Sheffield, J., E. Wood, and M. Roderick (2012), Little change in global drought over the past 60 years., *Nature*, *491*(7424), 435–438.

Shen, C., W.-C. Wang, Z. Hao, and W. Gong (2008), Characteristics of anomalous precipitation events over eastern China during the past five centuries, *Climate Dynamics*, *31*(4), 463–476.

Shindell, D. (2007), Estimating the potential for twenty-first century sudden climate change, *Philosophical Transactions of the Royal Society A - Mathematical, Physical, and Engineering Sciences*, *365*(1860), 2675–2694.

Shindell, D., G. Schmidt, M. Mann, D. Rind, and A. Waple (2001), Solar forcing of regional climate change during the Maunder Minimum., *Science*, *294*(5549), 2149–2152.

Shindell, D., G. Schmidt, R. Miller, and M. Mann (2003), Volcanic and Solar Forcing of Climate Change during the Preindustrial Era, *Journal of Climate*, *16*(24), 4094–4107.

Siegfried, T., T. Bernauer, R. Guiennet, S. Sellars, A. Robertson, J. Mankin, P. Bauer-Gottwein, and A. Yakovlev (2012), Will climate change exacerbate water stress in Central Asia?, *Climatic Change*, *112*(3), 881–899.

Simmons, A., K. Willett, P. Jones, P. Thorne, and D. Dee (2010), Low-frequency variations in surface atmospheric humidity, temperature, and precipitation: Inferences from reanalyses and monthly gridded observational data sets, *Journal of Geophysical Research*, *115*(D1), D01,110.

Skuras, D., and D. Psaltopoulos (2012), A broad overview of the main problems derived from climate change that will affect agricultural production in the Mediterranean area, in: *Building resilience for adaptation to climate change in the agriculture sector. Proceedings of a Joint FAO/OECD Workshop* (Meybeck, A., J. Lankoski, S. Redfern, N. Azzu, and V. Gitz, eds.), p. 346, FAO/OECD, Rome.

Smakhtin, V. (2001), Low flow hydrology: a review, *Journal of Hydrology*, *240*(3-4), 147–186.

Smiatek, G., H. Kunstmann, R. Knoche, and A. Marx (2009), Precipitation and temperature statistics in high-resolution regional climate models: Evaluation for the European Alps, *Journal of Geophysical Research*, *114*(D19), D19,107.

Smith, J., and J. Lazo (2001), A Summary of Climate Change Impact Assessments from the U.S. Country Studies Program, *Climatic Change*, *50*(1), 1–29.

Smith, J., S. Schneider, M. Oppenheimer, G. Yohe, W. Hare, M. Mastrandrea, A. Patwardhan, I. Burton, J. Corfee-Morlot, C. Magadza, H.-M. Füssel, A. Pittock, A. Rahman, A. Suarez, and J.-P. van Ypersele (2009a), Assessing dangerous climate change through an update of the Intergovernmental Panel on Climate Change (IPCC) "reasons for concern"., *Proceedings of the National Academy of Sciences of the United States of America*, *106*(11), 4133–4137.

Smith, R., C. Tebaldi, D. Nychka, and L. Mearns (2009b), Bayesian Modeling of Uncertainty in Ensembles of Climate Models, *Journal of the American Statistical Association*, *104*(485), 97–116.

Smith, S., and T. Wigley (2006), Multi-Gas Forcing Stabilization with the MiniCAM, *Energy Journal, Special Is*, 373–391.

Somot, S., F. Sevault, M. Déqué, and M. Crépon (2008), 21st century climate change scenario for the Mediterranean using a coupled atmosphereocean regional climate model, *Global and Planetary Change*, *63*(2-3), 112–126.

Sorg, A., T. Bolch, M. Stoffel, O. Solomina, and M. Beniston (2012), Climate change impacts on glaciers and runoff in Tien Shan (Central Asia), *Nature Climate Change*, *2*(10), 725–731.

Soulé, P. (1992), Spatial patterns of drought frequency and duration in the contiguous USA based on multiple drought event definitions, *International Journal of Climatology*, *12*(1), 11–24.

Sousa, P., R. Trigo, P. Aizpurua, R. Nieto, L. Gimeno, and R. Garcia-Herrera (2011), Trends and extremes of drought indices throughout the 20th century in the Mediterranean, *Natural Hazards and Earth System Science*, *11*, 33–51.

Sowers, J., A. Vengosh, and E. Weinthal (2011), Climate change, water resources, and the politics of adaptation in the Middle East and North Africa, *Climatic Change*, *104*(3-4), 599–627.

Stahl, K., H. Hisdal, J. Hannaford, L. Tallaksen, H. van Lanen, E. Sauquet, S. Demuth, M. Fendekova, and J. Jódar (2010), Streamflow trends in Europe: evidence from a dataset of near-natural catchments, *Hydrology and Earth System Sciences*, *14*, 2367–2382.

Stainforth, D., T. Aina, C. Christensen, M. Collins, N. Faull, D. Frame, J. Kettleborough, S. Knight, A. Martin, J. Murphy, C. Piani, D. Sexton, L. Smith, R. Spicer, A. Thorpe, and M. Allen (2005), Uncertainty in predictions of the climate response to rising levels of greenhouse gases, *Nature*, *433*, 403–406.

Stainforth, D., M. Allen, D. Frame, J. Kettleborough, C. Christensen, T. Aina, and M. Collins (2004), Climateprediction.net: a global community for research in climate physics, in: *Environmental Online Communication* (Scharl, A., ed.), chap. 12, pp. 101–112, Springer, London, UK.

Stainforth, D., M. Allen, E. Tredger, and L. Smith (2007a), Confidence , uncertainty and decision-support relevance in climate predictions, *Philosophical Transactions of the Royal Society A - Mathematical, Physical, and Engineering Sciences*, *365*, 2145–2161.

Stainforth, D., T. Downing, R. Washington, A. Lopez, and M. New (2007b), Issues in the interpretation of climate model ensembles to inform decisions, *Philosophical Transactions of the Royal Society A: Mathematical, Physical and Engineering Sciences*, *365*(1857), 2163–2177.

STARDEX (2005), *STARDEX*, Tech. rep., Available at: http://www.cru.uea.ac.uk/projects/stardex/.

Stefan, S., M. Ghioca, N. Rimbu, and C. Boroneant (2004), Study of meteorological and hydrological drought in southern Romania from observational data, *International Journal of Climatology*, *24*(7), 871–881.

Steinemann, A. (2003), Drought Indicators and Triggers: A Stochastic Approach to Evaluation, *Journal of the American Water Resources Association*, *39*(5), 1217–1233.

Steinemann, A., and L. Cavalcanti (2006), Developing Multiple Indicators and Triggers for Drought Plans, *ASCE Journal of Water Resources Planning and Management*, *132*(3), 164–174.

Steinemann, A., M. Hayes, and L. Cavalcanti (2005), Drought and Water Crises, in: *Drought and Water Crises: Science, Technology, and Management Issues* (Wilhite, D., ed.), pp. 71–92, Marcel Dekker, NY.

Stoll, S., H. Hendricks Franssen, M. Butts, and W. Kinzelbach (2011), Analysis of the impact of climate change on groundwater related hydrological fluxes: a multi-model approach including different downscaling methods, *Hydrology and Earth System Sciences*, *15*, 21–38.

Stott, P. (2003), Attribution of regional-scale temperature changes to anthropogenic and natural causes, *Geophysical Research Letters*, *30*(14), 1728.

Stott, P., and J. Kettleborough (2002), Origins and estimates of uncertainty in predictions of twenty-first century temperature rise, *Nature*, *416*(6882), 723–726.

Stott, P., D. Stone, and M. Allen (2004), Human contribution to the European heatwave of 2003, *Nature*, *432*, 610–614.

Strzepek, K., and D. Yates (1997), Climate change impacts on the hydrological resources of Europe: a simplified continental scale analysis, *Climatic Change*, *36*(1), 79–92.

Stuiver, M., P. Grootes, and T. Braziunas (1995), The GISP2 δ18O Climate Record of the Past 16,500 Years and the Role of the Sun, Ocean, and Volcanoes, *Quaternary Research*, *44*(3), 341–354.

Sumner, G., R. Romero, V. Homar, C. Ramis, S. Alonso, and E. Zorita (2003), An estimate of the effects of climate change on the rainfall of Mediterranean Spain by the late twenty first century, *Climate Dynamics*, *20*(7), 789–805.

Sun, S., H. Chen, W. Ju, J. Song, H. Zhang, J. Sun, and Y. Fang (2013), Effects of climate change on annual streamflow using climate elasticity in Poyang Lake Basin, China, *Theoretical and Applied Climatology*, *112*(1-2), 169–183.

Svensmark, H., and E. Friis-Christensen (1997), Variation of cosmic ray flux and global cloud coverage-a missing link in solar-climate relationships, *Journal of Atmospheric and Solar-Terrestrial Physics*, *59*(11), 1225–1232.

Tabrizi, A., D. Khalili, A. Kamgar-Haghighi, and S. Zand-Parsa (2010), Utilization of Time-Based Meteorological Droughts to Investigate Occurrence of Streamflow Droughts, *Water Resources Management*, *24*(15), 4287–4306.

Tallaksen, L., H. Madsen, and B. Clausen (1997), On the definition and modelling of streamflow drought duration and deficit volume, *Hydrological Sciences Journal*, *42*(1), 15–33.

Tallaksen, L., K. Stahl, and G. Wong (2011), *Space-time characteristics of large-scale droughts in Europe derived from streamflow observations and WATCH multi-model simulations. WATCH Technical Report No. 48*, Tech. rep.

Tao, F., M. Yokozawa, and Z. Zhang (2009), Modelling the impacts of weather and climate variability on crop productivity over a large area: A new process-based model development, optimization, and uncertainties analysis, *Agricultural and Forest Meteorology*, *149*(2), 831–850.

Tarhule, A., and M.-K. Woo (1997), Towards an Interpretation of Historical Droughts in Northern Nigeria, *Climatic Change*, *37*(4), 601–616.

Tebaldi, C., K. Hayhoe, J. Arblaster, and G. Meehl (2006), Going to the extremes: An intercomparison of model-simulated historical and future changes in extreme events, *Climatic Change*, *79*(3-4), 185–211.

Tebaldi, C., and R. Knutti (2007), The use of the multi-model ensemble in probabilistic climate projections, *Philosophical Transactions of the Royal Society. Series A. Mathematical, Physical and Engineering Sciences*, *365*(1857), 2053–2075.

Tebaldi, C., and B. Sansó (2009), Joint projections of temperature and precipitation change from multiple climate models: a hierarchical Bayesian approach, *Journal of the Royal Statistical Society: Series A (Statistics in Society)*, *172*(1), 83–106.

Tebaldi, C., R. L. Smith, D. Nychka, and L. O. Mearns (2005), Quantifying Uncertainty in Projections of Regional Climate Change: A Bayesian Approach to the Analysis of Multimodel Ensembles, *Journal of Climate*, *18*(10), 1524–1540.

Teutschbein, C., F. Wetterhall, and J. Seibert (2011), Evaluation of different downscaling techniques for hydrological climate-change impact studies at the catchment scale, *Climate Dynamics*, *37*(9-10), 2087–2105.

Thodsen, H. (2007), The influence of climate change on stream flow in Danish rivers, *Journal of Hydrology*, *333*(2-4), 226–238.

Thom, H. (1958), A note on the gamma distribution, *Monthly Weather Review*, *86*(4), 117–122.

Thornthwaite, C. (1948), An approach towards a rational classification of climate, *Geographical Review*, *38*(1), 55–94.

Todd, M., R. Taylor, T. Osborn, D. Kingston, N. Arnell, and S. Gosling (2011), Uncertainty in climate change impacts on basin-scale freshwater resources preface to the special issue: the QUEST-GSI methodology and synthesis of results, *Hydrology and Earth System Sciences*, *15*(3), 1035–1046.

Trenberth, K. (2006), *The Impact of Climate Change and Variability on Heavy Precipitation, Floods, and Droughts*, pp. 1–11, John Wiley & Sons, Ltd.

Trigo, R., D. Pozo-Vázquez, T. Osborn, Y. Castro-Díez, S. Gámiz-Fortis, and M. Esteban-Parra (2004), North Atlantic oscillation influence on precipitation, river flow and water resources in the Iberian Peninsula, *International Journal of Climatology*, *24*(8), 925–944.

Türke, M., and H. Tatl (2009), Use of the standardized precipitation index (SPI) and a modified SPI for shaping the drought probabilities over Turkey, *International Journal of Climatology*, *29*(15), 2270–2282.

Valle, D., C. Staudhammer, W. Cropper, and P. Van Gardingen (2009), The importance of multimodel projections to assess uncertainty in projections from simulation models, *Ecological Applications*, *19*(7), 1680–1692.

van Aalst, M. (2006), The impacts of climate change on the risk of natural disasters., *Disasters*, *30*(1), 5–18.

van Asselt, M., and J. Rotmans (2002), Uncertainty in Integrated Assessment Modelling, *Climatic Change*, *54*(1-2), 75–105.

van der Ent, R., H. Savenije, B. Schaefli, and S. Steele-Dunne (2010), Origin and fate of atmospheric moisture over continents, *Water Resources Research*, *46*(9), W09,525.

van der Schrier, G., J. Barichivich, K. R. Briffa, and P. D. Jones (2013), A scPDSI-based global data set of dry and wet spells for 1901-2009, *Journal of Geophysical Research: Atmospheres*, *118*.

van der Schrier, G., K. Briffa, P. Jones, and T. Osborn (2010), Summer Moisture Variability across Europe, *Journal of Climate*, *19*(12), 2818–2834.

van der Schrier, G., P. Jones, and K. Briffa (2011), The sensitivity of the PDSI to the Thornthwaite and Penman-Monteith parameterizations for potential evapotranspiration, *Journal of Geophysical Research*, *116*(D3), D03,106.

van der Wateren-de Hoog, B. (1995), The effects of climate variability on discharge as dependent on catchment characteristics in the Upper Loire basin, France, *Hydrological Sciences Journal*, *40*(5), 633–646.

van Huijgevoort, M., P. Hazenberg, H. van Lanen, and R. Uijlenhoet (2012), A generic method for hydrological drought identification across different climate regions, *Hydrology and Earth System Sciences*, *16*(18), 2437–2451.

van Lanen, H., and E. Peters (2002), Temporal variability of recharge as an indicator for natural groundwater droughts in two climatically contrasting basins, in: *FRIEND 2002 - regional hydrology: bridging the gap between research and practice. Fourth International Conference on FRIEND (Flow Regimes from International Network Data)* (van Lanen, H., and S. Demuth, eds.), pp. 101–106, IAHS Press, Wallingford, ROYAUME-UNI, Cape Town, South Africa.

van Lanen, H., L. Tallaksen, and G. Rees (2007), Droughts and climate change, in: *Commission Staff Working Document Impact Assessment (SEC(2007) 993), Accompanying document to Communication Addressing the challenge of water scarcity and droughts in the European Union (COM(2007) 414)*, Commission of the European Communities, Brussels, Belgium.

Van Loon, A., M. Van Huijgevoort, and H. Van Lanen (2012), Evaluation of drought propagation in an ensemble mean of large-scale hydrological models, *Hydrology and Earth System Sciences*, *16*, 4057–4078.

Van Loon, A., and H. Van Lanen (2012), A process-based typology of hydrological drought, *Hydrology and Earth System Sciences2*, *16*(7), 1915–1946.

van Loon, H., and J. Rogers (1978), The Seesaw in Winter Temperatures between Greenland and Northern Europe. Part I: General Description, *Monthly Weather Review*, *106*(3), 296–310.

van Rooy, M. (1965), A rainfall anomaly index independent of time and space, *Notos*, *14*, 43–48.

van Ulden, A., and G. van Oldenborgh (2006), Large-scale atmospheric circulation biases and changes in global climate model simulations and their importance for climate change in Central Europe, *Atmospheric Chemistry and Physics*, *6*(4), 863–881.

van Vuuren, D., M. den Elzen, P. Lucas, B. Eickhout, B. Strengers, B. van Ruijven, S. Wonink, and R. van Houdt (2007), Stabilizing greenhouse gas concentrations at low levels: an assessment of reduction strategies and costs, *Climatic Change*, *81*(2), 119–159.

Vasiliades, L., A. Loukas, and G. Patsonas (2009), Evaluation of a statistical downscaling procedure for the estimation of climate change impacts on droughts, *Natural Hazards and Earth System Science*, *9*(3), 879–894.

Vaze, J., D. Post, F. Chiew, J.-M. Perraud, N. Viney, and J. Teng (2010), Climate non-stationarity - Validity of calibrated rainfall-runoff models for use in climate change studies, *Journal of Hydrology*, *394*(3-4), 447–457.

Vicente-Serrano, S. (2006), Spatial and temporal analysis of droughts in the Iberian Peninsula (1910-2000), *Hydrological Sciences Journal*, *51*(1), 83–97.

Vicente-Serrano, S., S. Beguería, and J. López-Moreno (2010), A Multiscalar Drought Index Sensitive to Global Warming: The Standardized Precipitation Evapotranspiration Index, *Journal of Climate*, *23*(7), 1696–1718.

Vicente-Serrano, S., J. González-Hidalgo, M. de Luis, and J. Raventós (2004), Drought patterns in the Mediterranean area: the Valencia region (eastern Spain), *Climate Research*, *26*(1), 5–15.

Vicente-Serrano, S., and J. López-Moreno (2005), Hydrological response to different time scales of climatological drought: an evaluation of the Standardized Precipitation Index in a mountainous Mediterranean basin, *Hydrology and Earth System Sciences*, *9*(5), 523–533.

Vidal, J.-P., and S. Wade (2009), A multimodel assessment of future climatological droughts in the United Kingdom, *International Journal of Climatology*, *29*(14), 2056–2071.

Vidale, P., D. Lüthi, R. Wegmann, and C. Schär (2007), European summer climate variability in a heterogeneous multi-model ensemble, *Climatic Change*, *81*(S1), 209–232.

Vogel, R., I. Wilson, and C. Daly (1999), Regional Regression Models of Annual Streamflow for the United States, *Journal of Irrigation and Drainage Engineering*, *125*(3), 148–157.

Walden, J. (2009), Construction industry, in: *Coping with climate change: risk and opportunities for insurers*, Chartered Insurance Institute, London.

Wanders, N., H. van Lanen, and A. van Loon (2010), *Indicators for drought characterization on a global scale. Technical Report No 24. WATCH deliverable D 4.2.1.*, Tech. rep.

Wang, G. (2005), Agricultural drought in a future climate: results from 15 global climate models participating in the IPCC 4th assessment, *Climate Dynamics*, *25*(7-8), 739–753.

Warren, R., R. Yu, T. Osborn, and S. de la Nava Santos (2012), European drought regimes under mitigated and unmitigated climate change: application of the Community Integrated Assessment System (CIAS), *Climate Research*, *51*(2), 105–123.

Weghorst, K. (1996), *The reclamation drought index: Guidelines and practical applications*, Bureau of Reclamation, Denver, CO [Available from Bureau of Reclamation, D-8530, Box 25007, Lakewood, CO 80226.].

Weigel, A., R. Knutti, M. Liniger, and C. Appenzeller (2010), Risks of Model Weighting in Multimodel Climate Projections, *Journal of Climate*, *23*(15), 4175–4191.

Weiss, J., C. Castro, and J. Overpeck (2009), Distinguishing Pronounced Droughts in the Southwestern United States: Seasonality and Effects of Warmer Temperatures, *Journal of Climate*, *22*(22), 5918–5932.

Weiss, M., and J. Alcamo (2011), A systematic approach to assessing the sensitivity and vulnerability of water availability to climate change in Europe, *Water Resources Research*, *47*, W02,549.

Weiss, M., M. Flörke, L. Menzel, and J. Alcamo (2007), Model-based scenarios of Mediterranean droughts, *Advances in Geosciences*, *12*, 145–151.

Wigley, T., and P. Jones (1985), Influences of precipitation changes and direct CO2 effects on streamflow, *Nature*, *314*(6007), 149–152.

Wigley, T., and S. Raper (1987), Thermal expansion of sea water associated with global warming, *Nature*, *330*(6144), 127–131.

Wigley, T., and S. Raper (1992), Implications for climate and sea level of revised IPCC emissions scenarios, *Nature*, *357*(6376), 293–300.

Wilby, R. (2010), Evaluating climate model outputs for hydrological applications, *Hydrological Sciences Journal*, *55*(7), 1090–1093.

Wilby, R., P. Whitehead, A. Wade, D. Butterfield, R. Davis, and G. Watts (2006), Integrated modelling of climate change impacts on water resources and quality in a lowland catchment: River Kennet, UK, *Journal of Hydrology*, *330*(1-2), 204–220.

Wilby, R., and T. Wigley (1997), Downscaling general circulation model output: a review of methods and limitations, *Progress in Physical Geography*, *21*(4), 530–548.

Wilhite, D. (1997), Responding to drought: common threads from the past, visions for the future, *Journal of the American Water Resources Association*, *33*(5), 951–959.

Wilhite, D. (2005), *Drought and Water Crises: Science, Technology, and Management Issues*, Taylor and Francis Group, Boca Raton, FL.

Wilhite, D., and M. Glantz (1985), Understanding: the Drought Phenomenon: The Role of Definitions, *Water International*, *10*(3), 111–120.

Williams, C., D. Kniveton, and R. Layberry (2010), Assessment of a climate model to reproduce rainfall variability and extremes over Southern Africa, *Theoretical and Applied Climatology*, *99*(1-2), 9–27.

Wilson, D., H. Hisdal, and D. Lawrence (2010), Has streamflow changed in the Nordic countries? Recent trends and comparisons to hydrological projections, *Journal of Hydrology*, *394*(3-4), 334–346.

Wise, M., K. Calvin, A. Thomson, L. Clarke, B. Bond-Lamberty, R. Sands, S. Smith, A. Janetos, and J. Edmonds (2009), Implications of limiting CO2 concentrations for land use and energy, *Science*, *324*(5931), 1183–1186.

WMO (2006), *Drought monitoring and early warning: concepts , progress and future challenges*, Tech. Rep. 1006, WMO-No. 1006.

Wong, W., S. Beldring, T. Engen-Skaugen, I. Haddeland, and H. Hisdal (2011), Climate Change Effects on Spatiotemporal Patterns of Hydroclimatological Summer Droughts in Norway, *Journal of Hydrometeorology*, *12*(6), 1205–1220.

Woo, M.-K., and A. Tarhule (1994), Streamflow droughts of northern Nigerian rivers, *Hydrological Sciences Journal*, *39*(1), 19–34.

Wood, A., L. Leung, V. Sridhar, and D. Lettenmaier (2004), Hydrologic Implications of Dynamical and Statistical Approaches to Downscaling Climate Model Outputs, *Climatic Change*, *62*(1-3), 189–216.

Xu, H., R. Taylor, and Y. Xu (2011), Quantifying uncertainty in the impacts of climate change on river discharge in sub-catchments of the Yangtze and Yellow River Basins, China, *Hydrology and Earth System Sciences*, *15*, 333–344.

Xu, Q. (2001), Abrupt change of the mid-summer climate in central east China by the influence of atmospheric pollution, *Atmospheric Environment*, *35*(30), 5029–5040.

Xu, Y., C. Xu, X. Gao, and Y. Luo (2009), Projected changes in temperature and precipitation extremes over the Yangtze River Basin of China in the 21st century, *Quaternary International*, *208*(1-2), 44–52.

Yevjevich, V. (1967), *An objective approach to definitions and investigations of continental hydrologic droughts*, Tech. Rep. 23, Hydrology Paper 23, Colorado State University, Fort Collins.

Yu, J., G. Fu, W. Cai, and T. Cowan (2010a), Impacts of precipitation and temperature changes on annual streamflow in the Murray-Darling Basin, *Water International*, *35*(3), 313–323.

Yu, Y., X. Zhang, and Y. Guo (2004), Global coupled ocean-atmosphere general circulation models in LASG/IAP, *Advances in Atmospheric Sciences*, *21*(3), 444–455.

Yu, Y., W. Zheng, B. Wang, H. Liu, and J. Liu (2010b), Versions g1.0 and g1.1 of the LASG/IAP Flexible Global Ocean-Atmosphere-Land System model, *Advances in Atmospheric Sciences*, *28*(1), 99–117.

Zemp, M., W. Haeberli, M. Hoelzle, and F. Paul (2006), Alpine glaciers to disappear within decades?, *Geophysical Research Letters*, *33*(13), L13,504.

Zhang, H., G. Huang, D. Wang, and X. Zhang (2011), Uncertainty assessment of climate change impacts on the hydrology of small prairie wetlands, *Journal of Hydrology*, *396*(1-2), 94–103.

Zhang, X., F. Zwiers, G. Hegerl, F. Lambert, N. Gillett, S. Solomon, P. Stott, and T. Nozawa (2007), Detection of human influence on twentieth-century precipitation trends, *Nature*, *448*(7152), 461–465.

Zheng, H., L. Zhang, R. Zhu, C. Liu, Y. Sato, and Y. Fukushima (2009), Responses of streamflow to climate and land surface change in the headwaters of the Yellow River Basin, *Water Resources Research*, *45*(7), W00A19.

Zierl, B. (2005), Global change impacts on hydrological processes in Alpine catchments, *Water Resources Research*, *41*(2), W02,028.

Zou, X., P. Zhai, and Q. Zhang (2005), Variations in droughts over China: 1951-2003, *Geophysical Research Letters*, *32*, L04,707.